Effects of increasing temperatures and CO_2 on phytoplankton and marine biogeochemical cycles

–

Combining experimental work and numerical modeling

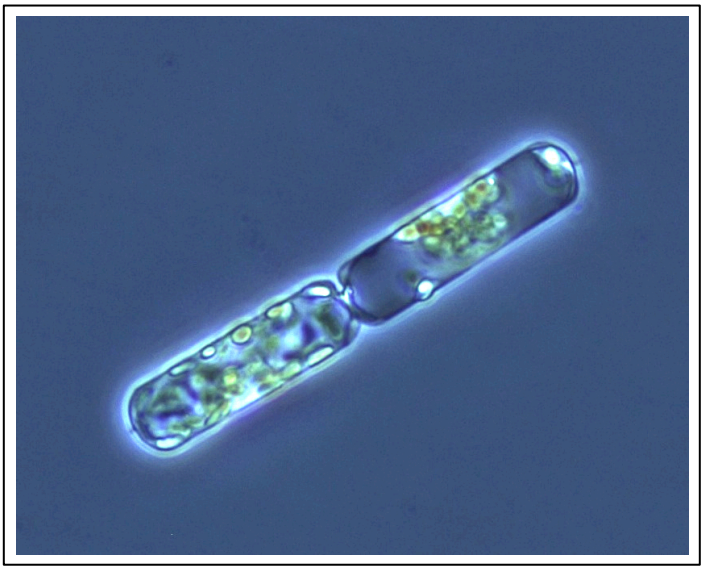

Dissertation

zur Erlangung des Doktorgrades

der Mathematisch-Naturwissenschaftlichen Fakultät

der Christian-Albrechts-Universität zu Kiel

vorgelegt von

Jan Taucher

Kiel, Oktober 2013

Referent: Prof. Dr. Andreas Oschlies
Koreferent: Prof. Dr. Ulf Riebesell
Tag der mündlichen Prüfung: 11.12.2013
Zum Druck genehmigt: 11.12.2013

gez. Prof. Dr. Wolfgang J. Duschl, Dekan

Contents

Summary

The ongoing increase in atmospheric carbon dioxide (CO_2) leads to a global increase in temperatures and its subsequent uptake by the ocean considerably alters the carbonate chemistry of seawater, a phenomenon generally referred to as “ocean acidification”. Both ocean warming and acidification occur at a pace unprecedented in recent geological history and are expected to significantly affect marine biota. In the present thesis, the sensitivity of marine ecosystems and biogeochemical cycling to increasing temperatures and CO_2 was investigated in a combined approach of numerical modeling and experimental work.

In a first step, the role of direct temperature effects in the response of marine ecosystems to ocean warming was investigated by simulating climate change in a global earth system model, based on emission scenarios for the 21st century. The study revealed fundamental uncertainties in our knowledge about temperature sensitivities of marine ecosystems and biogeochemical cycling. Depending on whether biological processes were assumed temperature sensitive or not, simulated marine NPP increased or decreased under projected climate change.

Motivated by the outcome of this modeling study, a mesocosm experiment was carried out to specifically investigate the temperature sensitivity of biogeochemically important processes in diatom-dominated plankton communities. The results from this mesocosm study suggested a pronounced increase in carbon uptake and production of organic matter in response to elevated temperatures, which was contrary to results from similar experiments. A major difference to previous mesocosm studies was the dominant phytoplankton species, suggesting that the physiological response of this species determined the biogeochemical response of the entire plankton community.

In order to test this hypothesis, culture experiments were conducted to compare the sensitivities of two globally important diatom species (*Thalassiosira weissflogii* and *Dactyliosolen fragilissimus*) to temperature and CO_2. The results of these experiments revealed a pronounced effect of temperature and CO_2 on carbon uptake and partitioning into particulate and dissolved organic matter, and especially the phenomenon of carbon overconsumption and the associated decoupling of carbon and nitrogen cycling. Furthermore, the experiments could show that the sensitivity of these processes to temperature and CO_2 varies substantially between species, thereby confirming the hypothesis derived from the preceding mesocosm study.

The findings from these various laboratory experiments were the basis for the development of a novel biogeochemical ecosystem model. Most models do not account for carbon overconsumption and dynamic stoichiometry, and sensitivities of associated processes to temperature and pCO_2, as observed in these experimental studies. Consequently, a model was constructed that simulates carbon overconsumption and its sensitivity to temperature and pCO_2. Application of this model may help to understand how carbon overconsumption and associated processes affect marine biogeochemical cycling.

Further work investigated how the warming-induced decrease seawater viscosity under global warming might affect sinking velocity of marine particles and the carbon flux to the deep ocean. Application of a global earth system model demonstrated that this previously overlooked 'viscosity effect' could have profound impacts on marine biogeochemical cycling and oceanic carbon uptake over the next centuries to millennia. In the model experiment, the viscosity effect significantly accelerated particle sinking, thereby effectively reducing the portion of organic matter that is respired in the surface ocean and enhancing the long-term sequestration of atmospheric CO_2 in the ocean.

The representation of particle sinking in biogeochemical models was investigated in more detail in an additional sensitivity analysis. Results of this study demonstrated that the inherent structure of commonly used ecosystem models sets an upper limit to the flux of organic matter from the euphotic zone to the deep ocean, even under light-saturated and nutrient-replete conditions. This upper limit is determined by the functional form of the various process descriptions in the simulated ecosystem, as well as their respective parameter settings. These findings indicate that, even though such relatively simple ecosystem models may show good skill in reproducing observed current distributions of biogeochemical tracers, it is questionable whether such models can realistically simulate the sensitivity of biogeochemical cycles to environmental change.

Altogether, this doctoral thesis revealed substantial sensitivities of marine carbon fluxes to increases in temperature and CO_2, which should be considered when assessing the impact of climate change on marine ecosystems and feedbacks on the global carbon cycle.

Zusammenfassung

Der stetige Anstieg atmosphärischer Kohlendioxidkonzentrationen (CO_2) führt zu einem globalen Temperaturanstieg. Gleichzeitig resultiert die Aufnahme von CO_2 durch die Ozeane in beträchtlichen Veränderungen der Carbonatchemie des Meerwassers – ein Phänomen, welches im Allgemeinen als „Ozeanversauerung“ bezeichnet wird. Sowohl die Erwärmung als auch die Versauerung der Ozeane geschehen mit einer Geschwindigkeit, die in der jüngeren geologischen Vergangenheit beispiellos ist. Es wird damit gerechnet, dass dies signifikante Auswirkungen auf marine Lebewesen haben wird.

In der vorliegenden Arbeit wurde die Sensitivität mariner Ökosysteme und biogeochemischer Kreisläufe gegenüber steigenden Temperaturen und CO_2-Konzentrationen untersucht. Dabei wurde ein kombinierter Forschungsansatz aus numerischer Modellierung und experimenteller Arbeit angewandt.

Zunächst wurde mit einem globalen Modell des Erdsystems untersucht, wie marine Ökosysteme auf Ozeanerwärmung reagieren und welche Bedeutung direkte Temperaturauswirkungen dabei spielen. Hierfür wurde der künftige Klimawandel basierend auf Emissionsszenarien für das 21. Jahrhundert simuliert. Die Studie offenbarte beträchtliche Unsicherheiten in unserem Verständnis der Temperatursensitivitäten mariner Ökosysteme und biogeochemischer Kreisläufe. In Simulationen des projizierten Klimawandels nahm die simulierte marine Primärproduktion entweder zu oder ab, abhängig davon, ob biologische Prozesse eine Temperatursensitivität beinhalteten oder nicht.

Das Resultat dieser Modellstudie war Motivation für die Durchführung eines Mesokosmenexperiments, um die Temperatursensitivität biogeochemisch bedeutender Prozesse in Planktongemeinschaften, welche von Diatomeen dominiert werden, spezifisch zu untersuchen. Die Ergebnisse dieser Studie deuteten im Gegensatz zu früheren vergleichbaren Experimenten auf eine ausgeprägte Zunahme der Kohlenstoffaufnahme bei erhöhten Temperaturen hin. Da ein Hauptunterschied zu vorherigen Mesokosmenexperimenten die dominante Phytoplanktonart war, bestimmte möglicherweise die physiologische Reaktion dieser Spezies die biogeochemische Reaktion der gesamten Planktongemeinschaft.

Um diese Hypothese zu testen wurden Kulturexperimente durchgeführt, in denen die Sensitivität zweier global bedeutender Diatomeenarten (*Thalassiosira weissflogii* und *Dactyliosolen fragilissimus*) gegenüber Temperatur und CO_2 vergleichend untersucht

wurde. Die Ergebnisse dieser Studie zeigten einen deutlichen Einfluss von Temperatur und CO_2 auf Kohlenstoffaufnahme und -partitionierung in partikuläres und gelöstes organisches Material, und insbesondere auf das Phänomen des übermäßigen Kohlenstoffkonsums sowie die damit verbundene Entkopplung von Kohlenstoff- und Stickstoffkreislauf. Des Weiteren konnten die Experimente zeigen, dass sich die Sensitivität dieser Prozesse gegenüber Temperatur und CO_2 deutlich zwischen den Arten unterscheidet. Damit konnte die Hypothese bestätigt werden, welche anknüpfend an die Mesokosmenstudie entstanden war.

Die Resultate der diversen Laborexperimente waren der Grundstein für die Entwicklung eines neuartigen biogeochemischen Ökosystemmodells. Die meisten Modelle berücksichtigen weder übermäßigen Kohlenstoffkonsum und dynamische Stöchiometrie, noch die Sensitivität der damit verbundenen Prozesse gegenüber Temperatur und CO_2, wie sie in den Laborexperimenten beobachtet wurde. Aus diesem Grund wurde ein Modell konstruiert, welches übermäßigen Kohlenstoffkonsum und dessen Sensitivität gegenüber Temperatur und CO_2 simuliert. Die Anwendung dieses Modells könnte dabei helfen zu verstehen, wie sich übermäßiger Kohlenstoffkonsum und damit verbundene Prozesse auf marine biogeochemische Kreisläufe auswirken.

Überdies wurde untersucht wie sich eine wärmebedingte Abnahme der Viskosität des Meerwassers im Zuge der globalen Erwärmung auf Sinkgeschwindigkeiten mariner Partikel und den Kohlenstoffffluss in die Tiefsee auswirken könnte. Die Anwendung eines globalen Erdsystemmodells konnte darlegen, dass dieser bisher übersehene „Viskositätseffekt“ in den nächsten Jahrhunderten und Jahrtausenden tiefgreifende Auswirkungen auf biogeochemische Stoffflüsse und Kohlenstoffaufnahme der Ozeane haben könnte. In dem Modellexperiment bewirkte der Viskositätseffekt eine signifikante Beschleunigung sinkender Partikel. Dies reduzierte effektiv den Anteil organischen Materials, welcher im oberflächennahen Ozean respiriert wurde und steigerte somit die langfristige Speicherung von atmosphärischem CO_2 im Ozean.

Die Repräsentation sinkender Partikel in biogeochemischen Modellen wurde in einer weiteren Sensitivitätsanalyse genauer untersucht. Die Ergebnisse dieser Studie deuten darauf hin, dass die Struktur verbreiteter Ökosystemmodelle dem Fluss organischen Materials aus der euphotischen Zone in die Tiefsee eine obere Begrenzung setzt, auch unter licht- und nährstoffgesättigten Bedingungen. Diese Obergrenze wird bestimmt durch die funktionale Form der verschiedenen Ökosystem-Prozessbeschreibungen sowie deren jeweiligen Parametereinstellungen. Diese Ergebnisse weisen darauf hin, dass es

fragwürdig ist, ob solche relativ simplen Ökosystemmodelle in der Lage sind, die Sensitivität biogeochemischer Flüsse gegenüber Umweltveränderungen zu simulieren, obwohl diese Modelle gegenwärtige Verteilungen biogeochemischer Tracer gut abbilden können.

Zusammenfassend hat die vorliegende Doktorarbeit beträchtliche Sensitivitäten mariner Kohlenstoffflüsse gegenüber steigenden Temperaturen und CO_2-Konzentrationen aufgezeigt. Diese sollten in künftigen Studien und Einschätzungen über die Folgen des Klimawandels auf marine Ökosysteme und Rückkopplungen im globalen Kohlenstoffkreislauf berücksichtigt werden.

I. General introduction

1. The role of phytoplankton in the marine carbon cycle

The ocean in the earth system

The world oceans cover 71% of the earth's surface and play a central role in biogeochemical cycling of elements. Of special importance is their key role in the global carbon cycle and thereby the climate system by regulating the atmospheric concentration of carbon dioxide CO_2 (Raven and Falkowski, 1999). The oceans constitute the second-largest pool of carbon (C) on earth, containing more than 38,000 GtC (Figure 1). Most of this carbon is present in the form of dissolved inorganic carbon (DIC, ~98%) and dissolved organic carbon (DOC, ~2%), whereas only a negligibly small fraction consists of particulate organic carbon, which comprises live biomass (Falkowski et al., 2000; Hansell et al., 2009; Sarmiento and Gruber, 2006).

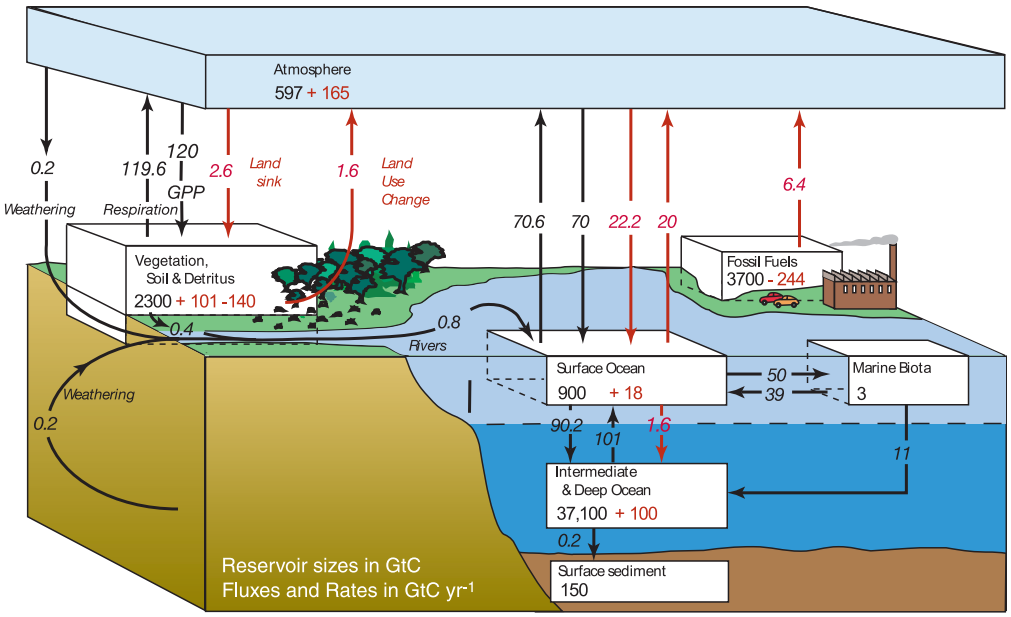

Figure 1: The global carbon cycle at the end of the 20th century. Shown are the main reservoirs [GtC] and fluxes [GtC yr^{-1}]. Black numbers and arrows denote pre-industrial reservoir sizes and fluxes, while red arrows and estimates denote anthropogenic fluxes and changes in pool sizes since the beginning of the industrial era. Source: IPCC (2007a).

However, even though the biomass of living photosynthetic organisms in the ocean only amounts to ~1 GtC, marine net primary production (NPP) is estimated to be ~50 GtC yr^{-1} (Falkowski et al., 1998; Field et al., 1998). This number roughly equals the estimates for

terrestrial primary production (Field et al., 1998). Furthermore, the proportion between NPP and biomass illustrates the rapid turnover of organic matter in marine ecosystem, which usually occurs on the timescale of days to weeks.

Phytoplankton in the sea

Marine primary production is almost entirely attributable to phytoplankton (Falkowski, 1994; Longhurst et al., 1995). These are free-floating, unicellular, photoautotrophic organisms living in the sunlit surface ocean. Approximately 5,000 marine phytoplankton taxa have been estimated so far (Sournia et al., 1991), even though diversity is expected to be orders of magnitude higher with an unknown number of undiscovered and unclassified species (Falkowski and Raven, 2007). Due to their large diversity, phytoplankton species with similar biogeochemical roles are commonly aggregated into functional types (Buitenhuis et al., 2013; Le Quéré et al., 2005; Moore et al., 2002). These include diatoms, which are often primary formers of plankton blooms and form a cell wall that is made of silica ("frustule"); dinoflagellates, which often have thick cellulose cell walls and have whip-like structures ("flagella") that are used for locomotion; coccolithophores with their ability to calcify and form an armor from small $CaCO_3$ plates ("coccoliths"); and nitrogen-fixing cyanobacteria, which are especially important in low-nutrient and less productive regions (Buitenhuis et al., 2013; Sarmiento and Gruber, 2006).

The focus of the work presented here was on diatoms, which are one of the most important groups of marine phytoplankton. They are cosmopolitan and display a wide range of morphologies, ranging from large, chain-forming species in polar and sub-polar regions to small and often single-celled diatoms in the tropical ocean (Boyd et al., 2010). It has been estimated that diatoms account for ~40% of marine primary production, which makes them key players in the biogeochemical cycling of carbon, nitrogen, phosphorus, silicon, and iron (Sarthou et al., 2005). They frequently form strong blooms and are commonly assumed to dominate particle flux and sequestration of carbon to the deep ocean (Boyd et al., 2010; Buesseler, 1998; Treguer et al., 1995).

The marine carbon cycle and the biological pump

A remarkable feature in ocean biogeochemistry is the pronounced vertical gradient of DIC, with relatively lower concentrations in the surface ocean and a sharp increase with depth. This gradient is maintained by two independent mechanisms that transport carbon from

the surface to the deep ocean: the solubility pump and the biological carbon pump (Sarmiento and Gruber, 2006; Volk and Hoffert, 1985). The solubility pump is an entirely physical mechanism: Through air-sea gas exchange, seawater can absorb CO_2 from the atmosphere. CO_2 is more soluble in colder water at high latitudes, where the formation of deep water takes place. This results in a transport of carbon-enriched water to the ocean interior via the meridional overturning circulation. It has been estimated that the solubility pump accounts for 35-40% of the surface-to-deep gradient of DIC (Toggweiler et al., 2003a). At the same time, this implies that the larger portion of the vertical DIC gradient is driven by the biological carbon pump (Toggweiler et al., 2003b). This term summarizes a myriad of biological processes that, in concert, transport carbon from the surface to the deep ocean (Fig. 2). In the surface layer of the ocean, the euphotic zone, DIC is converted into organic matter via photosynthesis by phytoplankton, which forms the base of the marine food web. Aggregation and sinking of particles result in a vertical transport of organic matter to the deep ocean.

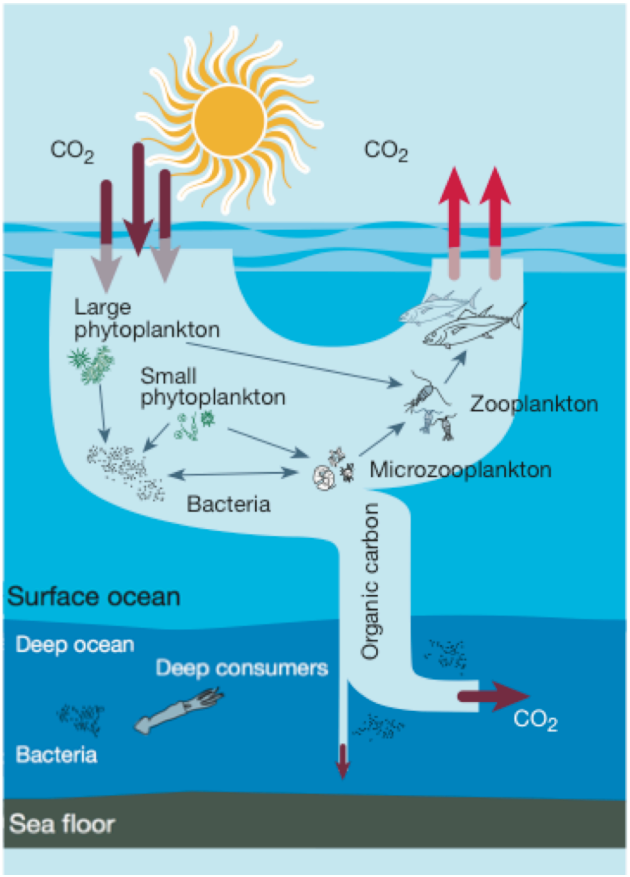

Figure 2: Schematic illustration of the biological pump. Sunlight and inorganic nutrients are used by phytoplankton to convert CO_2 to biomass, thereby forming the base of the marine food web. As the carbon passes through the foodweb in the surface ocean, most of it is converted back to CO_2 and released to the atmosphere. A variable fraction (10-20%) is transported to the ocean interior where the major fraction is remineralized to CO_2 by bacteria and other heterotrophs, while a small portion sediments on the sea floor. The net result of the biological pump is transport of CO_2 from the atmosphere to the deep ocean, where it remains for roughly ~1,000 years, on average. Illustration adapted and modified from Chisholm (2000).

Estimates for global carbon export out of the euphotic zone range from 5 GtC yr^{-1} (Henson et al., 2011) to 20 GtC yr^{-1} (Eppley and Peterson, 1979) with several estimates clustering around 10-12 GtC yr^{-1} (Dunne et al., 2007; Laws et al., 2000), corresponding to ~20% of marine NPP. As the biomass passes through the food web, a large fraction of the organic carbon gets respired through heterotrophic processes, thereby attenuating the vertical flux of organic matter with depth and releasing DIC back into deeper water layers. As these deeper water masses are not in contact with the atmosphere, the carbon which is taken up by the solubility and biological pump is effectively removed from the atmosphere until it reaches the surface ocean again, e.g. through upwelling on the continental margins, approximately one thousand years later. Consequently, the biological carbon pump plays a major role in the global carbon cycle, and it has been estimated that atmospheric CO_2 concentrations would be more than twice as high without this mechanism (Maier-Reimer et al., 1996).

Dissolved organic carbon and transparent exopolymer particles

With a size of ~662 GtC (Hansell et al., 2009), DOC constitutes the second larges carbon reservoir in the ocean and is comparable to the reservoir of atmospheric CO_2, which has been estimated to amount to ~750 GtC (IPCC, 2007a). The most important source for DOC is exudation by phytoplankton, although other processes, such as grazing and excretion by zooplankton, or bacterial decomposition of organic particles can also lead to production of DOC. While the largest portion of DOC is rather refractory, and consequently displays an average age of 4,000 years, a small fraction experiences rapid turnover by biological processes (Carlson, 2002; Hansell et al., 2009). The main sink of DOC is microbial remineralization, through which DOC is reintroduced into the food web as bacterial biomass, which is then available to higher trophic levels through grazing by protists and mesozooplankton. This trophic pathway is commonly referred to as the “microbial loop” (Azam et al., 1983). It has been estimated that up to 50% of primary production can be channeled into the DOC pool and rapid bacterial respiration (Hansell et al., 2009).

Besides its importance in the microbial food web, DOC also plays a significant role in the transport of carbon to the deep ocean. Although the biological carbon pump is dominated by the flux of particulate organic matter, it has been shown that DOC can significantly contribute to transport of carbon to the deep ocean through transport via deep water formation and mixing. Estimates of this surface-to-depth transport of DOC range between

1.2 to 1.8 GtC yr^{-1}, corresponding to approximately 10-15% of global export production (Hansell and Carlson, 1998; Hansell et al., 2009).

Furthermore, it has been demonstrated that a substantial fraction of exuded DOC can be transformed into gel-like transparent exopolymer particles (TEP) by abiotic coagulation and aggregation processes (Engel et al., 2004b; Passow, 2000). TEP mainly consist of acidic polysaccharides and exhibit a high degree of stickiness, which makes them an important player in the formation of marine aggregates ("marine snow") and thereby in the sedimentation of plankton blooms and transport of carbon into the deep ocean (Alldredge et al., 1993; Passow, 2002).

Elemental stoichiometry – the composition of organic matter

The stoichiometric (i.e. molar) ratio of carbon (C), nitrogen (N), and phosphorus (P) in particulate organic matter appears to be fairly constant across the globe. Based on measurements of the elemental composition of phytoplankton, the oceanographer A.C. Redfield found the stoichiometric ratio of C:N:P to be surprisingly uniform at 106:16:1 ("Redfield ratio") (Redfield, 1934). The fact that autotrophic organisms utilize chemical elements in specific stoichiometric ratios seems logical, considering the differential elemental requirements for the cell machinery and the synthesis of proteins, lipids, carbohydrates or nucleic acids (Geider and La Roche, 2002). However, the Redfield ratio represents an average value of all particulate organic matter and does therefore not take into account variations among species. Furthermore, a variety of studies have shown that there are large variations in phytoplankton stoichiometry and the ratio at which carbon and inorganic nutrients are acquired and synthesized into biomass (Banse, 1994; Brzezinski, 1985). In fact, a substantial portion of carbon uptake can occur after nutrient depletion, thereby leading to a notable decoupling of carbon and nitrogen uptake. This phenomenon is commonly referred to as "carbon overconsumption" (Toggweiler, 1993) and has been observed in various experiments and field studies (Banse, 1994; Körtzinger et al., 2001; Sambrotto et al., 1993). These stoichiometric variations have been primarily linked to the availability of nutrients, but other environmental factors, such as light, temperature and CO_2 are assumed to play an important role as well (Biddanda and Benner, 1997; Feng et al., 2008; Kim et al., 2011; Riebesell et al., 2007).

2. The ocean in the 21st century

The earth system and climate – past, present and future

Over the past centuries, human activities have led to substantial impacts on the global environment, e.g. through deforestation, destruction of habitats, pollution, or overfishing, to name only a few (Steffen et al., 2004). Besides these direct alterations of the environment, global climate change increasingly alters the earth system and global biogeochemical cycles (Falkowski et al., 2000; IPCC, 2007a).

Present day atmospheric concentrations of the greenhouse gases carbon dioxide (CO_2) and methane (CH_4) far exceed preindustrial values. Since the beginning of the industrial era in the middle of the 18th century, the concentration of atmospheric CO_2 has increased from its preindustrial value of 280 ppmv (parts per million volume) to almost 400 ppmv in the early 21st century (Figure 3A), which is higher than at any time during the last 800,000 years (Lüthi et al., 2008), and potentially the last 3 to 20 million years (IPCC, 2007a).

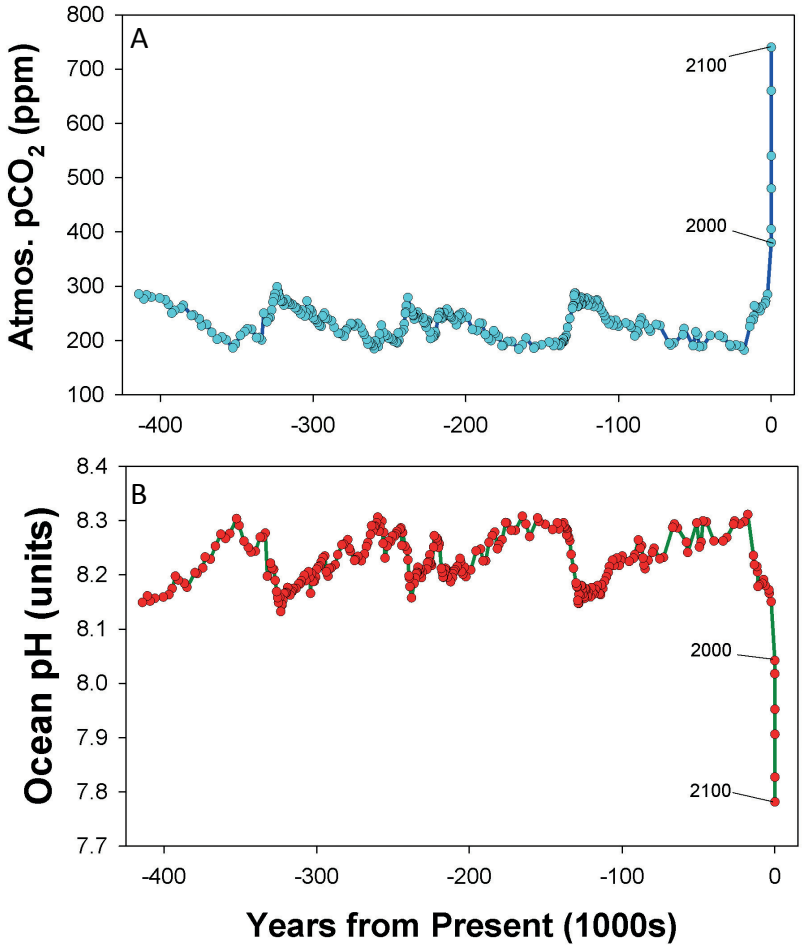

Figure 3: (A) Atmospheric CO_2 from ice core records and (B) estimated ocean pH in the Quaternary. Source: Barry et al. (2010)

This increase in greenhouse gas emissions from human activities, such as fossil fuel burning and land use change, has accelerated over the last decades and is tracking high-end emission scenarios as described and used in the assessment report of the Intergovernmental Panel On Climate Change. The result is an increasing imbalance in the earth's energy budget and a corresponding increase in global mean surface air temperatures of 0.74 °C over the last century (IPCC, 2007a). Warming of the ocean occurs slower than on land due to the higher thermal capacity of water and associated thermal inertia. Thus, the increase in global ocean sea surface temperatures over the same time period is slightly lower, amounting to 0.6 °C (Figure 4) (IPCC, 2007a). Furthermore, it is noteworthy that the warming signal has already penetrated the deeper ocean, displaying a global average increase of 0.18 °C of the upper 700 m since 1955, and an accelerating trend over the last decade (Balmaseda et al., 2013; Levitus et al., 2012).

Future projections of global warming depend on the underlying scenario for future greenhouse gas emissions. Estimates for the increase in global mean surface temperature range from 1.1 °C to 6.4 °C until the end of the 21st century, thereby also leading to a further warming of the ocean (IPCC, 2007a).

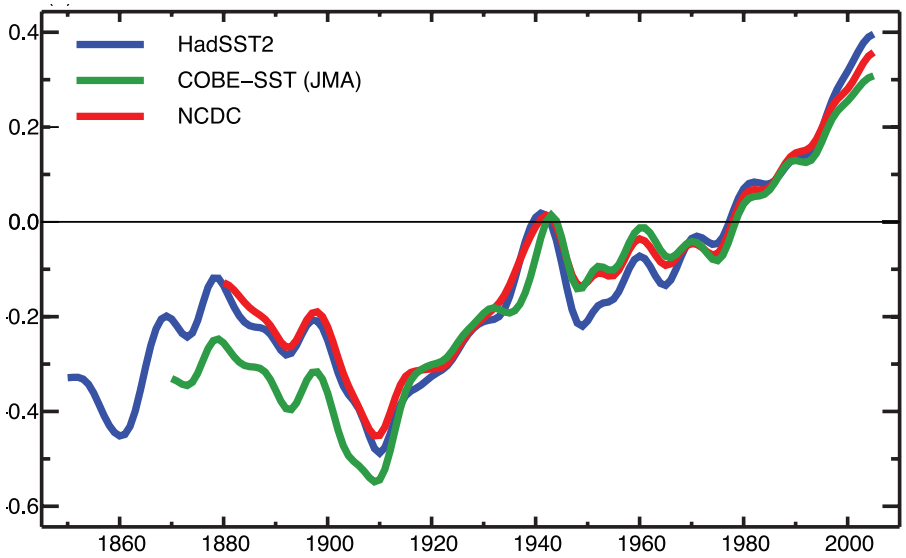

Figure 4: Annual global sea surface temperature anomalies, relative to 1961 to 1990 [°C] from three different observational datasets. Source: IPCC (2007a)

In addition to warming, the world oceans have absorbed almost one third of the emitted anthropogenic carbon (Sabine et al., 2004), thereby substantially altering its chemical balance: The uptake of atmospheric CO_2 leads to shifts in seawater carbonate chemistry,

with an increase in dissolved CO_2, bicarbonate (HCO_3^-), and free protons (H^+), and an associated decrease in carbonate (CO_3^{2-}), and pH (Zeebe and Wolf-Gladrow, 2001). This reduction in pH of seawater is commonly referred to as "ocean acidification" (Broecker and Clark, 2001; Caldeira and Wickett, 2003). Since preindustrial times, surface ocean pH has already dropped by approximately 0.1 units, and a further decrease between 0.3-0.4 units is expected until the end of the 21st century (Figure 3B) (Orr et al., 2005).

Impacts of global warming and ocean acidification on marine phytoplankton and ecosystems

Climate change will lead to severe changes in the marine realm, ranging from ocean warming, increased thermal stratification and reduced upwelling, sea level rise, loss of sea ice, to ocean acidification and deoxygenation (Doney et al., 2009a; Gruber, 2011; IPCC, 2007b). In the scope of this work, the focus was put on direct temperature effects and ocean acidification, both of which will affect marine ecosystems and biogeochemical cycling in a variety of ways (Passow and Carlson, 2012; Riebesell et al., 2009). However, while future changes of the abiotic environment can be reasonably projected within a certain range, their effects on marine organisms, biological processes and biogeochemical cycling are much less understood (Bopp et al., 2013; Sarmiento et al., 2004).

One of the major environmental factors that control biological processes is temperature, since most cellular functions, such as enzymatic reactions, are directly temperature-dependent. This affects many essential processes, such as growth and metabolic rates, and is therefore of great importance for the physiology and ecology of organisms (Gillooly et al., 2001). The sensitivity to temperature is commonly given as the Q_{10} factor, which describes the factorial increase of a rate for a 10 °C increase in temperature. A relationship between temperature and phytoplankton growth has long been recognized, suggesting rather low temperature sensitivity with a Q_{10} value between 1 and 2 (Eppley, 1972). Furthermore, recent studies in the context of ocean warming suggested e.g. a decrease in cell size (Moran et al., 2010), shifts in phenology (Sommer and Lengfellner, 2008), effects on carbon uptake of phytoplankton communities (Wohlers et al., 2009), as well as alterations on the ecosystem level e.g. in food web structure (O'Connor et al., 2009). However, observed effects of increasing temperatures vary substantially among studies and investigated species. Furthermore, the response to warming is expected to be different among the various components of marine ecosystems, especially between autotrophic and heterotrophic organisms (Riebesell et al., 2009).

At the same time, ocean acidification is expected to influence marine phytoplankton either through a decrease in pH (and the corresponding increase in H^+ ions) or the shift in carbonate speciation, e.g. the availability of CO_2 vs. HCO_3^- for carbon assimilation and photosynthesis (Doney et al., 2009a; Rost et al., 2008). There is a large number of studies on the effects of ocean acidification on a variety of organisms, especially calcifying phytoplankton such as coccolithophores, showing a marked influence of carbonate chemistry on factors such as growth rate and calcification (Iglesias-Rodriguez et al., 2008; Riebesell et al., 2000). Furthermore, it has been shown that "ocean carbonation", i.e. increasing concentrations of dissolved CO_2 in seawater (Bach et al., 2011), can affect non-calcifying phytoplankton, such as cyanobacteria (Hutchins et al., 2007) or diatoms (Burkhardt et al., 2001). At least some groups of phytoplankton, especially those with a relatively inefficient mechanism for CO_2 acquisition, might even benefit from the increased availability of aqueous CO_2 (Beardall et al., 2009; Rost et al., 2008).

Observed biological impacts that have been linked to ongoing climate change include biogeographical, phenological, physiological, and species abundance changes (Beaugrand, 2009; Grebmeier et al., 2006; Richardson and Schoeman, 2004). A number of studies based on different data sources, such as satellite and *in-situ* ocean chlorophyll measurements, found a decline of marine primary production and phytoplankton stocks, which they linked to recent trends in climate, particularly the increase in sea surface temperatures (Behrenfeld et al., 2006; Boyce et al., 2010). While observations on oceanic uptake of anthropogenic CO_2 and the decrease in seawater pH are consistent (Gattuso and Hansson, 2011), the consequences of ocean acidification and shifts in carbonate chemistry on oceanic ecosystems are just beginning to be understood (Doney et al., 2009a), and *in situ* observations of their effects on marine life are not available yet.

3. Motivation for this work and thesis outline

There are very different approaches to improve our understanding of biological processes in the ocean and their sensitivity to environmental changes, including field observations, laboratory experiments, and numerical models.

Experiments on different spatial and temporal scales are the primary source of biological data acquisition and are essential for process understanding and the exploration of sensitivities to environmental drivers. Experimental setups range from batch cultures and chemostats, to mesocosms or even manipulations in the field. Each of these approaches addresses different questions and has their own strengths and weaknesses (Riebesell et al., 2010). However, extrapolation of experimental results to large spatial and temporal scales is difficult.

In this regard, numerical models of marine biological processes have become and increasingly important tool in marine research. Such models can be viewed as a simplified representation of the real world, where processes are simulated with a formal mathematical description (Oschlies et al., 2010). They range from very simplistic models that are usually applied in studies of marine biogeochemistry on a global scale, to more sophisticated representations of physiological and ecological mechanisms. One of the most widespread applications of models in current marine research is hypothesis testing ("what if" experiments), and the identification of large-scale sensitivities to changing environmental drivers. In this regard, models are closely linked to laboratory and field work, as these deliver the data and process understanding that is necessary in order to allow for an adequate representation of biological processes in a model. However, exchange of data and knowledge between experimentalists and the modeling community tends to be slow and fraught with problems.

One of the aims of this thesis was to close this gap and combine experimental work and numerical modeling to identify sensitivities of ecosystem processes and carbon fluxes under projected climate change. A particular focus was to improve our understanding of ocean warming and acidification on carbon uptake and partitioning by phytoplankton, and potential implications for the carbon flux to the deep ocean. Over the last few years, an increasing number of studies have investigated the question of how marine ecosystems and biogeochemistry might respond to climate change and ocean acidification (Bopp et al., 2013; Oschlies et al., 2008; Steinacher et al., 2010). However, some of these results are quite contradictory. For instance, it is not even clear whether marine primary production

will increase or decrease in response to ocean warming (Sarmiento et al., 2004; Steinacher et al., 2010), how different phytoplankton species will react to changes in carbonate chemistry (Rost et al., 2008) and multiple environmental changes occurring at the same time (Beardall et al., 2009; Boyd et al., 2010). This illustrates that our understanding of the functioning of marine ecosystems, and how they will respond to a changing environment, is still far from perfect, thus making it difficult to describe and parameterize these processes in earth system models. Therefore, another major aim of this thesis was to gain a better mechanistic understanding of processes that are sensitive to temperature and carbonate chemistry, and implement the observed relationships into biogeochemical ecosystem models.

Chapter 1 presents results from a global modeling study, which investigates the role of direct temperature effects in the response of marine ecosystems and biogeochemical cycling to ocean warming. Although an increasing number of global modeling studies have investigated effects of climate change on marine ecosystems, the treatment of biological processes in most of these studies is rather rudimentary. Furthermore, most of these studies focused on the indirect effects of global warming, such as changes in nutrient supply or light availability. Only little attention has been given to direct effects of higher temperatures on marine biological processes, even though experimental evidence suggests substantial effects of warming on marine biota. In the presented study, we applied different configurations of an earth system model, with and without temperature dependence of biological processes, to simulate present conditions and projected future climate change. The model output was compared against observational data to assess the role of temperature sensitivity in reproducing observed distributions of biogeochemical tracers. Furthermore, the implications for marine ecosystem dynamics in a warming ocean are discussed.

Chapter 2 shows results from a mesocosm experiment in which temperature-driven changes in carbon and nitrogen cycling by a natural plankton community were investigated. While a large number of studies have identified a key role of temperature on metabolic rates, phenology or trophic interactions, the implications for biogeochemical cycling are far less understood. Furthermore, little is known about whether observed temperature sensitivities are a general pattern across marine ecosystems, or if the response of key processes in carbon cycling depends on the composition of the

phytoplankton assemblage. In the presented study, we investigated the temperature sensitivity of a summer plankton community in the Baltic Sea. Therefore, we induced a bloom via addition of inorganic nutrients and monitored carbonate chemistry and the build-up and elemental composition of particulate and dissolved organic matter for a period of one month.

Chapter 3 shows results from batch culture experiments, where the effects of temperature and pCO_2 on carbon uptake and partitioning by two diatom species were investigated. Both, warming and ocean acidification, are expected to alter the path and processing of carbon through marine food webs, and ultimately the biological pump. A particular focus of the presented study is on post-bloom dynamics after nutrient depletion, when carbon overconsumption becomes most prominent. Since carbon uptake and its allocation between the particulate and dissolved phase by primary producers on the one side, and heterotrophic consumption of this organic matter on the other side, operate simultaneously and are closely intertwined under natural conditions, it is usually difficult to disentangle the underlying mechanisms. In the presented experiments, production of POM and DOM was separated from their consumption and degradation through heterotrophic processes. Thereby, the mechanisms whereby elevated CO_2 and temperature alter the uptake and partitioning of carbon by phytoplankton can be elucidated and better understood for use in mechanistic ecosystem models.

Chapter 4 discusses the results of a model study that investigated the potential impact of temperature-driven changes in seawater viscosity on marine particle flux. Besides generally recognized direct effects of temperature changes on marine biota, ocean warming also leads to a decrease in seawater viscosity, which is expected to accelerate sinking velocities of marine particles. By applying an earth system model, we investigate how this “viscosity effect” could affect the export of photosynthetically fixed carbon into the deep ocean, and discuss its potential role as a feedback mechanism in the climate system.

Chapter 5 examines the general capability of commonly used biogeochemical models to realistically capture export production in the ocean, and the mechanisms that control its magnitude and spatiotemporal dynamics. Sinking of organic matter from the euphotic zone to the deep ocean plays a key role in marine biogeochemical cycling and the

distribution of inorganic nutrients and carbon in the ocean. Thus, a realistic simulation of the magnitude and spatiotemporal pattern of export production in earth system models is an essential prerequisite for correctly simulating observed nutrient fields, biogeochemical fluxes, and their potential sensitivity to ongoing environmental change. The presented study applies commonly used ecosystem model structures to identify which processes exert the strongest control on simulated export production, and discusses whether some existing models deliver realistic results for the wrong reasons.

The thesis concludes with a comprehensive **synthesis**, which discuses the results of the different chapters and embeds them into current knowledge on climate change and possibilities to combine experimental work and modeling. Furthermore, the findings from the various presented studies are synthesized and used for the development of a model that simulates carbon overconsumption and its sensitivity to temperature and CO_2.

II. Thesis Chapters

First-author publications and declaration of contribution

Chapter 1:

Taucher, J., and A. Oschlies (2011): Can we predict the direction of marine primary production change under global warming?, *Geophysical Research Letters*, 38(2).

Idea and experimental design: Andreas Oschlies, Jan Taucher
Modeling work: Jan Taucher
Data analysis: Jan Taucher
Manuscript preparation: Jan Taucher with comments from Andreas Oschlies

Chapter 2:

Taucher, J., K. G. Schulz, T. Dittmar, U. Sommer, A. Oschlies, and U. Riebesell (2012), Enhanced carbon overconsumption in response to increasing temperatures during a mesocosm experiment, *Biogeosciences*, 9(9), 3531-3545.

Idea and experimental design: Ulrich Sommer, Ulf Riebesell, Jan Taucher
Experimental work: Jan Taucher
Sample analysis: Jan Taucher, assisted by Thorsten Dittmar
Data analysis: Jan Taucher with comments from Kai Schulz
Manuscript preparation: Jan Taucher with comments from Kai Schulz, Thorsten Dittmar, Ulrich Sommer, Andreas Oschlies, Ulf Riebesell

Chapter 3:

Taucher, J., J. Jones, A. James, M. Brzezinski, C. A. Carlson, A. Oschlies, U. Riebesell, and U. Passow (2013): Effects of warming and elevated pCO_2 on carbon overconsumption and partitioning of the marine diatoms *Thalassiosira weissflogii* and *Dactyliosolen fragilissimus*. To be submitted to *Limnology and Oceanography*.

Idea and experimental design: Jan Taucher, Uta Passow, Ulf Riebesell, Andreas Oschlies, Mark Brzezinski, Craig Carlson
Experimental work: Jan Taucher, assisted by Jonathan Jones and Anna James
Sample analysis: Jan Taucher, assisted by Jonathan Jones and Anna James
Data analysis: Jan Taucher
Manuscript preparation: Jan Taucher with comments from Uta Passow, Mark Brzezinski, Craig Carlson

Chapter 4:

Taucher, J., L. T. Bach, U. Riebesell, A. Oschlies (2013): The viscosity effect on marine particle flux – a climate relevant feedback mechanism, currently under review at *Global Biogeochemical Cycles*.

Idea and experimental design: Jan Taucher, Lennart Bach, Andreas Oschlies
Modeling work: Jan Taucher
Data analysis: Jan Taucher, Lennart Bach
Manuscript preparation: Jan Taucher and Lennart Bach in equal contribution, with comments from Andreas Oschlies and Ulf Riebesell

Chapter 5:

Taucher, J., and A. Oschlies (2013): What sets the upper limit of export production in marine ecosystem models? To be submitted to *Global Biogeochemical Cycles*

Idea and experimental design: Andreas Oschlies, Jan Taucher
Modeling work: Jan Taucher
Data analysis: Jan Taucher
Manuscript preparation: Jan Taucher with comments from Andreas Oschlies

Chapter 1: Can we predict the direction of marine primary production change under global warming?

J. Taucher[1] and A. Oschlies[1]

[1]GEOMAR Helmholtz Centre for Ocean Research, Kiel, Germany

Correspondence to: J. Taucher (jtaucher@geomar.de)

Geophysical Research Letters
Received 22 October 2010; revised 1 December 2010; accepted 6 December 2010; published 21 January 2011.

Abstract

A global Earth System model is employed to investigate the role of direct temperature effects in the response of marine ecosystems to climate change. While model configurations with and without consideration of explicit temperature effects can reproduce observed current biogeochemical tracer distributions and estimated carbon export about equally well, carbon flow through the model ecosystem reveals strong temperature sensitivities. Depending on whether biological processes are assumed temperature sensitive or not, simulated marine NPP increases or decreases under projected climate change driven by a business-as-usual CO_2 emission scenario for the 21st century. This suggests that indirect temperature effects such as changes in the supply of nutrients and light are not the only relevant factors to be considered when modeling the response of marine ecosystems to climate change. A better understanding of direct temperature effects on marine ecosystems is required before even the direction of change in NPP can be reliably predicted.

1. Introduction

Climate change is expected to have diverse impacts on marine ecosystems (Riebesell et al., 2009). Estimates of possible future changes in marine net primary production (NPP) are generally based on numerical models. Most model studies addressing the response of marine ecosystems and biogeochemistry to climate change have, so far, focused on the effects of changes in nutrient or light availability. These are mostly attributable to enhanced stratification and weaker vertical mixing (Bopp et al., 2001; Boyd and Doney, 2002; Plattner et al., 2001) and are thus indirect effects of rising surface temperatures. An analysis of different biogeochemical climate models found a coherent decline of both NPP and export production under projected 21st century global warming (Steinacher et al., 2010). In contrast, *Sarmiento et al.* (2004) found an increase in projected 21st century NPP, using a semi-empirical approach, which combines climate model projections and satellite-based primary production algorithms. They identified the temperature sensitivities of the primary production algorithm as the main cause for the predicted increase in primary production.

Up to now, modeling studies have paid only little attention to the direct biological impacts of higher temperatures in simulations of global warming, although experimental evidence suggests a positive correlation between temperature and phytoplankton growth (Duarte, 1995; Eppley, 1972) and effects of elevated temperatures at the ecosystem level (Muren et al., 2005; Wohlers et al., 2009). Yet, the description of direct temperature effects differs considerably among different models (Steinacher et al., 2010). Here we specifically investigate the sensitivity of simulated 21st century's changes in marine primary production to the consideration of direct temperature effects on metabolic processes.

2. Methods

The model employed is the University of Victoria (UVic) global Earth system model (Schmittner et al., 2008; Weaver et al., 2001). It includes a simple NPZD type marine ecosystem model with the two nutrients phosphate and nitrate, two phytoplankton classes (nitrogen fixers and other phytoplankton) and one zooplankton type. Furthermore it contains a parameterization of fast nutrient recycling as a representation of the microbial loop and the cycling of dissolved organic matter (Schartau and Oschlies, 2003). In the standard version (Schmittner et al., 2008), hereafter called TEMP, biological production and remineralization processes depend on temperature via an Eppley formula

(Eppley, 1972) with a Q_{10} value of 1.88. In a sensitivity experiment (NOTEMP), all temperature-dependent rate coefficients are replaced by constant values.

Rate constants of the NOTEMP run are chosen as flux-weighted global averages of the temperature-dependent rates of the TEMP experiment. For instance, the maximum growth rate of phytoplankton is directly dependent on temperature:

$$J_{max} = a \cdot b^{cT}$$

The term b^{cT} is calculated with temperature *T* and the sensitivity parameters *b*=1.066 and *c*=1.0. In configuration NOTEMP the temperature-sensitivity *c* is 0.0 [°C^{-1}], and thus b^{cT} = 1.0. To ensure that global biogeochemical fluxes are as close as possible to those of experiment TEMP, other parameters describing the respective biological processes are readjusted by the process-weighted global-mean temperature term $b^{c\overline{T}_{proc}}$ with $\overline{T}_{proc}$, in the case of NPP, given by:

$$\overline{T}_{NPP} = \frac{\overline{(NPP \cdot Temperature)}}{\overline{NPP}}$$

Thereby parameter *a* is increased from 0.2 d^{-1} in run TEMP to 0.71 d^{-1} in run NOTEMP. All parameter changes are listed in Table 1.

Table 1: Changes of model parameters from configuration TEMP to NOTEMP

Parameter	**Symbol**	**TEMP**	**NOTEMP**
Phytoplankton (P_O, P_D)			
Maximum growth rate at 0°C [day^{-1}]	a	0.2	0.71
Temperature dependence of maximum growth rate [°C^{-1}]	c	1.0	0.0
Linear mortality coefficient (fast recycling) [day^{-1}]	μ_{P0}	0.014	0.0545
Handicap of diazotrophs w.r.t. other phytoplankton	c_D	0.5	0.25
Zooplankton (Z)			
Excretion [day^{-1}]	γ_2	0.01	0.0385
Detritus (D)			
Remineralization rate [day^{-1}]	μ_{D0}	0.048	0.139

After a spin-up of 4,000 years with preindustrial boundary conditions (e.g. insolation, fixed atmospheric CO_2 of 280 ppm), the models are forced using fossil fuel and land use carbon emissions as well as solar, volcanic and anthropogenic aerosol forcing reconstructed from different datasets for the period 1765 to 2000 (Schmittner et al., 2008). From year 2000 onwards, the model is forced by anthropogenic CO_2 emissions following the IPCC SRES A2 ("business-as-usual") scenario. Consequently, both model simulations account for indirect temperature effects of CO_2-driven global warming, such as changes in circulation and stratification and associated impacts on nutrient and light supply. However only model TEMP accounts for the direct effects of elevated temperatures on metabolic rates.

3. Results and Discussion

Present day conditions

Simulated nutrient, carbon, and oxygen fields in both models agree well with observations (Figure 1). Compared to data from the World Ocean Atlas (Garcia et al., 2006b) the global average root mean square (RMS) error for phosphate is 0.138 mmol m^{-3} in run TEMP and 0.157 mmol m^{-3} in model NOTEMP. This RMS error is at the lower end of errors found in previous modeling studies (Doney et al., 2009b; Kriest et al., 2010). Global marine net primary production (NPP) simulated for the year 2000 amounts to 49.0 GtC yr^{-1} in model TEMP and 56.0 GtC yr^{-1} in model NOTEMP. Both numbers are in good agreement with diverse satellite-based estimates of 49 to 60 GtC yr^{-1} for NPP in the world oceans (Behrenfeld et al., 2006; Carr et al., 2006). Datasets on NPP used here (Figure 2a) give 54.1 GtC yr^{-1} (Behrenfeld and Falkowski, 1997) and 56.7 GtC yr^{-1} (Westberry et al., 2008). Export production is also of similar magnitude in both model configurations, reaching 8.7 GtC yr^{-1} in run TEMP and 11.3 GtC yr^{-1} in run NOTEMP (Figure 2d). These numbers also agree with observation-based estimates from previous studies (Oschlies, 2001; Schlitzer, 2004).

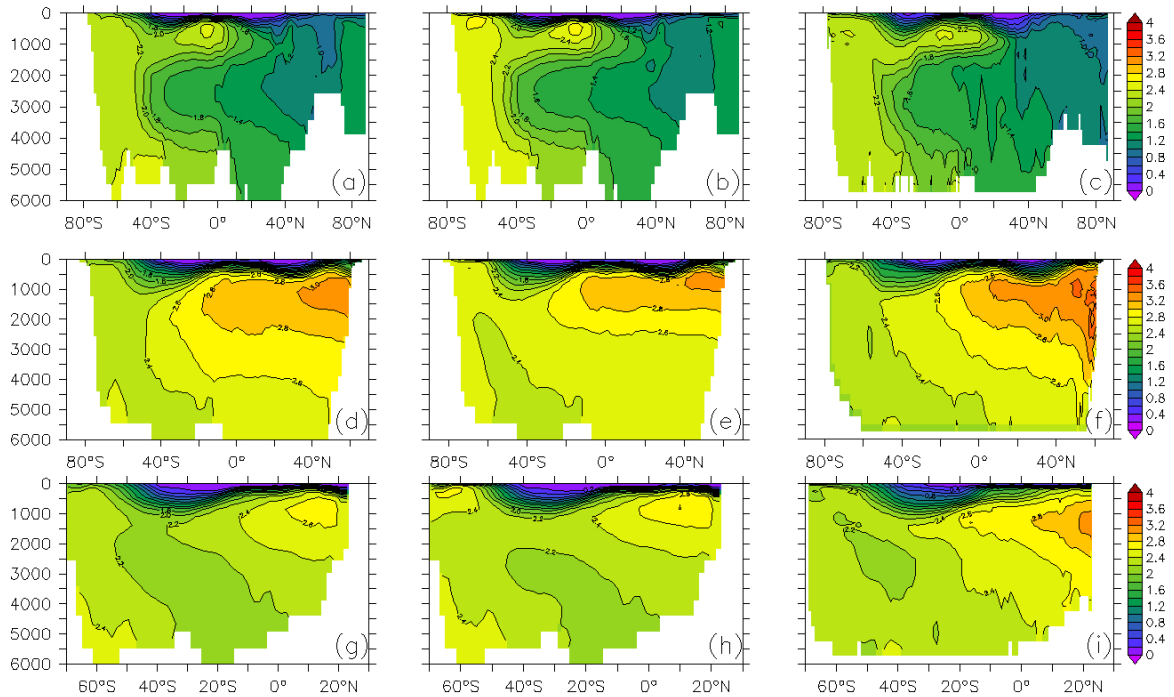

Figure 1. Depth-latitude sections of phosphate concentrations [mmol m^{-3}] in the Atlantic (a-c), Pacific (d-f) and Indian Ocean (g-i) in model TEMP (left), NOTEMP (middle) and from World Ocean Atlas (Garcia et al., 2006b) data (right).

Despite these similarities on the global scale, the spatial patterns and underlying controls of the various biological processes show some major differences between the two model configurations (Figure 2 a-d): In configuration TEMP, high values of NPP in the tropical oceans are accompanied by high recycling rates, especially remineralization and fast recycling via the microbial loop from phytoplankton back to dissolved inorganic nutrients, since all these processes occur faster at higher temperatures. Essentially, a short circuit is established, in which NPP is again fueled by rapidly regenerated nutrients and relatively little biomass is exported to depth (~10% of NPP). In run NOTEMP, the absence of a direct positive effect of temperature on metabolic rates yields lower tropical NPP, lower remineralization and less intense recycling of phytoplankton biomass back to nutrients. However, simulated export production in the tropical ocean turns out to be even higher in run NOTEMP, as less biomass is lost through recycling processes, leaving a higher fraction of NPP (~19%) available for export to depth. At high latitudes the pattern is reversed. NPP reaches high levels in run NOTEMP. However, a large portion of organic matter is recycled in the surface ocean, as there is no slowdown by low water temperatures.

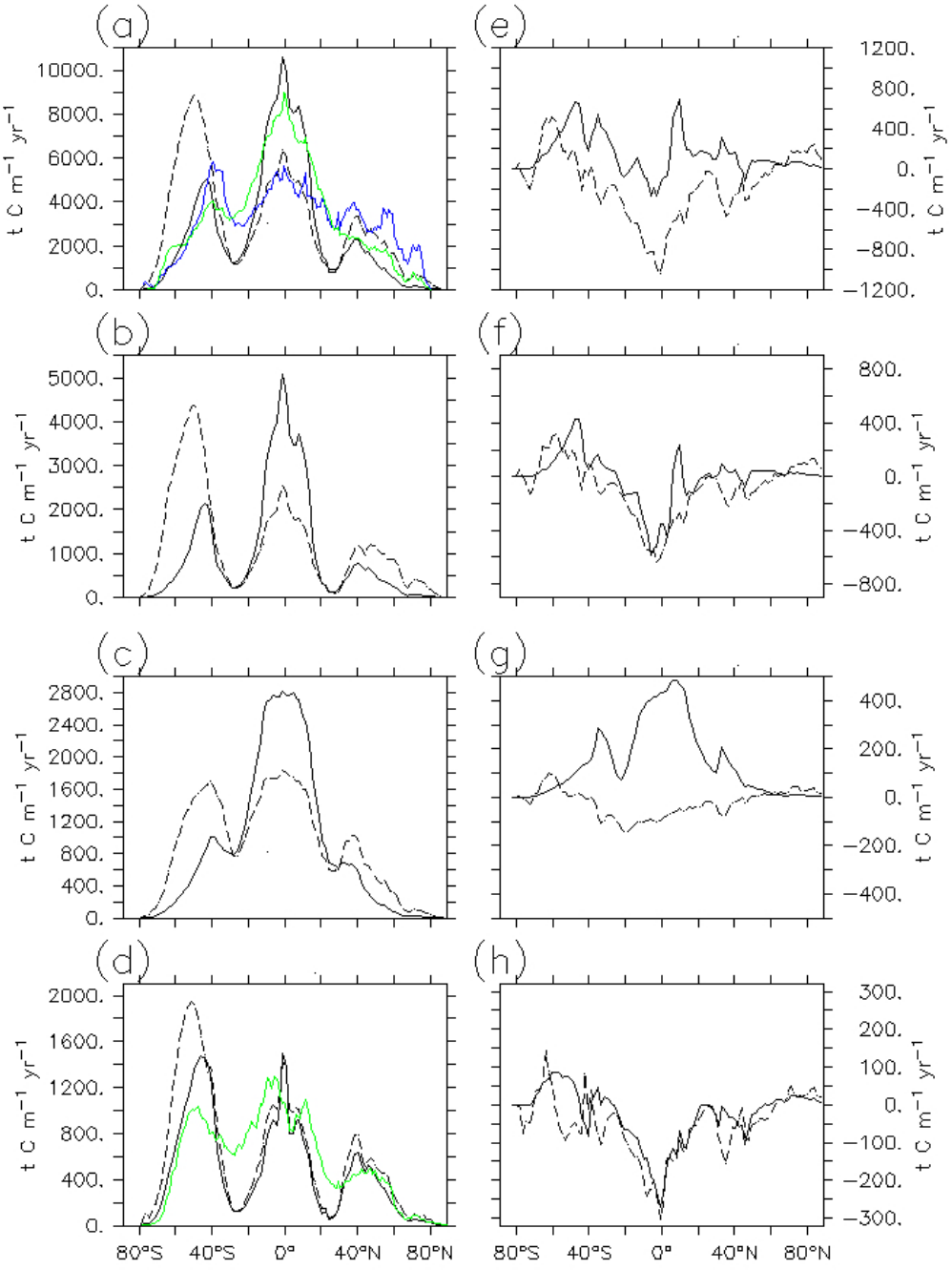

Figure 2. Zonal distribution of marine ecosystem processes in the model with (solid) and without temperature dependence (dashed) in the year 2000 (a-d) and their respective change from 2000 through 2100 (e-h). From top: Net Primary Production [tC °lat^{-1} yr^{-1}], Remineralization of detritus [tC °lat^{-1} yr^{-1}], Fast Recycling [tC °lat^{-1} yr^{-1}], Export of organic matter (including turbulent mixing) [tC °lat^{-1} yr-1]. NPP (a) includes SeaWiFS estimates using VGPM (Behrenfeld and Falkowski, 1997) (blue) and CBPM2 (Westberry et al., 2008) (green) algorithms, and export of organic matter (d) includes observation-based export estimates (Schlitzer, 2002, 2004) (green).

Consequently, the amount of organic matter that is exported to depth is relatively small compared to the high level of NPP (~13%). In run TEMP, the high-latitude ecosystem works at a much lower level of biomass production. NPP is inhibited by low temperatures and reaches not even a quarter of high-latitude NPP of run NOTEMP. All recycling processes are also slowed down by low temperatures in run TEMP, channeling a relatively large fraction of simulated high-latitude NPP (~33%) into export of sinking particles. Regional differences in export production between the two model configurations are relatively small compared to the pronounced differences in NPP. Also, NPP and export production in both models compare about equally well with observation-based estimates (Figure 2a,d).

Response to climate change

Following the SRES A2 emission scenario, simulated global sea surface temperatures increase by 2.0 °C in the 21st century (Schmittner et al., 2008). Physical changes of the ocean, like enhanced thermal stratification, reduced upwelling and weaker vertical mixing lead to reduced supply of nutrients to the surface ocean in both models. Being closely tied to simulated nutrient supply, global export production responds very similarly in both model configurations over the period 2000-2100, with a decrease from 8.7 to 8.2 GtC yr^{-1} (-6.1%) in model TEMP and a decrease from 11.3 to 10.3 GtC yr^{-1} (-7.2%) in model NOTEMP (Figure 3). The response also shows a similar spatial pattern in both model simulations (Figure 2h). In contrast, changes in individual ecological processes turn out to differ considerably among the two model configurations: In run NOTEMP, all globally-averaged carbon and nitrogen fluxes associated with any biological process decrease in response to climate change (Figure 3b). In particular, simulated annual NPP decreases from 56.0 to 53.0 GtC yr^{-1} from year 2000 to 2100 (-5.3%). This change is directly linked to the decrease in nutrient supply. In contrast, in configuration TEMP simulated global NPP increases from 49.0 to 51.7 GtC yr^{-1} (+5.2%) during the same period (Figure 3a) despite the decline in export production. Besides NPP, fast recycling of phytoplankton increases significantly from 16.0 to 18.7 GtC yr^{-1} (+16.9%) in model TEMP. This indicates a faster spinning of the microbial loop under elevated temperatures, and a corresponding increase in regenerated production.

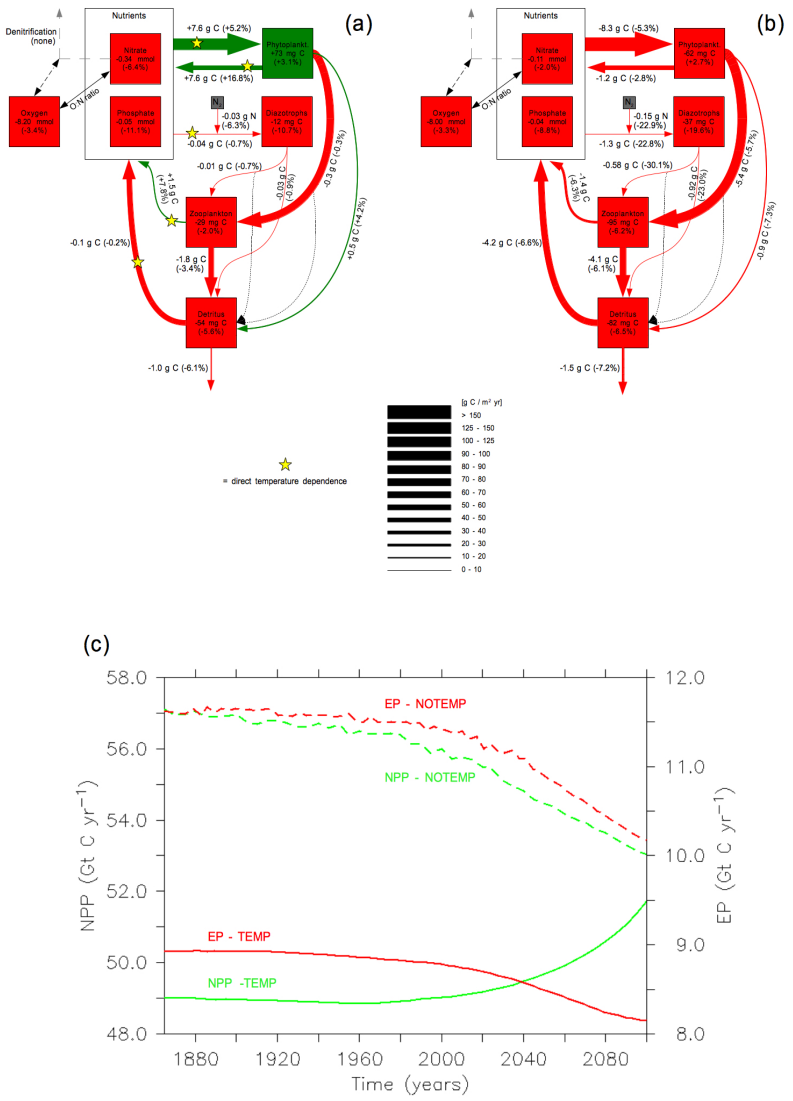

Figure 3. Global average change in nutrient and oxygen concentrations [mmol m^{-3}], biomass [mgC m^{-3}] and biogeochemical flows in carbon equivalents [gC m^{-3} yr^{-1}] in the surface ocean (0-130 m) in model TEMP (a) and NOTEMP (b) for the period 2000 to 2100. Percentage change given in brackets. Timeseries of global Net Primary Production (NPP) and Export Production (EP) of organic matter out of the upper 130 m in model TEMP and NOTEMP (c).

Latitudinal differences in the response to simulated climate-induced changes in metabolic rates are shown in Figure 2e-h: At high latitudes NPP and phytoplankton biomass moderately increase in both model configurations. This is mainly due to the shoaling of the mixed layer, the retreat of sea ice and a longer growing season. The increase in high-latitude NPP is also accompanied by an increase in export production in both models.

Major differences between the two models occur at low and intermediate latitudes. In model TEMP, both NPP and phytoplankton biomass increase in most parts of the tropical and subtropical oceans (Figure 2e). The strongest response can be observed for fast recycling from phytoplankton back to inorganic nutrients (Figure 2f). Its acceleration is tightly coupled to NPP, since the build-up of biomass provides the substrate for fast recycling, which in turn restores nutrients and thereby fuels NPP. At the same time, simulated export production remains closely tied to nutrient supply, which is affected only indirectly by temperature and hence shows a similar decrease under global warming in runs TEMP and NOTEMP. However, in run NOTEMP, both NPP and biomass of phytoplankton also show a decrease in the tropical and subtropical oceans. Without the enhancement of recycling processes by higher temperatures, regenerated production decreases along with new production (Figure 2e,h). Consequently, spatial differences in the simulated response of NPP among the two model configurations correspond to differences in the simulated response of the microbial loop to global warming.

The global-warming induced increase in NPP in configuration TEMP appears contradictory to the results of studies by *Gregg et al.* (2003) and *Behrenfeld et al.* (2006) which are based on satellite measurements and suggest a predominantly negative correlation of increasing temperatures and marine NPP. However, these studies cover a relatively short time span and do not disentangle direct and indirect effects of temperature changes. When satellite NPP algorithms were applied to changes in the physical environment projected for the end of the 21st century, *Sarmiento et al.* (2004) inferred an increase in marine NPP in response to warming, which would agree with the results of our model configuration TEMP.

The results of model TEMP also appear to agree better with empirical evidence on the relationship between temperature and phytoplankton growth (Eppley, 1972; Moisan et al., 2002) and with observed responses of marine ecosystem processes to elevated temperatures. Recent mesocosm experiments revealed a clear effect of elevated temperatures on ecosystem functioning and carbon cycling, with a generally stronger temperature dependence of heterotrophic processes (Muren et al., 2005; Wohlers et al., 2009). While a coherent effect of elevated temperatures on primary production could not be observed in these experiments, the stronger response of respiration relative to autotrophic production to elevated temperatures favors a shift towards a more

heterotrophic system and associated lower vertical export of organic matter, which is consistent with the results of model TEMP.

4. Conclusions

The model experiments presented here reveal that temperature sensitivities of metabolic rates have the potential to play an important role in controlling marine ecosystem processes and their response to climate change. Depending on whether or not metabolic rates are assumed temperature dependent in the model, not only the magnitude, but even the direction of global-warming induced change is different for global NPP and the associated cycling of carbon and nutrients through the model ecosystem. Our model results also show that it is possible to adjust models with and without explicit temperature dependence about equally well to observed biogeochemical tracer distributions, which alone do not seem to provide sufficient information to judge which of the two model configurations TEMP or NOTEMP and, by inference, which sign of projected 21st century NPP change is more realistic.

In contrast to NPP, simulated export production and thereby the effective drawdown of carbon appear closely tied to the physically driven supply of nutrients and respond almost equally to climate change, regardless of whether direct temperature effects on biology are included in the model or not. In this regard, our results are consistent with results from previous studies (Bopp et al., 2001; Cox et al., 2000; Fung et al., 2005), which all project a decrease in export production in response to global warming. However, a number of global models also simulate a future decrease in primary production (Steinacher et al., 2010), which is not found in our model configuration TEMP, where elevated temperatures lead to higher NPP and accelerated carbon cycling. Our results also indicate that changes in NPP are closely linked to the temperature sensitivities of recycling processes and especially the microbial loop, which are not considered in most other global models (Steinacher et al., 2010). However, the intricate balance between production and respiration under increasing temperatures is still not understood properly and needs further research (Riebesell et al., 2009).

Our study has shown that the simulated response of NPP to climate change depends on the assumptions made about the temperature dependencies of metabolic processes. Here we used the same temperature function for both autotrophic and heterotrophic

processes. However, marine phytoplankton growth and photosynthesis are mainly controlled by light supply and nutrient availability and are therefore commonly assumed to show a weaker response to elevated temperatures than heterotrophic processes such as bacterial degradation (Pomeroy and Wiebe, 2001; Riebesell et al., 2009). Including these considerations in refined models might further accelerate the simulated microbial loop and thereby enhance the discrepancy in the responses of NPP and export production to global warming. We conclude, that a better understanding and model representation of direct temperature effects on biological processes is required in order to obtain robust estimates of even the direction of marine primary production changes under global warming.

Acknowledgement: This study was supported by the Deutsche Forschungsgemeinschaft (DFG).

Chapter 2: Enhanced carbon overconsumption in response to increasing temperatures during a mesocosm experiment

J. Taucher[1], K. G. Schulz[1,2], T. Dittmar[3], U. Sommer[1] , A. Oschlies[1] and U. Riebesell[1]

[1]GEOMAR Helmholtz Centre for Ocean Research Kiel, Kiel, Germany
[2]Now at: Southern Cross University, Lismore, Australia
[3]Max-Planck Research Group for Marine Geochemistry, University of Oldenburg, Oldenburg, Germany

Correspondence to: J. Taucher (jtaucher@geomar.de)

Biogeosciences
Received: 8 March 2012 – Published in *Biogeosciences Discuss*ions: 20 March 2012
Revised: 4 August 2012 – Accepted: 8 August 2012 – Published: 5 September 2012

Abstract

Increasing concentrations of atmospheric carbon dioxide are projected to lead to an increase in sea surface temperatures, potentially impacting marine ecosystems and biogeochemical cycling. Here we conducted an indoor mesocosm experiment with a natural plankton community taken from the Baltic Sea in summer. We induced a plankton bloom via nutrient addition and followed the dynamics of the different carbon and nitrogen pools for a period of one month at temperatures ranging from 9.5 °C to 17.5 °C, representing a range of ±4 °C relative to ambient temperature. The uptake of dissolved inorganic carbon (DIC) and the net build-up of both particulate (POC) and dissolved organic carbon (DOC) were all enhanced at higher temperatures and almost doubled over a temperature gradient of 8 °C. Furthermore, elemental ratios of carbon and nitrogen (C:N) in both particulate and dissolved organic matter increased in response to higher temperatures, both reaching very high C:N ratios of >30 at +4 °C. Altogether, these observations suggest a pronounced increase in excess carbon fixation in response to elevated temperatures. Most of these findings are contrary to results from similar experiments conducted with plankton populations sampled in spring, revealing large uncertainties in our knowledge of temperature sensitivities of key processes in marine carbon cycling. Since a major difference to previous mesocosm experiments was the dominant phytoplankton species, we hypothesize that species composition might play an important role in the response of biogeochemical cycling to increasing temperatures.

1. Introduction

Climate change is expected to affect marine ecosystems and biogeochemical cycling in the oceans in a variety of ways (IPCC, 2007b; Riebesell et al., 2009). Since the beginning of the 20th century, global average sea surface temperatures have already increased by 0.6 °C. Recent climate projections suggest an increase in global surface air temperatures by about 1.1 to 6.4 °C by the end of this century (relative to 1980-1999), thereby also leading to a further warming of the upper ocean (IPCC, 2007a). This will affect marine ecosystems indirectly as thermal stratification of the water column becomes stronger, leading to changes in the availability of nutrients and light. It is also likely that sea surface warming will have pronounced direct effects on pelagic ecosystems and marine carbon cycling, as temperature is a major environmental factor controlling the rates of biological processes (Brown et al., 2004). Experimental evidence suggests a clear relationship between temperature and phytoplankton growth (Eppley, 1972).

A number of studies have already investigated the effects of increasing temperatures at the ecosystem level. Common observations were a decrease in body size of planktonic organisms (Daufresne et al., 2009; Moran et al., 2010), effects on timing of the bloom (Lassen et al., 2010; Sommer and Lengfellner, 2008), coupling of phytoplankton and bacterial processes (Hoppe et al., 2008), as well as changes in food web dynamics, i.e. a shift from autotrophic to more heterotrophic states of the respective ecosystems (Muren et al., 2005; O'Connor et al., 2009). In some of these experiments a lower overall biomass was found in response to warming (Lassen et al., 2010; O'Connor et al., 2009)

However, most of these studies did not explicitly monitor biogeochemical dynamics. A recent mesocosm study with a natural plankton community investigated possible impacts of warming on biogeochemical cycling under spring bloom conditions (Wohlers et al., 2009). The results suggested an acceleration of respiratory carbon consumption over autotrophic production and an associated decrease in carbon drawdown at elevated temperatures. Furthermore, they found that warming shifted the partitioning of organic matter between the particulate and dissolved phase, with a higher fraction building up as dissolved material. This observation is also supported by another similar mesocosm experiment (Kim et al., 2011). Yet, little is known about whether these observed temperature sensitivities are a general pattern in marine ecosystems, or if the response of key processes in carbon cycling to sea surface warming depends on the phytoplankton assemblage. In both of the above mesocosm experiments, the dominant phytoplankton species was the diatom *Skeletonema costatum*. In this study, we investigated the effect of

temperature changes on marine carbon cycling in a natural plankton community in summer and discuss differences to previous experiments.

2. Material and Methods

Experimental Setup

The indoor mesocosm study was carried out between 16th June and 16th July 2010 at the Helmholtz Centre for Ocean Research Kiel (GEOMAR) in Kiel, Germany. Nine cylindric mesocosms with a volume of 1,400 L (water depth: ~100 cm, diameter ~140 cm) each were set up in triplicates in three temperature controlled climate chambers, and filled simultaneously with unfiltered seawater from approximately 6 m depth in Kiel Fjord (Western Baltic Sea). Thus, the water in the mesocosms contained a natural summer plankton community representative for this region at that time.

Mesozooplankton (copepods of the species *Acartia clausi*) was added from net catches (64 µm mesh size) with densities of ~10 individuals L^{-1}. Since *Acartia clausi* is the dominant mesozooplankton species (>90%) during most years in this region and the density of 10 ind L^{-1} is a reasonable number for this region and time of year (Behrends, 1996), we believe that our added mesozooplankton provides an adequate representation of field conditions.

To investigate the effects of temperature on a summer bloom situation, the temperatures in the three climate chambers were adjusted to 9.5 °C, 13.5 °C and 17.5 °C (in the following referred to as “low”, “intermediate” and “high” temperature, respectively). The intermediate temperature level of 13.5 °C corresponded to the temperature of near-surface water (~5m depth) in the Kiel Fjord at the start of the experiment. The other temperature regimes were equivalent to in situ +4 °C and in situ -4 °C, thereby establishing an overall temperature gradient of 8 °C. Previous mesocosm experiments had only considered a temperature gradient in the direction of warming. In our experimental setup a temperature gradient towards both cooling and warming was established in order to ensure that the observed effects are truly associated with the absolute temperature and are not merely a stress response to a temperature change in either direction. Mesocosms had been filled one day before the experiment started (t-1) as it took ~24h until target temperatures were reached. It should be noted that temperature regulation was not perfect with standard deviations between 0.4 and 0.8 °C in the different treatments. This is mainly attributable to the experimental setup, i.e. the airflow in the

climate chambers. Thereby, the temperature of one of the replicates was ~1 °C lower than in the other two mesocosms at all temperatures. However, this variability within treatments is still much smaller than variability between treatments.

Light supply during the experiment was provided by a computer-controlled system, generating a light curve with a light/dark cycle of ~17/7 hours. It contained full-spectrum light tubes (12 × 80 W per mesocosm; 10 × 4,000 K and 2 × 9,000 K color temperature) covering the full range of photosynthetically active radiation (PAR: 400-700 nm). The daily light dose was calculated for the respective latitude and day of the year following Brock (1981), resulting in a theoretical maximum irradiance intensity (at noon) of ~690 W m^{-2} at the water surface. The actual target intensity was 32%, corresponding to a daily maximum irradiance of ~270 W m^{-2}. However, the maximum realized intensity with our light supply was ~80 W m^{-2} or 400 µmol photons m^{-2} s^{-1}. Therefore, a plateau of maximum light intensity was established, holding the realized maximum light intensity long enough to compensate for the lack of desired maximum intensity. This way the desired integrated light supply of ~1100 Wh m^{-2} could be achieved.

Measured concentrations of dissolved inorganic nutrients in the mesocosms on day t1 amounted to ~0.1 µmol L^{-1} phosphate (PO_4^{3-}), ~1.5 µmol L^{-1} nitrate (NO_3^-), ~0.4 µmol L^{-1} ammonium (NH_4) and ~12.2 µmol L^{-1} silicate ($Si(OH)_4$). In order to initiate a phytoplankton bloom, inorganic nutrients were added to the mesocosms in Redfield stoichiometry on day t1, with concentrations of 16.0 µmol L^{-1} NO_3^- and 1.0 µmol L^{-1} PO_4^{3-}. While these nutrient concentrations are not typical of summer conditions in the field, such nutrient pulses can regularly occur in summer in this region and uce summer plankton blooms, e.g. through wind-induced convective events (Carstensen et al., 2004). In our mesocosm experiment this nutrient addition was necessary to induce a plankton bloom with the processes and dynamics we intended to study in a time frame of weeks.

Throughout the experiment, the water in the mesocosms was gently mixed by attached propellers. This way, settling of particulate organic matter onto the bottom of the mesocosms was minimized as far as possible and a homogenous water body was maintained, allowing discrete water samples to be representative of the whole mesocosm. Therefore, this mixing should not be confused with convective mixing in the real ocean, as the mesocosms in our experiment were intended to mimic a water parcel in the surface ocean that would not mix with water from the deeper ocean.

After the addition of nutrients on 17th June (t1) the development and decline of the plankton bloom were followed over 30 days with samples being taken three times a week from intermediate depth with a silicon tube.

Measurements

Temperature, salinity and pH were measured with a WTW conductivity / pH probe (calibrated with NBS buffer). Biomass estimates for community composition of phytoplankton are based on cell counts and cell volume conversion to carbon following (Menden-Deuer and Lessard, 2000). Samples for dissolved inorganic nitrate, nitrite, ammonium, phosphate and silicate were prefiltered through 0.2 µm cellulose acetate filters and measured with an autoanalyzer (AA II) (Hansen and Koroleff, 2007).

Dissolved inorganic carbon (DIC) was measured spectrophotometrically on an autoanalyzer (Stoll et al., 2001). Samples were sterile filtered (0.2 µm) and stored in borosilicate bottles, sealed with butyl / PTFE septa at temperatures below 10°C until analysis.

For the determination of particulate organic carbon and nitrogen (POC and PON), samples were filtered onto precombusted (5 hours at 450 °C) glassfibre filters (Whatman, GF/F, 0.7 µm nominal poresize), rinsed immediately after filtering of samples in order to avoid accumulation of DOM on the filters, and frozen (at -20 °C) until analysis. POC filters were fumed overnight with hydrochloric acid (37%) in order to remove particulate inorganic carbon (PIC) and dried at 60 °C for approximately 12 hours. Afterwards they were analyzed on a Eurovector EuroEA-3000 elemental analyzer (Sharp, 1974).

Samples for dissolved organic carbon and total dissolved nitrogen (DOC and TDN) were filtered through precombusted GF/F filters, with the filtrate being collected in acid-washed (HCl, 10%) and precombusted (12 hours at 250 °C) glass vials and frozen (at -20 °C) until analysis. Prior to measurements, the pH was adjusted to pH=2 with HCl (p.a.) and automatically purged with synthetic air in the DOC analyzer to remove inorganic carbon. The analysis was carried out by catalytic high-temperature combustion on a Shimadzu TOC-V analyzer with a total nitrogen module (TNM-1). The accuracy of the analysis was confirmed with deep-sea reference water samples provided by the University of Miami. The accuracy with respect to deep-sea water was within 5% relative error and detection limits were 5 µmol L^{-1} for DOC and 1 µmol L^{-1} for TDN. Procedural blanks did not yield detectable amounts of DOC and TDN. Dissolved organic nitrogen (DON) was calculated as

the difference between TDN and the sum of all dissolved inorganic nitrogen species (nitrate, nitrite, and ammonium).

Calculations

Calculation of additional carbonate system variables (such as pCO_2) from measured DIC and pH were carried out with the program CO2SYS (Lewis and Wallace, 1998), using the dissociation constants for carbonic acid as refitted by Dickson and Millero (1987). The pH values used for these calculations were measured on the NBS scale. The salinity of our seawater was ~13 and thus did not allow the use of certified reference buffers for calibration on the total scale. While we are aware that this might create electrode-specific uncertainties in measured pH, it would not change the observed dynamics of calculated pCO_2 over the course of the experiment, i.e. significantly lower minimum values at higher temperatures.

Air-water gas exchange of CO_2 between mesocosms and atmosphere was estimated following the stagnant boundary layer model of Smith (1985), with molecular diffusivity calculated as described in Jähne et al. (1987) and a chemical enhancement factor derived from pH as in Kuss and Schneider (2004). The main equation used for gas exchange, following Smith (1985), is given by

(1) $$F = \frac{k \times K_0 \times \Delta pCO_2 \times area_{meso}}{volume_{meso}}$$

In equation (1), F is the air-water flux of CO_2 and k is the gas transfer velocity. The latter is a function of temperature and the thickness of the boundary layer, which in turn is a function of windspeed (Jähne et al., 1987). Furthermore, K_0 is the solubility of CO_2 in water, with K_0 being a function of temperature and salinity, and ΔpCO_2 is the difference between partial pressure in water, calculated from measured pH and DIC and an assumed constant atmospheric value of 390 µatm.

However, this approach was originally developed for field conditions and not specifically for conditions such as those in our experimental setup, with constant mechanical mixing of the water column and a wind speed close to zero. Because of mixing-induced overturning of the water body, gas exchange is strongly underestimated when wind speed is set to zero in the calculations and mixing of the mesocosms is not accounted for. Without gas exchange, the amount of total carbon (DIC+POC+DOC) should not increase, as biological processes only lead to shifts between the different pools. Therefore, any change

in total carbon concentrations is attributable to gas exchange, assuming no loss of carbon, e.g. through sinking. The temporal development of total carbon (DIC+POC+DOC) in the mesocosms suggests a net carbon uptake of ~200, 310 and 420 µmol C L^{-1} at low, intermediate and high temperatures, respectively, over the course of the experiment (Fig. 4B).

Equation (1) shows that the only way to account for the turnover of the water column through mechanical mixing is the adjustment of wind speed, and thereby the thickness of the boundary layer and the gas transfer velocity. To account for the observed increase in total carbon, wind speed was set to a value of 6 m s^{-1} in our calculations, yielding the best fit to the observed net carbon uptake (on day t30) in the mesocosms at different temperatures. Of course, this number for wind speed seems quite high for an indoor experiment, without any actual wind in our culture rooms. Even though mechanical mixing of the mesocosms does not lead to "surface roughness" as due to wind, the net effect of both mechanical mixing and wind mixing is the same: It leads to a rapid turnover of the water body. Thereby, the boundary layer, which is exchanging gas with the atmosphere, is constantly renewed and rapid air-water gas exchange is facilitated even at virtually zero wind speed. Consequently, our estimates of air-sea CO_2 exchange are different from previous studies (Delille et al., 2005; Wohlers et al., 2009) that did not apply the modifications described above. Equation (1) also illustrates that the flux is dependent on the surface-to-volume relationship of the mesocosms. The diameter of ~140 cm is relatively high to the volume of 1,400 L (with ~100 cm depth), thereby further facilitating high rates of gas exchange.

In fact, the magnitude of gas exchange in our mesocosm setup has been tested in a follow-up experiment, where the gas exchange of an injected tracer (N_2O) was investigated in isolation, i.e. without the influence of biological processes (data not published yet). The results from that study support the high rates of gas exchange presented in this study and confirm that a parameterization of wind speed in the range of 4-8 m s^{-1} is necessary to account for the mechanical mixing of the mescosms and to explain the observed changes in the tracer.

Nutrient concentrations for day t0 are estimated from data of day t1, since sampling and measurements only started on day t1, immediately prior to nutrient addition. These measurements revealed already slight differences between temperature treatments, which were probably caused by different biological activities at different temperatures. Concentrations of NO_3^- on day t1 ranged from ~0.7 to 2.6 µmol L^{-1} between warm and

cold mesocosms. Since nutrient uptake was slowest in the colder mesocosms, we assumed the initial nutrient concentrations in all mesocosms on day t0 to correspond to the concentrations in the low temperature treatment as the best approximation possible. For day t1 the presented nutrient data was calculated as the sum of measured values and nutrient addition (16.0 µmol NO_3^- L^{-1}) for the respective mesocosms.

Statistical analysis

To test whether there are significant differences between the temperature treatments, a multivariate statistical analysis was carried out, as the different biogeochemical parameters are not independent from each other. Two-way ANOSIM (analysis of similarity) was applied on DIC, POC, DOC, NO_3, PON and DON data to test whether there were significant differences between the temperature treatments and to illustrate the effect of time. Since we investigated dynamics during a plankton bloom, the biogeochemical parameters, and thus the effects of temperature, are of course strongly changing over time. This was also confirmed by the results of the two-way ANOSIM. Consequently, we additionally performed a one-way ANOSIM using only data from the day of the peak of the phytoplankton bloom (t12). To reveal which parameters were responsible for most of the differences between temperature treatments, a SIMPER (similarity percentages) analysis was carried out on the same datasets used for ANOSIM.
Furthermore, the effects of temperature on maximum drawdown of DIC, maximum build-up of POC and DOC, and maximum ratios of POC:PON and DOC:DON were analyzed with a linear regression model. This approach was chosen since it provides valuable quantitative information for ecological and biogeochemical modeling. Coefficients of determination (R^2) and *p*-values of the applied regression models are given in the figure legends.

3. Results

Bloom development and community composition

At the beginning of the experiment, the phytoplankton community was composed of ~54% diatoms and ~46% cryptophytes in terms of biomass. After nutrient addition and with the onset of the bloom, diatoms became strongly dominant (>99% of biomass) in all mesocosms, in particular the species *Dactyliosolen fragilissimus*. Other functional groups

(e.g. dinoflagellates) remained at very low abundances throughout the bloom (<1%) and are thus likely negligible for the overall dynamics of the plankton bloom.

Copepod abundance remained approximately at initial levels of ~10 ind L^{-1} during the phytoplankton bloom in the first half of the experiment and was not affected by temperature (not shown). In the second half of the experiment, copepod numbers increased slightly and abundance of juveniles (copepodites) began to rise, indicating a stronger increase at lower temperatures (data not shown; manuscript in preparation).

The development of the phytoplankton bloom was characterized by a rapid decline in dissolved inorganic nutrients (Fig. 1), the drawdown of dissolved inorganic carbon and the build-up of particulate organic matter (Fig. 3). Temperature had a significant effect on all biogeochemical parameters over the course of the entire experiment (Table 1), most pronounced during the peak of the plankton bloom (Table 2). Most of the observed differences between the temperature treatments (almost 90%) could be explained by POC, DIC and DOC (Table 3).

Table 1: Results of a two-way crossed ANOSIM of the effects of temperature and time on biogeochemical parameters (DIC, POC, DOC, NO_3, PON and DON), including pairwise tests for differences between temperature treatments.

	R	**p**
Overall (temperature)	0.73	<0.01
Overall (time)	0.69	<0.01
18 °C vs. 14 °C	0.56	<0.01
18 °C vs. 10 °C	0.95	<0.01
14 °C vs. 10 °C	0.73	<0.01

Table 2: Results of a one-way ANOSIM of the effects of temperature on biogeochemical parameters (DIC, POC, DOC, NO_3, PON and DON) at the time of the peak of the plankton bloom (day t12), including pairwise tests for differences between temperature treatments.

For data from t12	**R**	**p**
Overall	0.84	<0.05
18 °C vs. 14 °C	0.78	<0.1
18 °C vs. 10 °C	1.00	<0.1
14 °C vs. 10 °C	0.74	<0.1

Data shown in Figures 1-3, 4A (upper panel), 4B and 5 are measured values. Data shown in figure 4A (lower panel), 4C and 4D are based on carbonate system calculations (see methods).

Nutrient consumption

Calculated initial concentrations (on day t0) of NO_3^- and PO_4^{3-} in the mesocosms were 2.6 and 0.2 µmol L^{-1}, respectively. Initial levels of silicate were 12.3 µmol L^{-1}. With the addition of 16.0 µmol NO_3^- L^{-1} and 1.0 µmol PO_4^{3-} L^{-1}, the total amount of available nutrients added up to 18.6 µmol L^{-1} NO_3^- and 1.2 µmol L^{-1} PO_4^{3-}. Following the addition of nitrate and phosphate on day t1, inorganic nutrients were consumed very rapidly and were depleted in all mesocosms a few days after nutrient addition (Fig. 1). While both NO_3^- and PO_4^{3-} were already exhausted on day t5, the consumption of silicate was slightly slower, with exhaustion on day t7. The depletion of silicate is in line with analysis of phytoplankton species composition, suggesting diatoms constituted a major fraction of phytoplankton biomass.

Nutrient concentrations on day t2 of the experiment were lower in the mesocosms at higher temperatures, thus indicating a faster consumption with increasing temperatures. After reaching exhaustion on day t5, concentrations of NO_3^- stayed below 1.0 µmol L^{-1} and those of PO_4^{3-} below 0.1 µmol L^{-1} for the rest of the experiment. Ammonium concentrations were almost constant and not affected by temperature, with concentrations in all mesocosms fluctuating between ~0.2 and 0.6 µmol L^{-1} throughout the experiment (not shown).

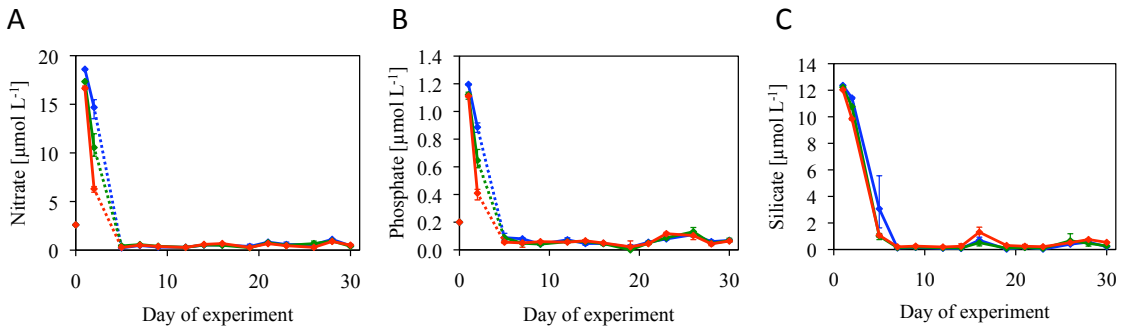

Fig. 1: Temporal development of (A) nitrate, (B) phosphate, and (C) silicate in the mesocosms at low (blue), intermediate (green) and high (red) temperature. Vertical lines denote range of replicates within each temperature treatment.

Table 3: Results of a SIMPER analysis for the contributions of different biogeochemical variables to the differences between temperature treatments. Shown are biogeochemical variables that contribute to 90% of dissimilarity, with average concentration (square root transformed), average dissimilarity, ratio of average dissimilarity and respective standard deviation, as well as percentages of contribution and cumulative contribution. Average dissimiliarity between temperature treatments: 18 °C & 14 °C = 5.30, 18 °C & 10 °C = 7.08, and 14 °C and 10 °C = 5.32.

	Avg. Conc. (transformed)	Avg. Conc. (transformed)	Avg. Diss.	Diss / SD	Contrib. %	Cum. %
	18 °C	**14 °C**				
POC	17.10	15.42	2.09	1.28	39.45	39.45
DIC	39.35	40.51	1.39	1.43	26.29	65.75
DOC	22.02	20.71	1.20	1.40	22.53	88.28
NO_3	0.82	0.90	0.27	0.61	5.04	93.32
	18 °C	**10 °C**				
POC	17.10	12.33	3.19	1.74	45.12	45.12
DIC	39.35	41.52	1.62	1.47	22.89	68.01
DOC	22.02	19.56	1.55	1.72	21.86	89.86
NO_3	0.82	3.57	0.32	1.63	4.55	94.41
	14 °C	**10 °C**				
POC	15.42	12.33	2.35	1.50	44.13	44.13
DIC	40.51	41.52	1.11	1.41	20.91	65.04
DOC	20.71	19.56	1.08	1.37	20.25	85.28
NO_3	0.90	3.57	0.33	0.58	6.28	91.56

Nitrogen

After addition of inorganic nutrients, particulate organic nitrogen (PON) built up in all mesocosms from initial concentrations of ~4.4 µmol N L^{-1} to maximum concentrations of ~20.2, 17.9 and 15.2 µmol N L^{-1} around day t5 at low, intermediate and high temperatures, respectively (Fig. 2A). Accordingly, maximum build-up of PON was lower at higher temperatures. After the peak of the bloom, PON decreased in all mesocosms until the end of the experiment. PON concentrations at the end of the experiment were higher at elevated temperatures, reaching concentrations of ~8.0, 9.9 and 12.2 µmol N L^{-1} at low, intermediate and high temperatures, respectively.

Concentrations of dissolved organic nitrogen (DON) increased constantly throughout the experiment, reaching final concentrations of ~18.7 µmol N L^{-1} averaged over all mesocosms. An effect of temperature on the accumulation of DON could not be observed (Fig. 2B).

The total amount of nitrogen (PON+DON+DIN) decreased in all mesocosms over the course of the experiment (Fig. 2C). Initial concentrations were ~25.4 µmol N L^{-1} and maximum concentrations occurred one day after nutrient addition (day t2) with ~40.5, 38.3 and 37.7 µmol N L^{-1} in the mesocosms at low, intermediate and high temperatures, respectively. During the bloom phase, total nitrogen decreased in all mesocosms (until t14 to t16). Afterwards, total nitrogen fluctuated strongly, reaching final concentrations (day t30) of ~27.2, 29.3 and 32.3 µmol N L^{-1} at low, intermediate and high temperatures, respectively. Thus, total nitrogen at the end of the experiment was higher at high temperatures, though this difference was pronounced only during the last few days of the experiment (Fig. 2C).

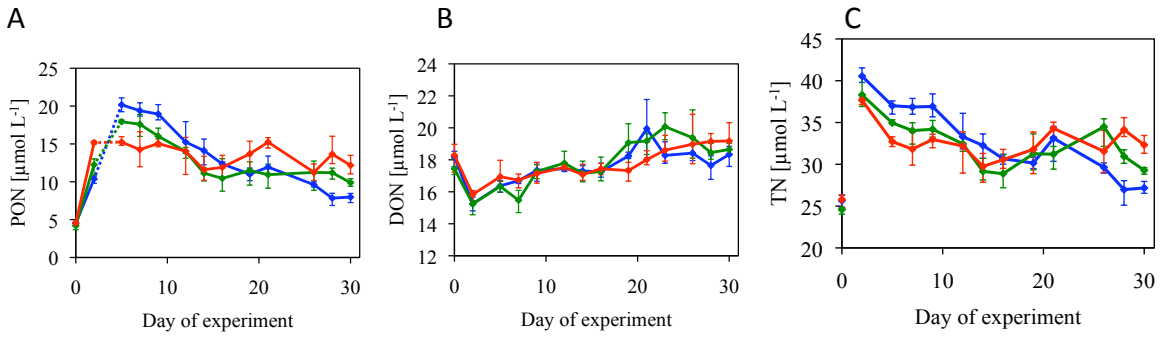

Fig. 2: Temporal development of (A) PON, (B) DON and (C) total nitrogen. Style and color-coding follow that of Fig. 1.

Carbon

DIC uptake

The consumption of inorganic nutrients was accompanied by photosynthetic uptake of dissolved inorganic carbon (DIC). Temporal dynamics of DIC concentrations showed a clear response to temperature, with average concentrations in the replicate mesocosms decreasing from initial levels of ~1860 µmol L^{-1} on day t0 to a minimum of ~1590, 1475 and 1310 µmol L^{-1} until day t12 at low, intermediate and high temperatures, respectively (Fig. 3A). This corresponds to a maximum DIC drawdown of ~280 µmol C L^{-1} on average at

low, 390 µmol C L^{-1} at intermediate, and 550 µmol C L^{-1} at high temperatures (Fig. 3D). Accordingly, the magnitude of biologically mediated drawdown of DIC was significantly enhanced at higher temperatures. After the peak of the bloom, i.e. from day t12 onwards, concentrations of DIC in the mesocosms increased again for the rest of the experiment, reaching approximately initial concentrations on day t30.

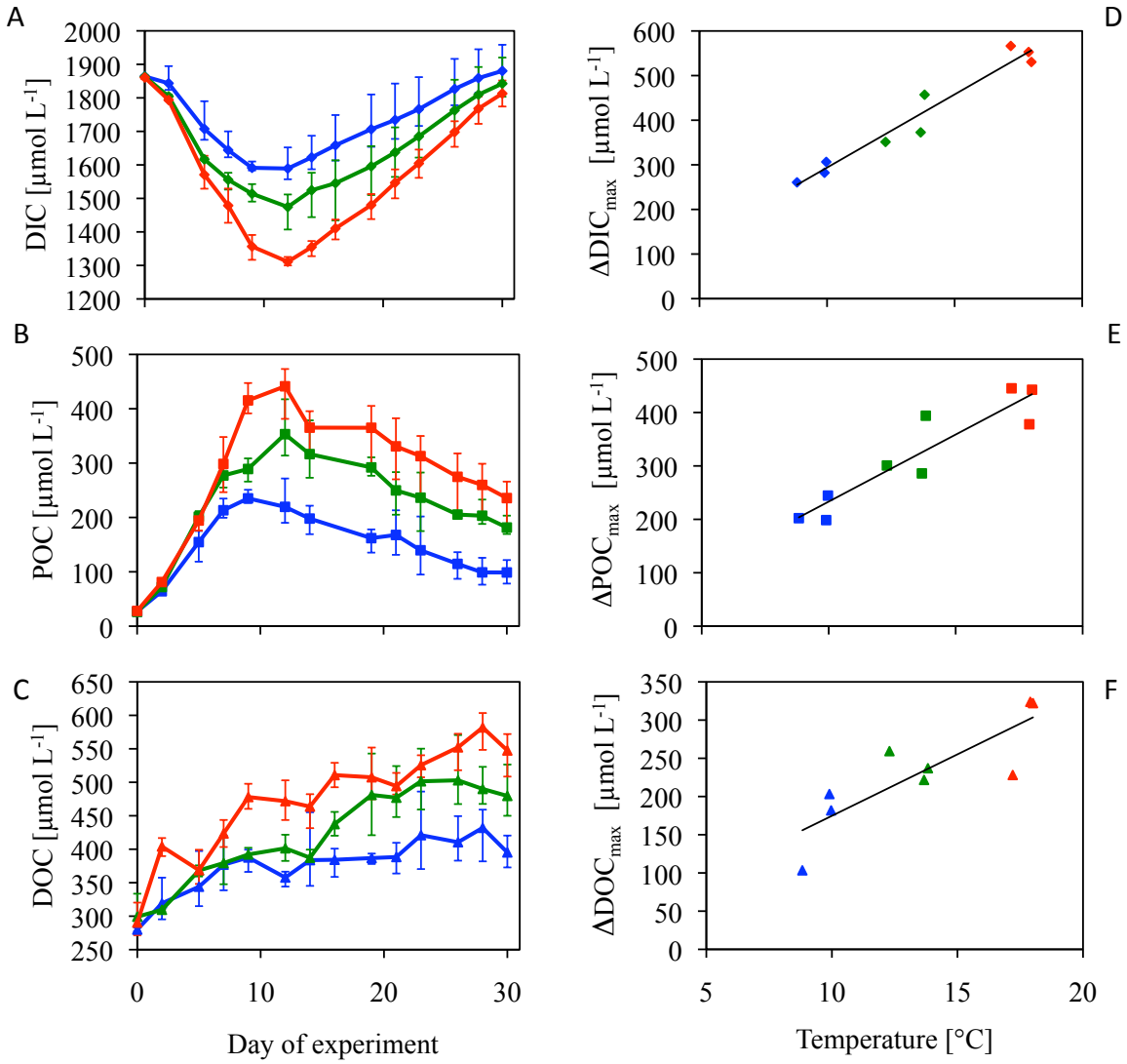

Fig. 3: Temporal development of measured concentrations of (A) DIC, (B) POC and (C) DOC. Style and color-coding follow that of Figure 1. (D) Maximum drawdown in DIC, (E) maximum build-up of POC and (F) DOC as a function of temperature. Color-coding as in Fig. 1. Solid lines denote linear regressions (n=9; ΔDIC_{max}: R^2=0.95, p<0.0001; POC_{max}: R^2=0.85, p<0.0005; ΔDOC_{max}: R^2=0.71, p<0.005).

When correcting for air-water gas exchange (see methods), the maximum uptake of DIC reached ~380 µmol C L^{-1} on average at low, 520 µmol C L^{-1} at intermediate, and 700 µmol C L^{-1} at high temperatures (Fig. 4A), corresponding to an increase in maximum DIC consumption of ~40 µmol C L^{-1} °C^{-1}. Accordingly, the rate of net DIC consumption during the bloom phase increased with higher temperatures, accelerating from an average of ~32 µmol C L^{-1} d^{-1} in the cool mesocosms, to 44 µmol C L^{-1} d^{-1} at intermediate, and 56 µmol C L^{-1} d^{-1} at high temperatures. This corresponds to a Q_{10} value of ~2.0 for net DIC uptake.

POC build-up

The drawdown of DIC was reflected in a concomitant build-up of particulate organic carbon (POC), which peaked between days t9 and t12 in the different mesocosms (Fig. 3B). Starting from initial levels of ~25-30 µmol C L^{-1}, POC concentrations rapidly increased and reached maximum build-ups of POC of ~210 µmol C L^{-1} at low, 325 µmol C L^{-1} at intermediate, and 410 µmol C L^{-1} at high temperatures. This corresponds to a linear increase of maximum POC build-up with temperature of 26 µmol C L^{-1} °C^{-1}. Thus, similar to DIC uptake, the magnitude of POC build-up was significantly elevated at higher temperatures (Fig. 3E). Accordingly, the rate of POC build-up during the bloom phase showed a clear response to higher temperatures, amounting to ~22, 27 and 39 µmol C L^{-1} d^{-1} at low, intermediate and high temperatures, respectively. This corresponds to a Q_{10} value of ~2.0 for net POC build-up.

After the peak of the bloom, POC concentrations in the water column decreased again. However, in contrast to DIC concentrations, POC did not reach initial levels but remained at concentrations much higher than at the beginning of the experiment.

DOC accumulation

Along with the decrease in DIC and build-up of POC, a substantial increase in dissolved organic carbon (DOC) was observed over the course of the experiment in all mesocosms (Fig. 3C). Starting from initial concentrations of ~290 µmol C L^{-1}, DOC concentrations increased steadily over the course of the experiment, with maximum accumulation of DOC amounting to ~160 µmol C L^{-1} at low, 240 µmol C L^{-1} at intermediate, and 290 µmol C L^{-1} at high temperatures. Thus, maximum build-up of DOC was significantly higher at elevated temperatures (Fig. 3F). This corresponds to a linear increase of maximum DOC accumulation of 16 µmol C L^{-1} °C^{-1}. The rate of net DOC accumulation showed a positive relationship with temperature as well, increasing from an average of 3.8 µmol C L^{-1} d^{-1} at

low, to 6.0 µmol C L^{-1} d^{-1} at intermediate, and 8.6 µmol C L^{-1} d^{-1} at high temperatures. This increase corresponds to a Q_{10} value of ~2.7 for the net build-up of DOC.

Carbon budget

After the peak of the bloom, the amount of total organic carbon (TOC), i.e. the sum of particulate and dissolved organic carbon decreased relatively slowly and remained at levels much higher than initial concentrations until the end of the experiment (Fig. 4A). The decrease in POC was closely balanced by the increase in DOC, resulting in almost constant levels of TOC in the mesocosms at all temperatures. However, TOC concentrations after the bloom remained elevated at higher temperatures until the end of the experiment, amounting to ~490, 660 and 780 µmol C L^{-1} at low, intermediate and high temperature, respectively, on t30.

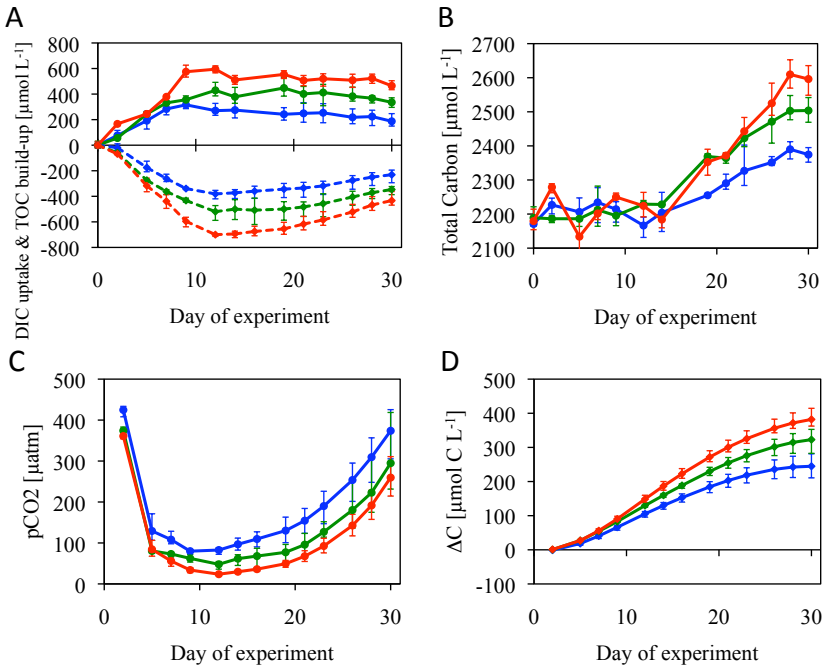

Fig. 4: Temporal development of (A) corrected (air-water gas exchange) DIC uptake (dashed) and measured TOC build-up (solid), (B) measured total carbon concentrations, (C) calculated pCO_2 (water) in the mesocosms and (D) calculated cumulative air-water carbon flux into the mesososms. Style and color-coding follow that of Fig. 1.

In contrast to TOC, an increase of DIC concentrations began in all mesocosms with the decline of the bloom, with DIC approaching initial levels again at the end of the experiment (Fig. 3A). The phytoplankton bloom and the associated uptake of DIC were accompanied by a sharp decrease in the partial pressure of carbon dioxide (pCO_2) in the

water. Early levels of calculated pCO_2 (day t2) were between ~360 and 430 µatm in all mesocosms, and thus near equilibrium with the atmosphere. Through biological uptake of DIC during the phytoplankton bloom, pCO_2 dropped to minimum values of ~78 µatm at low, 45 µatm at intermediate, and 24 µatm at high temperatures in the relatively weakly buffered low-salinity Baltic Sea water (Fig. 4C). This gradient between pCO_2 in water and air led to a flux of CO_2 from the atmosphere into the water in all mesocosms. This CO_2 flux was stronger in the mesocosms at higher temperatures, where more inorganic carbon had been taken up and converted to organic carbon and consequently higher air-water pCO_2 gradients were reached (Fig. 4C,D). This fact is also reflected in the total amount of carbon (i.e. the sum of organic and inorganic carbon) in the mesocosms at the end of the experiment. Concentrations of total carbon on day t30 were clearly elevated at higher temperatures amounting to ~2380, 2500 and 2600 µmol C L^{-1} at low, intermediate and high temperatures, respectively (Fig. 4B). Furthermore, there is a positive effect of temperature on gas transfer velocity, enabling higher rates of gas exchange at higher temperatures (~25% higher at 17.5 °C than at 9.5°C).

Our estimates of cumulative DIC increase due to air-water gas exchange suggest a clear effect of temperature, ranging from ~240 µmol C L^{-1} at low, to ~320 µmol C L^{-1} at intermediate, and ~380 µmol C L^{-1} at high temperatures over the course of the whole experiment (Fig. 4D).

Stoichiometry

Drawdown of carbon and nitrogen

While the same amount of NO_3^- was consumed in the mesocosms at all temperatures (~18.3 µmol L^{-1}), the decrease in DIC concentrations and the calculated uptake of DIC (corrected for gas exchange) showed a significant increase with temperature (see 3.3.1). Accordingly, the ratio of maximum DIC uptake to the maximum consumption of NO_3^- increased from ~20.8 at low, over 29.0 at intermediate, to 38.5 at high temperatures. This trend of increasing consumption of carbon over nitrogen at higher temperatures is reflected in the elemental ratios of particulate and dissolved organic matter (POM and DOM). Differential build-up and removal of particulate and dissolved organic matter led to temporal variations in the respective elemental ratios.

C:N of POM

The molar ratio of carbon to nitrogen (C:N) of particulate organic matter was ~6.1 in all mesocosms at the beginning of the experiment, and thereby close to the Redfield value of 6.6. From day t4 on, POC:PON started to increase in all mesocosms, and showed a positive correlation with temperature (Fig. 5A). The maximum ratio of POC:PON was significantly enhanced at higher temperatures and reached 15.9 at low, 29.0 at intermediate, and 33.7 at high temperatures (Fig. 5B; $p<0.0005$). After the decline of the bloom, POC:PON began to decrease again, however not back to initial values.

C:N of DOM

The elemental ratios of dissolved organic matter already deviated significantly from Redfield stoichiometry at the beginning of the experiment, with an average molar DOC:DON ratio of 16.1 over all mesocosms. C:N ratios of DOM were steadily increasing before, during and after the phytoplankton bloom over the entire course of the experiment, showing clear differences between temperature treatments (Fig. 5C). The maximum ratio of DOC:DON was significantly affected by temperature and reached 25.6 at low, 28.1 at intermediate, and 30.8 at high temperatures (Fig. 5D; $p<0.005$).

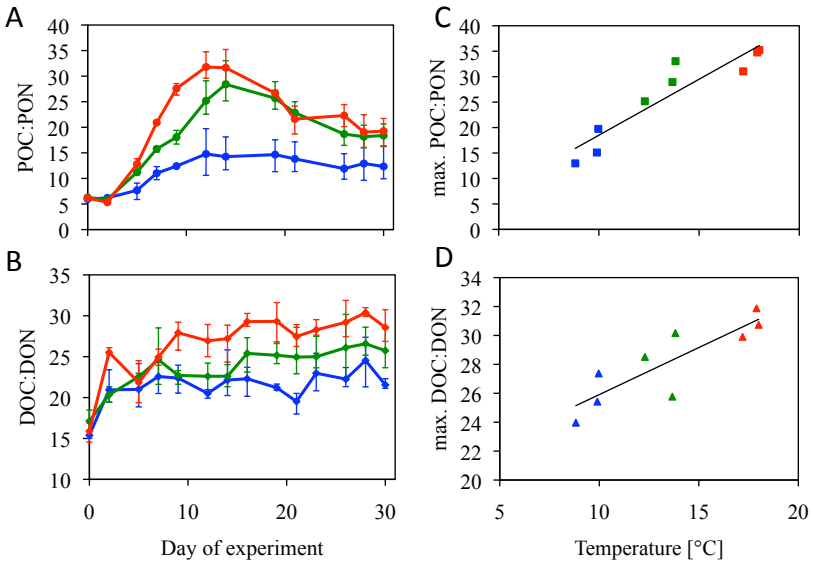

Fig. 5: Temporal development of C:N in (A) particulate and (B) dissolved organic matter. Maximum C:N of (C) particulate and (D) dissolved organic matter as a function of temperature. Style and color-coding follow that of Fig. 3. Solid lines denote linear regressions (n=9; $POC:PON_{max}$: $R^2=0.86$, $p<0.0005$; $DOC:DON_{max}$: $R^2=0.73$, $p<0.005$).

4. Discussion

Budgets of nitrogen and carbon

Loss of organic matter

The temporal development of total nitrogen (PON+DON+DIN) suggests a loss of organic matter over the course of the experiment. Total nitrogen decreased in all mesocosms by ~8.4 µmol N L^{-1}, most pronounced during the first half of the experiment until day t14 (Fig. 2C). In mesocosm experiments, organic matter can potentially get lost through wall growth or sinking of organic matter to the bottom of the mesocosms. However, it is difficult to quantify the proportional effect of these mechanisms for the observed loss in our experiment. Based on repeated inspections, no visible growth of algae could be found on the mesocosm walls. Furthermore, using a similar experimental setup, Sommer et al. (2007) concluded that it takes 7-8 weeks until the development of wall growth plays a significant role. On the other hand, the sedimentation of particles to the bottom of the mesocosms cannot be ruled out. Previous studies have shown, that sinking of organic matter can lead to a considerable loss of biomass from the surface layer in mesocosm experiments (Keller et al., 1999; Wohlers et al., 2009). Since high concentrations of POC and PON were reached very rapidly in our experiment, it is possible that some of this newly produced biomass sunk to the bottom of the mesocosms. Although mixing of the water column by the propeller should minimize particle settling, this can obviously never be excluded entirely, and it can be assumed that the loss of organic matter would have been much higher without any mixing of the water in the mesocosms. Possibly the formation of fast sinking aggregates played an important role in this regard. This mechanism could also explain why the loss of organic matter differed among the different temperature treatments. Higher build-up of DOM and extracellular gel-particles (TEP) at higher temperatures might have facilitated particle aggregation (Burd and Jackson, 2009; Passow, 2002), thereby leading to a larger sinking loss of organic matter in the warmer mesocosms. While we did not measure TEP in our experiment, POC and POC:PON data suggest that TEP might have contributed substantially to the observed POC dynamics. Furthermore, other loss terms that could be potentially responsible for a loss of nitrogen can be excluded. It is very unlikely that denitrification occurred in the well-mixed (and thus well-oxygenated) mesocosms, and the data does not suggest a significant contribution of degassing of regenerated ammonium. Therefore, sinking of particles is likely to be the dominant mechanism for the observed loss of organic matter.

Air-water gas exchange

Without external sources or sinks, the amount of total carbon (DIC+POC+DOC) in the mesocosms would be constant, as biological processes do not influence the overall mass balance of carbon but only shift matter between the different pools. If at all, one would expect a loss of total carbon in such an experiment, e.g. through wall growth or sinking of organic matter to the bottom of the mesocosms. However, we observed a strong increase of total carbon in the mesocosms, with clearly elevated concentrations at higher temperatures at the end of the experiment (Fig. 4B). Accordingly, this increase in total carbon could only be attributable to an external input of carbon into the mesocosms, which was only possible through continuous and rapid air-water gas exchange of CO_2 in our experiment. Due to the rapid decrease in pCO_2 associated with DIC uptake (Fig. 4C), a considerable air-water flux of CO_2 started with the onset of the bloom and prevailed for the rest of the experiment (see Fig. 4A). High rates of gas exchange were facilitated through continuous mixing of the water column by propellers attached to the mesocosms. Thereby, the boundary layer that exchanges gas with the atmosphere was constantly renewed and rapid air-water gas exchange was facilitated. Since more DIC was consumed and converted to organic matter during the bloom phase at higher temperatures, the air-water difference in pCO_2 and the magnitude of gas exchange were also enhanced at higher temperatures. The positive effect of temperature on gas transfer velocity additionally facilitated gas exchange at higher temperatures. Consequently, temperature affected carbon uptake by the water column in two ways: directly, by enhancing the gas transfer velocity, and indirectly, by enhancing biological carbon drawdown and the associated effect on pCO_2.

It is very likely that the observed loss of nitrogen was accompanied by a corresponding loss of carbon in the first half of the experiment. If the C:N of the missing fraction of total N is comparable to the C:N of organic matter that was identified, another substantial amount of carbon is also missing in the total carbon (DIC+POC+DOC). The delay between rapidly decreasing seawater pCO_2 levels and the increase in total carbon in the mesocosms supports this assumption, since an increase in total carbon should have been immediately visible with the onset of air-water gas exchange (Fig. 4B,D). Consequently, this loss of carbon is not taken into account for the estimate of gas exchange, which is based only on the observable increase in total carbon. Therefore, actual gas exchange could have been even higher but was compensated by the loss of carbon in the first half of the experiment (approximately until day t14). The calculated uptake of DIC through gas

exchange (until t14), which did not translate into an observed increase in total carbon concentration, and by inference an estimate for the loss of organic carbon, amounts to ~100, 120 and 180 µmol C L^{-1} at low, intermediate and high temperatures, respectively (Fig. 4B,D). However, an even higher input of carbon through gas exchange would be necessary to account for the observed loss of nitrogen (~8.4 µmol N L^{-1}), assuming C:N ratios of measured POM of up to >30. Since our estimate of gas exchange neglects this potential loss of carbon due to settling of particles and / or TEP in the initial phase of the experiment, it can, in this respect, be regarded as a conservative estimate for air-sea carbon flux.

Even though gas exchange had a substantial effect on measured concentrations of DIC, and a certain amount of organic matter may have been lost during the experiment, our results do not indicate a relevant influence of these processes on our main conclusions, i.e. the temperature sensitivity of carbon overconsumption and the build-up of POC and DOC.

Carbon overconsumption and temperature

Dynamics of DIC and particulate organic matter

Our results suggest a positive effect of temperature not only on the relative consumption of DIC over nutrients, but also on the build-up and elemental ratios of POM for the plankton community in our experiment. Especially after nutrient depletion, strong differences in POC dynamics occurred between the different temperature treatments (Fig. 3B), revealing a clear effect of temperature on the POC:PON ratio (Fig. 5A,C). It has to be noted that the observed temporal dynamics in POC:PON might be partly attributable to different concentrations of PON that were affected by possibly differential loss of organic matter. However, the major differences in POC:PON occurred between t12 and t14, when the differences in PON among the temperature treatments had become very small again and differences in POC were the main driver for differences in POC:PON.

The main mechanism responsible for the higher uptake of DIC and build-up of organic carbon at higher temperatures in our experiment was the higher relative consumption of carbon over nitrogen and its associated conversion to biomass. Excess uptake of DIC over inorganic nitrogen, a phenomenon called carbon overconsumption (Toggweiler, 1993), has been observed in previous experiments and field studies. Some earlier studies which found enhanced drawdown of carbon over nitrogen did not find changes in POC:PON as in

our experiment (Banse, 1994; Riebesell et al., 2007). Instead, a common assumption was that the excess carbon is exuded by phytoplankton mainly in the form of DOC (Kähler and Koeve, 2001). However, in agreement with our study, an increasing number of studies have reported a decoupling of carbon and nitrogen dynamics in phytoplankton blooms and an associated increase of the POC:PON ratio (Biddanda and Benner, 1997; Engel et al., 2002; Wetz and Wheeler, 2003). Generally, elemental stoichiometry of phytoplankton and POM can vary widely, depending on nutrient status and environmental conditions (Finkel et al., 2010; Geider and La Roche, 2002). An increasing cellular quota of carbon to nitrogen in phytoplankton has been found for different species under nutrient limitation (Goldman, 1992; Harrison et al., 1977), and there is also evidence for an influence of temperature on intracellular C:N ratios, at least for some species (Berges et al., 2002; Thompson et al., 1992). Hence, this mechanism might have contributed to the high C:N ratios of POM in our experiment.

Since an increase in POC:PON is usually observed after nutrient exhaustion, carbon overconsumption is commonly assumed to be associated with nutrient stress (Biddanda and Benner, 1997; Wetz and Wheeler, 2003). This is in line with the observations in our experiment: While PON reached its highest levels at the same time as nutrients were exhausted (day t5), minimum levels of DIC and maximum concentrations of POC occurred much later (between day t9 and t11). Furthermore, the major differences in drawdown of DIC and build-up of POC and DOC among the different temperature treatments occurred after nutrient depletion (Fig. 5). These observations further support the major role of excess carbon fixation for biogeochemical dynamics and its response to increasing temperatures in our experiment.

Engel et al. (2002) also observed an increase in POC:PON, which they concluded to be attributable to excess carbon fixation. However, they found a significant portion of excess carbon fixation to be channeled into the pool of transparent extracellular particles (TEP). Since we observed a massive build-up of POC and an associated strong increase in POC:PON, it is likely that at least part of these dynamics are attributable to the accumulation of carbon-rich (and nitrogen-poor) extracellular organic matter. This consideration is also supported by the strong build-up of dissolved organic matter in our experiment, as previous studies have shown that a considerable fraction of excess POC can be associated with TEP that form from dissolved polysaccharides (Engel et al., 2004a). The transformation of DOC into extracellular POC via aggregation of TEP has been shown before in experimental studies (Mopper et al., 1995), and the underlying mechanisms

have already been investigated and discussed (Passow, 2002). Furthermore, it is unlikely that the increase in POC:PON is entirely attributable to changes in the elemental composition of phytoplankton. Intracellular C:N ratios of diatoms are usually <10 (Goldman, 1992; Thompson et al., 1992) and do not exceed a value of 15 even under nutrient starvation (Harrison et al., 1977). Thus, we believe that the accumulation of carbon-enriched extracellular particles is the most likely explanation for the strong decoupling of POC and PON in our experiment.

An effect of temperature on the magnitude of POC production and POC:PON resulting from carbon overconsumption as observed in our experiment has, to the best of our knowledge, not been reported so far. Nor did previous mesocosm experiments (Wohlers et al., 2009) find an effect of temperature on POC:PON. It is also notable, that POC:PON reached very high absolute values in comparison to previous studies (between 16 and 34 at temperatures ranging from 9.5 to 17.5 °C). This suggests relatively high levels of carbon overconsumption, which increase with temperature.

Furthermore, results from single-species culture experiments suggest that TEP production is highly variable between phytoplankton species and that it is a function of temperature (Claquin et al., 2008). Accordingly, species-specific differences in TEP production could also contribute to the observed differences in carbon dynamics between our and earlier mesocosm experiments.

Differences in POC and the POC:PON ratio did not occur when nutrients were still replete. Thus, our results are in line with previous studies that did not observe an effect of temperature on C:N ratios in exponentially growing cultures, i.e. under nutrient-replete conditions (Feng et al., 2009; Hare et al., 2007; Hutchins et al., 2007). Since carbon overconsumption is usually closely tied to nutrient-limited growth, and our results suggest that the main effects of temperature in our experiment were related to this process, it can be hypothesized that the implications of our results are mainly important in advanced or declining plankton blooms.

These conclusions are not affected by our estimates of gas exchange. Since the amount of inorganic nitrogen was similar in all mesocosms, the temperature-related difference in inorganic carbon drawdown (from raw DIC data, Fig. 3A) alone supports the hypothesized temperature effect on carbon overconsumption. This is further supported by the presented data on POC and DOC, as well as the C:N ratios of particulate and dissolved organic matter. Air-water gas exchange only enhances the magnitude of DIC uptake in the mesocosms.

Dynamics of dissolved organic matter

Another remarkable observation in our experiment was the substantial build-up of DOC and its clear relationship with temperature. While the dynamics of DON did not show any response to temperature (Fig. 2B), the accumulation of DOC was clearly enhanced at higher temperatures (Fig. 3C,F), with the maximum build-up of DOC being enhanced by +47% and +79% at intermediate and high temperatures, respectively, compared to low temperatures.

Net accumulation of DOC usually occurs when biological production and loss processes are temporarily decoupled, which often happens in phytoplankton blooms (Carlson, 2002). A large portion of up to 50% of primary production can be channeled into the DOC pool (Hansell et al., 2009). The release of DOC by phytoplankton is generally assumed to increase with the onset of nutrient limitation (Biddanda and Benner, 1997). However, only few studies on the influence of temperature on DOC production exist and the results from single-species experiments are controversial. While Verity et al. (1981) could not observe an effect of temperature on dissolved primary production after acclimatization, Zlotnik and Dubinsky (1989) found clearly higher DOC excretion with increasing temperatures. However, they used different phytoplankton species in their studies. More recent findings from short-term warming experiments with natural plankton communities support the latter study, suggesting an increase of dissolved primary production at elevated temperatures (Moran et al., 2006). This is in line with the observed effect of temperature on net DOC accumulation in our experiment and other recent mesocosm studies (Engel et al., 2011; Kim et al., 2011; Wohlers et al., 2009). Thus, our results strongly support the assumption that phytoplankton exudation of DOM is temperature sensitive.

The ratio of DOC:DON also increased with temperature in our experiment, suggesting enhanced exudation of DOC over DON by phytoplankton at higher temperatures (Fig. 5D). Since a temperature effect on autotrophic production is also mirrored in the response of POC and POC:PON to higher temperatures, enhanced release of carbon-enriched DOM by phytoplankton due to carbon overconsumption is the most likely explanation for the observed dynamics of DOC accumulation and the DOC:DON ratio.

The net accumulation of DOC throughout the experiment (Fig. 3C) and the relative constancy of TOC after the peak of the bloom (Fig. 4B) did not indicate any substantial decrease of organic matter through microbial consumption. Unfortunately, bacterial production was not measured in our experiment, making it impossible to give statements about gross rates. Thus, there is a possibility that microbial consumption of organic matter

occurred, and that it was approximately balanced by production. On the other hand, inhibition of microbial degradation of DOC might also explain our finding. This has been observed before, e.g. due to high resistance of fresh DOC to microbial decomposition (Fry et al., 1996) or nutrient limitation by bacteria leading to inefficient bacterial decomposition (Thingstad et al., 1997). Further factors such as the molecular weight and chemical composition of DOM play a crucial role in its availability for bacterial degradation, although there are still huge gaps in our understanding of these aspects (Dittmar and Paeng, 2009).

Why is the response to temperature changes so different from previous experiments?

Temperature is a key factor in controlling ecological processes through its effect on metabolic rates (Brown et al., 2004). Our study revealed a strong effect of temperature on the dynamics of particulate organic matter, which was not observed in previous experiments. Most comparable studies investigating effects of temperature on marine ecosystems report negative impacts of increasing temperatures, e.g. on production of biomass derived from cell counts (Lassen et al., 2010; Muren et al., 2005; O'Connor et al., 2009) as well as on the build-up of measured POC (Kim et al., 2011; Wohlers et al., 2009). In contrast, both the magnitude and the rate of POC build-up were considerably elevated at higher temperatures in our experiment. Maximum build-up of POC increased by +52% and +96% at intermediate and high, compared to low temperatures, respectively. The calculated Q_{10} value of ~2.0 for the rate of POC build-up in our experiment lies at the upper end of estimates for the temperature dependence of autotrophic processes such as phytoplankton growth and photosynthesis ($1 < Q_{10} < 2$), which are also limited by light and nutrients (Eppley, 1972). The net build-up of DOC, which likely originates from exudation by phytoplankton, revealed an even higher effect of temperature (Q_{10} ~2.7). This tendency of enhanced DOC accumulation at elevated temperatures (Fig. 3F) is in line with results from previous mesocosm studies (Kim et al., 2011; Wohlers et al., 2009). Our results suggest that these high Q_{10} values are mainly attributable to the temperature sensitivity of carbon overconsumption by phytoplankton and could hence be interpreted as net Q_{10} factors for processes related to excess carbon fixation.

The previously reported shift from autotrophy to heterotrophy in response to warming (Muren et al., 2005; O'Connor et al., 2009; Wohlers et al., 2009) and an associated decrease in overall biomass could not be observed in our experiment. Wohlers et al.

(2009) found a lower consumption of DIC at elevated temperatures (decrease of up to -31% when increasing temperature by 2-6 °C), which they attributed mainly to a stronger effect of warming on respiratory consumption relative to autotrophic production. Such an effect could not be observed in our experiment, where the drawdown of DIC was strongly enhanced at higher temperatures (+39% and +94%, Fig. 3A,B). Possibly, the temperature effect on carbon overconsumption and DOC exudation prevented a substantial imbalance between production and consumption of organic matter in our experiment. Altogether, our results revealed a fundamentally different response of carbon cycling to sea surface warming compared to earlier studies. Consequently, the question is why our results are so different to those of previous studies.

One possible explanation for the different temperature sensitivity of biogeochemical dynamics might be the taxonomic composition of the phytoplankton assemblage prior to the bloom and especially the dominant species. At the beginning of our experiment (day t0) it consisted of ~53% diatoms and 47% cryptophytes in terms of biomass. After nutrient addition diatoms dominated the phytoplankton bloom (>99%), which is in line with previous mesocosm experiments (Kim et al., 2011; Wohlers et al., 2009). However, the prevailing diatom species was different to that in these previous studies. While *Skeletonema costatum* dominated in the two earlier experiments, *Dactyliosolen fragilissimus* was the dominant species in our experiment, constituting 80-99% of phytoplankton biomass. It has been shown in a number of studies that different diatom species can have different cellular composition and produce different amounts of extracellular carbohydrates. (Goldman, 1992; Myklestad, 1974; Wetz and Wheeler, 2003, 2007). Furthermore, differences in the response to changing temperatures among diatom species have been observed. While reports on possible temperature effects on the cellular composition of diatoms are contradictory (Montagnes and Franklin, 2001), the release of DOC (Zlotnik and Dubinsky, 1989) and production of TEP (Claquin et al., 2008) seem to increase with temperature.

Although no study on the physiology of *Dactyliosolen fragilissimus* and the mechanisms related to carbon overconsumption exists to the best of our knowledge, we hypothesize that physiological properties of this dominant phytoplankton species (e.g. carbon fixation, exudation of DOM and TEP, intracellular C:N) could be decisive for the response of the whole ecosystem, and may thus explain the different response to temperature changes compared to previous experiments. This is supported by the fact that the bloom was strongly dominated by this single species, and other mechanisms such as grazing dynamics

appear to be of minor importance in our experiment and do not seem to deviate substantially from earlier studies.

The abundance of the copepod *Acartia clausi* was rather low and very similar at all temperatures during the bloom phase (~10 individuals L^{-1}) when the major differences in carbon and nitrogen cycling occurred. Even though copepod numbers slightly increased and the abundance of juveniles (copepodites) began to rise during the second half of the experiment (manuscript in preparation), copepod grazing cannot explain the large differences in element cycling between our temperature treatments. Assuming typical values for grazing rates (0.1-0.5 µmol C ind^{-1} d^{-1}) and body mass (3-5 µg C ind^{-1}) of *Acartia clausi* (Fileman et al., 2010), we estimate that copepod grazing effects are too small to substantially affect biogeochemical dynamics, e.g. the loss of organic matter or temperature-related differences in POC and DOC concentrations.

The overall higher temperatures in our experiment might also have contributed to the differences to previous experiments. Higher temperatures and associated higher levels of metabolic rates might have revealed temperature effects on processes such as carbon overconsumption that could not be found in previous experiments at lower temperatures, where these processes might have been inhibited or temperature-driven differences were too small to be detected. Furthermore, the present study had higher light levels compared to previous experiments, as it was intended to mimic the summer conditions in the field at the time of the experiment. This may have additionally favored excess carbon fixation of phytoplankton, since exudation of DOC has been observed to increase with irradiance (Verity, 1981; Zlotnik and Dubinsky, 1989). Possibly, these different boundary conditions also contributed to the response of biogeochemical element cycling to temperature in our experiment.

5. Conclusion

The balance between build-up and decline of organic matter in the surface ocean plays a major role in marine biogeochemical cycling, as it strongly affects the uptake and sequestration of carbon and other elements to the deep ocean. The present study revealed large uncertainties in our knowledge of temperature sensitivities of key processes in marine carbon cycling.

Our results show that increasing temperatures can have previously unconsidered effects on the build-up of organic matter and uptake of carbon dioxide by marine ecosystems.

The response of some processes was contrary to previous experiments, suggesting that temperature effects on biogeochemical cycling are potentially dependent on the composition of the phytoplankton assemblage. Especially processes such as carbon overconsumption and exudation of DOM seem to be highly temperature sensitive and might play an important role in the ecosystem response to temperature changes, i.e. under future sea surface warming or in past cooler times, such as glacial periods. This could not only alter the balance between production and consumption of organic matter, but also the partitioning between particulate and dissolved organic matter and their respective elemental composition and carbon uptake under changing temperatures.

Thus, our findings also imply further challenges for ecosystem modeling and climate change projections. Only little attention has been paid to the effects of increasing temperatures on biological processes in global warming simulations. Current representations of temperature sensitivity differ greatly among marine ecosystem models. Consequently, it is currently not possible to forecast how the effect of future sea surface warming on marine carbon cycling might look like on a global scale (Taucher and Oschlies, 2011). Furthermore, our study clearly shows that increasing sea surface temperatures might have substantial impacts on marine ecosystems and that we do not even know the direction in which some key physiological and ecosystem processes will respond under future warming. We therefore conclude that temperature effects on these processes require further research, both in experimental and modeling studies, in order to improve our understanding of possible impacts of sea surface warming on marine biogeochemical cycling.

Acknowledgements:

This study was supported by Deutsche Forschungsgemeinschaft (DFG). Furthermore, we thank Aljoša Zavišić for assistance with POC and PON measurements, Jana Meyer for assistance with DIC measurements, Matthias Friebe for technical assistance with DOC and TDN analysis, Bente Gardeler for measurements of inorganic nutrients and Jamileh Javidpour for organizing and coordinating the mesocosm experiment. We also thank David Hutchins and two anonymous reviewers for their constructive comments.

Chapter 3: Effects of warming and elevated pCO_2 on carbon overconsumption and partitioning of the marine diatoms *Thalassiosira weissflogii* and *Dactyliosolen fragilissimus*

J. Taucher[1], J. Jones[2], A. James[2], M. Brzezinski[2], C. A. Carlson[2], A. Oschlies[1], U. Riebesell[1], U. Passow[2]

[1]GEOMAR Helmholtz Centre for Ocean Research, Kiel, Germany
[2]University of California Santa Barbara, Santa Barbara, United States of America

Correspondence to: J. Taucher (jtaucher@geomar.de)

To be submitted to *Limnology and Oceanography*

Abstract

Little is known about the effects of future increases in temperature and pCO_2 on carbon uptake and partitioning of marine diatoms, one of the most important phytoplankton functional groups and a major player in global biogeochemical cycling. In particular, the sensitivities of processes under nutrient limitation, such as carbon overconsumption, to environmental factors have only received little attention so far, even though it has been shown that a substantial fraction of carbon uptake can occur after nutrient depletion. We carried out batch culture experiments with the two globally important diatom species, *Thalassiosira weissflogii* and *Dactyliosolen fragilissimus*, under four conditions: ambient control (15 °C, 400 µatm), high CO_2 (15 °C, 1000 µatm), high temperature (20 °C, 400 µatm), and combined (20 °C, 1000 µatm). We followed biogeochemical dynamics over the entire course of the diatom blooms from exponential growth until 6 days after nitrogen depletion.

Both temperature and pCO_2 had pronounced effects on uptake of dissolved inorganic carbon (DIC), build-up of particulate (POM) and dissolved organic matter (DOM), as well as their elemental composition, and the accumulation of transparent exopolymer particles (TEP). These effects were most prominent during senescence after nitrogen depletion, where a substantial fraction of carbon uptake (up to 70%) and organic matter production occurred. Elevated temperatures increased carbon uptake and build-up of organic matter and TEP by *T. weissflogii*, but had the opposite effect on *D. fragilissimus*. At the same time, elevated pCO_2 enhanced DIC uptake by up to 8% for *T. weissflogii* and by up to 39% for *D. fragilissimus*. Furthermore, the build-up of organic matter, its carbon-to-nitrogen ratio, and TEP formation by *D. fragilissimus* were all substantially elevated under high pCO_2.

Our results suggest that, contrary to common assumptions, diatoms could be highly sensitive to changes in oceanic carbonate chemistry. Additionally, the temperature sensitivity of the two diatom species differed notably, suggesting that the response to future warming will strongly depend on the temperature range and physiological optima of the affected species.

1. Introduction

Over the past centuries, atmospheric carbon dioxide (CO_2) concentrations increased from preindustrial levels of approximately 280 ppmv (parts per million volume) to around 400 ppmv in the year 2013 (IPCC, 2007a). Current atmospheric CO_2 concentrations are higher than during at least the past 800,000 years and almost one third of this anthropogenic carbon input to the global carbon cycle has been taken up by the ocean (Lüthi et al., 2008; Sabine et al., 2004). This increase in atmospheric CO_2 leads to a global increase in temperatures and its subsequent uptake results in a decrease in ocean pH, both occurring at a pace unprecedented in recent geological history (Doney et al., 2009a; IPCC, 2007a). The reduction in seawater pH, a phenomenon commonly referred to as ocean acidification (Caldeira and Wickett, 2003), is accompanied by changes in carbonate chemistry, leading to a strong decrease of the carbonate ion (CO_3^{2-}) concentration, a slight increase in bicarbonate (HCO_3^-), and a strong increase in dissolved CO_2 and protons (H^+) (Zeebe and Wolf-Gladrow, 2001). At the same time, global average sea surface temperatures have already increased by 0.6 °C since the beginning of the 20th century. Recent climate projections suggest an increase in global surface air temperatures of 1.1 to 6.4 °C by the end of this century (relative to 1980–1999), thereby also leading to a further warming of the upper ocean (IPCC, 2007a). Both warming and ocean acidification are expected to affect marine ecosystems and carbon cycling in a variety of ways (for reviews see e.g. Riebesell et al. (2009), Passow and Carlson (2012)).

Temperature is a major environmental driver controlling metabolic rates, such as enzymatic reactions, thereby substantially affecting phytoplankton (Boyd et al., 2013; Duarte, 2007). Furthermore, it has been found that ocean warming might lead to a decrease in cell size (Moran et al., 2010), shifts in phenology (Sommer and Lengfellner, 2008), and alterations in carbon cycling by phytoplankton (Taucher et al., 2012; Wohlers et al., 2009). At the same time, ocean acidification is expected to influence marine phytoplankton either through a decrease in pH (and the corresponding increase in H^+ ions) or the shift in carbonate speciation, e.g. the relative availability of CO_2 and HCO_3^- for carbon assimilation and photosynthesis. Over the last few years an increasing number of studies investigated effects of ocean acidification on various functional groups of phytoplankton, showing e.g. a marked influence of carbonate chemistry on growth and calcification in coccolithophores (Bach et al., 2011; Iglesias-Rodriguez et al., 2008) and nitrogen fixation in cyanobacteria (Hutchins et al., 2007). Furthermore, it has been demonstrated that simultaneous changes in temperature and CO_2 can have interactive

effects on growth rates, photosynthesis and elemental composition of various marine phytoplankton (Feng et al., 2008; Fu et al., 2007; Fu et al., 2008).

Relatively few studies exist on ocean acidification effects on diatoms, which account for 40% of total primary production in the ocean (Nelson et al., 1995), frequently form massive blooms, and are commonly assumed to dominate export production (Buesseler, 1998; Lampitt, 1985; Treguer et al., 1995), making them major players in marine biogeochemical cycling and sequestration of carbon to the deep ocean (Boyd et al., 2010; Sarthou et al., 2005). Diatoms, like most other non-calcifying phytoplankton, have been shown to be primarily affected by ocean acidification through changes in dissolved CO_2 and a shift in $CO_2 : HCO_3^-$ ratio, as different species take up CO_2 and HCO_3^- in varying proportions (Rost et al., 2003; Tortell et al., 1997; Trimborn et al., 2008). Most studies showed little or no change in photosynthetic rates and elemental composition of diatoms under elevated pCO_2, suggesting that carbon assimilation is essentially saturated under present-day CO_2 levels and thus unlikely to be affected by ocean acidification (Beardall et al., 2009; Burkhardt et al., 1999; Rost et al., 2008; Tortell and Morel, 2002). This is in contrast to the observed effect of elevated CO_2 on inorganic carbon uptake by diatoms in natural plankton communities (Riebesell et al., 2007; Tortell et al., 2008).

This controversy might result from the fact that laboratory-based studies usually do not take into account bloom dynamics and the post-bloom physiological states of diatoms. However, exponential growth under nutrient-replete conditions and constant carbonate chemistry is not necessarily reflective of behavior during a natural bloom, where substantial shifts in the carbonate system occur with pH increasing by up to one unit and associated drops in pCO_2 and dissolved CO_2 (Brussaard et al., 1996; Wohlers et al., 2009). Furthermore, it has long been recognized that a substantial portion of carbon uptake can occur after nutrient depletion. This leads to a notable decoupling of carbon and nitrogen uptake, a phenomenon commonly referred to as “carbon overconsumption” (Sambrotto et al., 1993; Toggweiler, 1993). Previous work has shown that dynamics during the declining phase of a bloom are particularly important for export production (Lampitt, 1985). Furthermore, results from previous mesocosm experiments with natural, diatom-dominated plankton communities suggested that carbon overconsumption is affected by both temperature (Taucher et al., 2012) and CO_2 (Riebesell et al., 2007). However, carbon uptake and its allocation between the particulate and dissolved phase by primary producers on the one side, and heterotrophic consumption of this organic matter on the other side, operate simultaneously and are closely intertwined under natural or semi-

natural conditions in such studies, making it difficult to disentangle the underlying mechanisms.

Here we specifically investigate the effects of warming and increased pCO_2 on carbon uptake and partitioning between the particulate and dissolved phase by two marine diatom species, *Thalassiosira weissflogii* and *Dactyliosolen fragilissimus,* with particular focus on dynamics after N-depletion. While the strain of *T. weissflogii* used in the presented experiments was obtained from a culture collection, *D. fragilissimus* had been isolated shortly before this study, to investigate whether species in nature behave similarly to those that have been cultured for numerous years and thousands of generations. Furthermore, the production of organic matter by the diatom cultures was explicitly separated from its consumption by heterotrophs for an improved mechanistic understanding of processes related to diatom physiology and transferability to ecosystem models.

2. Methods:

Experimental setup

Phytoplankton strains

All experiments were conducted with monoclonal cell cultures of two diatom species, using the single-celled and rather small species *Thalassiosira weissflogii* (10-20 µm cell diameter, strain CCMP 1336), and the larger, chain-forming species *Dactyliosolen fragilissimus* (50-100 µm cell diameter, isolated from the North Sea in September 2012).

Treatments: combination of temperature and CO_2

Eight gas-tight polyethylene bags with a volume of 20 L were set up in duplicate in a combination of two temperatures and two pCO_2 levels, with temperatures of 15 and 20 °C, initial partial pressure levels of CO_2 of 400 and 1000 µatm. In the following, these treatments will be referred to as: "ambient" (15 °C and 400 µatm), "high CO_2" (15 °C and 1000 µatm), "warming" (20 °C and 400 µatm), and "combined" (20°C and 1000 µatm), respectively. Light supply was set to a photon flux density of ~100 µEinst. m^{-2} s^{-1} and a light/dark cycle of 14/10 hours in all treatments.

Following the main experiments, an additional experiment (in the following called temperature gradient experiment) was conducted to investigate the temperature range and optimum of the two diatom species. Here, both species were grown in gas-tight

polycarbonate bottles (1 L) at ambient pCO_2 (400 µatm) over a broad temperature gradient with a total of six temperatures (10.0, 12.5, 15.0, 17.5, 20.0, and 22.5 °C) that were established with the help of temperature controlled water baths in the two climate-controlled rooms. Other environmental conditions, e.g. light supply and nutrient availability were identical to those of the main experiment.

Materials, seawater and nutrients

The bags for the large volume experiments were sterilized and dissolved organic carbon (DOC) leaching minimized by soaking in 10% HCl for at least 48 hours. Over the course of the experiments, the bags were placed in plastic tubs and submerged in distilled water to minimize temperature fluctuation and possible gas exchange through the bag walls. Preceding experiments showed no significant change in DIC or DOC over a period of 10 days in bags containing only sterile artificial seawater.

The experiment with *T. Weissflogii* was conducted with artificial seawater (ASW), following Kester et al., (1967). Since, *D. fragilissimus* did not grow well in ASW, experiments with this species were carried out in natural seawater (NSW) from the Santa Barbara Channel, which was collected in late April 2013 and subsequently filtered through 1.2 µm and 0.2 µm. Autoclaving was avoided to keep the carbonate system of the media in tact. Both culture media (ASW and NSW) were instead treated with a UV lamp (50 Watt) for 30 minutes to minimize DOC and bacterial contamination. Preceding experiments showed that such a UV-treatment minimizes bacterial production for at least a week.

ASW and FSW were enriched with inorganic nutrients in a modified version of f/2 medium (Guillard and Ryther, 1962), with concentrations calculated in such a way that the diatom cultures become nitrate limited. Initial additions of NO_3^- amounted to 15 µmol L^{-1} in both experiments, PO_4^{3-} was 6 and 8 µmol L^{-1}, and $Si(OH)_4$ was 16 and 50 µmol L^{-1} in the experiments with *T. Weissflogii* and *D. fragilissimus*, respectively. Trace metals and vitamins were according to f/8 medium. The higher concentrations of PO_4^{3-} and $Si(OH)_4$ in the experiment with *D. fragilissimus* were based on preceding experiments, which suggested a possibly higher Si and P demand compared to *T. weissflogii*. Furthermore, the artificial seawater was further enriched with 2 ml L^{-1} of filtered (0.2 µm) and UV-blasted natural seawater to provide possible micronutrients that are not included in the recipe of Guillard and Ryther (1962).

Carbonate chemistry manipulation

Carbonate chemistry in our experiments was manipulated following the "closed system approach", i.e. through addition of inorganic carbon, acid and base to an incubation container without headspace (Rost et al., 2008). For the experiments with ASW, the carbonate system was adjusted to target levels of pCO_2 and TA of 2350 µmol kg^{-1} through combined additions of 1 M solutions of HCO_3^- and NaOH.

The carbonate system in the experiments with NSW had to be adjusted differently. The collected water had a pH of 7.76 and TA of ~2290 µmol kg^{-1}. From that, we calculated the necessary amount of HCO_3^- addition to set the desired pCO_2 levels of 400 and 1000 µatm for the respective temperatures (15 and 20 °C).

In order to mimic the carbonate system dynamics of a natural plankton bloom, pCO_2 was adjusted only initially, and was then allowed to change freely, as driven by biological dynamics. Measurements confirmed that the desired initial experimental conditions were within ~0.02 pH units (or ~20 µatm pCO_2) of target conditions.

Acclimatization phase

Prior to the experiments, the diatom cultures had been acclimatized to the respective target conditions of temperature and pCO_2 for at least a week (~5-6 generations). During this acclimatization phase, the cultures were grown semi-continuously in gas-tight polycarbonate bottles (1 L) at low cell numbers (< 40,000 L^{-1}). When pCO_2 dropped below 200 µatm (for the 400 µatm treatment) or 700 µatm (for the 1000 µatm treatment), the cultures were diluted with fresh medium and pCO_2 was readjusted to target conditions. After acclimatization, diatom cultures were inoculated at a density of 500 (*T. weissflogii*) and 200 cells ml^{-1} (*D. fragilissimus*) to the respective experimental treatments.

Sampling and measurements

Sampling was carried out daily, immediately after the end of each light cycle. This maximized the comparability of samples between treatments and replicates, as all the cultures were sampled in the same state. The bags were mixed gently prior to sampling to obtain representative water samples of the enclosed water body. Samples for pH and DOC were taken directly from the bag (gravity-filtration through in-line GF/F filter). For all other parameters, subsamples were collected in 1 L polycarbonate bottles. Since a major focus

of our culture experiments was to determine carbon overconsumption and post-bloom dynamics, we continued sampling for (at least) 6 days after NO_3 depletion.

pH was measured spectrophotometrically (Thermo Scientific Genesys 105 VIS Spectrophotometer with a SPG 1A air-cooled single cell Peltier element) following Dickson et al. (2007), using *m*-cresol as an indicator dye. For maximum precision and accuracy the dye was calibrated against certified reference material (A. Dickson, La Jolla, California).

Dissolved inorganic carbon (DIC) was measured on a non-dispersive infrared (NDIR) analyzer following Bandstra et al. (2006). Samples were filtered through GF/F,filters and stored in ~400 ml borosilicate bottles, sealed gas-tight and stored at ~5 °C until analysis.

Samples for particulate organic carbon and nitrogen (POC and PON) were filtered onto precombusted (5 hours at 450 °C) GF/F filters, rinsed with artificial seawater immediately after filtering of samples in order to avoid accumulation of DOM on the filters, dried at ~60 °C for approximately 24 hours and stored under vacuum in a desiccator until analysis. Afterwards they were analyzed on a CHN organic elemental analyzer (model CEC 440HA, Control Equipment Corp., now Exeter Analytical).

Samples for dissolved organic carbon (DOC) were gravity-filtered through precombusted GF/F filters, with the filtrate collected in acid-washed (HCl, 10%) and precombusted (12 hours at 450 °C) glass vials and frozen (at -20 °C) until analysis. DOC was quantified via high-temperature combustion on a Shimadzu TOC-V as in Carlson et al., (2010), but with glucose calibration standards and Santa Barbara Channel reference standards that were routinely verified against DOM consensus reference water (Hansell, 2005), for a resolution of 1.5 µmol L^{-1}. Total dissolved nitrogen (TDN) was measured using the TOC-V (Farmer and Hansell, 2007). Dissolved organic nitrogen (DON) was calculated by subtracting dissolved inorganic nitrogen (measured as below) from TDN.

Samples for transparent exopolymer particles (TEP) were filtered onto 0.4 µm polycarbonate filters and subsequently stained with Alcian Blue following the procedure of Passow and Alldredge (1995). TEP concentration was measured colorimetrically on a spectrophotometer (Thermo Scientific Genesys 105 VIS Spetrophotometer) through absorption at 787 nm. The dye solution had previously been calibrated using Gum Xanthan and the concentration of TEP is expressed as µg Gum Xanthan equivalents per liter (µg GXeq L^{-1}).

Samples for dissolved inorganic nitrate, nitrite, phosphate and silicate were sterile-filtered through 0.2 µm surfactant-free cellulose acetate filters, collected in 20 ml HDPE vials, and

stored at -20 °C until analysis. Measurement was carried out on a flow injection analyzer (QuikChem 8000, Lachat Instruments, Zellweger Analytics).

Bacterial production (BP) was determined by the ^{3}H-leucine incorporation (^{3}H-leu, SA= 54.1 Ci mmo1^{-1}, Perkin Elmer, Boston, MA) method (Kirchman et al., 1986), using the microcentrifuge method (Smith and Azam, 1992), modified by decanting supernatant rather than aspirating. Samples were taken on the first day, shortly after N-depletion, and six days after N-depletion, dark-incubated for 1.5 to 3 h. Radioactivity was analyzed on a Beckman Coulter LS6500 scintillation counter. All incubations were carried out in triplicate. To convert the incorporation of ^{3}H-leucine into carbon production (µg C L^{-1} h^{-1}), a theoretical conversion factor of 1.5 kg C mol^{-1} leucine (Simon and Azam, 1989) was used.

In vivo dark-adapted chlorophyll fluorescence (F_T) was measured using an AquaPen-C fluorometer (Photon Systems Instruments, Czech Republic).

In the temperature gradient experiment, daily measurements were restricted to pH, NO_3^-, and in vivo fluorescence due to the small volume of the incubation bottles. Furthermore, samples for particulate and dissolved organic matter were taken on the first day of the experiment (t_0), the day the respective cultures reached NO_3 depletion (t_{N0}), and four days after NO_3 depletion (t_{N4}). Uptake of DIC was calculated from total alkalinity (TA) and pH.

Calculations

Calculation of additional carbonate system variables (such as dissolved CO_2) from measured DIC and pH were carried out with the program CO2SYS (Lewis and Wallace, 1998), using the dissociation constants for carbonic acid as refitted by Dickson and Millero (1987).

Statistical analysis

In the presented experiments, we applied a fully crossed two-factorial design with temperature and pCO_2 as the fixed factors and two treatment levels, respectively. Statistical analysis was applied to calculated maximum values of cumulative net uptake of DIC and net build-up of POM and DOM, relative to day 0 for each replicate. TEP was highly variable in the period after nitrogen depletion in the experiment with *D. fragilissimus*. Therefore, the average concentration after nitrogen depletion was used for detection of treatment effects.

Statistical analysis was carried out with a permutational analysis of variance (PERMANOVA), since assumptions of normality and homogeneity of variances were not met for all analyzed data (Anderson, 2001). PERMANOVA was applied using "Euclidean distance" matrices with 9999 permutations, and running pairwise (*post-hoc*) tests in case a significant effect (p-value < 0.05) was detected.

For data from the temperature gradient experiment, a polynomial regression was applied to growth rate (calculated from measured fluorescence), and rate of DIC uptake and build-up of TOC (POC+DOC). The latter two were calculated as the cumulative change from day 0 to day 4 after N-depletion and divided by the respective number of days.

3. Results

The development of the diatom bloom in both experiments was characterized by a rapid decline in dissolved inorganic nutrients, drawdown of dissolved inorganic carbon (DIC), decrease in dissolved CO_2, and build-up of particulate (POM) and dissolved (DOM) organic matter (Figure 1-3).

Nutrient uptake

Initial concentrations of NO_3^- amounted to 15 µmol L^{-1} in both experiments. In the experiment with *T. weissflogii*, NO_3^- was depleted faster at higher temperatures, reaching concentrations close to zero at t3 (20 °C) and t5 (15 °C) in both pCO_2 treatments (Figure 1-3). In the experiment with *D. fragilissimus*, NO_3 depletion occurred on t3 in all temperature and pCO_2 treatments (Figure 1-3). PO_4^{3-} dropped from initial concentrations of 6 and 9 µmol L^{-1} in the experiments with *T. weissflogii* and *D. fragilissimus*, respectively, but remained > 2 µmol L^{-1} and thus well above depletion. While Si remained replete in the *D. fragilissimus* experiment (~40 µmol $Si(OH)_4$ L^{-1}), it reached very low concentrations (< 2 µmol $Si(OH)_4$ L^{-1}) in the *T. Weissflogii* experiment on t4 and t7 at at 20 °C and 15 °C in both pCO_2 treatments, respectively. No effect of pCO_2 on the speed and magnitude of nutrient uptake could be detected in either of the experiments.

DIC uptake and build-up of POC, DOC and TEP

DIC uptake showed a significant response to temperature and pCO_2 in both experiments (Figure 1, Table 1,2). Maximum uptake of DIC by *T. weissflogii* amounted to 333.2±3.2

(ambient), 360.2±0.8 (high CO_2), 448.1±9.0 (warming) and 462.7±9.6 (combined) µmol C L^{-1}. In the *D. fragilissimus* experiment, maximum drawdown of DIC reached 420.7±8.4 (ambient), 516.9±10.7 (high CO_2), 271.6±11.6 (warming) and 358.4±9.1 (combined) µmol C L^{-1}. Elevated pCO_2 enhanced biologically mediated drawdown of DIC by both species, even though the magnitude of the effect was much larger for *D. fragilissimus* than for *T. weissflogii*. The temperature increase from 15 to 20 °C significantly enhanced DIC uptake by *T. weissflogii*. This response was more complex in the experiment with *D. fragilissimus*, where elevated temperatures led to a significant increase ($p<0.05$) decrease in DIC drawdown under nutrient-replete conditions, but had a negative effect once nitrogen was depleted (Figure 1B).

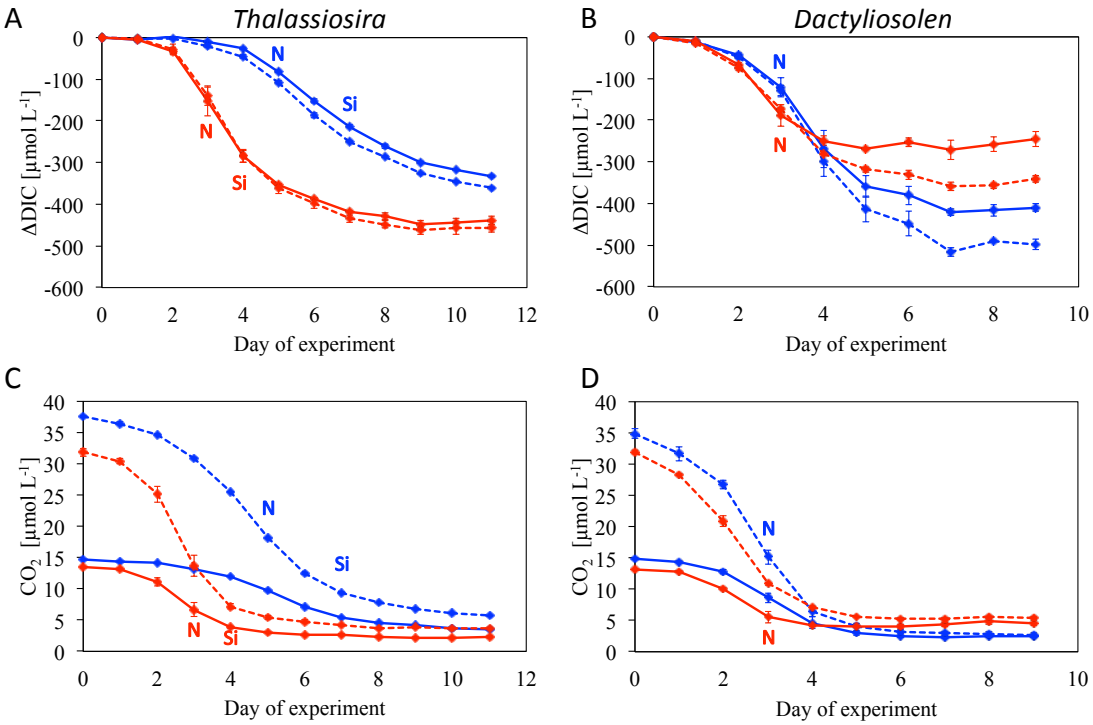

Figure 1: Temporal development of carbonate system variables in the experiment with *T. weissflogii* (left) and *D. fragilissimus* (right). Shown are (A,B) DIC uptake relative to initial values [µmol L^{-1}] and (B,C) concentrations of dissolved CO_2 [µmol L^{-1}] at 15 °C (blue) and 20 °C (red), and in the ambient CO_2 (solid) and high CO_2 treatments (dashed). Vertical error bars denote range of replicates within each treatment. Colored letters denote day when cultures reached depletion of inorganic nitrogen (N) and silica (Si) in the 15 °C (blue) and 20 °C (red) treatments.

The drawdown of DIC was reflected in a concomitant build-up of POC (Figure 2). In the *T. weissflogii* experiment, maximum POC build-up amounted to 288.7±8.3 (ambient), 314.7±13.0 (high CO_2), 412.0±14.0 (warming) and 418.1±3.5 (combined) µmol C L^{-1}. POC

build-up was enhanced at higher temperatures, whereas higher initial pCO_2 levels had no statistically significant effect (Figure 2A, Table 1). Build-up of POC by *D. fragilissimus* reached maximum values of 298.3±19.5 (ambient), 402.5±2.1 (high CO_2), 248.7±10.9 (warming) and 346.0±4.3 (combined) µmol C L^{-1}. Thus, both temperature and pCO_2 had a significant effect on maximum POC build-up, resulting in a decrease with higher temperatures, but an increase at elevated pCO_2 (Figure 2B, Table 2). Similar to DIC uptake, temperature had a significant positive effect on POC build-up before N-depletion ($p<0.05$), but a negative effect afterwards.

At the same time, accumulation of DOC was observed over the course of both experiments (Figure 2). In the *T. weissflogii* experiment, maximum DOC build-up amounted to 11.6±2.4 (ambient), 14.5±1.4 (high CO_2), 19.3±1.0 (warming) and 18.7±0.7 (combined) µmol C L^{-1}. Maximum accumulation of DOC was much greater in the *D. fragilissmus* experiment, reaching 123.9±6.2 (ambient), 136.4±24.6 (high CO_2), 70.0±8.3 (warming) and 63.2±0.3 (combined) µmol C L^{-1}. Consequently, elevated temperatures had a significant effect on DOC production by both species, resulting in an increase by *T. weissflogii*, but a decrease by *D. fragilissimus*. On the other hand, CO_2 did not have a statistically significant effect on DOC build-up in either of the experiments (Figure 2C,D, Table 1,2).

A notable accumulation of transparent exopolymer particles (TEP) accompanied the diatom blooms in both experiments (Figure 2). In the *T. weissflogii* experiment, average TEP accumulation in the period after N-depletion amounted to ~2,900±80 (ambient), 3,330±180 (high CO_2), 4,130±50 (warming) and 4,520±50 (combined) µg GXeq L^{-1}. Thus, increases in temperature and CO_2 both significantly enhanced TEP accumulation (Figure 2E, Table 1). The production of TEP by *D. fragilissimus* was generally much higher than that of *T. weissflogii*, reaching average concentrations of ~11,800±1,520 (ambient) 15,660±1,060 (high CO_2), 7,940±510 (warming) and 10,760±1,380 (combined) µg GXeq L^{-1} in the period after N-depletion. Thus, TEP accumulation averaged over the post-bloom phase was significantly decreased at higher temperatures, but elevated in the high CO_2 treatments (Figure 2F, Table 2).

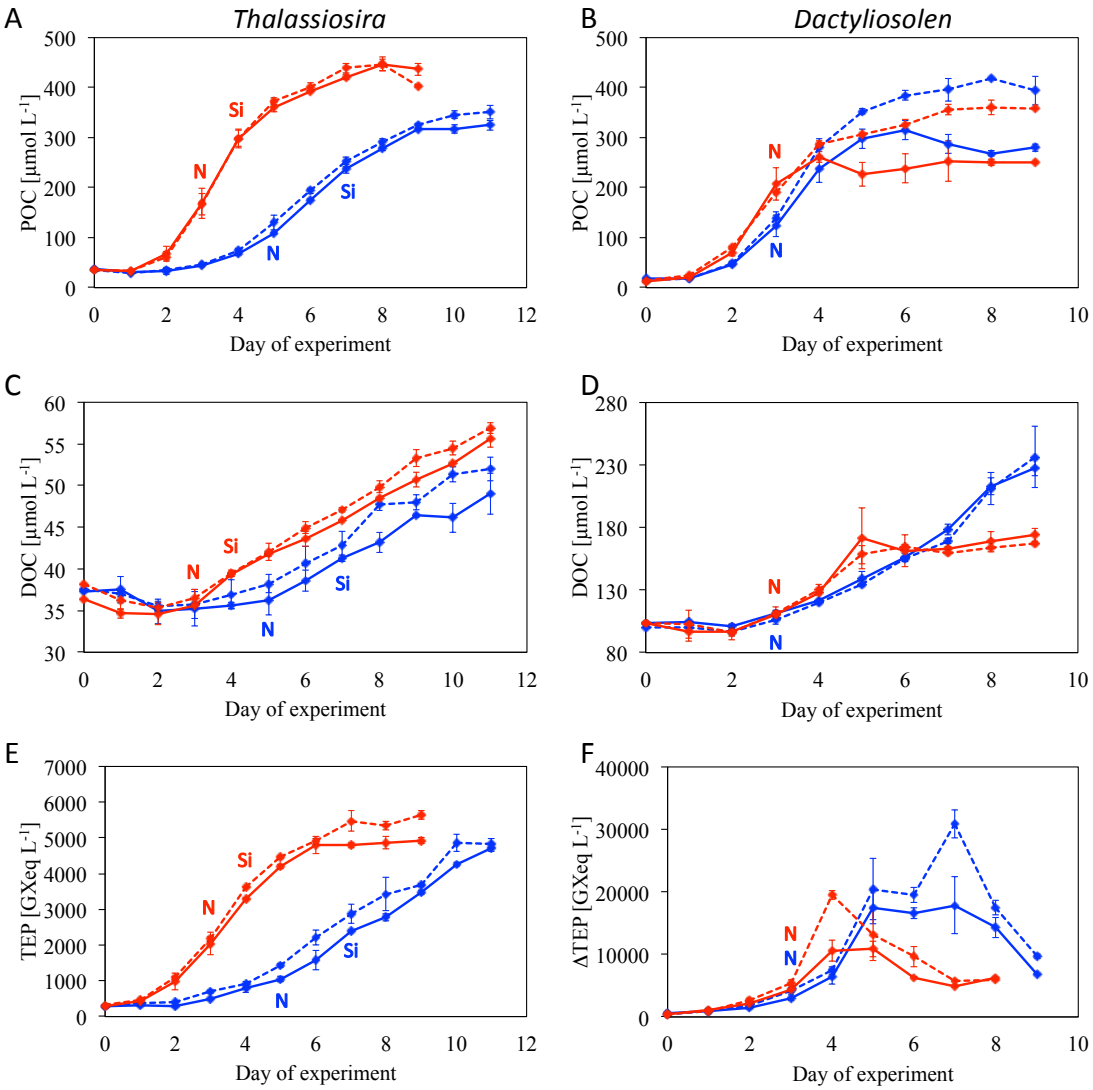

Figure 2: Temporal development of measured (A,B) POC and (C,D) DOC concentrations [µmol L^{-1}], and (E,F) TEP concentrations [µg GXeq L^{-1}] in the experiment with *T. weissflogii* (left) and *D. fragilissimus* (right). Style and color-coding as in figure 1.

Build-up of organic nitrogen

Particulate organic nitrogen (PON) increased by ~15.0±0.3 µmol N L^{-1} in both experiments. Dissolved organic nitrogen (DON) remained almost constant throughout the experiments, averaging around ~6.0±0.1 µmol N L^{-1} in the *T. weissflogii* experiment, and ~12.0±0.2 µmol N L^{-1} in the *D. fragilissimus* experiment. Neither temperature nor pCO_2 had an effect on PON or DON in any of the experiments. Furthermore, the total amount of nitrogen (i.e. the sum of inorganic N, PON, and DON) remained constant over the course of both experiments, indicating that no loss of material due to wall growth or denitrification, and no insufficient sampling occurred.

Stoichiometry

While the same amount of NO_3^- was consumed in all treatments and in both experiments, the uptake of DIC differed significantly across treatments and between experiments. In the *T. weissflogii* experiment, the uptake ratio of DIC over NO_3^- was elevated in the treatments with higher temperature and pCO_2. In contrast, the consumption of carbon relative to nitrogen by *D. fragilissimus* decreased at higher temperatures, but was enhanced in the high CO_2 treatments (Table 1,2).

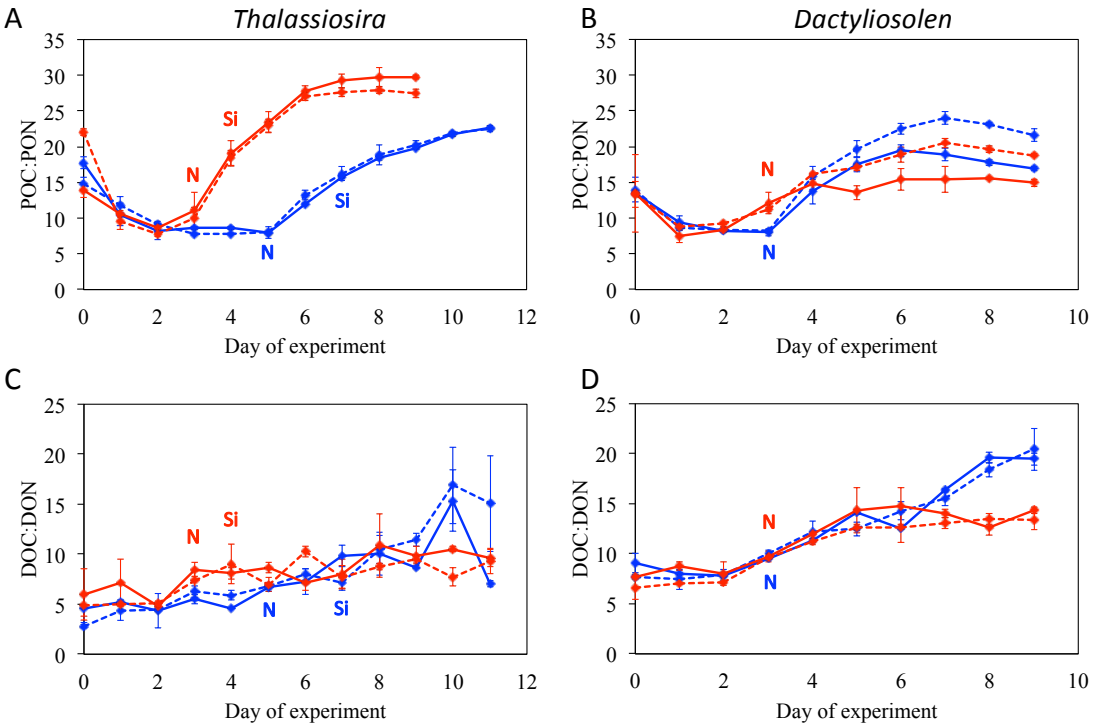

Figure 3: Temporal development of C:N in (A,B) particulate and (C,D) dissolved organic matter in the experiment with *T. weissflogii* (left) and *D. fragilissimus* (right). Style and color-coding as in figure 1.

This elevated consumption of carbon over nitrogen is also reflected in the elemental ratios of POM and DOM (Figure 3). The molar ratio of carbon to nitrogen (C:N) of POM under N-replete conditions remained between 8.0 and 9.0 in both experiments, and was thus only slightly higher than the Redfield value of 6.6. With the depletion of inorganic nitrogen, POC:PON increased in both experiments. Maximum values of POC:PON in the *T.*

weissflogii experiment increased at higher temperatures, but decreased in the high CO_2 treatments (Figure 3A, Table 1). In contrast, POC:PON values in the *D. fragilissimus* experiment display a decrease at higher temperatures but an increase at elevated pCO_2 (Figure 3B, Table 2). The C:N ratio of DOM was ~5.0 and 8.0 in the beginning of the experiment with *T. weissflogii* and *D. fragilissimus*, respectively. After N-depletion, DOC:DON slightly increased in the *T. weissflogii* experiment, however without a detectable effect of temperature or pCO_2 (Figure 3C, Table 1). In the experiment with *D. fragilissimus*, DOC:DON was significantly higher at lower temperatures, whereas an effect of pCO_2 could not be observed at either temperature (Figure 3D, Table 2).

Bacterial activity

Bacterial production (BP) in the experiment with *T. weissflogii* amounted to 1.77±0.22 µmol C L^{-1} in all treatments prior to N-depletion. After nitrogen was depleted, BP increased to 2.77±0.18 µmol C L^{-1}. A significant effect of temperature or CO_2 could not be detected when PERMANOVA was applied to both temperatures. However, CO_2 significantly enhanced BP at in the *T. weissflogii* cultures at 20 °C ($p<0.05$) (Figure 4A). In the experiment with D. fragilissimus, BP increased from initial levels of ~0.23±0.02 C L^{-1} d^{-1} under nutrient-replete conditions to 2.85±0.08 µmol C L^{-1} d^{-1} in the period after N-depletion, showing no significant difference between temperature and pCO_2 treatments (Figure 4B).

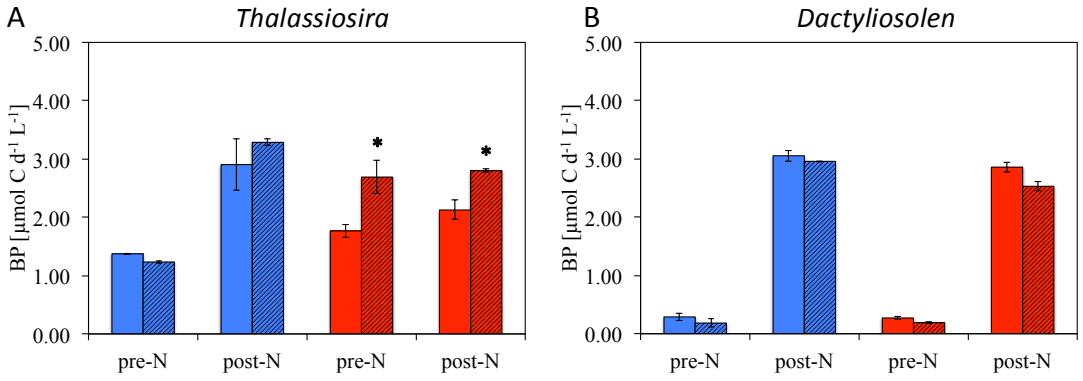

Figure 4: Average rates of bacterial production in the period before and after nitrogen depletion (denoted "pre-N" and "post-N", respectively) in the experiment with (A) *T. weissflogii* and (B) *D. fragilissimus* (right) at 15 (blue) and 20 °C (red), and in the ambient (solid) and high CO_2 treatment (hatched). Vertical error bars denote range of replicates within each treatment. Stars denote significant effect of CO_2 in the respective temperature treatment ($p<0.05$).

Table 1: Effects of temperature and CO_2 on biogeochemical parameters in the experiment with *T. weissflogii*. Shown are maximum net uptake of DIC, maximum net build-up of POC, and DOC [µmol C L^{-1}], maximum ratios of DIC:NO_3 uptake, POC:PON and DOC:DON build-up, and average TEP concentration after N-depletion [µg GXeq L^{-1}]. Effects of temperature and CO_2 were assessed by PERMANOVA. Significant effects are in bold (N=2, df=1).

	Value	Effect	SS	Pseudo-F	p(perm)
ΔDIC					
Ambient	333.2 ± 3.2				
High Temp.	448.1 ± 9.0	Temp.	14.8202	287.725	**0.004**
High CO_2	360.2 ± 0.8	CO_2	0.5687	11.041	**0.036**
Combined	462.7 ± 9.6	Temp.xCO_2	0.0740	1.438	0.360
ΔPOC					
Ambient	288.7 ± 8.3				
High Temp.	412.0 ± 14.0	Temp.	18.1083	112.407	**0.008**
High CO_2	314.7 ± 13.1	CO_2	0.4054	2.517	0.179
Combined	418.1 ± 3.5	Temp.xCO_2	0.1755	1.089	0.425
ΔDOC					
Ambient	11.6 ± 2.4				
High Temp.	19.3 ± 1.0	Temp.	1.1596	12.605	**0.013**
High CO_2	14.5 ± 1.4	CO_2	0.0572	0.621	0.485
Combined	18.7 ± 0.7	Temp.xCO_2	0.1140	1.239	0.345
ΔDIC:ΔNO_3					
Ambient	22.2 ± 0.2				
High Temp.	29.9 ± 0.6	Temp.	0.9880	287.631	**0.005**
High CO_2	24.0 ± 0.1	CO_2	0.0379	11.036	**0.034**
Combined	30.8 ± 0.6	Temp.xCO_2	0.0049	1.435	0.354
POC:PON					
Ambient	22.6 ± 0.1				
High Temp.	30.6 ± 0.5	Temp.	0.8699	274.266	**0.007**
High CO_2	22.5 ± 0.4	CO_2	0.0335	10.559	**0.037**
Combined	27.9 ± 0.5	Temp.xCO_2	0.0290	9.131	**0.039**
DOC:DON					
Ambient	11.6 ± 0.6				
High Temp.	11.8 ± 2.2	Temp.	0.0104	0.154	0.771
High CO_2	11.5 ± 0.6	CO_2	0.0223	0.332	0.647
Combined	10.4 ± 0.6	Temp.xCO_2	0.0154	0.229	0.721
TEP_{avg}					
Ambient	2898.7 ± 84.2				
High Temp.	4133.6 ± 49.3	Temp.	199.6363	116.221	**0.003**
High CO_2	3333.2 ± 183.8	CO_2	23.2679	13.546	**0.031**
Combined	4520.7 ± 50.8	Temp.xCO_2	0.4369	0.254	0.607

Table 2: Effects of temperature and CO_2 on biogeochemical parameters in the experiment with *D. fragilissimus*. Shown are maximum net uptake of DIC, maximum net build-up of POC, and DOC [µmol C L^{-1}], maximum ratios of DIC:NO_3 uptake, POC:PON and DOC:DON build-up, and average TEP concentration after N-depletion [µg GXeq L^{-1}]. Effects of temperature and CO_2 were assessed by PERMANOVA. Significant effects are in bold (N=2, df=1).

	Value	Effect	SS	Pseudo-F	p(perm)
ΔDIC					
Ambient	420.7 ± 8.4				
High Temp.	271.6 ± 11.6	Temp.	28.0617	204.642	**0.003**
High CO_2	516.9 ± 10.7	CO_2	9.4978	69.264	**0.006**
Combined	358.4 ± 9.1	Temp.xCO_2	0.0012	0.009	0.869
ΔPOC					
Ambient	298.3 ± 19.5				
High Temp.	248.7 ± 10.9	Temp.	2.2055	9.895	**0.045**
High CO_2	402.5 ± 2.1	CO_2	14.1741	63.593	**0.005**
Combined	346.0 ± 4.3	Temp.xCO_2	0.0958	0.429	0.538
ΔDOC					
Ambient	123.9 ± 6.2				
High Temp.	70.0 ± 8.3	Temp.	16.0904	22.938	**0.016**
High CO_2	136.4 ± 24.5	CO_2	0.2271	0.324	0.595
Combined	63.2 ± 0.3	Temp.xCO_2	1.4160	2.019	0.215
ΔDIC:ΔNO_3					
Ambient	28.0 ± 0.6				
High Temp.	18.1 ± 0.8	Temp.	1.8708	204.680	**0.003**
High CO_2	34.5 ± 0.9	CO_2	0.6331	69.270	**0.006**
Combined	23.9 ± 0.6	Temp.xCO_2	$8.30e^{-5}$	0.009	0.875
POC:PON					
Ambient	19.4 ± 0.9				
High Temp.	16.5 ± 0.7	Temp.	0.2545	17.128	**0.018**
High CO_2	24.0 ± 0.9	CO_2	0.4724	31.790	**0.004**
Combined	20.6 ± 0.6	Temp.xCO_2	$6.16e^{-5}$	0.004	0.908
DOC:DON					
Ambient	19.6 ± 0.5				
High Temp.	15.7 ± 1.0	Temp.	0.7846	28.535	**0.011**
High CO_2	20.9 ± 1.7	CO_2	$9.10e^{-4}$	0.033	0.793
Combined	14.3 ± 0.2	Temp.xCO_2	0.0505	1.836	0.248
TEP_{avg}					
Ambient	11795.8 ± 1525.3				
High Temp.	7944.4 ± 513.9	Temp.	833.7093	13.860	**0.029**
High CO_2	15658.0 ± 1062.2	CO_2	484.1105	8.048	**0.049**
Combined	10761.0 ± 1379.1	Temp.xCO_2	2.5173	0.042	0.853

Temperature range and optimum of *T. weissflogii* and *D. fragilissimus*

Growth rate, inorganic carbon uptake and build-up of organic carbon (TOC = POC+DOC) were significantly related to temperature in both diatom species (Figure 5). Growth rate, DIC drawdown and TOC build-up by *T. weissflogii* all increased over the entire range of temperatures from 10 to 22.5 °C, with an apparent optimum between 20 and 22.5 °C. In contrast, growth rate, DIC uptake and TOC build-up by *D. fragilissimus* increased over the range from 10 to 15 °C but decreased beyond that.

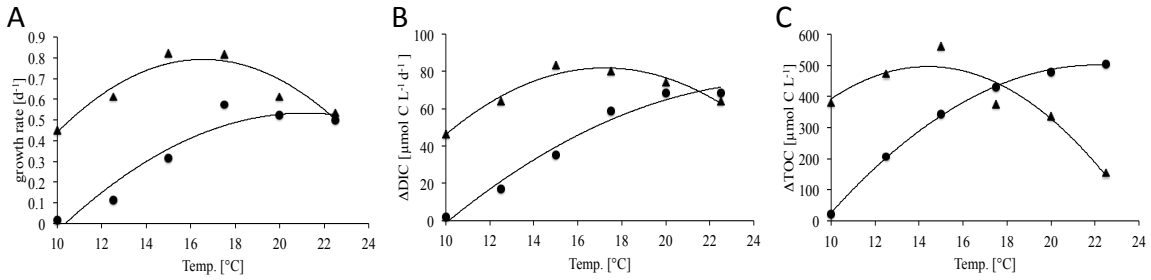

Figure 5: Effect of temperature on diatom growth and carbon cycling. Shown are (A) growth rate [d^{-1}] under nutrient-replete conditions (calculated from fluorescence), (B) rate of DIC uptake [µmol C L^{-1} d^{-1}] and (C) cumulative build-up of total organic carbon [µmol C L^{-1}] from onset of the experiment until day 4 after N-depletion for *T. weissflogii* (circles) and *D. fragilissimus* (triangles). Solid lines denote significant relationship of temperature and the respective parameter detected by polynomial regression ($p<0.05$, $n=6$).

4. Discussion

Effects of temperature and CO_2 on carbon overconsumption

The temporal development of DIC concentrations reveals that a substantial portion of carbon uptake and build-up of organic matter (up to 70 %) in the diatom cultures occurred after N-depletion, suggesting a strong decoupling of carbon and nitrogen cycling. Carbon overconsumption has been observed in previous experiments and field studies (Banse, 1994; Körtzinger et al., 2001; Sambrotto et al., 1993) and is commonly assumed to be associated with nutrient stress (Biddanda and Benner, 1997; Wetz and Wheeler, 2003). This is in line with the observations in our experiments, where uptake of DIC continued for several days after N-depletion and the magnitude of DIC uptake under N-depletion was even higher than DIC uptake during the period where inorganic N was still available (Figure 1).

Temperature effect on carbon overconsumption

Temperature had a strong effect on the magnitude of DIC uptake and carbon overconsumption in both experiments. However, the effect of temperature differed between the two diatom species (Figure 1). Warming from 15 to 20 °C resulted in an increase in carbon uptake for *T. weissflogii* (+34% and +28% at low and high CO_2, respectively), but a decrease for *D. fragilissimus* (-35% and -30% at low and high CO_2, respectively). Interestingly, *D. fragilissimus* grew faster at higher temperatures in the beginning of the experiments when nutrients were still available, with DIC uptake and POC build-up both accelerated. However, once inorganic nitrogen was depleted, DIC uptake and POC build-up by *D. fragilissimus* declined much faster at 20 °C than at 15 °C, suggesting that processes under N-replete and N-deficient conditions might have different temperature sensitivities. As bacterial activity was relatively low and similar across all treatments, this indicates that the observed effect of temperature is entirely attributable to physiological differences between the two diatom species.

Such a species-specific response of DIC uptake to elevated temperatures has been suggested before, e.g. by Taucher et al. (2012) who observed a strong positive relationship between temperature (9 to 17 °C) on carbon drawdown after nutrient depletion in a mesocosm experiment with a natural plankton community dominated by *D. fragilissimus*. In this regard, their findings were very different from a comparable experiment, where a negative effect of temperature on DIC uptake was found in a bloom that was dominated by *S. costatum* (Wohlers et al., 2009). Most comparable studies also reported generally negative impacts of increasing temperatures on marine ecosystems e.g. decreases in phytoplankton abundance (Lassen et al., 2010; O'Connor et al., 2009).

Our additional temperature gradient experiment demonstrates that the different responses to elevated temperature observed in the main experiments, depends on the respective temperature range and optimum of the two diatom species (Figure 5). According to growth rate, DIC uptake and build-up of organic carbon over the range from 10 to 22.5 °C, *T. weissflogii* seems to have an optimum around 20 °C and *D. fragilissimus* around 15 °C. Consequently, warming from 15 to 20 °C in the main experiment resulted in a rise from sub-optimal to optimal growth conditions for *T. weissflogii* (stimulating effect), but pushed *D. fragilissimus* beyond its temperature optimum, resulting in sub-optimal conditions and decreased carbon uptake after N-depletion (inhibiting effect).

Species-specific differences in the physiological response to warming ultimately arise from the temperature sensitivity of cellular processes. Temperature affects enzyme-catalyzed

reactions in phytoplankton cells, such as carbon fixation, whereas other cellular processes (e.g. light harvesting and electron transfer) are assumed to be mostly independent from temperature. However, these differential effects of temperature can create energetic imbalances within the cell, leading to inhibition of growth rate, cellular damage and eventually cell death when temperature increases beyond the species' optimum (Boyd et al., 2010; Finkel et al., 2010; Raven and Geider, 1988). Consequently, the net effect of temperature on carbon overconsumption after N-depletion is the sum of temperature-sensitivities of different physiological processes that affect cellular health and the efficiency of the photosynthetic apparatus, thereby giving rise to the differences in temperature-sensitivity between *T. weissflogii* and *D. fragilissimus*.

It has to be noted that *T. weissflogii* probably experienced co-limitation by N and Si later in the experiment, whereas *D. fragilissimus* remained only N-limited throughout the experiment (Figure 1-3). However, it can be assumed that cellular processes and photosynthesis are mainly limited by N, whereas availability of Si is mainly important for cell division. Since an effect of additional Si-limitation is not detectable in the data, this should not affect the main findings presented here.

CO_2 effect on carbon overconsumption

High pCO_2 enhanced the cumulative uptake of DIC in both experiments, with the effect being much stronger on *D. fragilissimus* than on *T. weissflogii*. While elevated initial pCO_2 lead to an increase in DIC uptake by 3-8% in the experiment with *T. weissflogii*, DIC drawdown by *D. fragilissimus* was enhanced by 22-39% in the high CO_2 treatments. Our findings are in line with a mesocosm experiment where DIC uptake of a natural diatom-dominated community was enhanced by 27% and 39% at pCO_2 levels of 700 and 1050 µatm, respectively, compared to the control treatment with 350 µatm (Riebesell et al., 2007). Remarkably, the CO_2 effect in our experiments was not detectable before N-depletion and when pCO_2 was still close to target levels of 400 and 1000 µatm. Instead, most of the differences in DIC uptake occurred after dissolved CO_2 dropped below ~10 µmol L^{-1} (Figure 1).

Therefore, the most likely explanation for the pCO_2 effect is the inhibition of carbon assimilation at low concentrations of dissolved CO_2, which decreased down to values of 2 µmol L^{-1} towards the end of the experiments. This is in line with previous studies, which demonstrated that carbon acquisition in diatoms is highly sensitive to CO_2, especially at low concentrations of dissolved CO_2 (Riebesell et al., 1993; Rost et al., 2003). Other

studies also reported a close correlation of growth rate and POC production with dissolved CO_2, suggesting growth inhibition below 5-7.5 µmol CO_2 (Bach et al., 2013; Engel, 2002). An important mechanism could be diffusive loss of CO_2 from the cell, outweighing inorganic carbon fixation once a critical lower threshold of dissolved CO_2 has been reached. Most phytoplankton species can actively take up HCO_3^- in addition to passive uptake of CO_2 via diffusion through operation of a carbon concentrating mechanism (CCM). Thereby, phytoplankton actively enhance their intracellular CO_2 and HCO_3^-, which creates a concentration gradient between inside and outside the cell. However, the primary carboxylating enzyme (RubisCO) is restricted to CO_2 for fixation of inorganic carbon, which is why accumulated HCO_3^- has to be converted to CO_2 before it can be used for photosynthesis (Hopkinson et al., 2011; Rost et al., 2003). Thus, at very low CO_2 concentrations surrounding the cell, the diffusion gradient between the chloroplast and the outside increases strongly. Since membranes have a high permeability to CO_2, the loss of carbon through CO_2 leakage becomes dominant when external CO_2 concentrations become very low and the gradient between the cell interior and exterior too strong (Bach et al., 2013; Hopkinson et al., 2011; Rost et al., 2006). Leakage has been found to be up to 79% at ambient pCO_2 levels for other phytoplankton species (Schulz et al., 2007) and shown to increase with decreasing concentrations of dissolved CO_2 (Rost et al., 2006). Accordingly, concentrations of aqueous CO_2 determine how much accumulated DIC remains within the cell and can be used for photosynthesis. With respect to our experiments, this implies that diatoms in the high pCO_2 treatments could take up more DIC until they reached very low CO_2 concentrations, where they might get carbon limited through the balance between carbon uptake and leakage.

This inhibition of carbon uptake at low CO_2 could have been additionally affected by N-limitation in our experiments. The functioning of the CCM depends on photosynthesis and harvesting of light energy can be compromised by N-limitation, e.g. through shortage in nitrogen for the synthesis of specific proteins that are required in the CCM (Giordano et al., 2005). Therefore, it is likely that the availability of nitrogen controls the amount of resources that a cell invests in carbon acquisition through a CCM. This mechanism could have further contributed to the observed effect of CO_2 on DIC uptake in our experiments.

Observed differences between *T. weissflogii* and *D. fragilissimus* in response to high CO_2 could either be species-specific or related to cell size in general. On the one hand, photosynthetic pathways of diatoms are diverse and there are substantial differences regarding the preference for the form of inorganic carbon (CO2 or HCO_3^-) among species

(Giordano et al., 2005; Roberts et al., 2007; Rost et al., 2003). Under elevated pCO_2 conditions, dissolved CO_2 increases much stronger than HCO_3^-. Thus, the more a species is dependent on CO_2, the more prominent the effect of high pCO_2 might become. Furthermore, it has been shown that the sensitivity of CCM to N-limitation varies strongly between species, with some up-regulating and some down-regulating their CCM in response to N-deficiency (Giordano et al., 2005). Such species-specific differences could explain why *D. fragilissimus* displayed a much stronger reaction to high pCO_2 than *T. weissflogii*.

On the other hand, the differences between the two experiments are possibly related to cell size of the diatoms. If the uptake of CO_2 is limited by diffusion, increasing CO_2 can be expected to have a stronger effect on larger than on smaller phytoplankton. Small cells should have an advantage under lower concentrations of CO_2 due to the larger surface area per unit volume, which can support more transporters on the cell surface and a thinner diffusion boundary layer (Finkel et al., 2010). In addition, larger cells that rely more heavily on a CCM than on diffusive uptake of CO_2 due to their low surface-to-volume ratio (at low CO_2) could be affected more severely by N-limitation of their CCM. The results from our experiments are in line with these considerations, where the effect of elevated CO_2 was much more prominent for the large, chain-forming *D. fragilissimus*, than for the rather small, unicellular *T. weissflogii*. Possibly, *D. fragilissimus* experienced a much stronger carbon limitation than *T. weissflogii*, thereby explaining the different magnitude of the CO_2 effect. Data from natural, mixed phytoplankton assemblages showed increasing abundances of larger phytoplankton species with additional dissolved CO_2 (Paulino et al., 2008; Tortell and Morel, 2002). Specifically for diatoms, elevated CO_2 favored large chain-forming diatoms over small single-celled diatoms in the Ross Sea, resulting in an overall increase in carbon fixation of the phytoplankton community (Tortell et al., 2008).

Fate of carbon overconsumption: Partitioning of organic matter as a function of temperature and pCO_2

Excess carbon fixation was accompanied by a substantial build-up of organic carbon in both experiments. However, partitioning between the particulate and dissolved phase differed notably between species. In the experiment with *T. weissflogii*, inorganic carbon uptake could almost entirely be traced to the POC pool (~95%). In contrast, a larger

fraction of DIC uptake accumulated as DOC (20-45%), and TEP concentrations were substantially higher in the experiment with *D. fragilissimus*. In both experiments, C:N of produced particulate and dissolved organic matter far exceeded Redfield stoichiometry, reaching C:N values of 20-25.

It has long been recognized that elemental composition is highly variable among different diatom species and that it is affected by environmental parameters (Brzezinski, 1985). Variations in POC:PON have previously been attributed to production of TEP (Engel, 2002), or variable cellular amounts of carbon-enriched compounds, such as lipids and carbohydrates (Bach et al., 2013; Goldman, 1992). For diatoms, it has been shown that lipids can amount to 30-45% of total biomass (Chen, 2012), and that the lipid content can increase several fold under N-depletion (McGinnis et al., 1997). However, it is unlikely that the increase in POC:PON observed in the experiments presented here is entirely attributable to changes in the elemental composition of phytoplankton. Though highly species-specific, cellular C:N ratios of diatoms usually remain below 10 and do not exceed a value of 15 even under nutrient starvation (Brzezinski, 1985; Goldman, 1992; Harrison et al., 1977).

Since TEP concentrations in our experiments were very high, the most likely explanation for observed high POC:PON values is release of excess carbon in the form of DOC and subsequent formation of TEP or similar gel-like particles. Controlling cellular elemental ratios is fundamentally important for optimizing resources and maintaining the enzyme machinery that is necessary for survival and growth (Giordano et al., 2005). Release of DOC therefore acts as a "carbon overflow" mechanism that helps in maintaining the metabolic functionality of the cell (Fogg, 1983), protecting the photosynthetic apparatus from accumulated organic carbon in excess of growth requirements and maintaining the cellular balance of carbon and nitrogen when there is an imbalance between light and nutrients (Gordillo et al., 2003; Wood and van Valen, 1990). Previous studies suggested that carbon overconsumption is mainly channeled into an increase in DOC (Koeve, 2004; Sambrotto et al., 1993). However, in our experiments the major portion of carbon overconsumption was channeled into the POC pool. This is not necessarily contradictory to the assumption the excess carbon is released as DOC: It has been demonstrated that a substantial fraction of DOC exudates can be transformed into gel-like transparent exopolymer particles (TEP) by abiotic coagulation and aggregation processes (Engel et al., 2004a; Passow, 2000). TEP can constitute a substantial fraction of total POC usually have high C:N ratios averaging between 20 and 25 (Engel et al., 2004a; Mari et al., 2001; Wetz

and Wheeler, 2007). Since TEP and precursor material exist in a size continuum, bridging the boundary between particulate and dissolved organic matter (Verdugo et al., 2004), the major portion of TEP gets caught on GF/F filters and is subsequently measured as POC. Thus, the formation of TEP has important implications for estimates of POC and DOC. The fraction of released DOC consisting of dissolved precursor material, which subsequently aggregate to TEP, is mainly measured as POC. Accordingly, this mechanism can lead to an underestimation of the true DOC release (Verdugo et al., 2004; Wetz and Wheeler, 2007). Most likely, a large portion of released DOC comprised TEP-precursors in our experiments, which were then rapidly transformed into TEP. Formation of TEP occurs abiotically from dissolved extracellular polysaccharides that are released by phytoplankton, especially under nutrient limitation (Corzo et al., 2000; Passow, 2002; Passow et al., 1994). Thus, our results are in line with earlier studies, where excess carbon fixation after N-depletion could almost entirely be traced to POC and TEP (Engel et al., 2002; Wetz and Wheeler, 2007). Differences in the build-up of POC, DOC and TEP between *T. weissflogii* and *D. fragilissimus* might be attributable to the differences in the conversion of precursor material to TEP, which can occur very rapidly (Engel et al., 2004b). The production of DOC and TEP by *D. fragilissimus* was much higher than that by *T. weissflogii*, suggesting species-specific differences in the amount and quality of produced DOC, the fraction of precursors contained in this DOC, and their subsequent conversion to TEP.

Furthermore, build-up and elemental composition of organic matter in the experiments with *T. weissflogii* and *D. fragilissimus* were affected by temperature and CO_2, mirroring the respective effects on inorganic carbon uptake. A temperature increase from 15 to 20 °C resulted in higher build-up of POC, DOC, and TEP, and an associated increase in POC:PON in the experiment with *T. weissflogii*. The opposite was the case for *D. fragilissimus*, where the same temperature increase resulted in reduced build-up of POC, DOC, and TEP, and correspondingly lower C:N ratios in particulate and dissolved organic matter. Generally, our findings are in line with previous studies that observed an effect of temperature on build-up of POC (Taucher et al., 2012), exudation of DOC (Zlotnik and Dubinsky, 1989), production of TEP (Claquin et al., 2008), and elemental stoichiometry of organic matter (Taucher et al., 2012). However, observed effects in temperature are ambiguous and vary substantially among studies, suggesting either beneficial or negative effects of warming on phytoplankton (Taucher et al., 2012; Wohlers et al., 2009). Clearly, the direction and magnitude of the temperature effect depends on the temperature range and optimum, which has been shown to be strongly variable among species (Boyd et al.,

2013; Eppley, 1972; Thomas et al., 2012). While species living below their temperature optimum might benefit from warming, as was the case in the experiment with *T. weissflogii*, species that are pushed beyond the temperature optimum will be negatively affected by warming, e.g. through inhibition of carbon fixation, and consequently lower production of POC and DOC, as observed for *D. fragilissimus*.

While elevated pCO_2 enhanced DIC uptake by both diatom species, the fate of this additional carbon uptake varied strongly between species. In the experiment with *D. fragilissimus*, higher initial pCO_2 did not have a detectable effect on accumulation of DOC, but strongly enhanced build-up of POC, suggesting that most of the additional carbon under elevated pCO_2 was channeled into POC. In contrast, pCO_2 did not have a statistically significant effect on build-up of POC and DOC by *T. weissflogii*. However, the CO_2 response was related to temperature in this experiment, with no detectable effect of pCO_2 at 20 °C, but build-up of both POC and DOC slightly elevated under higher initial pCO_2 at 15 °C. Since TEP was elevated in the high CO_2 treatments in both experiments, it is most likely that most of the additional carbon uptake was released as DOC, of which a variable portion is transformed to TEP. This is in line with previous studies that found TEP build-up to be affected by CO_2, especially at CO_2 concentrations below ~10 µmol CO_2 (Borchard and Engel, 2012; Engel, 2002). This probably mirrors carbon limitation of photosynthesis at low CO_2 as discussed above. Thereby, effects of temperature and CO_2 on carbon uptake ultimately translate into partitioning of this carbon into POC, DOC, and TEP.

It has to be noted that actual DOC release might have been underestimated due to bacterial degradation. Net changes in measured DIC, POC and DOC include carbon fluxes mediated by bacterial consumption of organic matter. Even though measured bacterial production did not exceed 3 µmol L^{-1} d^{-1}, bacterial carbon demand (i.e. the gross flux of carbon through the bacteria pool) could have been higher, depending on the bacterial growth efficiency. Since DOC build-up by *T. weissflogii* was relatively low (< 20 µmol L^{-1}, Table 1), slight differences in bacterial activity might have a notable effect on DOC. Bacteria production was elevated in the high CO_2 treatments of *T. weissflogii* (Figure 4A). Enhanced bacterial consumption of freshly produced DOC could possibly explain why there was no visible effect of CO_2 on accumulation of DOC in this experiment. In contrast, DOC build-up by *D. fragilissimus* was much higher (~60 to 130 µmol L^{-1}, Table 2) and bacterial production was similar across all treatments (Figure 4B). Therefore, estimates on DOC release are probably only marginally affected by bacterial activity.

5. Conclusion - implications for the marine carbon cycle

It has been widely recognized that ocean warming and acidification could substantially alter marine ecosystems, e.g. through changes in community composition, shifts in suitable habitats, and associated changes in species succession.

Our experiments revealed a notable sensitivity of carbon uptake and production of organic matter of two diatom species under N-depletion to both temperature and CO_2. Remarkably, up to 70% of DIC uptake occurred after N-depletion in our experiments. While previous studies concluded that CO_2 is usually not a limiting factor for photosynthetic carbon fixation, with only small to negligible impacts of elevated CO_2 on diatoms, our results demonstrate that the effect becomes much more prominent when considering bloom dynamics and the post-bloom phase. Although the underlying mechanism might not be fully understood in its entire complexity yet, a higher initial pCO_2 can increase the amount of inorganic carbon that is taken up over the course of a bloom before CO_2 becomes a limiting factor. At the same time, our study demonstrated that the same magnitude of warming can have either stimulating or inhibiting effects on carbon uptake and production of biomass by diatoms, depending on the species-specific temperature range.

This physiological response of phytoplankton could act as a feedback mechanism in the marine carbon cycle. Whether the sensitivity of carbon overconsumption to temperature and CO_2 presented in this study results in a negative or positive climate feedback would depend on the fate of the organic carbon. It has been shown that DOC can significantly contribute to the carbon flux to the deep ocean through transport via deep water formation and mixing (Carlson et al., 2010; Hansell and Carlson, 1998). An increase in DOC release by phytoplankton could therefore enhance the transport of carbon from the atmosphere to the ocean interior. However, this strongly depends on the quality and bioavailability of the produced DOC (Carlson, 2002). If the additional DOC gets rapidly remineralized in the surface ocean, the net effect on carbon flux would be zero. Thus, more information on degradability of DOC release by phytoplankton is required. Changes in production of TEP could have even stronger effects on the biological pump. TEP facilitate the formation of marine aggregates through their high stickiness and thus play an important role in particle flux to the ocean interior (Alldredge et al., 1993; Logan et al., 1995; Passow, 2002). Assuming no changes in phytoplankton abundance, higher TEP production would result in faster formation of aggregates, thereby enhancing the particle flux out of the euphotic zone, and ultimately the biological pump (Arrigo, 2007). Since

sensitivities to temperature and CO_2 and partitioning of excess carbon fixation into DOC, POC and TEP seem to be highly variable among species, it is currently hard to predict whether ocean warming and acidification will lead to an enhancement of the biological pump or an acceleration of the microbial loop. The picture becomes even more complex when considering that the observed effects of temperature and CO_2 on elemental composition of organic matter could change their food quality for higher trophic levels (Sterner and Elser, 2002; van de Waal et al., 2010).

Ultimately, the effect of increasing temperatures and CO_2 on entire pelagic ecosystems will depend on the sensitivities of its most important species, as this will propagate into community composition and food web dynamics, as well as carbon uptake and the efficiency of the biological pump. Since the major fraction of DIC uptake and organic matter build-up occurred after N-depletion in our experiments, more attention should be paid to post-bloom dynamics in future studies. Complementary to experiments as in this study, these questions should be investigated on the ecosystem level, e.g. in mesocosm experiments. Both approaches in combination can deliver valuable information on physiology and ecosystem functioning. Single-species experiments as in this study are particularly important to identify sensitivities of specific processes that cannot be disentangled in mesocosm experiments that are close to natural conditions. Furthermore, our experimental setup could be applied to identify a more detailed functional relationship with each environmental parameter for different phytoplankton species in future work, e.g. in by establishing gradients of temperature and CO_2 under N-replete and N-deficient conditions. Eventually, such information is urgently required for further development of marine ecosystem models that are used for projections of climate change.

Acknowledgments:

This study was supported by the German Research Foundation (Deutsche Forschungsgemeinschaft, DFG), the German Academic Exchange Service (DAAD), and the National Science Foundation (NSF). We thank Julia Sweet for assistance with pH and TEP measurements, as well as Maverick Carey and Ellie Wallner for technical assistance with DOC and TDN measurements.

Chapter 4: The viscosity effect on marine particle flux – a climate relevant feedback mechanism

J. Taucher[1]*, L.T. Bach[1]*, U. Riebesell[1], A. Oschlies[1]

[1]GEOMAR Helmholtz Centre for Ocean Research Kiel, Kiel, Germany
*equal contribution

Correspondence to: J. Taucher (jtaucher@geomar.de)

Currently under review for *Global Biogeochemical Cycles* –submitted: 9 September 2013

Abstract

Oceanic uptake and long-term storage of atmospheric carbon dioxide (CO_2) are strongly driven by the marine 'biological pump', i.e. sinking of biotically fixed inorganic carbon and nutrients from the surface into the deep ocean (Sarmiento and Bender, 1994; Volk and Hoffert, 1985). Sinking velocity of marine particles depends on seawater viscosity, which is strongly controlled by temperature (Sharqawy et al., 2010). Consequently, marine particle flux is accelerated as ocean temperatures increase under global warming (Bach et al., 2012). Here we show that this previously overlooked 'viscosity effect' could have profound impacts on marine biogeochemical cycling and carbon uptake over the next centuries to millennia. In our global-warming simulation, the viscosity effect accelerates particle sinking by up to 25%, thereby effectively reducing the portion of organic matter that is respired in the surface ocean. Accordingly, the biological carbon pump's efficiency increases, enhancing the sequestration of atmospheric CO_2 into the ocean. This effect becomes particularly important on longer timescales when warming reaches the ocean interior. At the end of our simulation (4000 AD) oceanic carbon uptake is 17% higher, atmospheric CO_2 concentration is 180 ppm lower, and the increase in global average surface temperature is 8% weaker when considering the viscosity effect. Consequently, the viscosity effect could act as a long-term negative feedback mechanism in the global climate system.

1. Introduction:

In the surface ocean, inorganic carbon and nutrients are converted photosynthetically into organic matter by phytoplankton. As the carbon passes through the food web, most of it is converted back to CO_2 via respiration and released to the atmosphere. However, a small fraction of this organic matter escapes remineralization and is exported from the euphotic zone to deeper waters as sinking particles ("export production"). The biological pump plays a major role in the global carbon cycle (Sarmiento and Bender, 1994; Volk and Hoffert, 1985) and it has been estimated that atmospheric CO_2 concentrations would be more than twice as high without this mechanism (Maier-Reimer et al., 1996).

Various studies have shown that climate change might have pronounced impacts on marine primary production, export of organic matter, and consequently on the efficiency of the biological pump and associated oceanic uptake of atmospheric CO_2 (Bopp et al., 2001; Boyd and Doney, 2002; Passow and Carlson, 2012; Riebesell et al., 2009). No study to date, however, has addressed the potential effects of changing seawater viscosity on the sinking of organic matter, although a relationship between seawater viscosity and sinking velocity of marine particles has long been recognized (Smayda, 1970). Generally, gravitationally accelerated particles move faster at lower viscosities. As rising temperatures reduce seawater viscosity, the sinking velocity of particles will accelerate (Fig. 1a,c). Recent projections of climate change estimate an increase in global surface temperatures of 1.1 to 6.4 °C until 2100 AD and more in the following centuries (IPCC, 2007a). Empirical evidence shows that the associated changes in seawater viscosity may accelerate sinking velocities of natural marine particles such as zooplankton fecal pellets or marine aggregates by ~5% per °C warming, with yet unknown consequences for carbon sequestration in the oceans (Bach et al., 2012; Honjo and Roman, 1978). Here we apply an earth system model (UVic ESCM) to specifically investigate the potential global effect of temperature-driven changes in seawater viscosity on the sinking and export of organic matter, and discuss associated implications on marine biogeochemical cycling and a potential climate feedback.

2. Methods:

We applied an earth system model of intermediate complexity (UVic ESCM), which includes a commonly used marine ecosystem representation in two different configurations. The CONTROL model corresponds to a version applied in several previous

studies (Schmittner et al., 2008; Taucher and Oschlies, 2011), whereas the VISCOSITY model contains a modified parameterization for sinking of organic matter, where sinking velocity is dependent on seawater viscosity as described below. Particle sinking in the CONTROL model occurs for detritus with velocity calculated as:

$$\omega_D = \omega_{D0} + m_\omega z \qquad (1)$$

Sinking speed (ω_D) at the sea surface (ω_{D0}) is set to 6.0 m d^{-1} and increases linearly (with the factor m_ω) with depth (z), i.e. to ~45 m d^{-1} at 1000 m, and ~90 m d^{-1} at 2000 m. This formulation is consistent with observations from sediment traps, which suggest that the vertical pattern of POC flux is associated with an increase of sinking velocity with depth (Berelson, 2002; Clegg and Whitfield, 1990; Martin et al., 1987). This common parameterization of sinking velocity as a function of depth can be considered a reasonable approximation to observed conditions (Kriest and Oschlies, 2008). However, the sensitivity to environmental change may not be reflected correctly in relation (1). Accordingly, we test the impact of temperature-related changes in seawater viscosity on the vertical particle flux in the VISCOSITY model experiment. The dynamic viscosity of seawater ($\mu_{seawater}$) is a function of pressure, salinity and temperature among which temperature is by far the most important factor in a marine system (Bett and Cappi, 1965; Sharqawy et al., 2010). $\mu_{seawater}$ almost doubles from 25 to 0 °C (Fig. 1a), thereby showing considerable spatial and temporal variability. According to Stokes' Law and the effects of viscosity and excess particle density on sinking speed of particles, sinking velocity in the VISCOSITY model (ω_μ) is calculated as a function of density (ρ) of particles and seawater, and the dynamic viscosity of seawater (μ):

$$\omega_\mu = \alpha \times \frac{\mu_{(0°C)}}{\mu_{(T)}} \times \frac{\rho_{part} - \rho_{seawater(T)}}{\rho_{part} - \rho_{seawater(0°C)}} \qquad (2)$$

This term consists of three parts: a term that describes the temperature-driven viscosity effect on sinking velocity; a term that describes the influence of assumed excess particle density on the strength of the viscosity effect, and a multiplier (α) that is necessary to obtain similar global mean vertical profiles of sinking velocity for preindustrial conditions as in the CONTROL model, and thereby facilitate comparability of the different model

setups. In order to compute α, we inserted global mean values of viscosity and density for preindustrial conditions into the above formula (eq. 2) and fitted the multiplier α to achieve the same vertical profile of sinking velocity as in the CONTROL model (eq. 1). Since both the term for the viscosity effect and the term for the density effect decreases with depth (due to the decrease in temperature, see eq. 2), the multiplier α increases with depth:

$$\alpha = \alpha(z) = 0.04078z + \frac{1212}{(254.3 + z)} - 1.493 \qquad (3)$$

with z measured in meters. For the results presented from the VISCOSITY model, we assume an average particle density of 1,060 kg m^{-3} for eq. 2, a value that is based on estimates from literature (Bach et al., 2012; Logan and Hunt, 1987). However, since the viscosity-related increase in sinking velocity is modified by the density difference between particles and seawater (Fig. 1b, eq. 2), we also created model setups to test the effect of assumed particle densities of 1,035 and 1,200 kg m^{-3}, i.e. one value near the density of seawater and another value for higher density particles (e.g. diatoms or calcifying organisms), as well a model setup without an effect of particle density on sinking velocity at all. While the absolute values were slightly different between the model setups, the overall patterns and dynamics were very similar to the VISCOSITY model (data not shown). Furthermore, it should be noted that the validity of sinking velocity according to Stokes' Law depends on the Reynolds number, which is in turn a function of the size and shape of the particle, as well as the sinking velocity. For reasons of simplicity we did not implement a full particle-size spectrum model, as this is not necessary for the effects of viscosity investigated here. Assuming average particle size to be smaller than 1000 µm and sinking velocities not exceeding 150 m d^{-1}, which is reasonable for the largest portion of marine particles that contribute to particle mass flux (Clegg and Whitfield, 1990; Jackson et al., 1997; McDonnell and Buesseler, 2010; Stemmann et al., 2004), Reynolds numbers remain below a critical value in the ocean regions important for the scope of our study (Fig. 1c).

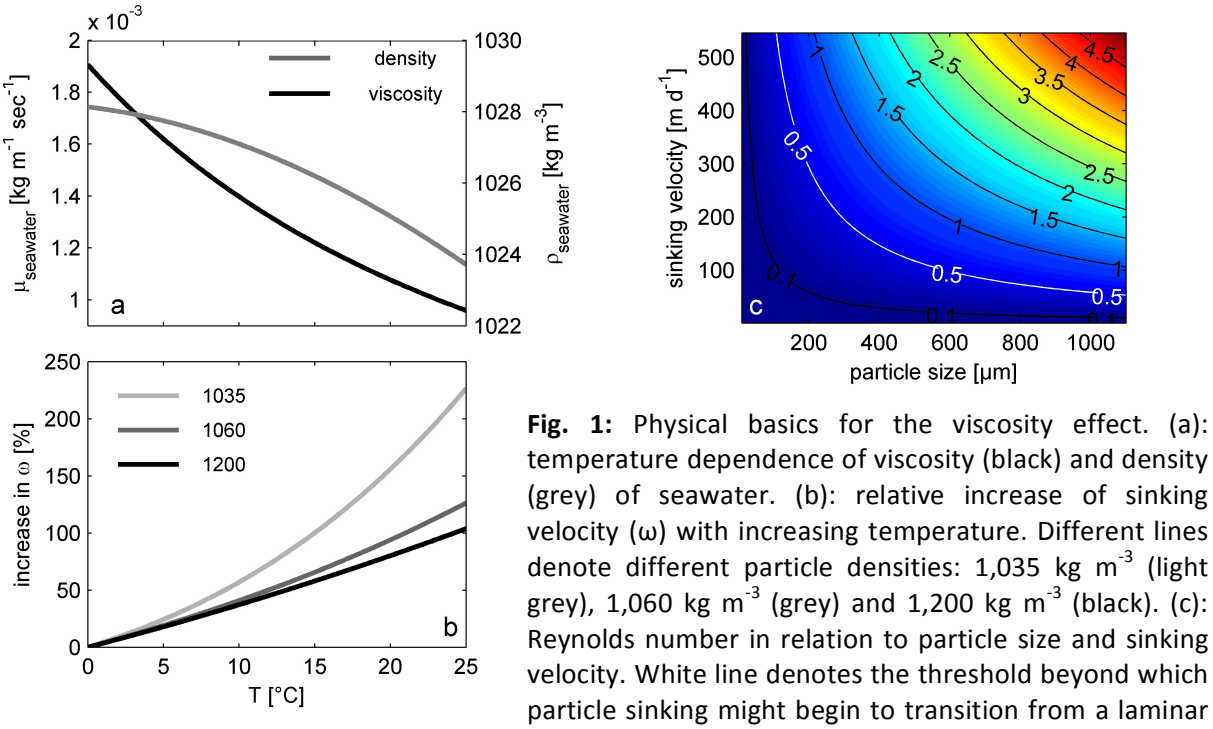

Fig. 1: Physical basics for the viscosity effect. (a): temperature dependence of viscosity (black) and density (grey) of seawater. (b): relative increase of sinking velocity (ω) with increasing temperature. Different lines denote different particle densities: 1,035 kg m^{-3} (light grey), 1,060 kg m^{-3} (grey) and 1,200 kg m^{-3} (black). (c): Reynolds number in relation to particle size and sinking velocity. White line denotes the threshold beyond which particle sinking might begin to transition from a laminar flow into a turbulent regime.

3. Results and discussion

Present day

Present day conditions of nutrient and oxygen fields are simulated almost equally well in the CONTROL run with climate-independent constant viscosity, and the VISCOSITY run, in which viscosity varies spatially and temporally as a function of local water temperature (see methods). Compared to data from the World Ocean Atlas (Garcia et al., 2010) the global average root mean square (RMS) error for phosphate is 0.152 mmol m^{-3} and 0.156 mmol m^{-3} in the CONTROL and VISCOSITY model, respectively. This RMS error is at the lower end of errors found for biogeochemical tracers in previous modeling studies (Doney et al., 2009b; Kriest et al., 2010). Biological rates in 2000 AD are also in the same range in both models. Global NPP reaches 59.4 GtC yr^{-1} in the CONTROL run and 53.6 GtC yr^{-1} in the VISCOSITY run. Export production (at 130 m depth) amounts to 6.56 and 6.37 GtC yr^{-1} in the respective models (Table 1). The slight differences between these numbers originate from spatial differences between the models: Since viscosity is an inverse function of temperature, sinking velocity and thus export production follow the spatial pattern of

water temperature and are lower at high latitudes and higher in the tropics in the VISCOSITY compared to the CONTROL simulation.

Long-term simulation

Following the SRES A2 emission scenario until year 2100 AD, and a subsequent linear decrease of emissions to zero in 2300 AD, simulated global sea surface temperatures increase from a global average of ~18 °C to ~24 °C around 2400 AD and stay almost constant thereafter. However, the warming signal continues to penetrate into the ocean interior over the course of the simulation (Figure 2a), thereby increasing sinking velocity in the upper (< 1000 m) ocean by more than 20% in the VISCOSITY model (Figure 2b). At the end of the model simulations (4000 AD), export production amounts to 6.85 and 6.55 GtC yr^{-1} in the CONTROL and VISCOSITY model, respectively, and is thus even slightly higher than under present day conditions (Table 1). NPP increases even stronger (+53% and +29% in the CONTROL and in the VISCOSITY model) between 2000 and 4000 AD (Table 1). This increase is mainly attributable to the direct effect of warming on metabolic rates. As both phytoplankton growth and remineralization processes are positively affected by increasing temperatures, the turnover of organic matter in the surface ocean is accelerated, i.e. NPP is fueled by rapidly regenerated nutrients. This also explains the divergent response of NPP and export production to climate change (Taucher and Oschlies, 2011). The different magnitude of change in NPP between the two model setups results from differences in nutrient availability: The viscosity effect leads to faster particle sinking under global warming, thereby stripping nutrients out of the euphotic zone more efficiently and transporting them to the ocean interior. Consequently, fewer nutrients are available to fuel NPP in the surface ocean in the VISCOSITY model (Fig. 3a,b).

Viscosity effect on the biological pump

While the response of export production to climate change is very similar in both models, the sequestration flux (Lampitt et al., 2008), i.e. the carbon flux to the ocean interior (here defined as > 1000 m depth) that removes atmospheric CO_2 on the timescale of centuries, reveals substantial differences between the two models. In 2000 AD, this “sequestration flux” amounts to 0.74 and 0.70 GtC yr^{-1} in the CONTROL and VISCOSITY run, respectively. In response to climate change, the carbon flux to the deep ocean decreases and remains below the preindustrial level in both models, which is mainly driven by an accelerating

effect of increasing temperatures on the remineralization of organic matter (Figure 2c,d). At the end of the simulation (year 4000), the sequestration flux is 0.47 and 0.63 GtC yr^{-1} in the CONTROL and VISCOSITY run, respectively, with the decrease being much lower in the VISCOSITY run (-10%) than in the CONTROL run (-36%) (Table 1). Thus, the weakening of the biological pump due to climate change is strongly reduced when the viscosity effect on particle sinking velocity is considered.

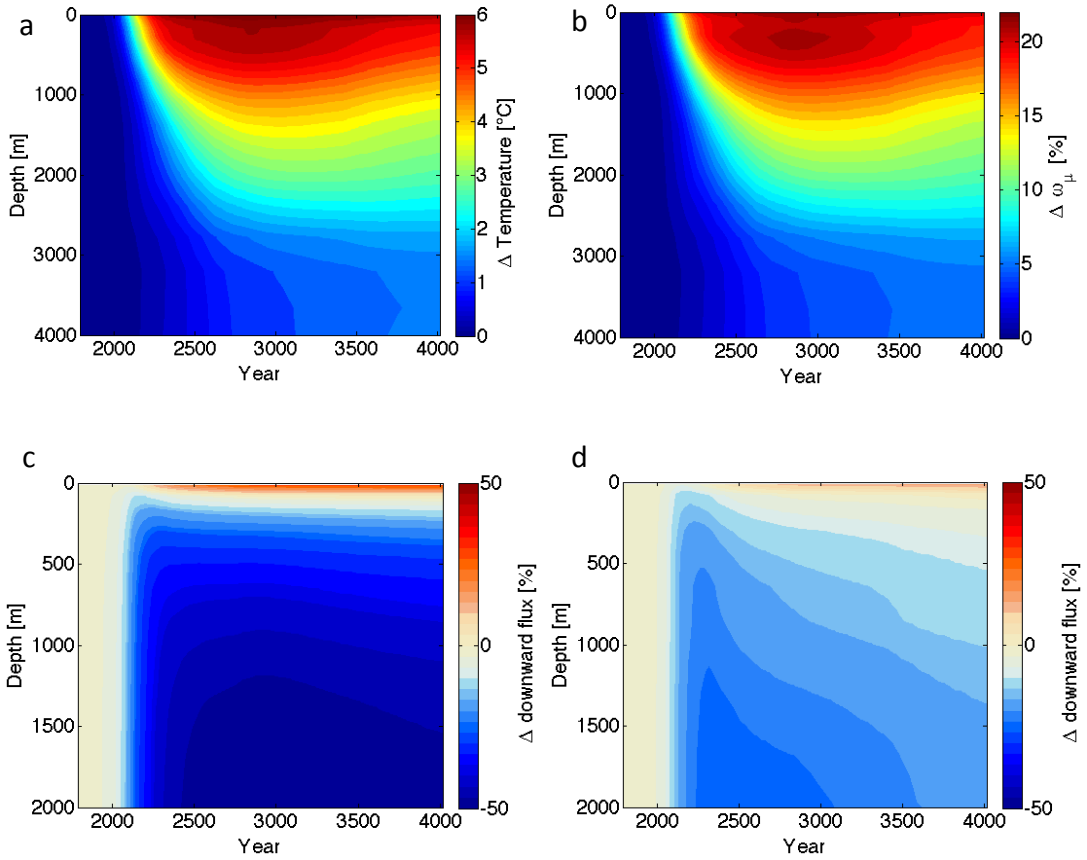

Fig. 2: Vertical profile of change relative to pre-industrial conditions in global mean ocean temperature in the VISCOSITY model (a) and associated global mean change in sinking velocity [%] in the VISCOSITY model (b). Change relative to pre-industrial conditions [%] of the global mean vertical particle flux in the CONTROL (c) and VISCOSITY (d) model.

The reason for this discrepancy between export production and sequestration flux is the different attenuation of the sinking flux of organic matter in the two models (Figure 2c,d). In the CONTROL model, where sinking velocity remains constant under ocean warming but remineralization rates increase with temperature, sinking particles are decomposed to a larger extent within the upper few hundred meters of the ocean (i.e. the mesopelagic

zone), thereby decreasing the portion of organic matter that sinks to the deeper ocean (Fig. 4). By contrast, increasing sinking velocities in the VISCOSITY model counteract accelerated bacterial decomposition in a warming ocean. This results in a more effective removal of organic matter from the surface ocean compared to the CONTROL run. Therefore, the efficiency of the biological pump in the future ocean is positively influenced by the viscosity effect, as a larger portion of organic matter escapes turnover through remineralization in the upper few hundred meters of the water column and reaches the deep ocean in this model setup (Fig. 4). In other words, the warming-induced increase in sinking velocity in the VISCOSITY model increases the remineralization length scale (RLS), i.e. the distance it takes until a certain amount of organic matter is respired (Fig. 3c).

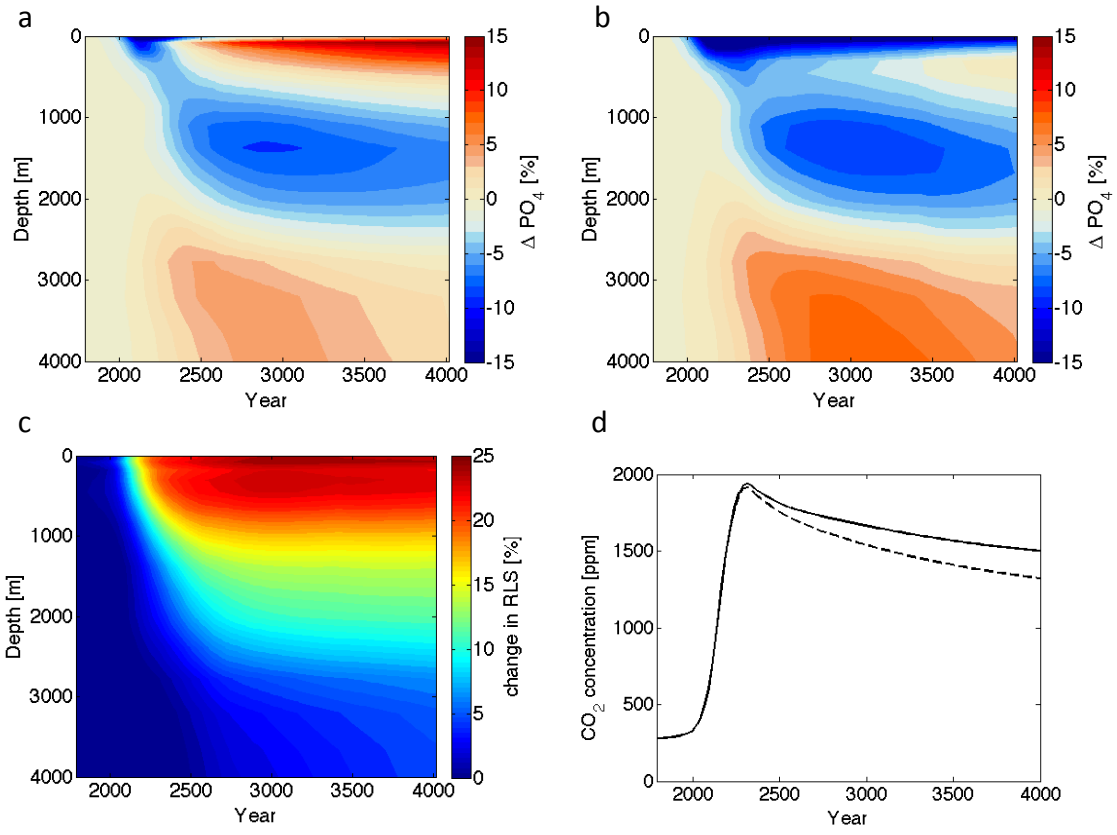

Fig. 3: Vertical profile of change relative to pre-industrial conditions [%] in global mean phosphate in the CONTROL (a) and VISCOSITY model (b). (c): Vertical profile of the relative difference in remineralization length scale (RLS) between the VISCOSITY and CONTROL model [%]. Increasingly red areas denote for the relatively longer RLS in the VISCOSITY compared to the CONTROL run. (d): Atmospheric CO_2 concentrations in the CONTROL (solid) and VISCOSITY simulation (dashed).

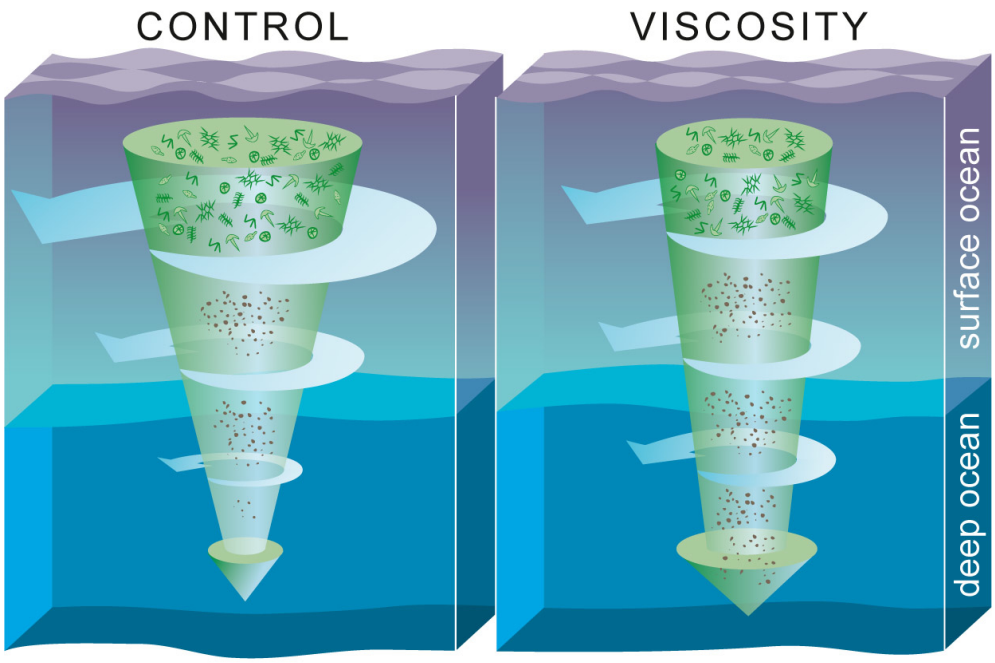

Fig. 4: Schematic diagram on the influence of the viscosity effect on particulate organic matter export in a warmer future ocean as simulated without (CONTROL) and including the viscosity effect on particle sinking velocity (VISCOSITY). Under CONTROL conditions, ocean warming does not reduce viscosity and therefore has no effect on sinking velocity. Compared to the VISCOSITY model, sinking particles remain longer above sequestration depth so that a larger fraction can be remineralized (illustrated by the green 'particle flux arrow' with greater attenuation and the larger circular blue 'respiration arrows') in the surface ocean. When the viscosity effect is implemented, particle sinking is accelerated and a larger fraction of organic matter escapes remineralization above sequestration depth. Thus, the remineralization length scale (the distance a particle sinks until a certain amount of organic matter is respired) is longer in the VISCOSITY model, which is indicated by a weaker attenuation of the green 'particle flux arrow' and the - over the water column - more homogenously distributed blue 'respiration arrows'. Furthermore, the higher efficiency of the biological pump (i.e. sinking of organic matter to the deep ocean) in the VISCOSITY setup leads to a stronger decrease in surface ocean nutrient concentrations and therefore also lower primary production and plankton standing stocks. This is indicated by the lower number of green phytoplankton particles in the surface box. Consequently, warming of the surface ocean results in a faster cycle of primary production and remineralization in the CONTROL model. Accelerated particle sinking velocities in the VISCOSITY model counteract this effect and enhance the efficiency of the biological carbon pump.

These results show that the carbon export to the deep ocean (and thereby effective long-term removal of carbon) is more effective when the influence of temperature-driven viscosity changes on particle sinking is taken into account. Net cumulative carbon uptake of the ocean over the course of the simulation (year 1780 to 4000) amounts to 2,415 GtC in the VISCOSITY model, compared to 2,061 GtC in the CONTROL model, and is thus 17% higher when considering the viscosity effect. This is also confirmed by the lower

concentrations of atmospheric CO_2 at the end of the simulation, which amount to 1,320 ppm in the VISCOSITY run compared to 1,500 ppm in the CONTROL model (Fig. 3d, Table 1). Correspondingly, global mean surface temperatures in 4000 AD are 0.6 °C lower and global warming is reduced by 8% with the viscosity effect being considered (Table 1). These findings confirm that slight changes in remineralization depth can have notable effects on oceanic carbon uptake, and consequently atmospheric CO_2 concentrations (Kwon et al., 2009).

Table 1: Differences between the model simulation without (CONTROL) and including the viscosity effect (VISCOSITY) in export production (at 130 m depth), sequestration flux (at 1000 m depth) and other climate relevant variables.

	CONTROL	VISCOSITY
Export Production, 2000 AD [GtC yr^{-1}]	6.56	6.37
Export Production, 4000 AD [GtC yr^{-1}]	6.85	6.55
Export production, relative change between 2000 and 4000 AD [%]	+4.4	+2.8
Sequestration flux, 2000 AD [GtC yr^{-1}]	0.74	0.70
Sequestration flux, 4000 AD [GtC yr^{-1}]	0.47	0.63
Sequestration flux, relative change between 2000 and 4000 AD [%]	-36.5	-10.0
Atmospheric CO_2, 4000 AD [ppm]	1,500	1,320
Net cumulative oceanic carbon uptake between 1780 and 4000 AD [GtC]	2,061	2,415
Global average increase in surface air temperature between 2000 and 4000 AD	7.7	7.1

Timescale of the viscosity effect

While warming of the surface follows climate change-driven atmospheric temperature increases on short timescales, the penetration of the warming signal to deeper layers is much slower, as it largely depends on physical transport via mixing and the meridional overturning circulation. Since the viscosity effect is directly coupled to changing seawater temperatures, it affects the global system on similar timescales as the warming signal is distributed in the ocean interior, i.e. centuries to millennia (Figure 2a-d). An instantaneous

impact of the viscosity effect on elemental cycling in the 21st century is largely restricted to water masses situated above the winter mixed layer, i.e. depths < 1000m. This limits the immediate feedback of the viscosity effect on the atmospheric CO_2 concentration, as the organic matter sequestration flux to water masses not in contact with the atmosphere is only slightly affected during this initial period (Fig. 3d). A significant influence of the viscosity effect on the atmospheric carbon dioxide concentration arises, therefore, most prominently on longer timescales in our model runs. However, it has been suggested recently that the global warming signal is transferred into the mesopelagic zone much faster than previously estimated, with 30% of the warming having occurred below 700 m over the last decade (Balmaseda et al., 2013). Such an accelerated penetration of warming to the ocean interior is not yet resolved by current earth system models and would allow for a much more rapid evolution of the viscosity effect than presented in our simulations.

4. Conclusion

Our findings demonstrate for the first time the potential global impact of temperature-driven changes in seawater viscosity on marine particle flux and consecutive changes in biogeochemical element cycling and carbon uptake of the oceans. The viscosity effect in response to ocean warming positively influences the efficiency of the biological pump and results in a larger remineralization length scale. As a larger portion of organic matter reaches the deep ocean, this ultimately increases the long-term sequestration of carbon in the ocean interior. Since the viscosity effect could potentially act as a previously overlooked negative climate feedback we suggest that this effect should be considered in future studies investigating long-term effects of climate change.

Acknowledgements:

This study was supported by the Deutsche Forschungsgemeinschaft (DFG) and the Federal Ministry of Education and Research (BMBF) in the framework of the BIOACID project. Furthermore, we thank Rita Erven for assistance with graphical illustration.

Chapter 5: What sets the upper limit of export production in marine ecosystem models?

J. Taucher[1] and A. Oschlies[1]

[1]GEOMAR Helmholtz Centre for Ocean Research, Kiel, Germany

Correspondence to: J. Taucher (jtaucher@geomar.de)

To be submitted to *Global Biogeochemical Cycles*

Abstract

Sinking of organic matter out of the euphotic zone, a process commonly referred to as export production, plays an important role in marine biogeochemical cycling and the distribution of inorganic nutrients and carbon in the ocean. Thus, a realistic simulation of the magnitude and spatiotemporal pattern of export production in earth system models is an essential prerequisite for correctly modeling marine carbon fluxes, reproducing observed nutrient fields, as well as for capturing biogeochemically important features, such as high-nutrient low-chlorophyll (HNLC) regions, and their potential sensitivity to ongoing environmental change.

In this study we demonstrate that already the inherent structure of common NPZD models sets an upper limit to modeled export production, even under light-saturated and nutrient-replete conditions. This upper limit is determined by the functional form of the various ecosystem process descriptions, and their respective parameter settings, suggesting that ecosystem structure itself may regulate the amount of organic matter that sinks out of the euphotic zone. This finding is in contrast to the assumption that the amount of new and export production is essentially controlled through limitation of primary production by irradiance and nutrient supply. Our model results suggest that it may be difficult to decide whether bottom-up or top-down control of phytoplankton is more important in controlling ecosystem matter fluxes, since both approaches can yield a similar limitation of export production. Although relatively simple NPZD-type models may show good skill in reproducing observed current distributions of biogeochemical tracers, the question arises whether such models, in which export production is implicitly controlled by model structure and parameter values, can realistically simulate the sensitivity of biogeochemical cycles to environmental change.

1. Introduction

Marine ecosystem models have become increasingly important tools for improving our understanding of marine biogeochemical cycles, their role in the climate system and their sensitivity to environmental change. The suite of current marine ecosystem models ranges from highly simplified representations and parameterizations of marine biological processes to more sophisticated models, sometimes including different functional types of phytoplankton, multiple trophic levels or micronutrients such as iron (Kriest et al., 2010; Moore et al., 2004). Of major interest with regard to climate change and carbon uptake of the ocean is the simulation of export production, i.e. the vertical transport of organic matter out of the surface layer into the ocean interior due to gravitational sinking (Sarmiento and Bender, 1994; Volk and Hoffert, 1985). Historically, the surface layer was usually taken to be the euphotic zone (Eppley and Peterson, 1979), though on time scales of years or longer the depth of the winter mixed layer offers a more adequate delineation with respect to impacts on the atmosphere-ocean partitioning of CO_2 (Oschlies and Kähler, 2004). Export of organic matter occurs mostly in form of particles that sink through the water instead of moving with it and can therefore transport matter much faster into the ocean interior than can passive transport with the large-scale overturning circulation. The magnitude of export production is not only important with respect to carbon fluxes associated with the biological pump, but also determines concentrations of unutilized nutrients at the surface (Ito and Follows, 2005). In many regions, including the vast subtropical gyres, surface nutrients are generally depleted, indicating that biological uptake and export is large enough to balance the upward supply of new nutrients into the euphotic zone. Other regions, such as high-nutrient low-chlorophyll (HNLC) regions of the Southern Ocean, the eastern equatorial Pacific, and the subpolar North Pacific, display – in today's ocean – substantial amounts of surface nutrients all year round, indicating that export production in this regions is limited by processes other than the supply rate of macronutrients (Minas et al., 1986). The ability of models to correctly simulate the resulting patterns of surface nutrients is often used as one criterion to evaluate the quality of models. A realistic simulation of surface nutrients is particularly relevant in the context of climate change, because changes in the distribution of biotically unutilized nutrients can have a direct impact on the marine biological carbon pump and oceanic CO_2 uptake (Marinov et al., 2008). A realistic representation of surface nutrient concentrations will, in turn, depend on a reasonable simulation of spatial and temporal patterns of export production. Surface nutrient concentrations, export production, and the marine carbon

pump are thus closely interlinked, as is their sensitivity to environmental change. However, there is still a large gap in our understanding of many biological processes and their interplay, thus making it difficult to adequately describe them in marine ecosystem models.

A number of different methods have emerged and been applied to estimate export production from observations, e.g. based on sediment traps, oxygen consumption rates or thorium isotopes (Martin et al., 1987; Savoye et al., 2006). However, all of these techniques have their difficulties and assumptions, and consequently quantitative estimates of actual export production in the world oceans are still rare and are often available for specific locations only. Estimates of global patterns of export production are therefore often based on inverse modeling or empirical relationships of the ratio between particle export and primary production (ef-ratio) (Laws et al., 2000; Schlitzer, 2002). Consequently, estimates for global carbon export out of the euphotic zone spread widely, ranging from 5 GtC yr^{-1} (Henson et al., 2011) to 20 GtC yr^{-1} (Eppley and Peterson, 1979).

Since export production plays such a substantial role in the spatiotemporal distribution of inorganic carbon and nutrients, one would assume that a good representation of ecosystem dynamics and ultimately export production is a necessary condition for a good fit of model output to observational data of biogeochemical tracers. However, it has been shown that even very simplified models can reproduce global tracer distributions relatively well (Doney et al., 2009b; Kriest et al., 2010). This arises the question whether there is a "malfunctioning" in marine ecosystem models, that enables them to reproduce the "correct" magnitude in uptake and export of inorganic carbon and nutrients for the "wrong" reasons. This can be illustrated by HNLC regions as an example. It is commonly assumed and backed by observational evidence that HNLC areas are related to limitation of phytoplankton growth by the micronutrient iron when sufficient light and macronutrients are available (Boyd et al., 2000; Kolber et al., 1994; Martin et al., 1994). These regions can be reproduced with some success in numerical biogeochemical models that explicitly account for iron limitation (Aumont and Bopp, 2006). However, it has been shown that nutrient uptake of an ecosystem can be limited through other mechanisms, such as grazing (Armstrong, 1994; Sarmiento and Gruber, 2006). Thereby, supply of nutrients can exceed their utilization, resulting in a HNLC situation even when possible limitation by micronutrients is not accounted for. Furthermore, models that do not explicitly resolve iron, such as the model of Schmittner et al. (2008) can show good skill in reproducing non-zero surface nutrient concentrations in HNLC areas. We here

hypothesize that this apparent success is related to a maximum in export production implicitly imposed by the structure and parameter choices in such models.

Motivated by an analysis of some sensitivity tests with the global NPZD model by Schmittner et al. (2009, 2008) that showed an unexpectedly weak response of export production to changes in ocean circulation and associated nutrient supply to the surface layer, we here investigate whether and how an upper limit of export production may be imposed by the structure of commonly used global ecosystem models. To this extent, a NPZD-type marine ecosystem model is employed in different configurations, in order to investigate inherent mechanisms controlling export production. The potential implications will be discussed, also with their possible relevance to global applications of such ecosystem models in climate change simulations.

2. Methods

This study employs a hierarchy of structurally different marine ecosystem models is used, ranging from a very simple nutrient-phytoplankton-detritus (NPD) model to an NPZD type ecosystem model that has been successfully applied in centennial to millennial-scale biogeochemical simulations in the UVic global earth system model (Schmittner et al., 2008; Taucher and Oschlies, 2011). In all models, co-limitation of phytoplankton growth by light and nutrients is accounted for either by the minimum of the individual limitation factors (Liebig and Playfair, 1840) or by a multiplicative combination of these terms (Droop, 1983), as these are still the two most common approaches for representing co-limitation in large-scale biogeochemical models (but see recent approaches by Pahlow and Oschlies (2009) and Pahlow et al. (2013)). For the present study, we neglect nitrogen fixing diazotrophs and anaerobic remineralization. Consequently, modeled nitrogen and phosphorus fluxes are proportional to each other, and results are shown only for the nitrogen cycle.

For the sensitivity experiments reported here, the models are run in a 0-D version, i.e. one homogenously mixed surface ocean grid box with a thickness of 50 m is simulated for prescribed environmental conditions. In all experiments presented, continuous nutrient supply is set to an artificially high value of $flux_{NO_3}$ = 10,000 mmol N m^{-2} yr^{-1} (200 mmol N m^{-3} yr^{-1}). This ensures nutrient-replete conditions and the sensitivity of export production to different ecosystem processes can be investigated in isolation. Initial concentrations are 0.05 mmol N m^{-3} for phytoplankton and 0.025 mmol N m^{-3} for zooplankton (in the model

setups where zooplankton are included). Environmental forcing was, in a first step, calculated for 0° N and June (Brock, 1981), and thus simulates light-saturating conditions and relatively high temperatures allowing for high growth rates and a fast establishment of steady-state conditions. In the latitude-seasonality-experiments, the models are then run for different combinations of latitude, irradiance, day length and temperature, which are all kept constant for each individual model run. This way, environmental forcing for different oceanic regions can be mimicked. For example, the results for 80°N in June are obtained for an average irradiance and day length for this latitude and time of the year (calculated after Brock (1981)), and monthly average sea surface temperature (derived from World Ocean Atlas, see (Locarnini et al., 2006)). For all simulations environmental forcing is kept constant and each model is run for 180 days for the respective combination of latitude and month of the year. Although longer than the typical persistence of these conditions in the annual cycle, this procedure ensures that a steady state is reached and the results are independent of the initial conditions of the model simulations. This steady-state was usually reached after 3-4 weeks, which is still a reasonable time period for the assumption of relatively stable light and temperature conditions. Nevertheless, it has to be noted that the results represent a potential equilibrium state for given conditions and are not directly comparable to results from seasonally variable global earth system models, which include temporal variations of nutrient input and environmental forcing as well as vertical and lateral transports.

We tested the sensitivity of export production simulated by different structural model complexities to environmental changes. We generally begin with the simplest model possible and add complexity until the complete NPZD model is recovered. Thereby, the different factors that are commonly assumed to control HNLC regions (micronutrients, grazing, irradiance) can be investigated separately. Initial parameter values were adapted from the original NPZD setup used in previous global studies (Schmittner et al., 2008, 2009; Taucher and Oschlies, 2011) and modified in the various model runs to explore the model sensitivities to these values (see Table 1).

3. Model setups and results

Model hierarchy and complexity

Phytoplankton growth & mortality (NPD)

This is the structurally simplest model setup studied here. It has to be noted that some global models apply even simpler parameterizations of biological processes, some containing only nutrients as a state variable and a parameterization for uptake and sinking (Bacastow and Maier-Reimer, 1990; Kriest et al., 2010). However, such models cannot be considered as ecosystem models, but rather as purely biogeochemical models for global applications and are therefore not further discussed in the scope of this study. Marine ecosystem models may be regarded to require at least three compartments to explicitly export production: nutrients (here NO_3), phytoplankton and detritus, which is usually the only compartment that gravitationally sinks through the water column. The only phytoplankton loss term is the often assumed, but empirically difficult to constrain, phytoplankton mortality.

This phytoplankton loss is channeled into the detritus pool, allowing for sinking of organic matter and export production (EP) Source-minus-sinks terms (S) in this model setup are:

$$S(NO_3) = flux_{NO_3} + \mu_D D - J_P P \qquad (1)$$

where remineralization is calculated as a function of the remineralization rate at 0 °C (μ_{D0}) and temperature (T) via $\mu_D = \mu_{D0} b^{cT}$, J_P is the growth rate of phytoplankton (P), which is calculated as a minimum function of the light-limited growth rate (J_I) and nutrient-limited growth rate (J_{NO3}):

$$J_P(I, NO_3) = \min(J_I, J_{NO_3}) \qquad (2)$$

$$J_I = \frac{J_{max}\alpha I}{\sqrt{J_{max}^2 + (\alpha I)^2}} \qquad (3)$$

$$J_{NO_3} = J_{max} \cdot u_{NO_3} \qquad (4)$$

where α is the initial slope of the photosynthesis-irradiance-curve (P-I-curve) and J_{max} is the maximum phytoplankton growth rate, with the latter being calculated as a exponential function of temperature (T) following Eppley (1972) with the fixed parameters a, b, and c:

$$J_{max} = a \cdot b^{cT} \quad (5)$$

For the nutrient-limited growth rate, nitrate-limitation (u_{NO3}) is calculated with a Michaelis-Menten formulation including a half-saturation constant for nitrate (k_N):

$$u_{NO_3} = \frac{NO_3}{(k_N + NO_3)} \quad (6)$$

Changes in phytoplankton concentrations are then calculated as phytoplankton growth minus mortality:

$$S(P) = J_P P - \mu_P P \quad (7)$$

where μ_P denotes the phytoplankton mortality coefficient. Accordingly, the change in detritus (D) is calculated as phytoplankton mortality minus remineralization and sinking of detritus, where sinking occurs at a constant rate (ω_D).

$$S(D) = \mu_P P - \mu_D D - \omega_D D \quad (8)$$

(a) Linear phytoplankton mortality

In the first model setup phytoplankton mortality is linear, i.e. a constant fraction of phytoplankton biomass is turned into detritus every time step. Rapidly growing phytoplankton leads to increasing light-limitation through self-shading, which eventually leads to a decrease in light availability in the simulated water parcel and consequently decreases the realized specific growth rate (Figure 1). Consequently, when a certain concentration of phytoplankton is reached (~15 mmol N m^{-3}), primary production (NPP) is balanced by loss through mortality and export production remains constant while nutrients start to accumulate. Accordingly, NO_3 concentrations show a continuous

increase after this steady state is reached, where the realized growth rate equals the mortality of phytoplankton:

$$J_P = \mu_P \qquad (10)$$

For the parameter values of the original model setup (see Table 1) export production in steady state amounts to 5177.8 mmol N m^{-2} yr^{-1}. Assuming Redfield stoichiometry, this is be equivalent to 411 gC m^{-2} yr^{-1}, which is higher than observational estimates in most ocean regions. Depending on the parameter choice for maximum growth rate J_{max} and mortality μ_P, the system reaches a balanced state more or less quickly (on a timescale of days to weeks), and also the steady-state level of export production depends on the chosen parameter values. However, the sensitivity to export production to changes in mortality is relatively low. Increasing (decreasing) μ_P by 10% results in a decrease (increase) of EP by not even 1%. This underlines that the reason for the cease in phytoplankton growth is not driven by mortality, but rather by the effect of self-shading on light-limitation and associated growth inhibition. Accordingly, sensitivity to the maximum phytoplankton growth rate is larger: increasing (decreasing) J_{max} by 10% increases (decreases) EP by 7-8%.

(b) Quadratic phytoplankton mortality

In an attempt to reduce the otherwise unrealistically high phytoplankton concentrations simulated by the above model configuration, a quadratic phytoplankton mortality function can be employed. This increases mortality particularly at high phytoplankton concentrations and is often applied in marine ecosystem models. A quadratic mortality term also helps to make models more robust in terms of avoiding very high peaks of biomass concentrations. This quadratic relation can be considered as simulating loss due to viruses or aggregation, which both depend on the mutual encounter rate of phytoplankton cells.

$$S(NO_3) = flux_{NO_3} + \mu_D D - J_P P \qquad (11)$$

$$S(P) = J_P P - \mu_{P2} P^2 \qquad (12)$$

$$S(D) = \mu_{P2} P^2 - \mu_D D - \omega_D D \qquad (13)$$

The model behavior is generally very similar to the setup with linear mortality. Initially, at low phytoplankton concentrations the specific growth rate of phytoplankton J_P is higher than its mortality $\mu_{P2}P^2$, leading to growth under nutrient-replete and light-saturated conditions in the beginning of the simulation. Increasing light limitation through self-shading of phytoplankton then leads to a continuous decrease of J_P, reaching a steady state when loss balances growth (Figure 1):

$$J_P P = \mu_{P2} P^2 = \mu_D D + \omega_D D \qquad (14)$$

The system reaches equilibrium faster and at lower phytoplankton concentrations (~3.5 mmol N m^{-3}) than in the model with linear mortality, as the density-dependent formulation introduces an additional stabilizing feedback mechanism. Lower standing stocks of phytoplankton lead to lower rates of ecosystem processes and export production, which reaches its maximum at still relatively high 4423.0 mmol N m^{-2} yr^{-1} (352 gC m^{-2} yr^{-1} according to Redfield stoichiometry) in steady state.

Parameter sensitivity is similarly small as in the linear-mortality model. Increasing (decreasing) the quadratic mortality coefficient μ_{P2} by ±10% changes export production by only ±1%, whereas varying growth rate by ±10% results in a change in export production of ±8%.

The main difference between the models with quadratic and linear mortality is the level of maximum export production and the time until it is reached. In both cases, this occurs when light limitation through self-shading becomes so strong, that growth is balanced by loss through mortality. This scenario emerges from the structure of the ecosystem model and can be compared with the competition for space as the limiting factor in terrestrial ecosystems (Smetacek, 2012). Since the application of a quadratic mortality term can be considered more reasonable from a biological point of view (e.g. viral infections at higher densities) than a linear mortality function. This functional form is often used in ecosystem models (Schmittner et al., 2008) and will also be used in the following sections.

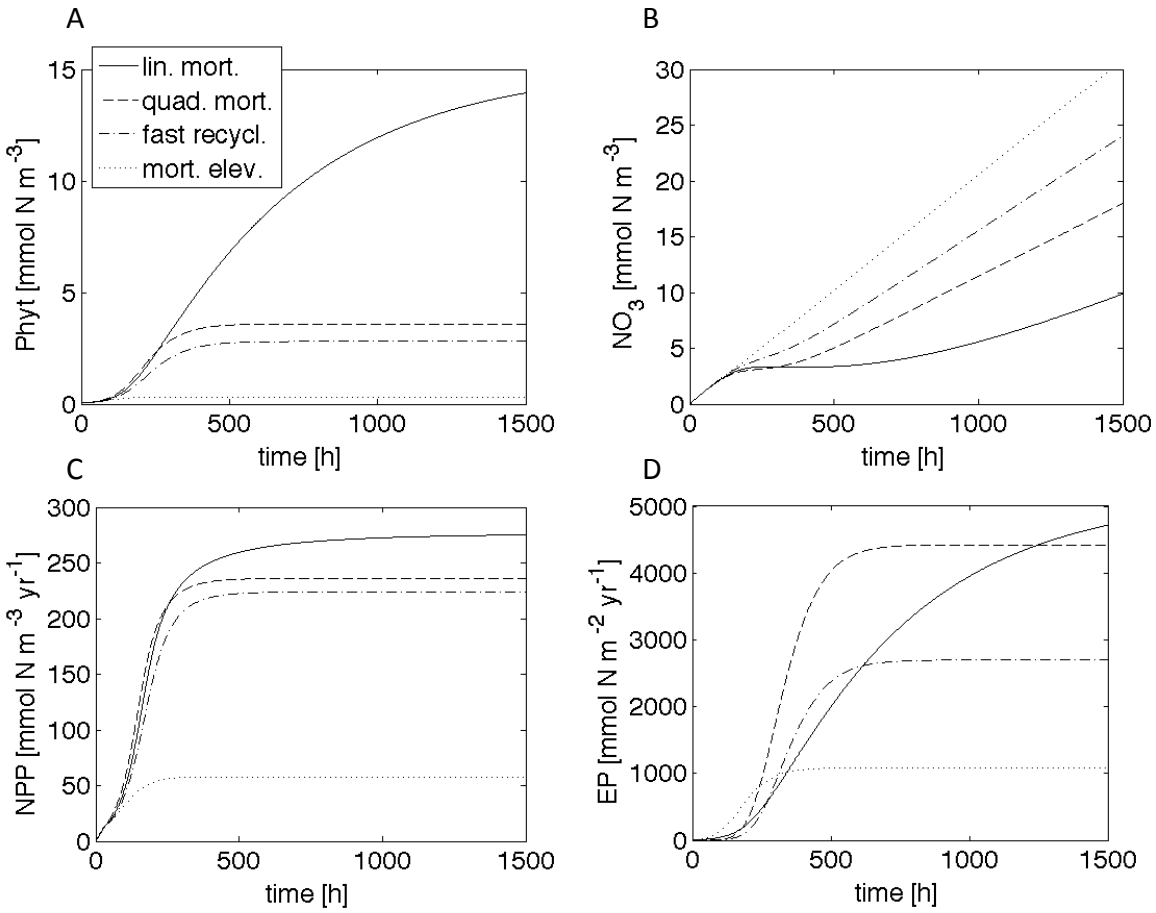

Figure 1: Ecosystem dynamics in the 0-D simulations with different model setups of the NPD model. (A): Phytoplankton [mmol N m^{-3}], (B) nitrate [mmol N m^{-3}], (C) net primary production [mmol N m^{-3} yr^{-1}], and (D) export production [mmol N m^{-2} yr^{-1}]. Shown are: NPD with linear mortality of phytoplankton (solid), NPD with quadratic phyto mortality (dashed), N-P-D with elevated quadratic phytoplankton mortality (morp=1.5, dotted), and NPD with fast recycling (dashed-dotted).

(c) Addition of a parameterization of the microbial loop

A second loss term to phytoplankton, fast recycling to inorganic nutrients, is introduced in this model setup. It consists of a linear loss term and can be considered a simplified representation of DOM cycling and the microbial loop. The specific rate of fast recycling μ_{P*} is determined by the linear mortality coefficient μ_{P0} and also depends on temperature in the same way as the maximum growth rate. However, this loss term is not channeled into the sinking detritus pool, but is directly remineralized back into dissolved inorganic nutrients:

$$\mu_{P*} = \mu_{P0} \cdot b^{cT} \quad (15)$$

$$S(NO_3) = flux_{NO_3} + \mu_D D + \mu_{P*} P - J_P P \quad (16)$$

$$S(P) = J_P P - \mu_{P*} P - \mu_{P2} P^2 \quad (17)$$

The general behavior of this system resembles that of the configurations discussed above (Figure 1). However, the inclusion of fast recycling as an additional loss term for phytoplankton lowers the maximum export production compared to the "mortality-only" case. Equilibrium phytoplankton stocks and primary production levels are lower, as a substantial fraction of phytoplankton is turned over by fast recycling. For the standard parameters, simulated export production in steady state reaches 2698.1 mmol N m^{-2} yr^{-1}, which is ~37% lower than in the setup with quadratic mortality only and corresponds to 214 gC m^{-2} yr^{-1}. Thus, turnover by fast recycling has a dampening impact on maximum possible export production, since the flow to the detritus pool still occurs only through phytoplankton mortality in this setup. Increasing (decreasing) the fast recycling coefficient μ_{P0} by 10% results in a decrease (increase) of export production of about 5%.

NPZD: mortality, fast recycling & grazing

By including zooplankton and grazing, a NPZD model is obtained that corresponds to the original model setup used in previous studies on a global scale (Schmittner et al., 2008; Taucher and Oschlies, 2011). It includes a grazing formulation of zooplankton on phytoplankton, in which the grazing rate depends on food concentrations (*Holling III*) (Gentleman et al., 2003; Holling, 1959). Loss of zooplankton biomass occurs through excretion and quadratic mortality. The grazing rate of zooplankton is calculated as:

$$G(P) = \frac{g\varepsilon P^2}{g + \varepsilon P^2} \quad (18)$$

where g denotes the maximum grazing rate and ε is the assimilation efficiency of zooplankton. Note that grazing is not temperature-dependent in this reference model setup. Change in Zooplankton (Z) concentration is then calculated as:

$$S(Z) = \gamma_1 G(P) Z - \gamma_2 Z - \mu_Z Z^2 \quad (19)$$

where γ_1 is the assimilation efficiency, γ_2 is the excretion rate and μ_Z is the mortality rate of zooplankton. Accordingly, the other source-minus-sink terms are given by:

$$S(NO_3) = flux_{NO_3} + \mu_D D + \mu_{P*} P + \gamma_2 Z - J_P P \quad (20)$$

$$S(P) = J_P P - \mu_{P*} P - G(P)Z - \mu_{P2} P^2 \quad (21)$$

$$S(D) = (1-\gamma_1)G(P)Z + \mu_{P2} P^2 + \mu_Z Z^2 - \mu_D D - \omega_D D \quad (22)$$

Compared to the previous model setups, grazing pressure strongly inhibits high standing stocks of phytoplankton and high rates of primary production (Figure 2A,C), as a large fraction of NPP is grazed by zooplankton. Lower phytoplankton concentrations keep self-shading effects small and the light-limited growth rate does not show large temporal changes and remains relatively high. Hence, phytoplankton is top-down controlled in this model setup, as opposed to the bottom-up controlled systems with the NPD model. Since a part of zooplankton biomass is lost through excretion and is, in this model setup, instantaneously remineralized to inorganic nutrients, only part of the grazed biomass is ultimately removed from the modeled box through vertical export. While the fraction of detritus that is remineralized remains the same as in the models above, detritus concentrations are lower in this model setup, as grazing pressure exerts strong top-down limitation on phytoplankton and consequently keeps overall biomass in the ecosystem relatively low. Consequently, maximum export production is much smaller compared to the previous model setups and amounts to 1025.1 mmol N m^{-2} yr^{-1} (or 81gC m^{-2} yr^{-1}), which is 65% lower than in the setup without grazing and well within the typical range of observational estimates. Interestingly, increasing (decreasing) the maximum grazing rate g by 10% results in a decrease (increase) of export by only ±1.5%. This relatively low sensitivity to parameter changes suggests that the model structure itself (i.e. including a density-dependent grazing term) stabilizes the system.

Modification of the closure term, i.e. zooplankton mortality μ_Z, does not show a large effect either. Increasing (decreasing) μ_Z by 10% (in the standard setup) leads to an increase (decrease) in export production of ±4%. The reason for this slight difference is that a higher mortality leads to a slower increase in zooplankton concentrations. Thus, a stronger phytoplankton bloom can develop, ultimately resulting in higher export production in steady state. Applying a linear formulation of mortality instead of the quadratic zooplankton mortality increases export from 1025.1 to 1378.6 mmol N m^{-2} yr^{-1}. The mechanism is similar to the above, i.e. a linear mortality leads to a higher loss of

zooplankton at low concentrations and thus the increase in predator biomass is slower, thereby allowing for a stronger bloom development and higher export production.

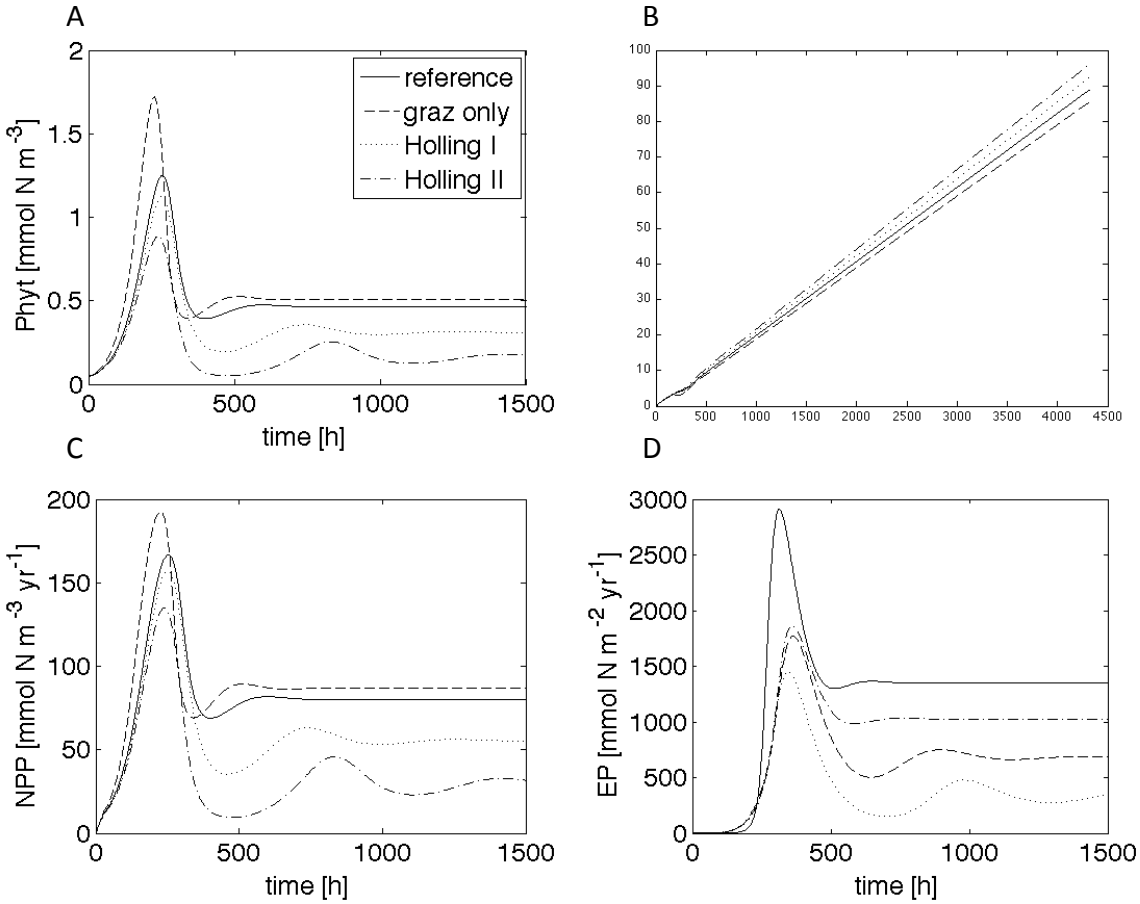

Figure 2: Ecosystem dynamics in the 0-D simulations with different model setups of the NPZD model. (A): Phytoplankton [mmol N m^{-3}], (B) nitrate [mmol N m^{-3}], (C) net primary production [mmol N m-3 yr-1], and (D) export production [mmol N m^{-2} yr^{-1}]. Shown are: NPZD reference (solid), NPZD only grazing as loss term (dashed), N-P-Z-D with Holling-I grazing formulation (dotted), and NPZD with Holling-II grazing formulation (dashed-dotted).

(a) Switching off phytoplankton mortality and fast recycling (grazing only)

Having seen that a stepwise increase in structural model complexity from a simple NPD to a more common NPZD-type model always leads to a finite maximum value of export production under nutrient-replete conditions, we now explore whether switching off part of the phytoplankton loss terms can lead to qualitatively different results. Accordingly, concentrations of state variables are calculated as:

$$S(NO_3) = flux_{NO_3} + \mu_D D + \gamma_2 Z - J_P P \quad (23)$$

$$S(P) = J_P P - G(P)Z \quad (24)$$

$$S(Z) = \gamma_1 G(P)Z - \gamma_2 Z - \mu_Z Z^2 \quad (25)$$

$$S(D) = (1-\gamma_1)G(P)Z + \mu_Z Z^2 - \mu_D D - \omega_D D \quad (26)$$

When switching off phytoplankton mortality and fast recycling, the model behavior is similar to the original NPZD model setup including all loss terms (Figure 2), however the absolute values are different and steady-state nutrient-replete export production amounts to 1349.2 mmol N m^{-2} yr^{-1}. However, this is only ~32% higher than in the original model with all loss terms, indicating that most of the potential increase in phytoplankton stocks and associated processes that would be expected through less mortality and fast recycling gets compensated through intensified zooplankton grazing. Also note that export production in this setup is still much lower than in the simulations with only mortality and fast recycling (compare Figure 2D and 1D),

Parameter sensitivity to the maximum grazing rate *g* is similarly small as in the original NPZD model. Increasing (decreasing) *g* by 10% changes export production by only ±2%. Since grazing is density-dependent, increasing (decreasing) the grazing parameters only results in slightly stronger phytoplankton increase, until concentrations are high enough for grazing to intensify irrespective of the chosen grazing parameters (through density-dependence). In this respect, the shape of the functional response is much more important than the particular parameter choice.

Altogether, these findings demonstrate that even a relatively large change in the parameterization of top-down control on phytoplankton does not allow as high levels of export production as in the setups without grazing. Thus, the structural change in the model through switching from bottom-up to top-down control of phytoplankton has a significant effect on the regulation of nutrient utilization and export production in our typical NPZD model.

Sensitivity to variations in functional forms

Having seen that all NPD and NPZD-type model configurations investigated so far yield some upper limit of simulated export production under nutrient-replete conditions, we now investigate whether this is due to the particular functional forms used in these

models. We investigate the sensitivity of our above results first to changes in the functional form of phytoplankton primary production and then to grazing.

Co-limitation of phytoplankton growth

To investigate whether the formulation for co-limitation of phytoplankton growth by light and nutrients has an impact on the results, a multiplicative approach for co-limitation is tested to replace the previously applied minimum function:

$$J_P(I, NO_3) = J_I \cdot u_{NO_3} \qquad (27)$$

Simulated export production is almost equal to the original model setup with the minimum function and amounts to 1011.1 mmol N m^{-3} yr^{-1}. Differences between this and the original model setup mainly occur at very low nutrient concentrations, i.e. when nutrient limitation is relatively strong and the product of the terms for nutrient and light limitation is significantly lower than the value returned by the minimum function used in the simulations presented above. However, the results suggest that the overall behavior of the system and simulated export production are barely affected by the formulation of co-limitation by light and nutrients.

Sensitivity to different grazing formulations

It is commonly assumed that grazing exerts a strong top-down control on phytoplankton in the real ocean and thus it can be expected that the same should be true for the modeled ecosystem. As shown above, incorporating a grazing formulation into the ecosystem model substantially alters the sensitivity of the model. This suggests that changes in the grazing function may have a strong impact on representation of ecosystem dynamics and the spatial and temporal pattern of export production in marine ecosystem models. In order to test the sensitivity of the ecosystem model to the grazing formulation, several aspects are investigated here: The role of different functional responses in the grazing formulation (Holling I – III), the structural complexity of the grazing formulation (i.e. predation on multiple prey types), and the effect of temperature-dependent grazing rates.

(a) Functional response to prey density

The functional response of grazing to prey density, i.e. the shape of the grazing function has a considerable impact on ecosystem dynamics and export production in our model

simulations (Figure 3A). We tested the three most common types of functional responses for the grazing formulation (de Boyer Montégut et al., 2004; Gentleman et al., 2003).

While the original NPZD model that applies a Holling III-type (sigmoidal) function reaches export production of 1025.1 mmol N m^{-2} yr^{-1}, maximum export production is limited to 682.5 and 330.6 mmol N m^{-2} yr^{-1} with the Holling I (linear), and Holling II (saturating, Michaelis-Menten) function for otherwise same parameter values (Figure 2D). A model setup without phytoplankton mortality and fast recycling (i.e. grazing as the only loss term) shows the same sensitivity with export production amounting to 1349.2 (Holling III), 471.2 (Holling II) and 967.5 mmol N m^{-2} yr^{-1} (Holling I). Even though these differences occur at relatively high rates of export production, they are mainly attributable to the different shape of the grazing functions at low phytoplankton concentrations (< 1 mmol N m^{-3}), as this has a substantial effect on the development of the bloom (Figure 3C): Initial concentrations of phytoplankton in the presented NPZD simulations are low (0.05 mmol N m^{-3}) and rarely exceed 1.5 mmol N m^{-3} even during the bloom (Figure 2A). Thus, differences in grazing pressure at low concentrations strongly modify bloom dynamics and thereby steady-state export production (Figure 2D). The higher the grazing pressure during the bloom development, the lower the maximum phytoplankton biomass and export production in steady state. The Holling II function (Michaelis-Menten) exerts the strongest grazing pressure at low phytoplankton concentrations, followed by Holling I (linear) and Holling III (sigmoidal).

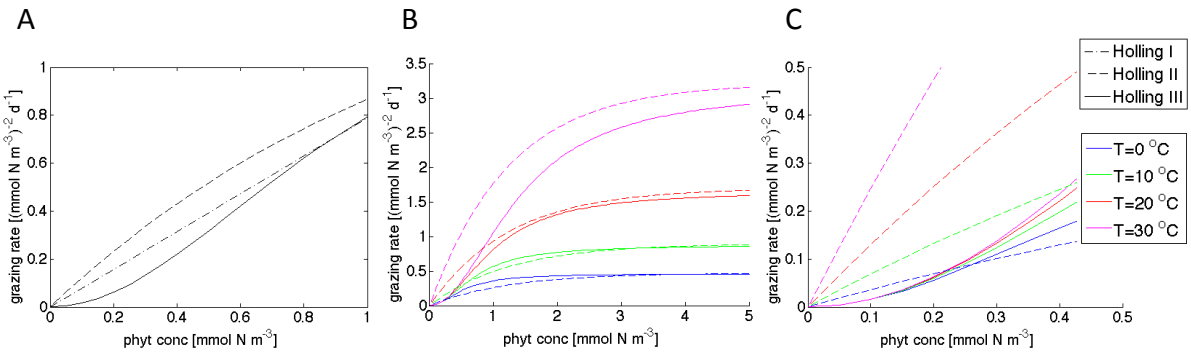

Figure 3: (A) Functional response of the grazing rate in relation to prey density using Holling I (dashed-dotted), Holling II (dashed) and Holling III (solid) functions. (B) Relationship between phytoplankton density and zooplankton grazing in the original model using Holling III (solid) and with Holling II (dashed) at different temperatures: 0°C (blue), 10°C (green), 20°C (red) and 30°C (magenta). (B): covering a broader spectrum of prey densities (from 0 – 5 mmol m-3) in panel (B). (C) Close-up of insert of panel B to illustrate differences between the models at low prey concentrations (< 0.5 mmol m^{-3}).

(b) Structural complexity of top-down control: Switching between different prey items

This setup includes a more complex grazing formulation with zooplankton switching between different food sources and respective food preferences, as has recently been included in the new ecosystem model component developed by (Keller et al., 2012) for the UVic model (see Table 1). In contrast to the original model (2008, 2009) model, zooplankton is now assumed to also graze on detritus and other zooplankton (self-predation). Grazing is a function of prey density and is described by a multiple-prey Holling II functional response in the setup applied by Keller at al. (2012). Preferences (ψ) are assigned for different kinds of prey. The rate of grazing on phytoplankton (*P*), detritus (*D*) and zooplankton (*Z*) is calculated as:

$$G(P) = gZ\theta_P P \quad (28)$$

$$G(D) = gZ\theta_D D \quad (29)$$

$$G(Z) = gZ\theta_Z Z \quad (30)$$

where:

$$\theta_P = \psi_P/\varphi \quad (31)$$

$$\theta_D = \psi_D/\varphi \quad (32)$$

$$\theta_Z = \psi_Z/\varphi \quad (33)$$

and φ is the sum of all available prey and the half-saturation constant for grazing k_{graz}:

$$\varphi = P + D + Z + k_{graz} \quad (34)$$

The sum over all food preferences is one, and the maximum grazing rate g is temperature-dependent in this standard model setup (Keller et al., 2012):

$$g = g_0 \cdot b^{cT} \quad (35)$$

where g_0 is the maximum grazing rate at 0 °C and *b*, *c* are parameters as used in eq. 4. For a more detailed description and rationale behind these equations see (Keller et al., 2012). Maximum export production is this model setup amounts to 466.4 mmol N m^{-2} yr^{-1} (37 gC m^{-2} yr^{-1}), and is thus considerably lower than in the model with the original grazing formulation. However, the number is very similar to the setup with the Holling II

formulation. Consequently, differences between this grazing formulation and the original model mainly occur due to the shape of the grazing function at low phytoplankton concentrations, which has a substantial impact on simulated bloom dynamics as discussed above. On the other hand, the structural complexity that is introduced by adding multiple types of prey and self-predation seems to be of minor importance for simulated bloom dynamics and the amount of export production.

Summary of 0-D simulations: Limitation of export production without typical HNLC factors

Altogether, the results presented above demonstrate that all applied NPD and NPZD models contain an upper limit of export production and under nutrient-replete and high-irradiance conditions. At the same time, non-utilized nutrients accumulate, leading to a HNLC situation without accounting for the micronutrient iron, and even without grazing. In this regard it is noteworthy that even a very simplistic, bottom-up limited model structure, as applied in the experiments with the NPD model, is already sufficient to set an upper limit to nutrient uptake and export production. This limitation arises without simulating either zooplankton grazing or micronutrients, and is solely attributable to the increase in light limitation through self-shading at certain cell densities. This is surprising, as it should be expected that growth is light-saturated at high irradiance (~250 W m^{-2}) and phytoplankton concentrations that are commonly observed in the ocean (Körtzinger et al., 2001).

Adding more structural complexity by including a higher trophic level (zooplankton) revealed a substantial effect on the upper limit of export production. The experiments with the NPZD model demonstrated that while this upper limit is strongly controlled by the functional form of the various parameterizations of e.g. grazing or mortality, the sensitivity to parameter changes of the different processes is relatively small. This suggests that the upper limit of export production may be entirely attributable to the model structure itself, and relatively independent of parameter choice. In the following it will be shown how this simulated limitation of export production translates into spatiotemporal patterns, and it will be discussed what this might imply for interpreting results of global marine ecosystem models.

Table 1: Ocean Ecosystem and Carbon Cycle Model Parameters used in the sensitivty experiments.

Parameter	Symbol	Units	NPZD (Schmittner et al. 2008)	NPZD (Keller et al. 2012)
Phytoplankton (P)				
Maximum growth	a	d^{-1}	0.2	0.6
Temperature	b	dimensionless	1.066	1.066
Temperature	c	$°C^{-1}$	1.0	1.0
Initial slope of P-I-	α	$(W\ m^{-2})^{-1}\ d^{-1}$	0.1	0.1
Half-saturation	k_N	$mmol\ m^{-3}$	0.7	0.7
Mortality	μ_P	$(mmol\ m^{-3})^{-1}\ d^{-1}$	0.05	0.03
Fast recycling	μ_{P0}	d^{-1}	0.014	0.015
Zooplankton (Z)				
Assimilation	γ_1	dimensionless	0.925	0.7
Maximum grazing	g	d^{-1}	1.575	1.3
Prey capture rate	ε	$(mmol\ m^{-3})^{-2}\ d^{-1}$	1.6	
Mortality	μ_Z	$(mmol\ m^{-3})^{-2}\ d^{-1}$	0.34	0.06
Excretion	γ_2	d^{-1}	0.01	
Grazing half	k_{graz}	$mmol\ N\ m^{-3}$		0.15
Feeding	ψ_P	dimensionless		0.35
Feeding	ψ_Z	dimensionless		0.35
Feeding	ψ_D	dimensionless		0.3
Detritus (D)				
Remineralisation	μ_{D0}	d^{-1}	0.048	0.048
Sinking speed	ω_{D0}	$m\ d^{-1}$	7.0	10.0

Spatiotemporal patterns of export production

The results for the 0-D experiments in the previous section are valid for specific conditions (perpetual model forcing for 0°N and June) of the environmental parameters irradiance, day length, temperature, and nutrient supply, the latter of which was chosen to be very large in order to test whether or not the various ecosystem models reach some implicit upper limit of simulated export production. Simulated export production might reach higher values on the short term, e.g. during non-steady-state situations such as strong spring blooms where environmental control changes rapidly. Environmental conditions essentially control ecosystem processes and matter fluxes, and consequently the amount of export production is controlled by these boundary conditions, e.g. higher light levels and higher temperatures allow for higher growth rates of phytoplankton and faster

element cycling in the system. To mimic application of the different ecosystem models to fully three-dimensional global models, various zero-dimensional model runs were performed for different settings of environmental parameters, representing different latitudes and times of the year. Thereby the spatial and temporal pattern of maximum export production and its sensitivity to the model structure can be estimated. Note that these simulations still represent steady-state solutions for respective environmental parameters for an assumed 50m deep surface mixed layer, rather than fully dynamic 3-D ocean model simulations.

Different model structures

In the original NPZD model configuration (2008, 2009), simulated maximum export production under nutrient-replete conditions amounts to ~1000 mmol N m^{-2} yr^{-1} at low latitudes throughout the year and between 0 and ~700 mmol N m^{-2} yr^{-1} at high latitudes, depending on the month and associated temperatures and light availability (Figure 4A). These numbers are in the same range as estimates for export production in the open ocean based on observations (Laws et al., 2000; Schlitzer, 2004).

Switching off fast recycling leads to a general increase in the upper limit of export production by 20-30% (Figure 4B). This result is similar to the one from the equatorial 0-D simulations presented above.

When mortality and fast recycling are set to zero and grazing is the only top-down control on phytoplankton growth (Figure 4C), export production increases between 15 and 35% compared to the reference configuration with all phytoplankton loss terms switched on (Figure 4A). The largest differences are found at low latitudes, where the top-down control through temperature-dependent fast recycling is relatively high in the reference setup.

When grazing is set to zero, maximum export production increases substantially, by up to 300% at low and 500% at high latitudes compared to the original model setup (Figure 4D), depending on the relative influence of temperature on phytoplankton growth and loss processes at different latitudes. In the absence of grazing, export production at low latitudes is strongly controlled by fast recycling. This becomes visible when comparing the model setup with both grazing and fast recycling turned off and (quadratic) mortality being the only phytoplankton loss term (Figure 4E,F) with the model setup where fast recycling is included, and export production is much higher (Figure 4D).

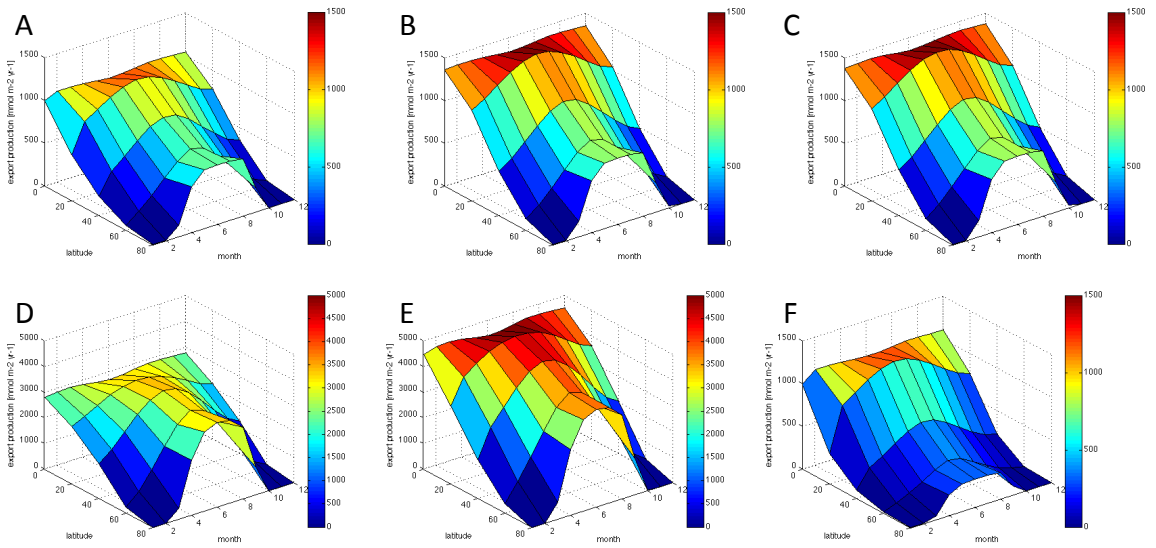

Figure 4: Effects of different model structures on the spatiotemporal pattern of export production [mmol N m^{-2} yr^{-1}] for (A) the original NPZD model, (B) the NPZD setup without fast recycling, (C) the NPZD model without phytoplankton mortality and fast recycling, i.e. grazing only, (D) the NPD setup without grazing (note that scale is 0-5000 mmol N m^{-2} yr^{-1} in this panel), (E) the NPD setup without both grazing and fast recycling (i.e. phytoplankton mortality only, note that scale is 0-5000 mmol N m^{-2} yr^{-1} in this panel), and (F) the NPD setup without both grazing and fast recycling (phytoplankton mortality only) with an increase of the phytoplankton mortality parameter from 0.05 to 1.5.

Generally, the spatial and seasonal variability of the maximum possible export production in the different model configurations confirms the results from the previous section, i.e. that an upper limit of export production is structurally inherent in commonly used (NPZD-type) ecosystem models, and that this limit is only modified through the various processes and loss terms. For typical model parameters, the maximum possible export production of the models may be reached in global model applications. While such models may be tuned to reproduce current observations, it cannot be ruled out that the sensitivity of simulated export production to environmental change is controlled by the model-implicit limits to export production.

Furthermore, it is notable that spatial and temporal patterns of maximum export production very similar to the original NPZD model can be achieved even in the simplest NPD model setup through self-shading and phytoplankton mortality as the only loss term, although the absolute magnitude of simulated export production is, for the standard parameter values, systematically larger for the NPD model compared to the NPZD model (Figure 4A,E). With suitable parameter values even a similar magnitude of maximum export production as in the original model setup can be achieved (Figure 4F). This already

indicates that very different functional controls can yield very similar results for a large range of environmental conditions.

Role of the functional response for grazing

The results of the 0-D experiments with the original NPZD model (3.1.1. through 3.1.3.) support the hypothesis that top-down control through grazing can be a strong mechanism in controlling export production.

As already apparent from the 0-D experiments, the functional response of grazing has a substantial impact on simulated ecosystem dynamics and export production, mostly due to its impact at low phytoplankton concentrations and therefore the development of a plankton bloom. This is also valid for the simulations of the spatiotemporal pattern. While maximum EP reaches ~1000 mmol N m^{-2} yr^{-1} at low latitudes and up to ~700 mmol m^{-2} yr^{-1} at high latitudes in the original NPZD model with a Holling III grazing formulation, it only amounts to ~330 (low latitudes) and ~100 mmol m^{-2} yr^{-1} (high latitudes) with Holling II, and ~700 (low latitudes) and ~250 mmol m^{-2} yr^{-1} (high latitudes) with Holling I, respectively (Figure 5A-C). Since phytoplankton concentrations rarely exceed 1-1.5 mmol N m^{-3} in the simulations, the behavior of the grazing function in the range between 0 and 1 mmol N m^{-3} has such a strong impact on bloom development and maximum export production.

Role of temperature dependence in grazing

(a) Holling III / original model

Temperature dependence of the maximum grazing rate (g) was incorporated according to eq. 35. Interestingly, this does not show a large effect on the upper limit of export production in the original model and the spatiotemporal pattern of export production changes only slightly compared to the original setup (Figure 5F). While maximum export production is very similar at low latitudes (~1000 mmol N m^{-2} yr^{-1}), the difference in export production gets slightly larger at high latitudes (up to 850 mmol N m^{-2} yr^{-1} compared to 700 mmol N m^{-2} yr^{-1} in the setup without temperature dependence). The reason is that temperature-dependent grazing is inhibited at low temperatures and consequently higher phytoplankton growth and export production occur compared to the model formulation with temperature-independent maximum grazing rate. However, the overall spatiotemporal pattern of export production is not substantially different from the model setup without temperature dependence. This is mainly attributable to the fact the

temperature effect on grazing is almost non-existent at low phytoplankton concentrations in this formulation (Figure 3B,C). Since phytoplankton concentrations do not reach values higher than ~1.5 mmol N m^{-3} in the model simulations (limited by grazing and other loss terms), the differences in actual grazing rates at different temperatures are relatively small with this grazing formulation. Consequently, the effects of including temperature dependence on grazing dynamics and overall model behavior are relatively minor.

(b) Holling I and II

In contrast to the Holling III grazing parameterization, temperature effects on grazing are already very pronounced even at low phytoplankton concentrations in the model setup with a Holling I and II grazing formulation (Figure 3B,C). This mechanism explains why the pattern between low and high temperatures (i.e. high and low latitudes) becomes so different when applying a Holling I or II formulation. Compared to the original model, maximum export production is much lower at low latitudes (< 300 mmol N m^{-2} yr^{-1}) and reaches much higher values (< 1500 mmol N m^{-2} yr^{-1}) at high latitudes when temperature effects are included (Figure 5D,E). At low latitudes, high temperatures result in high grazing rates and thus a strong top-down control on phytoplankton, inhibiting the development of high standing stocks of phytoplankton, and reaching a steady state with lower maximum export production than in the original model. The opposite effect occurs at high latitudes, where the maximum export production is much higher than in the original NPZD model. This is mainly attributable to a much weaker top-down control of grazing during the productive period when light is sufficient (late spring to early fall). Low temperatures slow down grazing substantially and thereby allow for a strong bloom development and high standing stocks of phytoplankton. Thus, the latitudinal pattern is the opposite than in the original NPZD model, with maximum values of export production now occurring at high rather than low latitudes. However, since estimates on global export production and associated spatial patterns are highly variable (Henson et al., 2011; Laws et al., 2000), it is not possible to determine which simulated latitudinal pattern is more realistic.

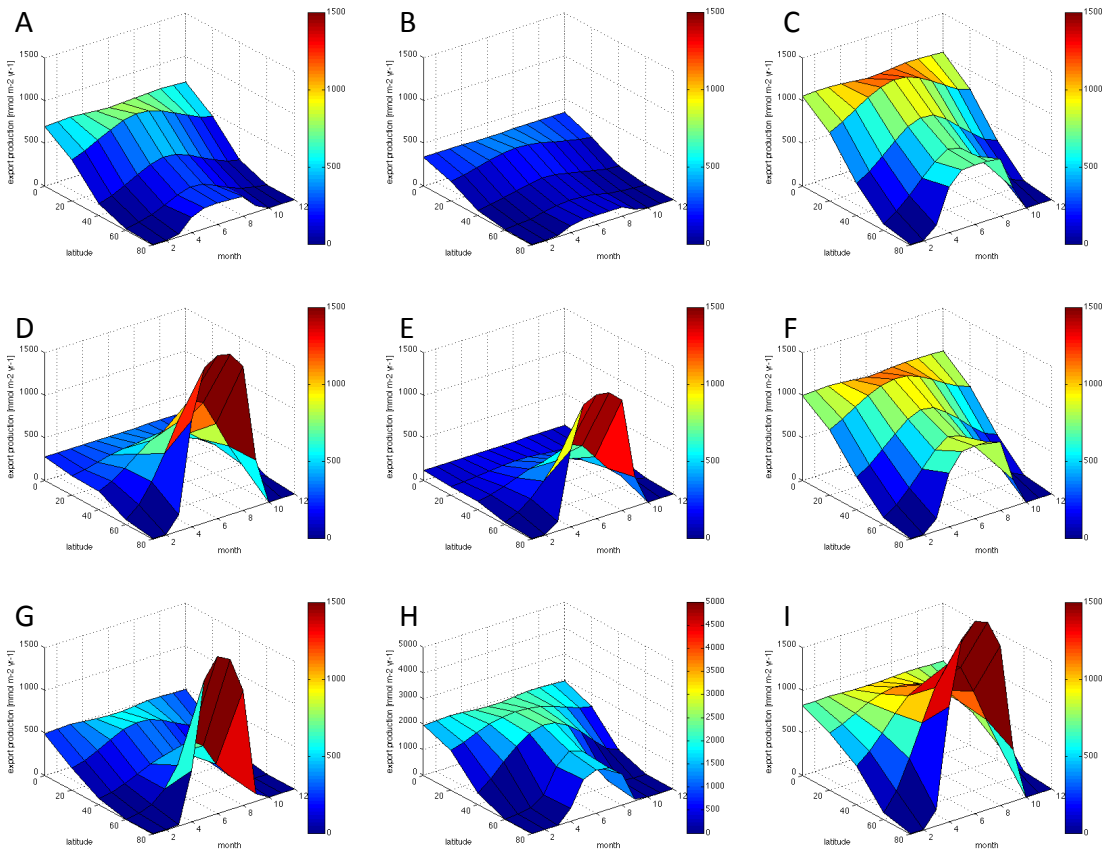

Figure 5: Effects of grazing control on the spatiotemporal pattern of export production [mmol N m^{-2} yr^{-1}]. Model setups with a (A) Holling I, (B) Holling II, and (C) Holling III formulation without temperature dependence. Model setups including temperature dependence for the maximum grazing rate for the (D) Holling I, (E) Holling II, (F) and Holling III formulation. (G,H) Model with and alternative grazing formulation (Keller et al., 2012) with (G) and without (H) temperature dependence for the maximum grazing rate (note that scale is 0-5000 mmol N m^{-2} yr^{-1} in panel H). (I) Original NPZD model setup without temperature dependence for any biological processes.

Switching off temperature dependence for all ecosystem processes

A model setup using the original NPZD model with Holling III grazing, however without any temperature sensitivities for autotrophic or heterotrophic processes shows a spatiotemporal pattern similar to the Holling-I and Holling-II model versions with temperature-dependent grazing (Figure 5D,E,I). Thus, including (the identical) temperature dependence either for all or none of the ecosystem processes results in a similar spatiotemporal pattern, where export production under nutrient-replete conditions is strongly elevated at high latitudes. As a consequence, such a model setup might need further factors, such as the micronutrient iron, in order to obtain lower export production in subpolar and polar HNLC regions. Nevertheless, the model configurations

with temperature-independent grazing suggest that this is also possible through the balance of production and loss terms, and their respective temperature dependence.

Does structural complexity of grazing matter?

In a global application of their modified NPZD model with the modified grazing formulation, Keller et al. (2012) argued that the incorporation of the micronutrient iron was necessary in order to correctly simulate HNLC regions. This seems to contradict our hypothesis of an inherent upper limit of export production and that very simple models with only one loss term are sufficient to capture the spatiotemporal pattern of global export production (given the parameters are accordingly adjusted).

The standard formulation of the Keller et al. (2012) model includes temperature dependence of the maximum grazing rate. The application of this Holling III grazing formulation leads to significant changes in the spatiotemporal pattern of modeled export production compared to the original Schmittner et al. (2008) model (Figure 5G), but is very similar to the Holling I and II models discussed above (Figure 5D,E). Maximum export production is much lower at low latitudes (~500 mmol N m^{-2} yr^{-1}) and reaches much higher values (~1800 mmol N m^{-2} yr^{-1}) at high latitudes (Figure 5G) than in the original Schmittner et al. (2008) NPZD model. The mechanism is basically the same as for the Holling I and II formulation with temperature dependent grazing, i.e. differential suppression of grazing at high latitudes and low latitudes leading to steady-states with more or less standing stocks of phytoplankton biomass. Switching off temperature dependence in the model with the new grazing formulation results in a spatiotemporal pattern more similar to the original NPZD model, i.e. higher values of export production at low latitudes and lower values at high latitudes, even though a reparameterization would be necessary to achieve a similar magnitude (Figure 5H). Consequently, the spatiotemporal pattern of simulated export production is controlled by different temperature sensitivities of the grazing on phytoplankton rather than by bottom-up limitation e.g. through micronutrients.

4. Synthesis: Model mechanisms that limit export production

We carried out a series of tests with a variety of model setups of different complexities and formulations of biological processes. The model simulations reveal the existence of an upper limit of phytoplankton productivity and ultimately export production in marine ecosystem models, which makes simulated export fluxes essentially insensitive to

enhanced nutrient supply once a threshold has been crossed. This maximum in simulated export production exists for all functional forms of NPD and NPZD models investigated. The maximum level of the simulated export production depends on the number and structural form of the loss terms and their relative influence (i.e. the chosen respective parameters). Values of simulated maximum export production in the order of ~1,000 mmol N m^{-2} yr^{-1} or ~80 g C m^{-2} yr^{-1} lie well in the range of observational data for export production (Henson et al., 2011; Laws et al., 2000; Martin et al., 1987).

Our results show that the strongest control on maximum export production in most ecosystem models is the top-down control of phytoplankton by zooplankton grazing. This is in line with previous work that demonstrated the varying effects of grazing limitation and nutrient limitation on marine ecosystems (Armstrong, 1994). According to our results, different formulations and temperature sensitivities of the simulated grazing pressure can have a strong influence on the spatial patterns and the magnitude of ecosystem nutrient uptake and export production, as well as on its simulated sensitivity to environmental change. The sensitivity experiments with different grazing formulations revealed that the functional response to prey density is crucial, particularly through its effect at very low phytoplankton concentrations and thereby on the bloom development.

Some of the model configurations explored above simulate maximum levels of export production at high latitudes that are much higher than observational estimates. This is no surprise as the nutrient supply prescribed in the models is also much higher than observed in the real ocean. Still, additional controlling factors on phytoplankton could be envisaged that further limit export production in (macro)nutrient replete conditions. Keller et al. (2012) have shown that this can, in a global model, be achieved with the introduction of iron as a micronutrient. This limits simulated phytoplankton growth and ultimately export production in large parts of the ocean with relatively low temperatures and high nutrients (e.g. the Northern Pacific, Southern Ocean) and is therefore required to capture HNLC regions in their model. However, this applies only to the combination of the NPZD model with the temperature-dependent Holling II grazing formulation used by Keller et al. (2012). Furthermore, the effect on spatiotemporal dynamics depends strongly on the type of the applied grazing formulations (here Holling II) and the balance between production and loss processes and, in particular, the inclusion of temperature dependence or not.

In this regard, a crucial aspect is temperature-dependence of all processes in the model. A growing body of experimental evidence suggests that different temperature sensitivities for autotrophic and heterotrophic processes might have a substantial impact on

ecosystem functioning and biogeochemical cycling (O'Connor et al., 2009; Taucher et al., 2012; Wohlers et al., 2009). Despite this increased attention of temperature effects in experimental studies, the representation of temperature dependence in ecosystem and biogeochemical modeling is still rudimentary and differs considerably among different models (Sarmiento et al., 2004; Steinacher et al., 2010), although it has been shown that temperature effects can have a significant impact on biogeochemical dynamics in global modeling studies (Taucher and Oschlies, 2011). A better implementation of temperature effects on different ecosystem processes could thus help to improve our understanding of the mechanisms controlling spatial and temporal distribution of export production, their sensitivity to environmental change and their representation in ecosystem models.

Furthermore, even in a model setup without top-down control by zooplankton, export production is limited by model structure, e.g. through phytoplankton mortality and self-shading. Our results show that even the simplest bottom-up model setup with only phytoplankton growth and mortality can, with the right parameterization, capture the same broad spatiotemporal pattern of export production as the more complex and realistic models. A broad range of models with different structural complexities was capable of simulating similar results, e.g. an upper limit to export production and associated spatiotemporal dynamics. Earlier global models used a very simplified representation of marine biogeochemistry, were export production was only a function of nutrient supply and surface nutrients were restored, and achieved reasonably realistic results with this simple bottom-up approach (Najjar et al., 1992). Over the last decades model development resulted in a variety of more sophisticated global biogeochemical models, ranging from still rather simple NPZD-type models to approaches with higher trophic levels or plankton functional types (Le Quéré et al., 2005; Steinacher et al., 2010). In accordance with the prevailing opinion of a strong control of higher trophic levels on marine ecosystem dynamics, all of these models rely on a strong top-down control on phytoplankton primary production and ultimately export production.

The varying importance of bottom-up and top-down mechanisms in different models can be illustrated with an example, the correct representation of HNLC regions, which has long been considered a huge challenge in global ocean modeling. There are different explanations for the persistence of these regions, ranging from light limitation, strong grazing control to iron limitation, with the latter being the most prominent one. A reasonable simulation would require low nutrient uptake and export production at high latitudes (e.g. in the North Pacific or the Southern ocean), as well as in some regions at

low latitudes (e.g. the Equatorial Pacific). Our model experiments show that, in principle, the simulation of HNLC areas is possible in models that do not account for limitation by the micronutrient iron and, in fact, not even the inclusion of grazing is necessary, when a single loss term is parameterized accordingly. The reason is that common model structures ultimately result in increasing light limitation through self-shading by phytoplankton. As soon as its biomass reaches a certain threshold value, primary production is balanced by mortality, thereby establishing an upper limit to biomass and export production. Consequently, there are different mechanisms that are capable of simulating a HNLC environment reasonably well: limitation by the micronutrient iron, strong top-down control by zooplankton, or – in the simplest way – limitation of phytoplankton growth by self-shading of the cells. Since all model approaches deliver similar results for given environmental conditions, this illustrates the difficulties of identifying the correct and most realistic mechanism and, associated with that, the proper sensitivity to environmental forcing.

The fact that the same amount of simulated export production can, in our model simulations, be achieved with structurally very different model setups also raises the question if the limitations on productivity in marine environments are properly understood and represented in biogeochemical modeling approaches. A comparison with terrestrial ecosystems might illustrate this. The paradigm for the limitation of productivity on land suggests that the dominant mechanism is the competition for resources, i.e. bottom-up limitation. If there is enough water, plants compete for light and bottom-up control is ultimately a competition for the occupation of space. Our model simulation suggests that this could also be the case for aquatic systems. Although, the common view suggests a dominant role of top-down control through predators, the model experiments show that the ultimate constraint is space. Without higher trophic levels exerting control on primary producers and assuming infinite nutrients, sufficient light supply is only available, until a certain cell density in the water body is reached. This corresponds to a bottom-up control much similar to that on land, suggesting that we cannot rule out that the factors that control growth on land and in the ocean are may be more similar as usually believed (Smetacek, 2012).

5. Conclusion

Our model experiments suggest that high-nutrient low-chlorophyll regions and upper limits of export production under nutrient-replete conditions can be reproduced with structurally very different types of ecosystem models. These may range from simple bottom-up ecosystem models, which include only nutrients, phytoplankton and one loss term, to more complex top-down controlled models that include higher trophic levels and food-web dynamics. As a consequence, this implies that at least some models may reproduce observed tracer fields (e.g. nutrient patterns) for the wrong reasons. In particular, sensitivities to environmental forcing and change might be erroneous, despite an apparently good fit to observations for the present ocean, thereby adding substantial uncertainties to simulations of ongoing climate change.

However, models cannot be simply improved by adding complexity and thereby "realism", e.g. through adding multiple functional types or size classes, as long as we lack the data to constrain parameter values and meaningfully represent ecological interactions (Anderson, 2005; Flynn, 2006). For instance, our results demonstrate that zooplankton grazing can play a major role in controlling the total biomass of the ecosystem and ultimately export production. However, many commonly used zooplankton grazing formulations are poorly constrained and sometimes based only on theoretical assumptions or data from fish (Ivlev, 1955). Furthermore, mechanistic descriptions of effects of temperature on zooplankton metabolism and trophic interactions are not sufficient for a realistic representation in ecosystem models. Warming is expected to affect respiration, reproduction, growth, development, and feeding rates of zooplankton (Durbin and Durbin, 1992). However, from available data it is not possible to estimate whether the net effect of temperature on different metabolic processes will result in enhanced or decreased grazing pressure. Such relationships could be derived from experiments designed in a way that makes it possible to quantify the parameters and rates that are needed for further model development. Therefore, a closer collaboration and communication between experimentalists and the modeling community is required for an improved and more realistic representation of ecosystem dynamics and their sensitivities to environmental factors.

III. Synthesis

1. The complex response of phytoplankton to warming

Possible responses to temperature changes

Warming of the ocean can either have direct effects on marine biota, by changing the metabolic rates of organisms, or indirect effects on nutrient supply and light availability through changes in mixing and stratification of the water column (Beardall et al., 2009; Riebesell et al., 2009). In the scope of this thesis, the focus was on direct effects of temperature. The global modeling study presented in chapter 1 demonstrated that temperature sensitivity of metabolic processes plays a major role in the response of marine ecosystems to ocean warming. Depending on the sensitivity of biological processes in our model experiment simulated NPP decreased or increased under projected climate change. The relationship between temperature and processes related to carbon cycling by phytoplankton were subject of the experiments presented in chapter 2 and 3, demonstrating that there is a large variability in temperature sensitivity among species, and that the response of the dominant species influences the biogeochemical response of the entire plankton community. Altogether, these results revealed large gaps in our understanding of temperature effects on marine biota, highlighting the need for a novel approach to represent temperature sensitivity of marine organisms in models on a global scale.

In general, there are three possible responses for organisms facing warming: (I) shifts in the spatial distribution of species as they spread to more hospitable habitats, (II) acclimation through physiological plasticity may allow species to live under warmer conditions, or (III) species may evolutionary adapt to the new conditions through genetic change and selection of more resistant genotypes (Hofmann and Todgham, 2010).

A common assumption is that ocean warming will mainly lead to a poleward shift of species (Sarmiento et al., 2004; Thomas et al., 2012). A number of reasons suggest that the response might be more complex. Temperature is an important, but not the only environmental factor that determines species distribution of phytoplankton, which form the base of the marine food web. Nutrient supply and light availability are equally or even more important factors influencing spatial and temporal patterns of phytoplankton. Important functional groups depend on supply of specific nutrients, e.g. diatoms require silicic acid to form their silicate shells, and nitrogen-fixing cyanobacteria have a higher

demand for the micronutrient iron than other phytoplankton (Boyd et al., 2010). The supply of silicic acid and iron is restricted to distinct regions in the ocean (Fung et al., 2000; Garcia et al., 2010), which is why these phytoplankton groups cannot simply migrate and follow their optimum temperature or temperature niche in a warming ocean. Consequently, in order to persist these organisms either need to physiologically acclimate or evolutionary adapt to the changing environmental conditions.

The physiological response to warming will differ greatly between phytoplankton groups and species. Even among species from the same group, temperature ranges for growth can be quite different. Thermal tolerance curves of organisms are generally unimodal and negatively skewed, i.e. the decline in fitness above the optimum temperature is stronger than below (Boyd et al., 2013; Eppley, 1972; Kingsolver, 2009). Consequently, species that already live close to their optimum temperature are very sensitive to warming and might be pushed them beyond their optimum, where they experience a sharp decline in fitness and growth. In contrast, species living well below their temperature optimum might even benefit from warming. Both responses were demonstrated in the experiments discussed in chapter 2 and 3. Field data showed that most phytoplankton species in polar and temperate regions live below optimum temperatures at present (Thomas et al., 2012), suggesting that these species could benefit from warming. On the other hand, some species have very narrow temperature ranges (Boyd et al., 2013; Suzuki and Takahashi, 1995), and projected ocean warming of 3-4 °C as projected (Gruber, 2011) might push these species beyond their optimum, thereby causing shifts in community composition.

Long-term adaption to warmer conditions at a given location is another possibility for survival of a species. A synthesis of field data revealed a strong relationship between optimum temperature of phytoplankton and mean annual temperature at the isolation location, suggesting that temperature is a major selective agent and that adaptation to local environmental conditions occurs in marine microbes despite the potential for long-distance dispersal through ocean currents (Thomas et al., 2012). Furthermore, there is increasing evidence that phytoplankton have the potential for relatively rapid genetic adaptation to changing temperatures, i.e. through the evolutionary processes of mutation and selection (Huertas et al., 2011). In this regard, species in temperate aquatic systems with relatively large thermal fluctuations all year round are assumed to have a higher potential for genetic thermal adaptation than species from cold-water communities (Hofmann and Todgham, 2010; Huertas et al., 2011).

However, it should be considered that even if a species physiologically acclimates or genetically adapts to higher temperatures, some temperature-dependent processes might still occur at a higher rate than in the original pre-warming state. These might include enzyme-mediated processes like photosynthetic carbon fixation, and consequently also carbon overconsumption and DOC exudation as shown in chapters 2 and 3.

The importance of species-specific temperature ranges

Generally, differences in the temperature range and optimum among phytoplankton species or components of the pelagic ecosystem should be taken into account, when trying to assess the overall response of marine ecosystems to ocean warming. Species-specific differences might also help to explain contrasting findings from experiments. For instance, temperature had a negative effect on carbon uptake in one mesocosm study (Wohlers et al., 2009), but a positive effect in a similar experiment (chapter 2). The main difference between these two studies was the temperature range and the community composition, particularly the dominant phytoplankton species. Temperatures were much lower in the study by Wohlers et al. (2-8 °C) than in the experiment presented in chapter 2 (9.5-17.5 °C), and the dominant diatom species was different (*Skeletonema costatum* in the study of Wohlers et al., *Dactyliosolen fragilissimus* in the experiment discussed in chapter 2). Wohlers et al. explained the decreased DIC uptake under elevated temperatures with an increase in heterotrophic respiration. However, it is likely that this response is only valid for that particular community in that particular temperature range. For *S. costatum* an optimum temperature of 15-25 °C has been found (Suzuki and Takahashi, 1995). Thus, temperatures as in the study by Wohlers et al. lie at the low end of the temperature range described for *S. costatum*, suggesting a negligible effect of temperature, whereas bacterial activity has been shown to be highly sensitive in the same temperature range, roughly doubling between 2 and 8 °C in the same study. Accordingly, the overall effect of elevated temperatures was that heterotrophic consumption of organic carbon dominated over autotrophic production. Assuming the same plankton community, the response of warming at a higher temperature range, e.g. between 12 and 18 °C, could have been entirely different, as it can be expected that temperature would have a strong positive effect on growth of *S. costatum* in that range. This could result in a similarly positive effect of temperature as observed in the experiment in chapter 2, where higher temperatures resulted in larger carbon uptake and production of organic carbon that outweighed its consumption by heterotrophs (Figure 1).

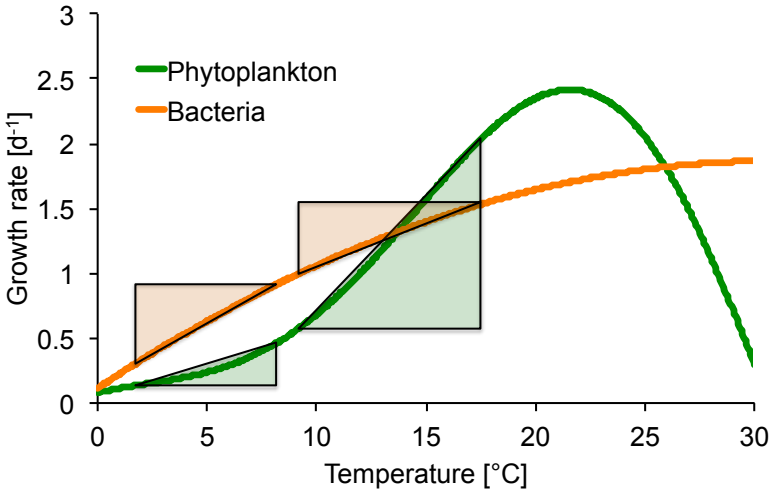

Figure 1: Functional responses to temperature of growth rates of phytoplankton (green) and bacteria (orange). Colored triangles mark the changes in growth rate over different temperature ranges. Contrasting responses between experiments can be explained by the different temperature sensitivities of autotrophic and heterotrophic communities. Depending on which component of the ecosystem exhibits a stronger sensitivity to a given change in temperature, the net response of the system will be positive or negative. Shown temperature functions assume a typical optimum curve for phytoplankton (Boyd et al., 2013; Eppley, 1972) and a quasi-linear (low temperature) to saturating (high temperature) function for bacteria based on data from Wohlers et al. (2009) and Adams et al. (2010), illustrating the generally wider temperature range of bacteria.

This example illustrates that it should be avoided to think of general effects of warming. Rather, the temperature sensitivities of various species and processes involved should be taken into account. What is important for the response of organisms or ecosystems is not warming in general, but the temperature change relative to the temperature range and optimum. This should be considered in both experimental and modeling studies.

Implications for modeling and data needs

Despite progress in the understanding of temperature effects on spatial distribution, physiological acclimation, and genetic adaption, we still lack the necessary information to accurately model these effects of warming on marine phytoplankton (chapter 1, (Chown et al., 2010)). Generally, the representation of physiological capacities of species, as well as capacities for genetic change are still underappreciated in ecological modeling in the context of responses to climate change (Chown et al., 2010; Helmuth et al., 2005). In many cases, direct temperature effects are either completely ignored in modeling studies

(e.g. Steinacher et al. (2010)), or strongly simplified (e.g. Bopp et al. (2013)), which seems questionable considering the key role of temperature in controlling biological processes (chapter 1-3). Most models that include temperature-dependence assume an exponential relationship following Eppley (1972) for a variety of biological processes (e.g. Bopp et al. (2013), Schmittner et al. (2008)). However, such an approach cannot account for variations in temperature sensitivity among species, functional groups or differences between autotrophic and heterotrophic communities. A recent study attempted to simulate the effects of ocean warming on species ranges and global diversity patterns of phytoplankton, combining an eco-evolutionary model with a physiological species distribution model (Thomas et al., 2012). In some regard, this approach seems overly simplistic, as it does not take into account important mechanisms, such as different nutrient requirements in different functional groups of phytoplankton, species succession, or trophic interactions. However, such studies emphasize the need to improve model representations of temperature effects on biological rates.

For a better understanding of the functional relationship between phytoplankton physiology and temperature, its implications for food web dynamics, and adequate representation of these relationships in marine ecosystem models, more comprehensive and comparable datasets are necessary. Scientific community-wide studies with specific protocols and coordinated lab efforts could help to provide the required data, e.g. by carrying out experiments with phytoplankton from different functional groups and across a wide range of marine environments (Boyd et al., 2013). Such data could be used to develop generally valid relationships between temperature and phytoplankton physiology, which could be implemented into global models, also for different functional types and biomes. This approach would also be suitable to constrain temperature sensitivity of other processes, such as bacterial degradation, that play an important role in marine biogeochemical cycling and are generally assumed to be strongly temperature-dependent (Lopez-Urrutia and Moran, 2007; Rivkin and Legendre, 2001). Altogether, a more realistic representation of temperature sensitivity of phytoplankton, or even a variety of functional phytoplankton groups, and other components of marine ecosystems is necessary for model development and to better assess potential impacts of ocean warming.

2. Post-bloom dynamics and carbon overconsumption – their relevance and representation in models

The fate of carbon overconsumption

The results from chapter 2 and 3 demonstrate that cycling of carbon and nitrogen can be substantially decoupled and notably deviate from Redfield stoichiometry, especially in post-bloom situations under nutrient depletion. Furthermore, the data showed that DOC and its conversion to TEP play major role in the fate of the excess carbon.

It has long been recognized that the relatively simple concept of fixed C:N stoichiometry following Redfield can be incompatible with observations. Carbon overconsumption, i.e. excess uptake of DIC over inorganic nutrients, has been observed in various experimental and field studies, with most pronounced increases after nutrient depletion (Körtzinger et al., 2001; Riebesell et al., 2007; Sambrotto et al., 1993; Wetz and Wheeler, 2003). The findings presented in chapter 2 and 3 support these earlier results. However, the fate of this additional carbon remained unclear for quite some time, as some of these studies (Riebesell et al., 2007; Sambrotto et al., 1993) did not observe a concomitant increase in either DOC or POC.

Nevertheless, a common assumption was that carbon fixed in excess of nitrogen by phytoplankton is exuded mainly in the form of DOC (Banse, 1994; Sambrotto et al., 1993), which could also be confirmed in some studies (Biddanda and Benner, 1997; Kähler and Koeve, 2001). Other studies, however, that observed a decoupling of carbon and nitrogen dynamics in phytoplankton blooms found that a large fraction of the additional carbon was channeled into the particulate pool and observed an associated increase in its C:N ratio (Engel et al., 2004a; Wetz and Wheeler, 2003). These two observations are not mutually exclusive, since a substantial fraction (~40%) of particulate organic matter can be comprised of TEP (Engel 2002). These in turn are formed from exuded carbohydrates that are measured as DOC. Thus, it depends on the conversion time of DOC to TEP, whether the excess carbon is measured in the dissolved or particulate pool. Usually this occurs within hours to days (Engel et al., 2004b; Passow, 2000). Since formation of TEP from precursor material is a physical process (Passow, 2002), it might also depend on the experimental setup (e.g. mixing of the water body) whether carbon overconsumption is predominantly detected in the DOC or POC pool.

A strong accumulation of particulate organic matter and increase in its C:N ratio, which was most likely related to production of TEP was also observed in the experiments

presented in chapter 2 and 3. Such experimental studies provide valuable insights and an improved mechanistic understanding of processes on the species or community level on relatively short time scales. However, the role of carbon overconsumption in the global marine carbon cycle and sequestration of carbon to the deep ocean via the biological pump is very complex and much less understood.

In the case that most of the additional carbon is channeled into the DOC pool, it can be assumed that a significant fraction of this fresh and biologically labile material is consumed and respired by bacteria relatively quickly. However, it has been estimated that up to 20% of net community production is released as semi-labile DOC that is not immediately remineralized and instead accumulates in the surface ocean (Hansell et al., 2009). This DOC is transported with the ocean circulation and can thereby be exported to deeper waters (Carlson et al., 2010). It has been suggested that export of semi-labile DOC out of the euphotic zone amounts to 1.2-1.8 GtC yr^{-1}, corresponding to 10-15% of global export production (Hansell and Carlson, 1998; Hansell et al., 2009). However, it has been shown that only a small fraction of this exported DOC (~0.2 GtC) reaches depths greater then 500 m (Hansell et al., 2009). This suggests that DOC is less important for the carbon flux to the deep ocean, but plays a substantial role in oxygen consumption in the upper ocean, contributing to as much as 70% of oxygen consumption in the upper 400 m (Doval and Hansell, 2000). The experiments in chapter 2 and 3 demonstrate that release of DOC by phytoplankton is sensitive to environmental factors, such as temperature or CO_2, and highly variable among species. However, in order understand the fate of this produced DOC and constrain its role for export production, more knowledge about its quality and bioavailability is required, e.g. through systematic DOC degradation experiments.

In the case that most of the excess carbon fixation is channeled into TEP, as indicated by the results in chapter 3, a larger portion of this additional carbon could be transported to depth. It has been demonstrated numerous times that the presence of TEP plays a major role in the formation of large, rapidly sinking marine aggregates and thus particle flux out of the euphotic zone, especially during diatom blooms (Alldredge et al., 1993; Engel et al., 2004a; Passow et al., 2001). Furthermore, it has been shown that the matrix of all marine aggregates, regardless of their origin and composition, consists of TEP (Alldredge et al., 1993; Passow, 2002; Passow et al., 1994). Besides their role in aggregate formation, TEP themselves may contribute appreciably to the vertical carbon flux, as they are carbon-enriched with high C:N ratios averaging between 20 and 25 (Engel and Passow, 2001; Mari et al., 2001). Therefore, formation of TEP can represent an important pathway in which

DOC released by phytoplankton can be transported from the euphotic zone to the deeper ocean. However, the relative contribution of TEP – and therefore carbon overconsumption – to the biological pump and carbon flux to the ocean interior is still controversial. There is strong evidence that substantial amounts of TEP can be exported out of the euphotic zone (Körtzinger et al., 2001; Passow et al., 2001). However, only a small fraction of TEP produced in the surface ocean seems to reach the deep ocean. Data from sediment traps usually show no sign of substantially elevated C:N ratios, and a study off the Californian coast suggested that only ~2% of produced TEP reached 500m (Passow et al., 2001). This would imply that other loss processes, such as grazing and bacterial degradation are important for the fate of TEP below the euphotic zone (Koeve, 2005; Passow et al., 2001). Therefore, it has been suggested that TEP does not contribute significantly to export and long-term sequestration of carbon (Koeve, 2005, 2006). On the other hand, C:N ratios of up to 10 or even 20 are frequently observed in the deep ocean, for instance in detritus freshly deposited on the seafloor (Beaulieu, 2002; Lampitt et al., 2001; Smith et al., 1998). While this is often attributed to preferential remineralization of N over C (Koeve, 2005, 2006; Lee and Cronin, 1984), it can not be excluded that fast-sinking aggregates rich in TEP also contribute to these elevated C:N values. Furthermore, a major role of TEP lies in the formation of fast-sinking particles, which are responsible for most of the POC flux to the deep ocean. Even if a large portion of the TEP comprising the matrix of aggregates is remineralized in the upper ocean, the formed aggregates and solid organic material (e.g. phytoplankton cells, fecal pellets) contained within them, continue sinking to the deep ocean. From this perspective, by initiating significant POC flux in the first place, TEP might rather contribute indirectly than directly to the long-term sequestration of carbon. Considering the generally weak flux of organic matter to the deep ocean, with only ~1% of NPP (~0.5 GtC yr^{-1}) ending up as sedimentation onto the ocean floor (Sarmiento and Gruber, 2002), it can be expected that the carbon flux mediated by TEP constitutes an important contribution to long-term carbon sequestration.

On the global scale, the ultimate fate of carbon overconsumption associated with post-bloom dynamics is yet unclear. The additional carbon might either remain as semi-labile DOC, which would then be transported with oceanic currents, or in the form of TEP, subsequently sinking to greater depths. Estimates of global export production vary greatly and range from 5-20 GtC yr^{-1} (Eppley and Peterson, 1979; Henson et al., 2011; Laws et al., 2000). While these differences are mainly attributable to the applied methodology, it has been suggested that even the highest estimates are not sufficient to balance

heterotrophic respiration in the mesopelagic and bathypelagic zone, (Burd et al., 2010; Henson et al., 2011) suggesting that DOC might contribute even more to transport of carbon to the deep ocean than previously assumed (del Giorgio and Duarte, 2002). Furthermore, there are major gaps in the coverage of *in situ* data, which makes it difficult to account for spatial and temporal variability in such global estimates, e.g. substantial episodic export events, such as phytoplankton blooms, where TEP and aggregation play major roles are not resolved in such estimates. However, it has been demonstrated that only moderate changes in C:N of particle flux to the ocean interior might have substantial impacts on biogeochemical cycling and the extent of oxygen minimum zones (Oschlies et al., 2008). Altogether, this illustrates that a better understanding of carbon overconsumption and its role for carbon export is urgently needed. Besides acquisition of data from experiments and field campaigns, this requires the development of new concepts and their implementation into biogeochemical ecosystem models.

Species-specific sensitivities of carbon overconsumption and implications for biogeochemical cycling

The experiments presented in chapter 2 and 3 demonstrated that carbon overconsumption and its fate are highly species-specific. Furthermore, the sensitivity to temperature and CO_2 is varies strongly among species. As shown in chapter 2 and section III.1, the physiology of the dominant phytoplankton species can determine the biogeochemical response of the entire plankton community. The plankton assemblage in the mesocosm experiment presented in chapter 2 was strongly dominated by *D. fragilissimus*. DIC uptake and production of POC and DOC were positively correlated to temperature over a gradient from 9.5 to 17.5 °C. However, it was not possible to exclude if other mechanisms contributed to the observed response, as many other processes occurred simultaneously in mesocosm experiments, e.g. zooplankton grazing and bacterial degradation. The culture experiments presented in chapter 3 eventually confirmed the inferences from the mesocosm study, demonstrating that the amount of excess carbon fixation by *D. fragilissimus* is substantial, and that it increases with temperature between 10 and 17.5 °C. The consistency of findings from the mesocosm study (chapter 2) and batch culture experiments (chapter 3) confirms the critical role of the dominant species' physiology in biogeochemical cycling of entire plankton communities. Consequently, such dominant species can also be considered as "biogeochemical key species": The experiments in chapter 3 indicated that the magnitude of carbon overconsumption, its

partitioning into POC and DOC, and the sensitivity of these processes to temperature and CO_2, is highly variable among species. Depending on the magnitude of excess carbon fixation and its partitioning into POC, DOC and TEP, cycling of organic matter and the strength and efficiency of the biological pump could decrease or increase under elevated temperatures and CO_2 (Figure 2). Thus, the sensitivity of such "biogeochemical key species" to ocean warming and acidification could determine the large-scale response of biogeochemical cycling and the biological pump in a changing ocean.

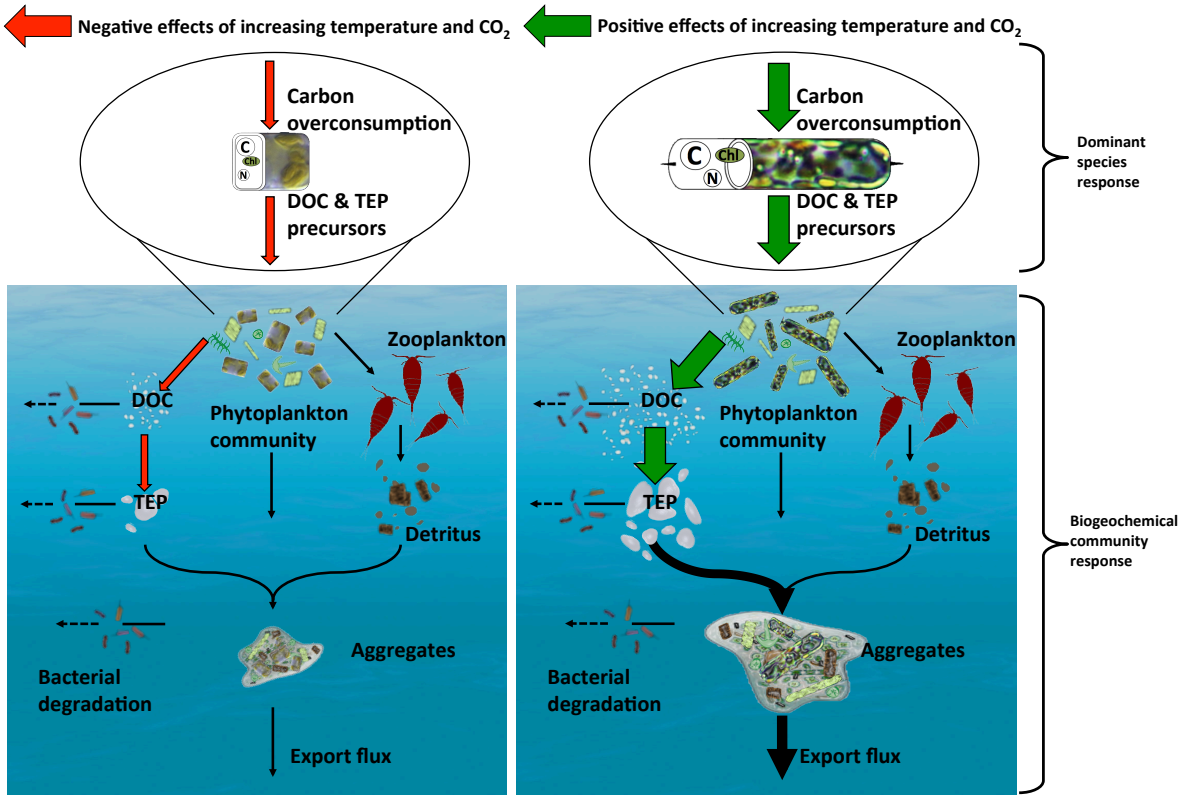

Figure 2: Conceptual diagram illustratiing how the response of dominant phytoplankton species to ocean warming and acidification can determine the biogeochemical response of the entire plankton assemblage. The physiology of "biogeochemical key species" exerts a strong control on organic matter cycling and the biological pump. Carbon overconsumption by phytoplankton has been shown to be sensitive to both temperature and CO_2 in the scope of this study, with substantially varying sensitivities among species. Most of this additional carbon is released as DOC, which, depending on its quality, will coagulate and form TEP. These play an important role in the formation of sinking aggregates from phytoplankton cells and detrital organic matter, and thus carbon flux to the deep ocean. Depending on the direction and magnitude of the physiological response of biogeochemical key species to rising temperatures and CO_2, environmental changes will result in a decrease (left panel) or increase (right panel) in the strength and efficiency of the biological pump.

A model for carbon overconsumption and its sensitivity to temperature and CO_2

Experimental studies as presented in chapter 2 and 3 can provide improved mechanistic understanding of processes such as carbon overconsumption, production of TEP, and formation of aggregates. To assess their relevance on the global scale and under climate change, the application of models including these processes and their sensitivities to environmental factors is required. The few modeling studies that include these mechanisms produce promising results e.g. in simulating mesocosm data (Schartau et al., 2007). However, these studies tend to focus on very detailed representations of coagulation and aggregation of TEP and neglect other important processes, such as zooplankton grazing and export of organic matter. Furthermore, they do not account for sensitivities to temperature and CO_2, which have been shown to be substantial in chapters 1, 2, and 3.

In the scope of this thesis, a new model was developed that includes the decoupling of carbon and nitrogen, dissolved organic matter and TEP, as well as more realistic representations of temperature and CO_2 dependence of various biological processes (Figure 3A, a more detailed description is presented in appendix A). Preliminary results show already good skill in capturing the temperature response of carbon cycling in two mesocosm experiments (Figure 3B). The parameters that are most important in capturing the biogeochemical dynamics from the experiments are the physiological parameters of simulated phytoplankton, as well as the temperature sensitivity of DIC uptake, release of DOC, and various other ecosystem processes.

This illustrates the need for a better mechanistic understanding of phytoplankton physiology, and its sensitivity to environmental factors. In this regard, more comprehensive datasets, e.g. from field studies or mesocosm experiments in the open ocean, are required for further model developing and validating such models. A particularly important objective is the identification of general patterns of carbon overconsumption and its fate across functional groups and species. Results from the studies presented in chapter 2 and 3 demonstrated that partitioning of carbon between the dissolved and particulate phase is highly variable among diatom species and significantly affected by temperature and CO_2. Such variations on the species or community level, as well as their sensitivity to environmental factors, need to be adequately represented in order to correctly simulate the fate of excess carbon in global biogeochemical models.

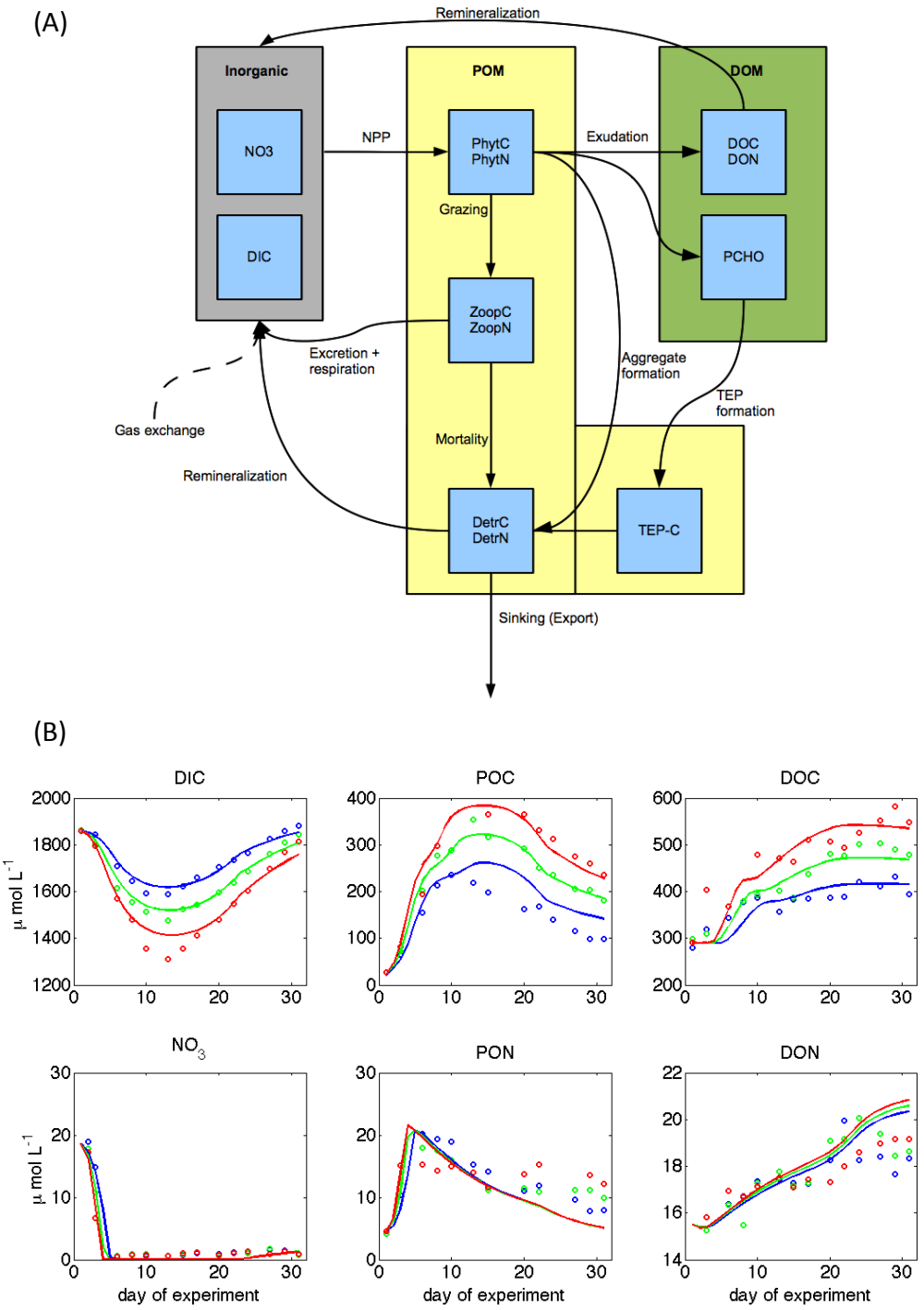

Figure 3: (A) Schematic illustration of major biogeochemical fluxes in the newly developed model. Main features are the decoupling of carbon and nitrogen and their separate calculation for each state variable. In addition, dissolved organic matter, polysaccharides and TEP are explicitly included, enabling the model to simulate carbon overconsumption and its sensitivity to temperature and CO_2. (B) Preliminary results from simulations of the mesocosm study presented in chapter 2. Solid lines denote model results, circles indicate measured data from the experiment. Colors represent different temperatures: 9.5 (blue), 13.5 (green), and 17.5 °C (red).

3. Methodological considerations – experiments vs. models

Even though it has long been proposed that a closer collaboration and communication between experimentalists and the modeling community is essential in marine science, the two approaches are usually still strictly separated from each other. One of the aims of this thesis was to bridge this gap between experimentalists and modelers in marine research and investigate a scientific question in a complementary approach. Accordingly, the work conducted during my doctoral thesis combined experimental work and numerical modeling, including parameter sensitivity studies to identify processes and aspects that need experimental data, acquisition of this required data in experimental work, and developing model parameterizations to make use of this data. Both, experimental work and modeling are suited for investigating specific questions and have their respective strengths and weaknesses. These will be discussed shortly in the following sections, before giving a conclusion about the combined approach conducted during the work on this thesis.

Comparison of different experimental approaches

Experimental approaches in marine research range from small-scale incubations of single species and volumes on the order of liters, to mesocosms with volumes ranging from less than one m^3 to several hundred m^3 containing entire communities. In the scope of this thesis, work was carried out in batch cultures (single phytoplankton species, 20 L per container) and in mesocosms (natural plankton community, ~1,400 L per mesocosm).

Small-scale experiments, such as batch cultures are a widely used method in marine research. They are relatively easy to set up, conduct and replicate, usually inexpensive, and provide controlled environment for investigation of a wide range of processes. On the downside, growth conditions are quite artificial, and therefore not very representative of the real ocean. This kind of experiments can provide valuable information about individual components and distinct processes of the complex marine ecosystems, e.g. on the sensitivity of single species to environmental drivers (see chapter 3).

In contrast, mesocosm experiments are more representative of the real world, containing entire communities and multiple trophic levels. Due to the large volume of mesocosms, natural populations can be enclosed under natural or semi-natural conditions, and the same populations can be sampled repeatedly over a long period of time. The major drawback is that mesocosm experiments are relatively expensive and require intensive maintenance, making it difficult to have a high number of replicates and treatments.

However, such experiments are essential as they provide the only means of investigating effects of e.g. warming and CO_2 on the community level.

Therefore, it is useful to apply both approaches complementarily. While small-scale experiments are only suitable for extrapolation to the real ocean to a very limited extent, they can be used to test hypothesis derived from mesocosm studies, or investigate specific processes that cannot be isolated in mesocosms with whole communities. This can be illustrated by the workflow during this thesis. The findings from the mesocosm study presented in chapter 2 were rather surprising and in sharp contrast to previous comparable experiments (see section III.1). However, due to the complexity of the system in the mesocosm it was difficult to disentangle processes and find a definite explanation for the observed response. This led to the development of a hypothesis, which was then tested in batch culture experiments presented in chapter 3. Since these contained only one single phytoplankton species at a time and no higher trophic levels, the effects of environmental drivers on carbon fluxes mediated by the respective diatom species could be constrained much better, eventually confirming the hypothesis that had been developed following the mesocosm experiment. Thus, a combination of small-scale and mesocosm experiments can facilitate to understand the complexity of marine ecosystems, and help in the further development of ecosystem models.

Types of models, needs for improvement

Generally, biogeochemical ecosystem models are an important tool for testing the understanding of a given system, e.g. by investigating if the model behaves as expected and if it reproduces the observational or experimental data (see chapter 1). Models can also be applied to put data of different types, e.g. from different locations, times or experiments, into a coherent context. In this respect, data assimilation has emerged as a valuable method, incorporating observational data into numerical models to identify patterns and improve forecasting in a given system. Furthermore, models are valuable for extrapolation in space and time, e.g. where data is sparse, or to simulate past and future conditions. In this regard, models are a commonly used for testing hypotheses (“what if” experiments) that were developed based on observations or experiments. The study presented in chapter 4 gives a good example where ideas emerging from results of a laboratory experiment (direct effect of temperature on sinking speeds) were incorporated into a model to test the observed sensitivity on a global scale.

Most ecosystem models applied on a global scale include very simplified representations of the marine ecosystem ("NPZD", e.g. Fasham et al., (1990), Steinacher et al., (2010)). Consequently, they are not able to capture complex processes, such as community changes, which are expected in response to climate change and ocean acidification and have already been observed in mesocosm experiments (Riebesell et al., 2007; Schulz et al., 2013). There have been increasing efforts for designing more complex and realistic models, including multiple functional types and size classes (e.g. Moore et al., (2002), Blackford et al., (2004), Le Quéré et al., (2005)). However, there has been an ongoing debate on the appropriate level of model complexity for a sufficiently realistic representation of marine ecosystems and their sensitivity to environmental change, especially regarding the large gaps in parameter constraints through lack of data, and little knowledge about ecological interactions (Anderson, 2005; Flynn, 2006; Kriest et al., 2010). Nevertheless, it is obvious that commonly used models that apply very simplified representations of marine ecosystems (e.g. NPZD) are very likely to miss physiological effects at the organism level, and associated interactions and effects at the community level. From the growing body of experimental and observational data it becomes increasingly clear that there is a severe lack of biological detail in most biogeochemical ecosystem models, especially those applied on the global scale. For instance, the experimental data presented in chapters 2 and 3 suggest a strong decoupling of carbon and nitrogen during phytoplankton blooms, which is also affected by temperature and pCO_2. While such a decoupling has been observed in various experimental and field studies, most marine ecosystem models still rely on fixed stoichiometry, and there have been relatively few attempts to model carbon overconsumption (see Schartau et al. (2007) and section III.2)

This illustrates the need for an adequate representation of biological processes and their sensitivities in models with respect to their predictive capability. While simulation and predictions of changes in the physical system, e.g. temperature increases and response of the carbonate system are quite robust (IPCC, 2007a; Orr et al., 2005), the response of biological processes and ecosystems is much more uncertain and at a very early stage (chapter 1, Oschlies et al. (2010)). Reasons for this uncertainty are numerous, including the complexity and interplay of system drivers, the variety of responses of different species, and ultimately the lack of required data from experiments.

Linkages between experiments and models

Models are closely linked to laboratory and field work, as these deliver the required data and process understanding that is necessary in order to allow for an adequate representation of biological processes in a model. Any model can only give predictions or insights about processes that are in some way included in its equations. For instance, mechanistic descriptions of carbon overconsumption, biogenic calcification, sensitivities of different zooplankton or fish life stages to changes in temperature and carbonate chemistry are not available yet. Studies as presented in chapter 3, where the sensitivity of processes are investigated in isolation, could help to bridge this gap and deliver the required information for model development. Even more complex are mechanisms on the ecosystem level, e.g. impacts of warming and ocean acidification on food web dynamics, such as the propagation of impacts from lower to higher trophic levels. Studies on the community level, as conducted in the mesocosm experiment presented in chapter 2, can provide valuable insights into the response at the community and ecosystem level, particularly when coupled with small-scale experiments as discussed above.

Thus, a complementary approach of experimental work and modeling, where those quantities and rates that are needed for these models are measured in experiments, could help in the improvement of ecosystem models. In this regard, modelers need to communicate what kind of data they require for model improvement, such as rate measurements of processes that are still poorly constrained. The modeling community could strongly profit from comprehensive datasets that could be used for model validation. At the same time, models can provide information highly relevant for experimental work. They can help in identifying problems with our conceptual understanding, e.g. through discrepancies between model output and observations, and ultimately also identify further research needs and development of new hypotheses. Furthermore, model simulations can facilitate experimental design, e.g. by estimating the appropriate perturbation levels for experiments (e.g. CO_2 levels), assessing the sensitivity to boundary conditions (e.g. initial community composition), or by identifying regions that are especially sensitive to environmental change. These considerations demonstrate how modeling and experimental work can benefit from mutual exchange of knowledge and scientific progress.

Personal experience: Combining experimental work and numerical modeling

One of the objectives of this thesis was a meaningful combination of numerical modeling and experimental work.

The starting point was a global modeling study (presented in chapter 1), which revealed the importance of temperature sensitivity of marine ecosystem processes under climate change, and fundamental uncertainties in our knowledge about them. Even though it has long been recognized that temperature is a major driver of biological processes, only few studies exist that systemically investigated temperature sensitivity of marine organisms in the context of biogeochemistry. Most studies focused on physiological or ecological questions, such as relationships between temperature and growth rate, cell size or phenology (Daufresne et al., 2009; Hoppe et al., 2008; O'Connor et al., 2009). On the other hand, the few studies that explicitly focused on biogeochemical dynamics, such as DIC uptake or C:N stoichiometry, gave contrasting results (Kim et al., 2011; Wohlers et al., 2009) and were restricted to few species.

Together with the results from the study presented in chapter 1, this was the motivation for the experiments presented in chapter 2 and 3. These experiments were specifically designed to investigate how temperature sensitivity of biogeochemically important processes differs between diatom-dominated ecosystems (chapter 2) and diatom species (chapter 3), and how it might interact with ocean acidification (also chapter 3).

The results of these experiments suggested a pronounced effect of temperature and pCO_2 on carbon uptake and partitioning into particulate and dissolved organic matter, and especially the phenomenon of carbon overconsumption and the associated decoupling of carbon and nitrogen cycling. Furthermore, the experiments could show that the sensitivity of these processes to temperature and pCO_2 varies substantially between species. Altogether, these findings were the motivation for development of a novel model. Most ecosystem models do not account for carbon overconsumption and dynamic stoichiometry, and respective sensitivities to temperature and pCO_2, as observed in the experiments shown in chapter 2 and 3. Consequently, a model has been constructed (work still ongoing) that simulates carbon overconsumption and its sensitivity to temperature and pCO_2 (see appendix of this thesis for a detailed mode description). Application of this model to various datasets can help to identify general patterns that might be related to functional groups or cell size, and ultimately investigate how carbon overconsumption and associated processes affect marine biogeochemical cycling (manuscript in preparation). Another good example is the study presented in chapter 4,

where ideas arising from findings of a laboratory experiment (effect of temperature-driven viscosity changes on sinking speeds) were incorporated into a model to test the observed sensitivities and their potential effects on a global scale. These reciprocal stimulations illustrate how the combined approach of experimental work and modeling during my thesis allowed for a more effective knowledge exchange and collaboration between both sides.

From a personal point of view, it was both challenging and fruitful to conduct research in a combination of experimental work and modeling. This complementary approach turned out to be very productive and efficient. Knowing the basic functioning, as well as the strength and weaknesses of both approaches facilitated the workflow and knowledge exchange, especially by gaining an understanding of how these two approaches are linked to each other. Altogether, this demonstrates how such a complementary work approach can facilitate and accelerate interdisciplinary exchange of data and knowledge, and can thus be of mutual benefit for both the experimental and modeling community.

4. Future perspectives

Future work might investigate questions that emerged from the observations and results presented in this thesis.

Complementary to existing studies, work presented here demonstrated that key processes in the marine ecosystem display a strong sensitivity to temperature (chapter 1 to 5) and CO_2 (chapter 3). It has become evident that these sensitivities vary between functional groups, species, or even strains of the same species (Boyd et al., 2010; Langer et al., 2009). Organisms can respond to environmental changes either through physiological acclimation, evolutionary adaption, or spatial migration. Most models do not adequately account for these mechanisms. Future model development should therefore focus on an integrative approach, in which all three possible responses are represented and simulated by the models. Of course, this requires a better mechanistic understanding of these processes. For instance, only few studies exist that investigated evolutionary adaption of phytoplankton (Collins and Bell, 2004; Lohbeck et al., 2012). One possibility to obtain datasets that can be used for model development are joint lab efforts in scientific community-wide studies. Using standardized protocols for data acquisition this would facilitate the investigation of a large variety of functionally different species in a consistent manner. The more comparable data is generated for different species, the more likely it is

that a general pattern can be identified, which could then be translated into functional relationships and implemented into ecosystem models. This is crucial for a more realistic simulation of the response of marine ecosystems to global change.

In the scope of this thesis, a key role of carbon overconsumption, DOC, and TEP in organic matter cycling was identified (chapter 2 and 3), which is in line with earlier studies (Passow et al., 2001; Riebesell et al., 2007; Sambrotto et al., 1993). However, its relevance for export flux and long-term carbon sequestration are controversially debated (Koeve, 2005; Passow and Carlson, 2012; Riebesell et al., 2007). Building on the work presented here, more experiments focusing on the connections between carbon overconsumption, TEP production, and export flux need to be conducted. In this regard, a major focus should be set on the role of dominant phytoplankton species in the response of the plankton community as a whole. Bringing together the results from the experiments in chapter 2 and 3 with findings from other mesocosm studies and model experiments indicated a biogeochemical key role of species dominating a plankton assemblage. Accordingly, the physiological response of such key species to environmental change (e.g. the sensitivity of carbon overconsumption to temperature and CO_2) could translate into large-scale biogeochemical responses of entire plankton communities. This hypothesis needs to be tested in future efforts. In this regard, open ocean mesocosm experiments could be an ideal framework, as they provide close-to-natural conditions and techniques to estimate export production have been recently developed (Riebesell et al., 2013). Together with small-scale laboratory experiments that are conducted simultaneously, focusing on individual components of the ecosystem and the dominant species found in the mesocosms, this could improve our understanding of the interplay between biogeochemical key species and biogeochemical dynamics on the community level. These mechanisms need to be understood to a degree that general patterns can be identified and such processes can be meaningfully represented in ecosystem models. The findings presented in chapter 1, 4, and 5 demonstrate that there are still large uncertainties regarding the representation of biological processes in biogeochemical ecosystem models. To date, most biogeochemical ecosystem models do not allow for decoupling of carbon and nitrogen, or do not even account for dissolved organic matter cycling. Given the relevance of these processes in biogeochemical dynamics and oceanic carbon uptake, they should be implemented mechanistically into ecosystem models.

Based on these findings we developed a new ecosystem model that includes these mechanisms and their sensitivities to temperature and CO_2 (see section III.2). Ongoing

work with this model includes validation against data from experiments presented in this thesis, as well as other available datasets, especially from mesocosm experiments. Considering the diversity in biogeochemical ecosystem models, ranging from very simplified NPZD models to more sophisticated models that include multiple size classes or functional types, it is obvious that these models need to be quantitatively compared regarding their predictive capabilities. Validation of ecological and biogeochemical models against experimental data constitutes an important part of model development (Vallino, 2000). For instance, measurements of standings stocks and process rates from mesocosm experiments can be used for validation and intercomparison of different models, and include ecosystem components or processes that might have been overlooked. Since mesocosm experiments cover all relevant physiological, ecological and biogeochemical parameters, they are perfectly suitable for such purposes. In this regard, an important prerequisite is the identification of general physiological and ecological patterns e.g. in response to changes in temperature and CO_2. This can only be achieved through synthesis of as many experiments as possible, ranging from single species to the community level. Meta-analyses of experimental datasets are a suitable tool to reveal and possibly quantify general patterns and should be carried out in addition to further model development. Altogether, the objective for future research is a complementary work approach that integrates experiments from the physiological to the community level, meta-analyses of obtained datasets, and application of numerical models to simulate the conducted experiments.

Appendix: A biogeochemical ecosystem model for the simulation of carbon overconsumption and its sensitivity to temperature and CO_2

Manuscript in preparation for *Biogeosciences*

1. Background and motivation

The currently developed model described in the following is based on the ecosystem module of the UVic Earth System and Climate Model (ESCM). In the original version, it comprised a commonly used NPZD-type ecosystem structure, i.e. simulating nutrients (N), phytoplankton (P), zooplankton (Z), and detritus (D) as the state variables, and applying fixed stoichiometry for cycling of carbon (C), nitrogen (N), and phosphorus (P) (Schmittner et al., 2008). While the model displayed good skill at reproducing observed global distributions of biogeochemical tracers, it was not able to correctly simulate recent mesocosm experiments, in which a strong decoupling of carbon and nitrogen was observed (e.g. chapter 2, Wohlers et al. (2009)).

Therefore, the model was modified in a way that enables it to capture biogeochemical dynamics from such studies. A major focus was the representation of carbon overconsumption and effects of temperature and CO_2 on carbon uptake and partitioning. Major modifications from the original model include decoupling of carbon and nitrogen, addition of dissolved organic matter (DOM) and transparent exopolymer particles (TEP).

Carbon and nitrogen decoupling for phytoplankton growth are mainly based on the model by Geider et al., (1998). The PCHO and TEP pathway is based on the model by Schartau et al., (2007). Biogeochemical fluxes, such as DOM exudation and bacterial remineralization are regulated by the N:C quotas of phytoplankton and DOM. C and N specific rates, and sensitivities to temperature and pCO_2 of various biological processes are based on experimental data from Wohlers et al. (2009) and the studies presented in chapter 2 and 3. For model skill assessment and validation, we applied the model to reproduce data of the aforementioned studies (see section III.2 in synthesis).

2. Detailed model description

Source-minus-sink terms

The equations terms describing changes in the concentration of biogeochemical state variables are as follows:

$$S(DIN) = \left(-N_{upt}\right)PhytN + \rho_{DetN}DetrN + \rho_{DON}DON + \varepsilon ZoopN$$

Dissolved inorganic nitrogen = nitrogen uptake by phytoplankton + remineralization of detritus nitrogen + remineralization of DON + nitrogen excretion by zooplankton

$$S(DIC) = \left(-C_{fix}\right)PhytC + \rho_{DetC}DetrC + \rho_{DOC}DOC + \rho_{TEP}TEP + \varepsilon ZoopC + flux_{air-sea}$$

DIC = carbon fixation by phytoplankton + remineralization of detritus carbon + remineralization of DOC + remineralization of TEP + carbon excretion by zooplankton + air-sea gas exchange of CO_2

$$S(PhytN) = (N_{upt} - \theta_{DON})PhytN - \gamma_P(PhytN)^2 - Aggr - graz \cdot ZoopN$$

Phytoplankton nitrogen = nitrogen uptake – leakage of DON – mortality – aggregation of cells – zooplankton grazing

$$S(PhytC) = (C_{fix} - \theta_{DOC})PhytC - \gamma_P\frac{(PhytN)^2}{q_P} - \frac{Aggr}{q_P} - graz \cdot \frac{ZoopN}{q_P}$$

Phytoplankton carbon = carbon fixation – exudation of DOC – mortality – aggregation of cells – zooplankton grazing

$$S(ZoopN) = graz \cdot ZoopN - \varepsilon_N ZoopN - \gamma_Z(ZoopN)^2$$

Zooplankton nitrogen = grazing on phytoplankton – excretion of nitrogen – mortality

$$S(ZoopC) = graz \cdot \frac{ZoopN}{q_P} - \varepsilon_C ZoopC - \gamma_Z\frac{(ZoopN)^2}{q_Z}$$

Zooplankton carbon = grazing on phytoplankton – respiration of carbon – mortality

$$S(DetrN) = \gamma_P(PhytN)^2 + (1-\sigma)\gamma_Z ZoopN + Aggr - \rho_{DetN}DetrN - \omega DetrN$$

Detritus nitrogen = phytoplankton mortality + zooplankton mortality (particulate fraction) + phytoplankton aggregation – detritus remineralization – sinking of organic matter

$$S(DetrC) = \gamma_P \frac{(PhytN)^2}{q_P} + \frac{(1-\sigma)\gamma_Z}{q_Z} ZoopN + \frac{Aggr}{q_P} + Aggr \cdot f_{TEP} TEP - \rho_{DetC} DetrC - \omega \frac{DetrN}{q_{Det}}$$

Detritus carbon = phytoplankton mortality + zooplankton mortality (particulate fraction) + phytoplankton aggregation + TEP contained in aggregates – detritus remineralization – sinking of organic matter

$$S(DON) = \theta_{DON} PhytN + \sigma\gamma_Z (ZoopN)^2 - \rho_{DON} DON$$

Dissolved organic nitrogen = leakage by phytoplankton + zooplankton mortality (dissolved fraction) – remineralization

$$S(DOC) = (1 - f_{PCHO})\theta_{DOC} PhytC + \sigma\gamma_Z \frac{(ZoopN)^2}{q_Z} - \rho_{DOC} DOC$$

Dissolved organic carbon (excluding PCHO) = exudation by phytoplankton + zooplankton mortality (dissolved fraction) – remineralization

$$S(PCHO) = f_{PCHO}\theta_{DOC} PhytC - (\beta_1 PCHO^2 + \beta_2 PCHO \cdot TEP)$$

Polysaccharides = exudation by phytoplankton – aggregation of PCHO with each other – aggregation of PCHO with TEP

$$S(TEP) = (\beta_1 PCHO^2 + \beta_2 PCHO \cdot TEP) - \rho_{TEP} TEP - Aggr_{TEP} TEP$$

Transparent exopolymer particles = aggregation of PCHO with each other + aggregation of PCHO with other DOC + aggregation of PCHO with TEP – remineralization of TEP – TEP contained in aggregates

For comparison with experimental data, model output was merged to measured biogeochemical quantities:

$$POC = PhytC + ZoopC + DetrC + TEP$$
$$PON = PhytN + ZoopN + DetrN$$
$$DOC_{total} = DOC + PCHO$$

Phytoplankton

Net primary production of phytoplankton is calculatedly separately for carbon and nitrogen, thereby allowing for flexible stoichiometry.

Carbon fixation is a function of irradiance (*I*), the cellular nitrogen-to-carbon ratio (q_P), temperature (*T*), and carbonate chemistry (CO_2):

$$C_{fix} = f(I, q_P, T, pCO_2) \quad (1)$$

It is calculated as:

$$C_{fix} = \mu_I R_{C-fix}^{NC} \quad (2)$$

where μ_I is the light-limited growth rate (as in Schmittner et al. (2008), following Evans and Parslow (1985)):

$$\mu_I = \frac{\mu_C \alpha I}{\sqrt{\mu_C^2 + (\alpha I)^2}} \quad (3)$$

where α is the initial slope of the photosynthesis-irradiance-curve (P-I-curve) and μ_C is the light-saturated carbon assimilation rate, which in turn is a function of temperature (*T*) and CO_2 according to:

$$\mu_C = \mu_{C0} \cdot f(T) \cdot f(CO_2) \quad (4)$$

$$f(T) = b^{cT} \quad (5)$$

$$f(CO_2) = \frac{CO_2}{(k_{CO_2} + CO_2)} \quad (6)$$

with the parameters maximum carbon assimilation rate μ_{C0}, the temperature sensitivity parameters *b*, *c,* and the half-saturation constant for CO_2 k_{CO_2}. Note that ongoing work investigates the impact of applying different functional responses to temperature (e.g. optimum curves) that are not discussed here. Accordingly carbon assimilation increases

exponentially with temperature. The sensitivity to dissolved CO_2 concentrations is represented with a Michaelis-Menten function, where carbon fixation decreases below a critical threshold (where cellular leakage of CO_2 increasingly counteracts C-fixation see chapter 3 and Rost et al., (2006)).

Besides light-limitation, the rate of carbon fixation is also controlled by the cell quota, following Geider et al., (1998) and Schartau et al., (2007):

$$R_{C-fix}^{NC} = \frac{q_P - q_{P_{min}}}{q_{P_{max}} - q_{P_{min}}} \qquad (7)$$

Here q_P is the simulated cell quota and $q_{P_{min}}$ and $q_{P_{max}}$ the prescribed minimum and maximum quotas. The lower the N:C content of the cell, the lower carbon fixation. Future work will include variable minimum and maximum cell quotas, depending on environmental conditions.

Nitrogen uptake is a function of the external and internal nutrient availability, i.e. the concentration of inorganic nitrogen (here NO_3) dissolved in water, temperature, and the cell quota:

$$N_{upt} = f(NO_3, T, q_P) \qquad (8)$$

It is calculated as:

$$N_{upt} = \mu_N R_{N-upt}^{NC} \qquad (9)$$

where μ_N is the N-limited growth rate using a Michaelis-Menten formulation including a half-saturation constant for nitrate (k_N), the maximum N-uptake rate μ_{N0} and temperature dependence as above:

$$\mu_N = \mu_{N0} f(T) \frac{NO_3}{(k_N + NO_3)} \qquad (10)$$

The regulation of N-uptake by the cell quota is calculated using a sigmoidal function:

$$R_{N-upt}^{NC} = 1 - exp\left[-\lambda_{NC}\left(\left|q_P - q_{P_{max}}\right| - \left(q_P - q_{P_{max}}\right)\right)^2\right] \qquad (11)$$

with the scaling parameter λ_{NC} and the maximum cell quota $q_{P_{max}}$.

Phytoplankton mortality (representing e.g. cell lysis and viral infection) is density dependent:

$$\gamma_P = \gamma_{P0}(PhytN)^2 \qquad (12)$$

where γ_{P0} denotes the phytoplankton mortality coefficient.

Zooplankton

The grazing rate of zooplankton on phytoplankton depends on food concentrations in the form of nitrogen. The functional response follows a sigmoidal shape (*Holling III*):

$$graz = \frac{g_{max}\eta(PhytN)^2}{g_{max}+\eta(PhytN)^2} \qquad (13)$$

where g_{max} denotes the maximum grazing rate and η is the assimilation efficiency of zooplankton.

Phytoplankton are grazed in their simulated N:C ratio, i.e. the amount of carbon that is grazed is inversely related to the phytoplankton cell quota.

$$grazC = \frac{1}{q_P} graz \qquad (14)$$

However, zooplankton are assumed to maintain their optimum cellular N:C ratio via homeostasis. When the C:N ratio of prey ingestion exceeds the optimum zooplankton cell quota, this excess carbon is immediately respired as CO_2:

For $q_Z \leq q_{Z_{min}}$ assimilation efficiency of carbon is calculated as: $\left(1 - \frac{q_P}{q_Z}\right)$

Excretion of nitrogen ε_N and respiration of carbon ε_C are then given as:

$$\varepsilon_N = \varepsilon_0 f(T) ZoopN \qquad (15)$$

and

$$\varepsilon_C = \frac{\varepsilon_N}{q_Z} + \left(1 - \frac{q_P}{q_Z}\right) grazC \qquad (16)$$

where ε_0 is the excretion coefficient and $f(T)$ denotes the temperature-sensitivity of excretion and respiration.
Mortality of zooplankton is density dependent:

$$\gamma_Z = \gamma_{Z0} T_f (ZoopN)^2 \qquad (17)$$

with the mortality coefficient γ_{Z0}.

Dissolved organic matter

The primary source of DOM is exudation by phytoplankton. Release of DOC is controlled by temperature and the cell quota, increasing with a decreasing N:C ratio:

$$\theta_{DOC} = \theta_{DOC_0} f(T) \frac{q_{P_{max}} - q_P}{q_{P_{max}} - q_{P_{min}}} \qquad (18)$$

DON leakage is assumed to occur predominantly passively and is therefore calculated a fixed fraction of phytoplankton nitrogen, independent from temperature and cell quota:

$$\theta_{DON} = \theta_{DON_0} \qquad (19)$$

Bacterial remineralization of DOM is calculated separately for carbon and nitrogen and is a function of temperature and the elemental composition of DOM, which is used as a proxy for the substrate quality for bacteria:

$$\rho_{DON} = \rho_{DON_0} f(T) R_{DOM}^{NC} \quad (20)$$

$$\rho_{DOC} = \rho_{DOC_0} f(T) R_{DOM}^{NC} \quad (21)$$

Substrate quality is calculated with a Michaelis-Menten function, i.e. increasing with relative nitrogen content, and sharply decreasing at low N:C ratios:

$$R_{DOM}^{NC} = \frac{q_{DOM}}{k_{DOM} + q_{DOM}} \quad (22)$$

TEP and aggregation

Formation of TEP from polysaccharides (PCHO) is based on the model by Schartau et al. (2007) with several modifications.

PCHO are released by phytoplankton as a variable fraction of DOC release (f_{PCHO}) decreasing linearly with an increasing cellular N:C quota:

$$f_{PCHO} = f_{PCHO_{max}} \cdot \left[1 - \left(\frac{q_{P_{max}} - q_P}{q_{P_{max}} - q_{P_{min}}}\right)\right] \quad (23)$$

TEP are formed from PCHO through coagulation and aggregation of PCHO with each other and with TEP:

$$\beta_1 PCHO^2 + \beta_2 PCHO \cdot TEP \quad (24)$$

where β_1 and β_2 are the coagulation parameters.

TEP remineralization is a function of temperature, similar to remineralization of DOM:

$$\rho_{TEP} = \rho_{TEP_0} f(T) \quad (25)$$

TEP also play an important role in formation of aggregates, as TEP concentrations determine the "stickiness" of the water parcel ψ:

$$\psi = \psi_0 \cdot TEP \quad (26)$$

Aggregate formation is then calculated as:

$$Aggr = \psi \cdot (\phi_1 PhytN^2 + \phi_2 PhytN \cdot DetrN) \quad (27)$$

where ϕ_1 and ϕ_2 are the coagulation coefficients for phytoplankton with each other, and for phytoplankton with detritus, respectively.

An additional term calculates the loss of TEP, which forms the matrix of sinking aggregates:

$$Aggr_{TEP} = f_{TEP} \cdot \frac{Aggr}{q_P} \quad (28)$$

where f_{TEP} is the fraction of carbon contained in TEP in the amount of total carbon of aggregates.

Detritus

Remineralization of detritus is similar to that of DOM, i.e. it is calculated separately for carbon and nitrogen and is a function of temperature and the elemental composition of detritus, which is used as a proxy for the substrate quality for bacterial degradation:

$$\rho_{DetN} = \rho_{DetN_0} f(T) R_{Det}^{NC} \quad (29)$$

$$\rho_{DetC} = \rho_{DetC_0} f(T) R_{Det}^{NC} \quad (30)$$

Substrate quality is calculated with a Michaelis-Menten function, i.e. increasing with relative nitrogen content, and sharply decreasing at low N:C ratios:

$$R_{Det}^{NC} = \frac{q_{Det}}{k_{Det} + q_{Det}} \quad (31)$$

Sinking of organic matter and gas exchange

In the current model version, sinking of organic matter is calculated for detritus at a constant rate:

$$\omega = \omega_D \quad (32)$$

Future model development will include variable sinking speeds, depending on the composition of the sinking material.

Gas exchange is calculated following Smith (1985):

$$flux_{air-sea} = k \cdot K_0 \cdot \Delta pCO_2 \quad (33)$$

where k is the gas transfer velocity, K_0 the solubility coefficient, and ΔpCO_2 the air-water difference in partial pressure of CO_2.

The solubility coefficient of CO_2 in seawater (K_0) is calculated as a function of temperature and salinity (Weiss, 1974). ΔpCO_2 is calculated with the program CO2SYS (Lewis and Wallace, 1998), using simulated DIC and TA. The gas transfer velocity following Smith (1985) is calculated as:

$$k = \frac{D}{h} \quad (34)$$

where D is the molecular diffusivity as a function of temperature following Jähne et al., (1987):

$$D = f(T) \quad (35)$$

and h the thickness of the stagnant boundary layer as a function of windspeed (u):

$$h = 0.072 \cdot e^{-0.215u} \quad (36)$$

Note that wind speed can also be regarded as a proxy for mixing of the water column, e.g. in laboratory based experiments (see chapter 2).

References

Adams, H. E., Crump, B. C., and Kling, G. W.: Temperature controls on aquatic bacterial production and community dynamics in arctic lakes and streams, Environmental Microbiology, 12, 1319-1333, 2010.

Alldredge, A. L., Passow, U., and Logan, B. E.: The abundance and significance of a class of large transparent organic particles in the ocean, Deep-Sea Research Part I-Oceanographic Research Papers, 40, 1131-1140, 1993.

Anderson, M. J.: A new method for non-parametric multivariate analysis of variance, Austral Ecology, 26, 32-46, 2001.

Anderson, T. R.: Plankton functional type modelling: running before we can walk?, Journal of Plankton Research, 27, 1073-1081, 2005.

Armstrong, R. A.: Grazing limitation and nutrient limitation in marine ecosystems - steady state solutions of an ecosystem model with multiple food chains, Limnology and Oceanography, 39, 597-608, 1994.

Arrigo, K. R.: Carbon cycle - Marine manipulations, Nature, 450, 491-492, 2007.

Aumont, O. and Bopp, L.: Globalizing results from ocean in situ iron fertilization studies, Glob. Biogeochem. Cycle, 20, 2006.

Azam, F., Fenchel, T., Field, J. G., Gray, J. S., Meyerreil, L. A., and Thingstad, F.: The ecological role of water-column microbes in the sea Marine Ecology Progress Series, 10, 257-263, 1983.

Bacastow, R. and Maier-Reimer, E.: Ocean-circulation model of the carbon cycle, Climate Dynamics, 4, 95-125, 1990.

Bach, L. T., Mackinder, L. C. M., Schulz, K. G., Wheeler, G., Schroeder, D. C., Brownlee, C., and Riebesell, U.: Dissecting the impact of CO_2 and pH on the mechanisms of photosynthesis and calcification in the coccolithophore Emiliania huxleyi, New Phytologist, 199, 121-134, 2013.

Bach, L. T., Riebesell, U., and Schulz, K. G.: Distinguishing between the effects of ocean acidification and ocean carbonation in the coccolithophore Emiliania huxleyi, Limnology and Oceanography, 56, 2040-2050, 2011.

Bach, L. T., Riebesell, U., Sett, S., Febiri, S., Rzepka, P., and Schulz, K. G.: An approach for particle sinking velocity measurements in the 3-400 µm size range and considerations on the effect of temperature on sinking rates, Marine Biology, 159, 1853-1864, 2012.

Balmaseda, M. A., Trenberth, K. E., and Källén, E.: Distinctive climate signals in reanalysis of global ocean heat content, Geophys. Res. Lett., 40, 1754-1759, 2013.

Bandstra, L., Hales, B., and Takahashi, T.: High-frequency measurements of total CO_2: Method development and first oceanographic observations, Mar. Chem., 100, 24-38, 2006.

Banse, K.: Uptake of inorganic carbon and nitrate by marine plankton and the Redfield ratio, Glob. Biogeochem. Cycle, 8, 81-84, 1994.

Barry, J. P., Tyrrell, T., Hansson, L., Plattner, G. K., and Gattuso, J. P.: Atmospheric CO_2 targets for ocean acidification perturbation experiments. In: Guide to best practices for ocean acidification research and data reporting, Riebesell, U., Fabry, V. J., Hansson, L., and Gattuso, J. P. (Eds.), Publications Office of the European Union Luxembourg, 2010.

Beardall, J., Stojkovic, S., and Larsen, S.: Living in a high CO_2 world: impacts of global climate change on marine phytoplankton, Plant Ecology & Diversity, 2, 191-205, 2009.

Beaugrand, G.: Decadal changes in climate and ecosystems in the North Atlantic Ocean and adjacent seas, Deep-Sea Res. Part II-Top. Stud. Oceanogr., 56, 656-673, 2009.

Beaulieu, S. E.: Accumulation and fate of phytodetritus on the sea floor. In: Oceanography and Marine Biology, Vol 40, Gibson, R. N., Barnes, M., and Atkinson, R. J. A. (Eds.), Oceanography and Marine Biology, 2002.

Behrends, G.: Long-term investigations of seasonal mesozooplankton dynamics in Kiel Bight, Germany, Proceedings of the 13th symposium on Baltic and Marine Biology, Jurmala, Latvia (1993), 93-98, 1996.

Behrenfeld, M. J. and Falkowski, P. G.: Photosynthetic rates derived from satellite-based chlorophyll concentration, Limnology and Oceanography, 42, 1-20, 1997.

Behrenfeld, M. J., O'Malley, R. T., Siegel, D. A., McClain, C. R., Sarmiento, J. L., Feldman, G. C., Milligan, A. J., Falkowski, P. G., Letelier, R. M., and Boss, E. S.: Climate-driven trends in contemporary ocean productivity, Nature, 444, 752-755, 2006.

Berelson, W. M.: Particle settling rates increase with depth in the ocean, Deep-Sea Res. Part II-Top. Stud. Oceanogr., 49, 237-251, 2002.

Berges, J. A., Varela, D. E., and Harrison, P. J.: Effects of temperature on growth rate, cell composition and nitrogen metabolism in the marine diatom Thalassiosira pseudonana (Bacillariophyceae), Marine Ecology-Progress Series, 225, 139-146, 2002.

Bett, K. E. and Cappi, J. B.: Effect of Pressure on the Viscosity of Water, Nature, 207, 620-621, 1965.

Biddanda, B. and Benner, R.: Carbon, nitrogen, and carbohydrate fluxes during the production of particulate and dissolved organic matter by marine phytoplankton, Limnology and Oceanography, 42, 506-518, 1997.

Blackford, J. C., Allen, J. I., and Gilbert, F. J.: Ecosystem dynamics at six contrasting sites: a generic modelling study, Journal of Marine Systems, 52, 191-215, 2004.

Bopp, L., Monfray, P., Aumont, O., Dufresne, J. L., Le Treut, H., Madec, G., Terray, L., and Orr, J. C.: Potential impact of climate change on marine export production, Glob. Biogeochem. Cycle, 15, 81-99, 2001.

Bopp, L., Resplandy, L., Orr, J. C., Doney, S. C., Dunne, J. P., Gehlen, M., Halloran, P., Heinze, C., Ilyina, T., S√¯©f√¯©rian, R., Tjiputra, J., and Vichi, M.: Multiple stressors of ocean ecosystems in the 21st century: projections with CMIP5 models, Biogeosciences, 10, 6225-6245, 2013.

Borchard, C. and Engel, A.: Organic matter exudation by Emiliania huxleyi under simulated future ocean conditions, Biogeosciences, 9, 3405-3423, 2012.

Boyce, D. G., Lewis, M. R., and Worm, B.: Global phytoplankton decline over the past century, Nature, 466, 591-596, 2010.

Boyd, P. W. and Doney, S. C.: Modelling regional responses by marine pelagic ecosystems to global climate change, Geophys. Res. Lett., 29, 2002.

Boyd, P. W., Rynearson, T. A., Armstrong, E. A., Fu, F. X., Hayashi, K., Hu, Z. X., Hutchins, D. A., Kudela, R. M., Litchman, E., Mulholland, M. R., Passow, U., Strzepek, R. F., Whittaker, K. A., Yu, E., and Thomas, M. K.: Marine Phytoplankton Temperature versus Growth Responses from Polar to Tropical Waters - Outcome of a Scientific Community-Wide Study, Plos One, 8, 2013.

Boyd, P. W., Strzepek, R., Fu, F. X., and Hutchins, D. A.: Environmental control of open-ocean phytoplankton groups: Now and in the future, Limnology and Oceanography, 55, 1353-1376, 2010.

Boyd, P. W., Watson, A. J., Law, C. S., Abraham, E. R., Trull, T., Murdoch, R., Bakker, D. C. E., Bowie, A. R., Buesseler, K. O., Chang, H., Charette, M., Croot, P., Downing, K., Frew, R., Gall, M., Hadfield, M., Hall, J., Harvey, M., Jameson, G., LaRoche, J., Liddicoat, M., Ling, R., Maldonado, M. T., McKay, R. M., Nodder, S., Pickmere, S., Pridmore, R., Rintoul, S., Safi, K., Sutton, P., Strzepek, R., Tanneberger, K., Turner, S., Waite, A., and Zeldis, J.: A mesoscale phytoplankton bloom in the polar Southern Ocean stimulated by iron fertilization, Nature, 407, 695-702, 2000.

Brock, T. D.: Calculating solar radiation for ecological studies, Ecological Modelling, 14, 1-19, 1981.

Broecker, W. and Clark, E.: A dramatic Atlantic dissolution event at the onset of the last glaciation, Geochemistry Geophysics Geosystems, 2, 2001.

Brown, J. H., Gillooly, J. F., Allen, A. P., Savage, V. M., and West, G. B.: Toward a metabolic theory of ecology, Ecology, 85, 1771-1789, 2004.

Brussaard, C. P. D., Gast, G. J., van Duyl, F. C., and Riegman, R.: Impact of phytoplankton bloom magnitude on a pelagic microbial food web, Marine Ecology Progress Series, 144, 211-221, 1996.

Brzezinski, M. A.: The Si-C-N ratio of marine diatoms - Interspecific variability and the effect of some environmental variables, Journal of Phycology, 21, 347-357, 1985.

Buesseler, K. O.: The decoupling of production and particulate export in the surface ocean, Glob. Biogeochem. Cycle, 12, 297-310, 1998.

Buitenhuis, E. T., Vogt, M., Moriarty, R., Bednarsek, N., Doney, S. C., Leblanc, K., Le Quéré, C., Luo, Y. W., O'Brien, C., O'Brien, T., Peloquin, J., Schiebel, R., and Swan, C.: MAREDAT: towards a world atlas of MARine Ecosystem DATa, Earth Syst. Sci. Data, 5, 227-239, 2013.

Burd, A. B., Hansell, D. A., Steinberg, D. K., Anderson, T. R., Arístegui, J., Baltar, F., Beaupré, S. R., Buesseler, K., DeHairs, F., and Jackson, G. A.: Assessing the apparent imbalance between geochemical and biochemical indicators of meso- and bathypelagic biological activity: What the @$#! is wrong with present calculations of carbon budgets?, Deep Sea Research Part II: Topical Studies in Oceanography, 57, 1557-1571, 2010.

Burd, A. B. and Jackson, G. A.: Particle Aggregation. In: Annual Review of Marine Science, Annual Review of Marine Science, Annual Reviews, Palo Alto, 2009.

Burkhardt, S., Amoroso, G., Riebesell, U., and Sultemeyer, D.: CO_2 and HCO_3-uptake in marine diatoms acclimated to different CO_2 concentrations, Limnology and Oceanography, 46, 1378-1391, 2001.

Burkhardt, S., Zondervan, I., and Riebesell, U.: Effect of CO_2 concentration on C : N : P ratio in marine phytoplankton: A species comparison, Limnology and Oceanography, 44, 683-690, 1999.

Caldeira, K. and Wickett, M. E.: Anthropogenic carbon and ocean pH, Nature, 425, 365-365, 2003.

Carlson, C. A.: Production and Removal Processes. In: Biogeochemistry of Marine Dissolved Organic Matter, Hansell, D. A. and Carlson, C. A. (Eds.), Academic Press, San Diego, 2002.

Carlson, C. A., Hansell, D. A., Nelson, N. B., Siegel, D. A., Smethie, W. M., Khatiwala, S., Meyers, M. M., and Halewood, E.: Dissolved organic carbon export and subsequent remineralization in the mesopelagic and bathypelagic realms of the North Atlantic basin, Deep-Sea Res. Part II-Top. Stud. Oceanogr., 57, 1433-1445, 2010.

Carr, M. E., Friedrichs, M. A. M., Schmeltz, M., Aita, M. N., Antoine, D., Arrigo, K. R., Asanuma, I., Aumont, O., Barber, R., Behrenfeld, M., Bidigare, R., Buitenhuis, E. T., Campbell, J., Ciotti, A., Dierssen, H., Dowell, M., Dunne, J., Esaias, W., Gentili, B., Gregg, W., Groom, S., Hoepffner, N., Ishizaka, J., Kameda, T., Le Quere, C., Lohrenz, S., Marra, J., Melin, F., Moore, K., Morel, A., Reddy, T. E., Ryan, J., Scardi, M., Smyth, T., Turpie, K., Tilstone, G., Waters, K., and Yamanaka, Y.: A comparison of global estimates of marine primary production from ocean color, Deep-Sea Res. Part II-Top. Stud. Oceanogr., 53, 741-770, 2006.

Carstensen, J., Conley, D. J., and Henriksen, P.: Frequency, composition, and causes of summer phytoplankton blooms in a shallow coastal ecosystem, the Kattegat, Limnology and Oceanography, 49, 191-201, 2004.

Chen, Y. C.: The biomass and total lipid content and composition of twelve species of marine diatoms cultured under various environments, Food Chemistry, 131, 211-219, 2012.

Chisholm, S. W.: Stirring times in the Southern Ocean, Nature, 407, 685-687, 2000.

Chown, S. L., Hoffmann, A. A., Kristensen, T. N., Angilletta, M. J., Stenseth, N. C., and Pertoldi, C.: Adapting to climate change: a perspective from evolutionary physiology, Climate Research, 43, 3-15, 2010.

Claquin, P., Probert, I., Lefebvre, S., and Veron, B.: Effects of temperature on photosynthetic parameters and TEP production in eight species of marine microalgae, Aquat. Microb. Ecol., 51, 1-11, 2008.

Clegg, S. L. and Whitfield, M.: A generalized model for the scavenging of trace metals in the open ocean. I. Particle cycling, Deep-Sea Research Part a-Oceanographic Research Papers, 37, 809-832, 1990.

Collins, S. and Bell, G.: Phenotypic consequences of 1,000 generations of selection at elevated CO_2 in a green alga, Nature, 431, 566-569, 2004.

Corzo, A., Morillo, J. A., and Rodriguez, S.: Production of transparent exopolymer particles (TEP) in cultures of Chaetoceros calcitrans under nitrogen limitation, Aquat. Microb. Ecol., 23, 63-72, 2000.

Cox, P. M., Betts, R. A., Jones, C. D., Spall, S. A., and Totterdell, I. J.: Acceleration of global warming due to carbon-cycle feedbacks in a coupled climate model, Nature, 408, 184-187, 2000.

Daufresne, M., Lengfellner, K., and Sommer, U.: Global warming benefits the small in aquatic ecosystems, Proceedings of the National Academy of Sciences of the United States of America, 106, 12788-12793, 2009.

de Boyer Montégut, C., Madec, G., Fischer, A. S., Lazar, A., and Iudicone, D.: Mixed layer depth over the global ocean: An examination of profile data and a profile-based climatology, Journal of Geophysical Research: Oceans, 109, C12003, 2004.

del Giorgio, P. A. and Duarte, C. M.: Respiration in the open ocean, Nature, 420, 379-384, 2002.

Delille, B., Harlay, J., Zondervan, I., Jacquet, S., Chou, L., Wollast, R., Bellerby, R. G. J., Frankignoulle, M., Borges, A. V., Riebesell, U., and Gattuso, J. P.: Response of primary production and calcification to changes of pCO_2 during experimental blooms of the coccolithophorid Emiliania huxleyi, Glob. Biogeochem. Cycle, 19, 2005.

Dickson, A. G. and Millero, F. J.: A comparison of the equilibrium constants for the dissociation of carbonic acid in seawater media, Deep Sea Research Part A. Oceanographic Research Papers, 34, 1733-1743, 1987.

Dickson, A. G., Sabine, C. L., and Christian, J. R.: Guide to best practices for ocean CO_2 measurements - PICES Special Publication 3, 2007.

Dittmar, T. and Paeng, J.: A heat-induced molecular signature in marine dissolved organic matter, Nature Geoscience, 2, 175-179, 2009.

Doney, S. C., Fabry, V. J., Feely, R. A., and Kleypas, J. A.: Ocean Acidification: The Other CO_2 Problem, Annual Review of Marine Science, 1, 169-192, 2009a.

Doney, S. C., Lima, I., Moore, J. K., Lindsay, K., Behrenfeld, M. J., Westberry, T. K., Mahowald, N., Glover, D. M., and Takahashi, T.: Skill metrics for confronting global upper ocean ecosystem-biogeochemistry models against field and remote sensing data, Journal of Marine Systems, 76, 95-112, 2009b.

Doval, M. D. and Hansell, D. A.: Organic carbon and apparent oxygen utilization in the western South Pacific and the central Indian Oceans, Mar. Chem., 68, 249-264, 2000.

Droop, M. R.: 25 years of algal growth kinetics - a personal view, Botanica Marina, 26, 99-112, 1983.

Duarte, C. M.: Marine ecology warms up to theory, Trends in Ecology & Evolution, 22, 331-333, 2007.

Duarte, P.: A mechanistic model of the effects of light and temperature on algal primary productivity Ecological Modelling, 82, 151-160, 1995.

Dunne, J. P., Sarmiento, J. L., and Gnanadesikan, A.: A synthesis of global particle export from the surface ocean and cycling through the ocean interior and on the seafloor, Glob. Biogeochem. Cycle, 21, 2007.

Durbin, E. G. and Durbin, A. G.: Effects of temperature and food abundance on grazing and short-term weight change in the marine copepod Acartia hudsonica, Limnology and Oceanography, 37, 361-378, 1992.

Engel, A.: Direct relationship between CO_2 uptake and transparent exopolymer particles production in natural phytoplankton, Journal of Plankton Research, 24, 49-53, 2002.

Engel, A., Delille, B., Jacquet, S., Riebesell, U., Rochelle-Newall, E., Terbruggen, A., and Zondervan, I.: Transparent exopolymer particles and dissolved organic carbon production by Emiliania huxleyi exposed to different CO_2 concentrations: a mesocosm experiment, Aquat. Microb. Ecol., 34, 93-104, 2004a.

Engel, A., Goldthwait, S., Passow, U., and Alldredge, A.: Temporal decoupling of carbon and nitrogen dynamics in a mesocosm diatom bloom, Limnology and Oceanography, 47, 753-761, 2002.

Engel, A., Handel, N., Wohlers, J., Lunau, M., Grossart, H. P., Sommer, U., and Riebesell, U.: Effects of sea surface warming on the production and composition of dissolved organic matter during phytoplankton blooms: results from a mesocosm study, Journal of Plankton Research, 33, 357-372, 2011.

Engel, A. and Passow, U.: Carbon and nitrogen content of transparent exopolymer particles (TEP) in relation to their Alcian Blue adsorption, Marine Ecology Progress Series, 219, 1-10, 2001.

Engel, A., Thoms, S., Riebesell, U., Rochelle-Newall, E., and Zondervan, I.: Polysaccharide aggregation as a potential sink of marine dissolved organic carbon, Nature, 428, 929-932, 2004b.

Eppley, R. W.: Temperature and phytoplankton growth in sea, Fishery Bulletin, 70, 1063-1085, 1972.

Eppley, R. W. and Peterson, B. J.: Particulate organic matter flux and planktonic new production in the deep ocean, Nature, 282, 677-680, 1979.

Evans, G. T. and Parslow, J. S.: A model of annual plankton cycles, Biological Oceanography, 3, 327-347, 1985.

Falkowski, P. G.: The role of phytoplankton photosynthesis in global biogeochemical cycles, Photosynth Res, 39, 235-258, 1994.

Falkowski, P. G., Barber, R. T., and Smetacek, V.: Biogeochemical controls and feedbacks on ocean primary production, Science, 281, 200-206, 1998.

Falkowski, P. G. and Raven, J. A.: Aquatic photosynthesis, Princeton University Press, 2007.

Falkowski, P. G., Scholes, R. J., Boyle, E., Canadell, J., Canfield, D., Elser, J., Gruber, N., Hibbard, K., Hogberg, P., Linder, S., Mackenzie, F. T., Moore, B., Pedersen, T., Rosenthal,

Y., Seitzinger, S., Smetacek, V., and Steffen, W.: The global carbon cycle: A test of our knowledge of earth as a system, Science, 290, 291-296, 2000.

Farmer, C. and Hansell, D. A.: Determination of dissolved organic carbon and total dissolved nitrogen in sea water. In: Guide to best practices for ocean CO_2 measurements - PICES Special Publication 3, Dickson, A. G., Sabine, C. L., and Christian, J. R. (Eds.), 2007.

Fasham, M. J. R., Ducklow, H. W., and McKelvie, S. M.: A nitrogen-based model of plankton dynamics in the oceanic mixed layer, Journal of Marine Research, 48, 591-639, 1990.

Feng, Y., Hare, C. E., Leblanc, K., Rose, J. M., Zhang, Y. H., DiTullio, G. R., Lee, P. A., Wilhelm, S. W., Rowe, J. M., Sun, J., Nemcek, N., Gueguen, C., Passow, U., Benner, I., Brown, C., and Hutchins, D. A.: Effects of increased pCO_2 and temperature on the North Atlantic spring bloom. I. The phytoplankton community and biogeochemical response, Marine Ecology-Progress Series, 388, 13-25, 2009.

Feng, Y., Warner, M. E., Zhang, Y., Sun, J., Fu, F. X., Rose, J. M., and Hutchins, D. A.: Interactive effects of increased pCO_2, temperature and irradiance on the marine coccolithophore Emiliania huxleyi (Prymnesiophyceae), European Journal of Phycology, 43, 87-98, 2008.

Field, C. B., Behrenfeld, M. J., Randerson, J. T., and Falkowski, P. G.: Primary production of the biosphere: Integrating terrestrial and oceanic components, Science, 281, 237-240, 1998.

Fileman, E., Petropavlovsky, A., and Harris, R.: Grazing by the copepods Calanus helgolandicus and Acartia clausi on the protozooplankton community at station L4 in the Western English Channel, Journal of Plankton Research, 32, 709-724, 2010.

Finkel, Z. V., Beardall, J., Flynn, K. J., Quigg, A., Rees, T. A. V., and Raven, J. A.: Phytoplankton in a changing world: cell size and elemental stoichiometry, Journal of Plankton Research, 32, 119-137, 2010.

Flynn, K. J.: Reply to Horizons Article 'Plankton functional type modelling: running before we can walk' Anderson (2005): II. Putting trophic functionality into plankton functional types, Journal of Plankton Research, 28, 873-875, 2006.

Fogg, G. E.: The ecological significance of extracellular products of phytoplankton photosynthesis, Botanica Marina, 26, 3-14, 1983.

Fry, B., Hopkinson, C. S., and Nolin, A.: Long-term decomposition of DOC from experimental diatom blooms, Limnology and Oceanography, 41, 1344-1347, 1996.

Fu, F. X., Warner, M. E., Zhang, Y. H., Feng, Y. Y., and Hutchins, D. A.: Effects of increased temperature and CO_2 on photosynthesis, growth, and elemental ratios in marine Synechococcus and Prochlorococcus (Cyanobacteria), Journal of Phycology, 43, 485-496, 2007.

Fu, F. X., Zhang, Y. H., Warner, M. E., Feng, Y. Y., Sun, J., and Hutchins, D. A.: A comparison of future increased CO_2 and temperature effects on sympatric Heterosigma akashiwo and Prorocentrum minimum, Harmful Algae, 7, 76-90, 2008.

Fung, I. Y., Doney, S. C., Lindsay, K., and John, J.: Evolution of carbon sinks in a changing climate, Proceedings of the National Academy of Sciences of the United States of America, 102, 11201-11206, 2005.

Fung, I. Y., Meyn, S. K., Tegen, I., Doney, S. C., John, J. G., and Bishop, J. K. B.: Iron supply and demand in the upper ocean, Glob. Biogeochem. Cycle, 14, 281-295, 2000.

Garcia, H. E., Locarnini, R. A., Boyer, T. P., and Antonov, J. I.: World Ocean Atlas 2005, Volume 4: Nutrients., U.S. Government Printing Office, Washington, D.C., 2006b.

Garcia, H. E., Locarnini, R. A., Boyer, T. P., Antonov, J. I., Zweng, M. M., Baranova, O. K., and Johnson, D. R.: World Ocean Atlas 2009, Volume 4: Nutrients (phosphate, nitrate, silicate), U.S. Government Printing Office, Washington, D.C., 2010.

Gattuso, J.-P. and Hansson, L.: Ocean acidification, Oxford University Press, 2011.

Geider, R. J. and La Roche, J.: Redfield revisited: variability of C : N : P in marine microalgae and its biochemical basis, European Journal of Phycology, 37, 1-17, 2002.

Geider, R. J., MacIntyre, H. L., and Kana, T. M.: A dynamic regulatory model of phytoplanktonic acclimation to light, nutrients, and temperature, Limnology and Oceanography, 43, 679-694, 1998.

Gentleman, W., Leising, A., Frost, B., Strom, S., and Murray, J.: Functional responses for zooplankton feeding on multiple resources: a review of assumptions and biological dynamics, Deep-Sea Res. Part II-Top. Stud. Oceanogr., 50, 2847-2875, 2003.

Gillooly, J. F., Brown, J. H., West, G. B., Savage, V. M., and Charnov, E. L.: Effects of size and temperature on metabolic rate, Science, 293, 2248-2251, 2001.

Giordano, M., Beardall, J., and Raven, J. A.: CO_2 concentrating mechanisms in algae: Mechanisms, environmental modulation, and evolution. In: Annual Review of Plant Biology, Annual Review of Plant Biology, 2005.

Goldman, J. C., Hansell, D. A., Dennett, M. R.: Chemical characterization of three large oceanic diatoms: potential impact on water column chemistry, Marine Ecology Progress Series, 88, 257-270, 1992.

Gordillo, F. J. L., Jimenez, C., Figueroa, F. L., and Niell, F. X.: Influence of elevated CO_2 and nitrogen supply on the carbon assimilation performance and cell composition of the unicellular alga Dunaliella viridis, Physiologia Plantarum, 119, 513-518, 2003.

Grebmeier, J. M., Overland, J. E., Moore, S. E., Farley, E. V., Carmack, E. C., Cooper, L. W., Frey, K. E., Helle, J. H., McLaughlin, F. A., and McNutt, S. L.: A Major Ecosystem Shift in the Northern Bering Sea, Science, 311, 1461-1464, 2006.

Gregg, W. W., Conkright, M. E., Ginoux, P., O'Reilly, J. E., and Casey, N. W.: Ocean primary production and climate: Global decadal changes, Geophys. Res. Lett., 30, 2003.

Gruber, N.: Warming up, turning sour, losing breath: ocean biogeochemistry under global change, Philosophical Transactions of the Royal Society a-Mathematical Physical and Engineering Sciences, 369, 1980-1996, 2011.

Guillard, R. R. L. and Ryther, J. H.: Studies of marine planktonic diatoms. I. Cyclotella nana Hustedt, and Detonula confervacea (cleve) Gran, Canadian journal of microbiology, 8, 229-239, 1962.

Hansell, D. A.: Dissolved organic carbon reference material program, Eos, Transactions American Geophysical Union, 86, 318-318, 2005.

Hansell, D. A. and Carlson, C. A.: Net community production of dissolved organic carbon, Glob. Biogeochem. Cycle, 12, 443-453, 1998.

Hansell, D. A., Carlson, C. A., Repeta, D. J., and Schlitzer, R.: Dissolved organic matter in the ocean - A controversy stimulates new insights, Oceanography, 22, 202-211, 2009.

Hansen, H. P. and Koroleff, F.: Determination of nutrients, Wiley-VCH Verlag GmbH, 2007.

Hare, C. E., Leblanc, K., DiTullio, G. R., Kudela, R. M., Zhang, Y., Lee, P. A., Riseman, S., and Hutchins, D. A.: Consequences of increased temperature and CO_2 for phytoplankton community structure in the Bering Sea, Marine Ecology Progress Series, 352, 9-16, 2007.

Harrison, P. J., Conway, H. L., Holmes, R. W., and Davis, C. O.: Marine diatoms grown in chemostats under silicate or ammonium limitation. 3. Cellular chemical composition and morphology of Chaetoceros debilis, Skeletonema costatum, and Thalassiosira gravida, Marine Biology, 43, 19-31, 1977.

Helmuth, B., Kingsolver, J. G., and Carrington, E.: Biophysics, physiological ecology, and climate change - Does mechanism matter?, Annual Review of Physiology, 67, 177-201, 2005.

Henson, S. A., Sanders, R., Madsen, E., Morris, P. J., Le Moigne, F., and Quartly, G. D.: A reduced estimate of the strength of the ocean's biological carbon pump, Geophys. Res. Lett., 38, L04606, 2011.

Hofmann, G. E. and Todgham, A. E.: Living in the Now: Physiological Mechanisms to Tolerate a Rapidly Changing Environment. In: Annual Review of Physiology, Annual Review of Physiology, 2010.

Holling, C. S.: Some Characteristics of Simple Types of Predation and Parasitism, The Canadian Entomologist, 91, 385-398, 1959.

Honjo, S. and Roman, M. R.: Marine copepod fecal pellets - Production, preservation and sedimentation, Journal of Marine Research, 36, 45-57, 1978.

Hopkinson, B. M., Dupont, C. L., Allen, A. E., and Morel, F. M. M.: Efficiency of the CO_2-concentrating mechanism of diatoms, Proceedings of the National Academy of Sciences of the United States of America, 108, 3830-3837, 2011.

Hoppe, H. G., Breithaupt, P., Walther, K., Koppe, R., Bleck, S., Sommer, U., and Jurgens, K.: Climate warming in winter affects the coupling between phytoplankton and bacteria during the spring bloom: a mesocosm study, Aquat. Microb. Ecol., 51, 105-115, 2008.

Huertas, I. E., Rouco, M., Lopez-Rodas, V., and Costas, E.: Warming will affect phytoplankton differently: evidence through a mechanistic approach, Proceedings of the Royal Society B-Biological Sciences, 278, 3534-3543, 2011.

Hutchins, D. A., Fu, F. X., Zhang, Y., Warner, M. E., Feng, Y., Portune, K., Bernhardt, P. W., and Mulholland, M. R.: CO_2 control of Trichodesmium N-2 fixation, photosynthesis, growth rates, and elemental ratios: Implications for past, present, and future ocean biogeochemistry, Limnology and Oceanography, 52, 1293-1304, 2007.

Iglesias-Rodriguez, M. D., Halloran, P. R., Rickaby, R. E. M., Hall, I. R., Colmenero-Hidalgo, E., Gittins, J. R., Green, D. R. H., Tyrrell, T., Gibbs, S. J., von Dassow, P., Rehm, E., Armbrust, E. V., and Boessenkool, K. P.: Phytoplankton calcification in a high-CO_2 world, Science, 320, 336-340, 2008.

IPCC: Climate Change 2007: The Physical Science Basis. Contribution of Working Group I to the Fourth Assessment Report of the Intergovernmental Panel on Climate Change., Cambridge University Press, Cambridge, United Kingdom and New York, NY, USA, 2007a.

IPCC: Climate Change 2007: Impacts, Adaptation and Vulnerability. Contribution of Working Group II to the Fourth Assessment Report of the Intergovernmental Panel on Climate Change., Cambridge University Press, Cambridge, UK, 2007b.

Ito, T. and Follows, M. J.: Preformed phosphate, soft tissue pump and atmospheric CO_2, Journal of Marine Research, 63, 813-839, 2005.

Ivlev, V. S.: Experimental Ecology of the Feeding of Fishes, Pischepromizdat, Moscow, 1955.

Jackson, G. A., Maffione, R., Costello, D. K., Alldredge, A. L., Logan, B. E., and Dam, H. G.: Particle size spectra between 1 μm and 1 cm at Monterey Bay determined using multiple instruments, Deep-Sea Research Part I-Oceanographic Research Papers, 44, 1739-1767, 1997.

Jähne, B., Heinz, G., and Dietrich, W.: Measurement of the Diffusion Coefficients of Sparingly Soluble Gases in Water, J. Geophys. Res., 92, 10767-10776, 1987.

Kähler, P. and Koeve, W.: Marine dissolved organic matter: can its C : N ratio explain carbon overconsumption?, Deep-Sea Research Part I-Oceanographic Research Papers, 48, 49-62, 2001.

Keller, A. A., Oviatt, C. A., Walker, H. A., and Hawk, J. D.: Predicted impacts of elevated temperature on the magnitude of the winter-spring phytoplankton bloom in temperate coastal waters: A mesocosm study, Limnology and Oceanography, 44, 344-356, 1999.

Keller, D. P., Oschlies, A., and Eby, M.: A new marine ecosystem model for the University of Victoria Earth System Climate Model, Geosci. Model Dev., 5, 1195-1220, 2012.

Kester, D. R., Duedall, I. W., Connors, D. N., and Pytkowic.Rm: Preparation of artificial seawater, Limnology and Oceanography, 12, 176-&, 1967.

Kim, J. M., Lee, K., Shin, K., Yang, E. J., Engel, A., Karl, D. M., and Kim, H. C.: Shifts in biogenic carbon flow from particulate to dissolved forms under high carbon dioxide and warm ocean conditions, Geophys. Res. Lett., 38, 2011.

Kingsolver, J. G.: The Well-Temperatured Biologist, American Naturalist, 174, 755-768, 2009.

Kirchman, D. L., Newell, S. Y., and Hodson, R. E.: Incorporation versus biosynthesis of leucine: implications for measuring rates of protein synthesis and biomass production by bacteria in marine systems, Marine Ecology Progress Series, 32, 47-59, 1986.

Koeve, W.: Spring bloom carbon to nitrogen ratio of net community production in the temperate N. Atlantic, Deep-Sea Research Part I-Oceanographic Research Papers, 51, 1579-1600, 2004.

Koeve, W.: Magnitude of excess carbon sequestration into the deep ocean and the possible role of TEP, Marine Ecology-Progress Series, 291, 53-64, 2005.

Koeve, W.: C : N stoichiometry of the biological pump in the North Atlantic: Constraints from climatological data, Glob. Biogeochem. Cycle, 20, 2006.

Kolber, Z. S., Barber, R. T., Coale, K. H., Fitzwater, S. E., Greene, R. M., Johnson, K. S., Lindley, S., and Falkowski, P. G.: Iron limitation of phytoplankton photosynthesis in the equatorial Pacific Ocean, Nature, 371, 145-149, 1994.

Körtzinger, A., Koeve, W., Kahler, P., and Mintrop, L.: C : N ratios in the mixed layer during the productive season in the northeast Atlantic Ocean, Deep-Sea Research Part I-Oceanographic Research Papers, 48, 661-688, 2001.

Kriest, I., Khatiwala, S., and Oschlies, A.: Towards an assessment of simple global marine biogeochemical models of different complexity, Progress in Oceanography, 86, 337-360, 2010.

Kriest, I. and Oschlies, A.: On the treatment of particulate organic matter sinking in large-scale models of marine biogeochemical cycles, Biogeosciences, 5, 55-72, 2008.

Kuss, J. and Schneider, B.: Chemical enhancement of the CO_2 gas exchange at a smooth seawater surface, Mar. Chem., 91, 165-174, 2004.

Kwon, E. Y., Primeau, F., and Sarmiento, J. L.: The impact of remineralization depth on the air-sea carbon balance, Nature Geoscience, 2, 630-635, 2009.

Lampitt, R. S.: Evidence for the seasonal deposition of detritus to the deep-sea floor and its subsequent resuspension, Deep-Sea Research Part a-Oceanographic Research Papers, 32, 885-897, 1985.

Lampitt, R. S., Achterberg, E. P., Anderson, T. R., Hughes, J. A., Iglesias-Rodriguez, M. D., Kelly-Gerreyn, B. A., Lucas, M., Popova, E. E., Sanders, R., Shepherd, J. G., Smythe-Wright, D., and Yool, A.: Ocean fertilization: a potential means of geoengineering?, Philosophical Transactions of the Royal Society a-Mathematical Physical and Engineering Sciences, 366, 3919-3945, 2008.

Lampitt, R. S., Bett, B. J., Kiriakoulakis, K., Popova, E. E., Ragueneau, O., Vangriesheim, A., and Wolff, G. A.: Material supply to the abyssal seafloor in the Northeast Atlantic, Progress in Oceanography, 50, 27-63, 2001.

Langer, G., Nehrke, G., Probert, I., Ly, J., and Ziveri, P.: Strain-specific responses of Emiliania huxleyi to changing seawater carbonate chemistry, Biogeosciences, 6, 2637-2646, 2009.

Lassen, M. K., Nielsen, K. D., Richardson, K., Garde, K., and Schluter, L.: The effects of temperature increases on a temperate phytoplankton community - A mesocosm climate change scenario, Journal of Experimental Marine Biology and Ecology, 383, 79-88, 2010.

Laws, E. A., Falkowski, P. G., Smith, W. O., Ducklow, H., and McCarthy, J. J.: Temperature effects on export production in the open ocean, Glob. Biogeochem. Cycle, 14, 1231-1246, 2000.

Le Quéré, C., Harrison, S. P., Prentice, I. C., Buitenhuis, E. T., Aumont, O., Bopp, L., Claustre, H., Da Cunha, L. C., Geider, R., Giraud, X., Klaas, C., Kohfeld, K. E., Legendre, L., Manizza, M., Platt, T., Rivkin, R. B., Sathyendranath, S., Uitz, J., Watson, A. J., and Wolf-Gladrow, D.: Ecosystem dynamics based on plankton functional types for global ocean biogeochemistry models, Global Change Biology, 11, 2016-2040, 2005.

Lee, C. and Cronin, C.: Particulate amino acids in the sea: Effects of primary productivity and biological decomposition, Journal of Marine Research, 42, 1075-1097, 1984.

Levitus, S., Antonov, J. I., Boyer, T. P., Baranova, O. K., Garcia, H. E., Locarnini, R. A., Mishonov, A. V., Reagan, J. R., Seidov, D., Yarosh, E. S., and Zweng, M. M.: World ocean heat content and thermosteric sea level change (0–2000 m), 1955–2010, Geophys. Res. Lett., 39, L10603, 2012.

Lewis, E. and Wallace, D. W. R.: Program Developed for CO_2 System Calculations. ORNL/CDIAC-105., Carbon Dioxide Information Analysis Center, Oak Ridge National Laboratory, U.S. Department of Energy, Oak Ridge, Tennessee, 1998.

Liebig, J. and Playfair, L.: Organic chemistry in its applications to agriculture and physiology by Justus Liebig ; edited from the manuscript of the author by Lyon Playfair, Printed for Taylor and Walton, London, 1840.

Locarnini, R. A., Mishonov, A. V., Antonov, J. I., Boyer, T. P., and Garcia, H. E.: World Ocean Atlas 2005, Volume 1: Temperature., U.S. Government Printing Office, Washington, D.C., 2006.

Logan, B. E. and Hunt, J. R.: Advantages to microbes of growth in permeable aggregates in marine systems, Limnology and Oceanography, 32, 1034-1048, 1987.

Logan, B. E., Passow, U., Alldredge, A. L., Grossart, H. P., and Simon, M.: Rapid formation and sedimentation of large aggregates is predictable from coagulation rates (half-lives) of transparent exopolymer particles (TEP), Deep-Sea Res. Part II-Top. Stud. Oceanogr., 42, 203-214, 1995.

Lohbeck, K. T., Riebesell, U., and Reusch, T. B. H.: Adaptive evolution of a key phytoplankton species to ocean acidification, Nature Geosci, 5, 346-351, 2012.

Longhurst, A. R., Sathyendranath, S., Platt, T., and Caverhill, C.: An estimate of global primary production in the ocean from satellite radiometer data, Journal of Plankton Research, 17, 1245-1271, 1995.

Lopez-Urrutia, A. and Moran, X. A. G.: Resource limitation of bacterial production distorts the temperature dependence of oceanic carbon cycling, Ecology, 88, 817-822, 2007.

Lüthi, D., Le Floch, M., Bereiter, B., Blunier, T., Barnola, J. M., Siegenthaler, U., Raynaud, D., Jouzel, J., Fischer, H., Kawamura, K., and Stocker, T. F.: High-resolution carbon dioxide concentration record 650,000-800,000 years before present, Nature, 453, 379-382, 2008.

Maier-Reimer, E., Mikolajewicz, U., and Winguth, A.: Future ocean uptake of CO_2: interaction between ocean circulation and biology, Climate Dynamics, 12, 711-722, 1996.

Mari, X., Beauvais, S., Lemee, R., and Pedrotti, M. L.: Non-Redfield C : N ratio of transparent exopolymeric particles in the northwestern Mediterranean Sea, Limnology and Oceanography, 46, 1831-1836, 2001.

Marinov, I., Follows, M., Gnanadesikan, A., Sarmiento, J. L., and Slater, R. D.: How does ocean biology affect atmospheric pCO_2? Theory and models, J. Geophys. Res.-Oceans, 113, 2008.

Martin, J. H., Coale, K. H., Johnson, K. S., Fitzwater, S. E., Gordon, R. M., Tanner, S. J., Hunter, C. N., Elrod, V. A., Nowicki, J. L., Coley, T. L., Barber, R. T., Lindley, S., Watson, A. J., Vanscoy, K., Law, C. S., Liddicoat, M. I., Ling, R., Stanton, T., Stockel, J., Collins, C., Anderson, A., Bidigare, R., Ondrusek, M., Latasa, M., Millero, F. J., Lee, K., Yao, W., Zhang, J. Z., Friederich, G., Sakamoto, C., Chavez, F., Buck, K., Kolber, Z., Greene, R., Falkowski, P. G., Chisholm, S. W., Hoge, F., Swift, R., Yungel, J., Turner, S., Nightingale, P., Hatton, A., Liss, P., and Tindale, N. W.: Testing the iron hypothesis in ecosystems of the equatorial Pacific Ocean, Nature, 371, 123-129, 1994.

Martin, J. H., Knauer, G. A., Karl, D. M., and Broenkow, W. W.: VERTEX - Carbon cycling in the Northeast Pacific, Deep-Sea Research Part a-Oceanographic Research Papers, 34, 267-285, 1987.

McDonnell, A. M. P. and Buesseler, K. O.: Variability in the average sinking velocity of marine particles, Limnology and Oceanography, 55, 2085-2096, 2010.

McGinnis, K. M., Dempster, T. A., and Sommerfeld, M. R.: Characterization of the growth and lipid content of the diatom Chaetoceros muelleri, Journal of Applied Phycology, 9, 19-24, 1997.

Menden-Deuer, S. and Lessard, E. J.: Carbon to volume relationships for dinoflagellates, diatoms, and other protist plankton, Limnology and Oceanography, 45, 569-579, 2000.

Minas, H. J., Minas, M., and Packard, T. T.: Productivity in upwelling areas deduced from hydrographic and chemical fields, Limnology and Oceanography, 31, 1182-1206, 1986.

Moisan, J. R., Moisan, T. A., and Abbott, M. R.: Modelling the effect of temperature on the maximum growth rates of phytoplankton populations, Ecological Modelling, 153, 197-215, 2002.

Montagnes, D. J. S. and Franklin, D. J.: Effect of temperature on diatom volume, growth rate, and carbon and nitrogen content: Reconsidering some paradigms, Limnology and Oceanography, 46, 2008-2018, 2001.

Moore, J. K., Doney, S. C., Kleypas, J. A., Glover, D. M., and Fung, I. Y.: An intermediate complexity marine ecosystem model for the global domain, Deep-Sea Res. Part II-Top. Stud. Oceanogr., 49, 403-462, 2002.

Moore, J. K., Doney, S. C., and Lindsay, K.: Upper ocean ecosystem dynamics and iron cycling in a global three-dimensional model, Glob. Biogeochem. Cycle, 18, 2004.

Mopper, K., Zhou, J. A., Ramana, K. S., Passow, U., Dam, H. G., and Drapeau, D. T.: The role of surface-active carbohydrates in the flocculation of a diatom bloom in a mesocosm, Deep-Sea Res. Part II-Top. Stud. Oceanogr., 42, 47-73, 1995.

Moran, X. A. G., Lopez-Urrutia, A., Calvo-DÍaz, A., and Li, W. K. W.: Increasing importance of small phytoplankton in a warmer ocean, Global Change Biology, 16, 1137-1144, 2010.

Moran, X. A. G., Sebastian, M., Pedros-Alio, C., and Estrada, M.: Response of Southern Ocean phytoplankton and bacterioplankton production to short-term experimental warming, Limnology and Oceanography, 51, 1791-1800, 2006.

Muren, U., Berglund, J., Samuelsson, K., and Andersson, A.: Potential effects of elevated sea-water temperature on pelagic food webs, Hydrobiologia, 545, 153-166, 2005.

Myklestad, S.: Production of carbohydrates by marine planktonic diatoms. I. Comparison of nine different species in culture, Journal of Experimental Marine Biology and Ecology, 15, 261-274, 1974.

Najjar, R. G., Sarmiento, J. L., and Toggweiler, J. R.: Downward transport and fate of organic matter in the ocean: Simulations with a general circulation model, Glob. Biogeochem. Cycle, 6, 45-76, 1992.

Nelson, D. M., Treguer, P., Brzezinski, M. A., Leynaert, A., and Queguiner, B.: Production and dissolution of biogenic silica in the ocean. Revised global estimates, comparison with regional data and relationship to biogenic sedimentation, Glob. Biogeochem. Cycle, 9, 359-372, 1995.

O'Connor, M. I., Piehler, M. F., Leech, D. M., Anton, A., and Bruno, J. F.: Warming and Resource Availability Shift Food Web Structure and Metabolism, Plos Biology, 7, 2009.

Orr, J. C., Fabry, V. J., Aumont, O., Bopp, L., Doney, S. C., Feely, R. A., Gnanadesikan, A., Gruber, N., Ishida, A., Joos, F., Key, R. M., Lindsay, K., Maier-Reimer, E., Matear, R., Monfray, P., Mouchet, A., Najjar, R. G., Plattner, G. K., Rodgers, K. B., Sabine, C. L., Sarmiento, J. L., Schlitzer, R., Slater, R. D., Totterdell, I. J., Weirig, M. F., Yamanaka, Y., and Yool, A.: Anthropogenic ocean acidification over the twenty-first century and its impact on calcifying organisms, Nature, 437, 681-686, 2005.

Oschlies, A.: Model-derived estimates of new production: New results point towards lower values, Deep-Sea Res. Part II-Top. Stud. Oceanogr., 48, 2173-2197, 2001.

Oschlies, A., Blackford, J., Doney, S. C., and Gehlen, M.: Modelling considerations. In: Guide to best practices for ocean acidification research and data reporting, Riebesell, U., Fabry, V. J., Hansson, L., and Gattuso, J. P. (Eds.), Publications Office of the European Union Luxembourg, 2010.

Oschlies, A. and Kähler, P.: Biotic contribution to air-sea fluxes of CO_2 and O_2 and its relation to new production, export production, and net community production, Glob. Biogeochem. Cycle, 18, GB1015, 2004.

Oschlies, A., Schulz, K. G., Riebesell, U., and Schmittner, A.: Simulated 21st century's increase in oceanic suboxia by CO_2-enhanced biotic carbon export, Glob. Biogeochem. Cycle, 22, -, 2008.

Pahlow, M., Dietze, H., and Oschlies, A.: Optimality-based model of phytoplankton growth and diazotrophy, Marine Ecology Progress Series, 489, 1-16, 2013.

Pahlow, M. and Oschlies, A.: Chain model of phytoplankton P, N and light colimitation, Marine Ecology Progress Series, 376, 69-83, 2009.

Passow, U.: Formation of transparent exopolymer particles, TEP, from dissolved precursor material, Marine Ecology Progress Series, 192, 1-11, 2000.

Passow, U.: Transparent exopolymer particles (TEP) in aquatic environments, Progress in Oceanography, 55, 287-333, 2002.

Passow, U. and Alldredge, A. L.: A dye-binding assay for the spectrophotometric measurement of transparent exopolymer particles (TEP), Limnology and Oceanography, 40, 1326-1335, 1995.

Passow, U., Alldredge, A. L., and Logan, B. E.: The role of particulate carbohydrate exudates in the flocculation of diatom blooms, Deep-Sea Research Part I-Oceanographic Research Papers, 41, 335-357, 1994.

Passow, U. and Carlson, C. A.: The biological pump in a high CO_2 world, Marine Ecology Progress Series, 470, 249-271, 2012.

Passow, U., Shipe, R. F., Murray, A., Pak, D. K., Brzezinski, M. A., and Alldredge, A. L.: The origin of transparent exopolymer particles (TEP) and their role in the sedimentation of particulate matter, Continental Shelf Research, 21, 327-346, 2001.

Paulino, A. I., Egge, J. K., and Larsen, A.: Effects of increased atmospheric CO_2 on small and intermediate sized osmotrophs during a nutrient induced phytoplankton bloom, Biogeosciences, 5, 739-748, 2008.

Plattner, G. K., Joos, F., Stocker, T. F., and Marchal, O.: Feedback mechanisms and sensitivities of ocean carbon uptake under global warming, Tellus Series B-Chemical and Physical Meteorology, 53, 564-592, 2001.

Pomeroy, L. R. and Wiebe, W. J.: Temperature and substrates as interactive limiting factors for marine heterotrophic bacteria, Aquat. Microb. Ecol., 23, 187-204, 2001.

Raven, J. A. and Falkowski, P. G.: Oceanic sinks for atmospheric CO_2, Plant Cell and Environment, 22, 741-755, 1999.

Raven, J. A. and Geider, R. J.: Temperature and algal growth, New Phytologist, 110, 441-461, 1988.

Redfield, A.: On the proportions of organic derivations in sea water and their relation to the composition of plankton. In: James Johnstone Memorial Volume, Daniel, R. J. (Ed.), University Press of Liverpool, 1934.

Richardson, A. J. and Schoeman, D. S.: Climate impact on plankton ecosystems in the Northeast Atlantic, Science, 305, 1609-1612, 2004.

Riebesell, U., Czerny, J., von Brockel, K., Boxhammer, T., Budenbender, J., Deckelnick, M., Fischer, M., Hoffmann, D., Krug, S. A., Lentz, U., Ludwig, A., Muche, R., and Schulz, K. G.: Technical Note: A mobile sea-going mesocosm system - new opportunities for ocean change research, Biogeosciences, 10, 1835-1847, 2013.

Riebesell, U., Fabry, V. J., Hansson, L., and Gattuso, J. P.: Guide to best practices for ocean acidification research and data reporting, Publications Office of the European Union Luxembourg, 2010.

Riebesell, U., Kortzinger, A., and Oschlies, A.: Sensitivities of marine carbon fluxes to ocean change, Proceedings of the National Academy of Sciences of the United States of America, 106, 20602-20609, 2009.

Riebesell, U., Schulz, K. G., Bellerby, R. G. J., Botros, M., Fritsche, P., Meyerhofer, M., Neill, C., Nondal, G., Oschlies, A., Wohlers, J., and Zollner, E.: Enhanced biological carbon consumption in a high CO_2 ocean, Nature, 450, 545-U510, 2007.

Riebesell, U., Wolf-Gladrow, D. A., and Smetacek, V.: Carbon dioxide limitation of marine phytoplankton growth rates, Nature, 361, 249-251, 1993.

Riebesell, U., Zondervan, I., Rost, B., Tortell, P. D., Zeebe, R. E., and Morel, F. M. M.: Reduced calcification of marine plankton in response to increased atmospheric CO_2, Nature, 407, 364-367, 2000.

Rivkin, R. B. and Legendre, L.: Biogenic carbon cycling in the upper ocean: Effects of microbial respiration, Science, 291, 2398-2400, 2001.

Roberts, K., Granum, E., Leegood, R. C., and Raven, J. A.: C-3 and C-4 pathways of photosynthetic carbon assimilation in marine diatoms are under genetic, not environmental, control, Plant Physiology, 145, 230-235, 2007.

Rost, B., Riebesell, U., Burkhardt, S., and Sultemeyer, D.: Carbon acquisition of bloom-forming marine phytoplankton, Limnology and Oceanography, 48, 55-67, 2003.

Rost, B., Riebesell, U., and Sultemeyer, D.: Carbon acquisition of marine phytoplankton: Effect of photoperiod length, Limnology and Oceanography, 51, 12-20, 2006.

Rost, B., Zondervan, I., and Wolf-Gladrow, D.: Sensitivity of phytoplankton to future changes in ocean carbonate chemistry: current knowledge, contradictions and research directions, Marine Ecology Progress Series, 373, 227-237, 2008.

Sabine, C. L., Feely, R. A., Gruber, N., Key, R. M., Lee, K., Bullister, J. L., Wanninkhof, R., Wong, C. S., Wallace, D. W. R., Tilbrook, B., Millero, F. J., Peng, T. H., Kozyr, A., Ono, T., and Rios, A. F.: The oceanic sink for anthropogenic CO_2, Science, 305, 367-371, 2004.

Sambrotto, R. N., Savidge, G., Robinson, C., Boyd, P., Takahashi, T., Karl, D. M., Langdon, C., Chipman, D., Marra, J., and Codispoti, L.: Elevated consumption of carbon relative to nitrogen in the surface ocean, Nature, 363, 248-250, 1993.

Sarmiento, J. L. and Bender, M.: Carbon Biogeochemistry and Climate-Change, Photosynth Res, 39, 209-234, 1994.

Sarmiento, J. L. and Gruber, N.: Sinks for anthropogenic carbon, Physics Today, 55, 30-36, 2002.

Sarmiento, J. L. and Gruber, N.: Ocean biogeochemical dynamics, Princeton University Press, 2006.

Sarmiento, J. L., Slater, R., Barber, R., Bopp, L., Doney, S. C., Hirst, A. C., Kleypas, J., Matear, R., Mikolajewicz, U., Monfray, P., Soldatov, V., Spall, S. A., and Stouffer, R.: Response of ocean ecosystems to climate warming, Glob. Biogeochem. Cycle, 18, 2004.

Sarthou, G., Timmermans, K. R., Blain, S., and Treguer, P.: Growth physiology and fate of diatoms in the ocean: a review, Journal of Sea Research, 53, 25-42, 2005.

Savoye, N., Benitez-Nelson, C., Burd, A. B., Cochran, J. K., Charette, M., Buesseler, K. O., Jackson, G. A., Roy-Barman, M., Schmidt, S., and Elskens, M.: ^{234}Th sorption and export models in the water column: A review, Mar. Chem., 100, 234-249, 2006.

Schartau, M., Engel, A., Schroter, J., Thoms, S., Volker, C., and Wolf-Gladrow, D.: Modelling carbon overconsumption and the formation of extracellular particulate organic carbon, Biogeosciences, 4, 433-454, 2007.

Schartau, M. and Oschlies, A.: Simultaneous data-based optimization of a 1D-ecosystem model at three locations in the North Atlantic: Part I - Method and parameter estimates, Journal of Marine Research, 61, 765-793, 2003.

Schlitzer, R.: Carbon export fluxes in the Southern Ocean: results from inverse modeling and comparison with satellite-based estimates, Deep-Sea Res. Part II-Top. Stud. Oceanogr., 49, 1623-1644, 2002.

Schlitzer, R.: Export production in the equatorial and North Pacific derived from dissolved oxygen, nutrient and carbon data, Journal of Oceanography, 60, 53-62, 2004.

Schmittner, A., Oschlies, A., Matthews, H. D., and Galbraith, E. D.: Future changes in climate, ocean circulation, ecosystems, and biogeochemical cycling simulated for a business-as-usual CO_2 emission scenario until year 4000 AD, Glob. Biogeochem. Cycle, 22, 2008.

Schmittner, A., Oschlies, A., Matthews, H. D., and Galbraith, E. D.: Correction to "Future changes in climate, ocean circulation, ecosystems, and biogeochemical cycling simulated for a business-as-usual CO_2 emission scenario until year 4000 AD", Glob. Biogeochem. Cycle, 23, 2009.

Schulz, K. G., Bellerby, R. G. J., Brussaard, C. P. D., B√ºdenbender, J., Czerny, J., Engel, A., Fischer, M., Koch-Klavsen, S., Krug, S. A., Lischka, S., Ludwig, A., Meyerh√∂fer, M.,

Nondal, G., Silyakova, A., Stuhr, A., and Riebesell, U.: Temporal biomass dynamics of an Arctic plankton bloom in response to increasing levels of atmospheric carbon dioxide, Biogeosciences, 10, 161-180, 2013.

Schulz, K. G., Rost, B., Burkhardt, S., Riebesell, U., Thoms, S., and Wolf-Gladrow, D. A.: The effect of iron availability on the regulation of inorganic carbon acquisition in the coccolithophore Emiliania huxleyi and the significance of cellular compartmentation for stable carbon isotope fractionation, Geochimica Et Cosmochimica Acta, 71, 5301-5312, 2007.

Sharp, J. H.: Improved Analysis for "Particulate" Organic Carbon and Nitrogen from Seawater, Limnology and Oceanography, 19, 984-989, 1974.

Sharqawy, M. H., Lienhard, J. H., and Zubair, S. M.: The thermophysical properties of seawater: A review of existing correlations and data., Desalination and Water Treatment, 354–380, 2010.

Simon, M. and Azam, F.: Protein content and protein synthesis rates of planktonic marine bacteria, Marine Ecology Progress Series, 51, 201-213, 1989.

Smayda, T.: The suspension and sinking of phytoplankton in the sea, Oceanography and Marine Biology: An Annual Review, 8, 1970.

Smetacek, V.: Making sense of ocean biota: How evolution and biodiversity of land organisms differ from that of the plankton, Journal of Biosciences, 37, 589-607, 2012.

Smith, D. C. and Azam, F.: A simple, economical method for measuring bacterial protein synthesis rates in seawater using ^{3}H-leucine, Mar. Microb. Food Webs, 6, 107-114, 1992.

Smith, K. L., Baldwin, R. J., Glatts, R. C., Kaufmann, R. S., and Fisher, E. C.: Detrital aggregates on the sea floor: Chemical composition and aerobic decomposition rates at a time-series station in the abyssal NE Pacific, Deep-Sea Res. Part II-Top. Stud. Oceanogr., 45, 843-880, 1998.

Smith, S. V.: Physical, chemical and biological characteristics of CO_2 gas flux across the air-water interface, Plant, Cell & Environment, 8, 387-398, 1985.

Sommer, U., Aberle, N., Engel, A., Hansen, T., Lengfellner, K., Sandow, M., Wohlers, J., Zollner, E., and Riebesell, U.: An indoor mesocosm system to study the effect of climate change on the late winter and spring succession of Baltic Sea phyto- and zooplankton, Oecologia, 150, 655-667, 2007.

Sommer, U. and Lengfellner, K.: Climate change and the timing, magnitude, and composition of the phytoplankton spring bloom, Global Change Biology, 14, 1199-1208, 2008.

Sournia, A., Chretiennotdinet, M. J., and Ricard, M.: Marine phytoplankton: how many species in the world ocean?, Journal of Plankton Research, 13, 1093-1099, 1991.

Steffen, W., Sanderson, R. A., Tyson, P. D., Jäger, J., Matson, P. A., Moore III, B., Oldfield, F., Richardson, K., Schellnhuber, H.-J., Turner, B. L., and Wasson, R. J.: Global Change and the Earth System: a Planet under Pressure, Springer, Berlin, Germany, 2004.

Steinacher, M., Joos, F., Frolicher, T. L., Bopp, L., Cadule, P., Cocco, V., Doney, S. C., Gehlen, M., Lindsay, K., Moore, J. K., Schneider, B., and Segschneider, J.: Projected 21st century decrease in marine productivity: a multi-model analysis, Biogeosciences, 7, 979-1005, 2010.

Stemmann, L., Jackson, G. A., and Gorsky, G.: A vertical model of particle size distributions and fluxes in the midwater column that includes biological and physical processes - Part II: application to a three year survey in the NW Mediterranean Sea, Deep-Sea Research Part I-Oceanographic Research Papers, 51, 885-908, 2004.

Sterner, R. W. and Elser, J. J.: Ecological stoichiometry: the biology of elements from molecules to the biosphere, Princeton University Press, 2002.

Stoll, M. H. C., Bakker, K., Nobbe, G. H., and Haese, R. R.: Continuous-Flow Analysis of Dissolved Inorganic Carbon Content in Seawater, Analytical Chemistry, 73, 4111-4116, 2001.

Suzuki, Y. and Takahashi, M.: Growth responses of several diatom species isolated from various environments to temperature, Journal of Phycology, 31, 880-888, 1995.

Taucher, J. and Oschlies, A.: Can we predict the direction of marine primary production change under global warming?, Geophys. Res. Lett., 38, 2011.

Taucher, J., Schulz, K. G., Dittmar, T., Sommer, U., Oschlies, A., and Riebesell, U.: Enhanced carbon overconsumption in response to increasing temperatures during a mesocosm experiment, Biogeosciences, 9, 3531-3545, 2012.

Thingstad, T. F., Hagstrom, A., and Rassoulzadegan, F.: Accumulation of degradable DOC in surface waters: Is it caused by a malfunctioning microbial loop?, Limnology and Oceanography, 42, 398-404, 1997.

Thomas, M. K., Kremer, C. T., Klausmeier, C. A., and Litchman, E.: A Global Pattern of Thermal Adaptation in Marine Phytoplankton, Science, 338, 1085-1088, 2012.

Thompson, P. A., Guo, M.-x., and Harrison, P. J.: Effects of variation in temperature. I. On the biochemical compostion of eight species of marine phytoplankton, Journal of Phycology, 28, 481-488, 1992.

Toggweiler, J. R.: Carbon overconsumption, Nature, 363, 210-211, 1993.

Toggweiler, J. R., Gnanadesikan, A., Carson, S., Murnane, R., and Sarmiento, J. L.: Representation of the carbon cycle in box models and GCMs: 1. Solubility pump, Glob. Biogeochem. Cycle, 17, 2003a.

Toggweiler, J. R., Murnane, R., Carson, S., Gnanadesikan, A., and Sarmiento, J. L.: Representation of the carbon cycle in box models and GCMs: 2. Organic pump, Glob. Biogeochem. Cycle, 17, 2003b.

Tortell, P. D. and Morel, F. M. M.: Sources of inorganic carbon for phytoplankton in the eastern Subtropical and Equatorial Pacific Ocean, Limnology and Oceanography, 47, 1012-1022, 2002.

Tortell, P. D., Payne, C. D., Li, Y. Y., Trimborn, S., Rost, B., Smith, W. O., Riesselman, C., Dunbar, R. B., Sedwick, P., and DiTullio, G. R.: CO_2 sensitivity of Southern Ocean phytoplankton, Geophys. Res. Lett., 35, 2008.

Tortell, P. D., Reinfelder, J. R., and Morel, F. M. M.: Active uptake of bicarbonate by diatoms, Nature, 390, 243-244, 1997.

Treguer, P., Nelson, D. M., Vanbennekom, A. J., Demaster, D. J., Leynaert, A., and Queguiner, B.: The silica balance in the world ocean: a reestimate, Science, 268, 375-379, 1995.

Trimborn, S., Lundholm, N., Thoms, S., Richter, K. U., Krock, B., Hansen, P. J., and Rost, B.: Inorganic carbon acquisition in potentially toxic and non-toxic diatoms: the effect of pH-induced changes in seawater carbonate chemistry, Physiologia Plantarum, 133, 92-105, 2008.

Vallino, J. J.: Improving marine ecosystem models: Use of data assimilation and mesocosm experiments, Journal of Marine Research, 58, 117-164, 2000.

van de Waal, D. B., Verschoor, A. M., Verspagen, J. M. H., van Donk, E., and Huisman, J.: Climate-driven changes in the ecological stoichiometry of aquatic ecosystems, Frontiers in Ecology and the Environment, 8, 145-152, 2010.

Verdugo, P., Alldredge, A. L., Azam, F., Kirchman, D. L., Passow, U., and Santschi, P. H.: The oceanic gel phase: a bridge in the DOM-POM continuum, Mar. Chem., 92, 67-85, 2004.

Verity, P. G.: Effects of temperature, irradiance, and daylength on the marine diatom Leptocylindrus danicus Cleve. II. Excretion, Journal of Experimental Marine Biology and Ecology, 55, 159-169, 1981.

Volk, T. and Hoffert, M. I.: Ocean carbon pumps: Analysis of relative strengths and efficiencies in ocean-driven atmospheric CO_2 changes. In: The Carbon Cycle and Atmospheric CO_2: Natural Variations Archean to Present, Geophysical Monograph Series, AGU, Washington, D.C., 1985.

Weaver, A. J., Eby, M., Wiebe, E. C., Bitz, C. M., Duffy, P. B., Ewen, T. L., Fanning, A. F., Holland, M. M., MacFadyen, A., Matthews, H. D., Meissner, K. J., Saenko, O., Schmittner, A., Wang, H. X., and Yoshimori, M.: The UVic Earth System Climate Model: Model description, climatology, and applications to past, present and future climates, Atmosphere-Ocean, 39, 361-428, 2001.

Weiss, R. F.: Carbon dioxide in water and seawater: the solubility of a non-ideal gas, Mar. Chem., 2, 203-215, 1974.

Westberry, T., Behrenfeld, M. J., Siegel, D. A., and Boss, E.: Carbon-based primary productivity modeling with vertically resolved photoacclimation, Glob. Biogeochem. Cycle, 22, 2008.

Wetz, M. S. and Wheeler, P. A.: Production and partitioning of organic matter during simulated phytoplankton blooms, Limnology and Oceanography, 48, 1808-1817, 2003.

Wetz, M. S. and Wheeler, P. A.: Release of dissolved organic matter by coastal diatoms, Limnology and Oceanography, 52, 798-807, 2007.

Wohlers, J., Engel, A., Zollner, E., Breithaupt, P., Jurgens, K., Hoppe, H. G., Sommer, U., and Riebesell, U.: Changes in biogenic carbon flow in response to sea surface warming, Proceedings of the National Academy of Sciences of the United States of America, 106, 7067-7072, 2009.

Wood, M. A. and van Valen, L. M.: Paradox lost? On the release of energy-rich compounds by phytoplankton, Marine Microbial Food Webs, 103–116, 1990.

Zeebe, R. E. and Wolf-Gladrow, D.: CO_2 in Seawater: Equilibrium, Kinetics, Isotopes: Equilibrium, Kinetics, Isotopes, Access Online via Elsevier, 2001.

Zlotnik, I. and Dubinsky, Z.: The effect of light and temperature on DOC excretion by phytoplankton, Limnology and Oceanography, 34, 831-839, 1989.

Danksagung

Zuallererst möchte ich mich bei Andreas Oschlies bedanken, der mir überhaupt erst die Möglichkeit geboten hat diese Doktorarbeit durchzuführen, und mir als Erstbetreuer in Sachen Modellierung stets mit Rat und Tat zur Seite stand. Ein weiterer besonderer Dank gilt Ulf Riebesell, ohne den meine Arbeit im experimentellen Bereich nicht möglich gewesen wäre. Danke Euch beiden dafür, dass Ihr Euer Vertrauen in mich gesetzt und mich stets unterstützt habt, und dafür dass Ihr es mir ermöglicht habt diese innovative Kombination aus Modellierung und Experimenten in meiner Doktorarbeit anzuwenden. Vielen Dank auch an Uta Passow, die mich in ihrem Labor in Santa Barbara toll aufgenommen hat, und mir durch die tolle Zusammenarbeit dabei half, meine Erfahrungen in der experimentellen Arbeit zu erweitern. Bei Euch dreien möchte ich mich ganz besonders bedanken für die tolle Betreuung während der Doktorarbeit und dafür dass Ihr mich mit Eurer Begeisterung für die Meereswissenschaft angesteckt habt.

Ein großes Dankeschön geht auch an die gesamten Arbeitsgruppen „Biogeochemische Modellierung“ und „Biologische Ozeanographie“. Es war eine tolle und lehrreiche Zeit, und ich will Euch allen für Eure Hilfe und Unterstützung, und auch den Spaß während der letzten Jahre danken, besonders Lenni, Nora, Fi, Lionel, Kai Schulz, Kai (to-the-L), Jan C. und Jassi. Vielen Dank auch an meine Büromitbewohnerin Bei Su für eine angenehme Atmosphäre im Büro und das Teilen fernöstlicher Delikatessen wenn die Nahrungsmittelversorgung mal eng wurde. Danke auch an Mark Lenz für hilfreiche Beratung in der Parallelwelt der statistischen Analyse.

Ein Riesendankeschön an das Team an der UCSB in Santa Barbara, für eine spannenden und tollen Aufenthalt in Kalifornien. Julia Sweet, Jonathan Jones, Anna James, Mark Brzezinski, Craig Carlson, Maverick Carey, ich danke Euch!

Vielen Dank auch an das Team unserer Graduiertenschule ISOS um Avan Antia für viele interessante Kurse, Workshops, Vorträge, und finanzieller Unterstützung für Dienstreisen.

Ein besonderer Dank geht auch an Andrea Froughmel für ihre Freundschaft, und eine tolle und fröhliche Zeit auf dem Unwetterstein. Danke auch an meinen anderen Fisch-Buddy Robert Tillner für viele lustige Momente und dessen Adaption bayrischer Brauchtümer.

Vielen Dank auch an meine anderen, nicht namentlich genannten Kollegen am GEOMAR für Eure stetige Hilfsbereitschaft und die angenehme Arbeitsatmosphäre am Institut.

Bedanken will ich mich auch bei meinen WG-Mitbewohnern und Freunden außerhalb der Arbeit, Veit, Sascha, Julio, Meike, Marie, Kaddy, Steffi, Mello, Arnim, Arnd, und allen anderen. Danke für eine schöne und spaßige Zeit in Kiel, die hoffentlich noch einige Jahre andauert. Auch bei meinen langjährigen Freunden aus der Münchner Zeit will ich mich bedanken, besonders Garwin, Pipo, Franz, Yuri, Loibl Ese, Eva B., Katrin, Nati, und allen anderen Weggefährten der letzten Jahre.

Meinen ganz besonderen Dank richte ich an Hanife, die mein Leben so bereichert und mich in der turbulenten Endphase meiner Doktorarbeit so liebevoll unterstützt hat.

Zuletzt danke ich noch ganz herzlich meiner Familie für die immerwährende und bedingungslose Unterstützung während meiner gesamten Ausbildung und angehenden Wissenschaftskarriere.

Curriculum Vitae

Personal information:

Name:	Jan Taucher
Nationality:	German
Date of birth:	10/20/1982
Place of birth:	Nuremberg, Germany

Education and academic career

01/2012 – 06/2012 01/2013 – 05/2013	Research visit at the University of California Santa Barbara (UCSB), Marine Science Institute. Supervisors: Uta Passow, Craig Carlson, Mark Brzezinski
Since 05/2010	PhD Student at IFM GEOMAR. Research Division “Marine Biogeochemistry”.
02/2010	Diploma in Physical Geography. Grade point average: 1.2 (very good)
09/2009 – 02/2010:	Diploma Thesis at IFM GEOMAR: Modelling the impacts of climate change on marine ecosystems – Investigating the direct effects of temperature on biological processes in a global earth system model. Grade: 1.0 (very good).
02/2009 – 04/2009:	Research internship at the Bjerknes Centre for Climate Research (BCCR), working group “Ocean Carbon Cycles”. Modelling the impacts of climate change and ocean acidification on marine biogeochemistry and ecosystems. Supervisor: Dr. Richard Bellerby
04/2008 – 07/2008:	Research internship at the Helmholtz Centre for Environmental Research (UFZ) within the EVENT experiment (ecological

	impacts of climatic extreme events). Supervisor: Prof. Dr. Anke Jentsch
12/2007 – 09/2009:	Student assistant researcher at the chair for remote sensing and environmental modelling at the department for geosciences of the LMU Munich. Main work was carried out in the DFG project "TRAIT" for tsunami risk and vulnerability assessment. Supervisor: Prof. Dr. Ralf Ludwig
08/2007 – 10/2007:	Research internship at the German Aerospace Centre (DLR), institute for remote sensing in the framework of the tsunami early warning project "GITEWS". Department: Environment and security. Supervisor: Hannes Taubenböck
10/2004 – 02/2010:	Diploma program (equiv. Master of Science) in Physical Geography at the Ludwig-Maximilian-University (LMU) Munich, Germany. Main focus: Climate change and its impacts on natural systems. Minor subjects: bio- / ecoclimatology, remote sensing (until intermediate diploma also economics and political science). Intermediate diploma in October 2006, grade point average: 1.5 (very good)
1993 – 2002:	Secondary School, Gymnasium Pullach, Munich, Germany, Graduation (Abitur) in 2002

Publications (peer reviewed)

Taucher, J., J. Jones, A. James, M. Brzezinski, C. A. Carlson, A. Oschlies, U. Riebesell, and U. Passow (2013): Effects of warming and elevated pCO_2 on carbon overconsumption and partitioning of the marine diatoms *Thalassiosira weissflogii* and *Dactyliosolen fragilissimus*. To be submitted to *Limnology and Oceanography*.

Taucher, J., and A. Oschlies (2013): What sets the upper limit of export production in marine ecosystem models? Submitted to *Global Biogeochemical Cycles*

Taucher, J., L. T. Bach, U. Riebesell, A. Oschlies (2013): The viscosity effect on marine particle flux – a climate relevant feedback mechanism, currently under review at *Global Biogeochemical Cycles*.

Taucher, J., K. G. Schulz, T. Dittmar, U. Sommer, A. Oschlies, and U. Riebesell (2012), Enhanced carbon overconsumption in response to increasing temperatures during a mesocosm experiment, *Biogeosciences*, 9(9), 3531-3545.

Taucher, J., and A. Oschlies (2011): Can we predict the direction of marine primary production change under global warming?, *Geophysical Research Letters*, 38(2).

Eidesstattliche Erklärung

Hiermit erkläre ich, dass die vorliegende Dissertation mit dem Titel:

„Effects of increasing temperatures and CO_2 on phytoplankton and marine biogeochemical cycles – Combining experimental work and numerical modeling“

selbständig von mir angefertigt wurde. Die Dissertation – abgesehen von der Beratung durch die Betreuerin oder den Betreuer – ist nach Form und Inhalt meine eigene Arbeit und es wurden keine anderen als die angegebenen Quellen und Hilfsmittel verwendet. Die vorliegende Arbeit ist unter Einhaltung der Regeln guter wissenschaftlicher Praxis der Deutschen Forschungsgemeinschaft entstanden und wurde weder ganz noch zum Teil an anderer Stelle im Rahmen eines Prüfungsverfahrens vorgelegt oder veröffentlicht.

Weiterhin erkläre ich mich einverstanden, dass diese Dissertation an die Bibliothek des GEOMAR und die Universitätsbibliothek der CAU weitergeleitet wird.